ABSTRACT

Reconstruction of the Paleo-Redox Conditions of Reservoir Facies Using Chemostratigraphy and Core Descriptions of the Devonian Marcellus Formation, Pennsylvania

David W. Yeates, M.S.

Mentor: Stephen I. Dworkin, Ph.D.

The Marcellus Formation near Clinton County Pennsylvania has of average TOC of 2.8 wt %. TOC values found near the bottom of the Union Spring Member are >5 wt % and were created by high organic production which allowed for euxinic conditions on the seafloor. The Appalachian Basin had about 80% of open seawater conditions during Marcellus deposition. The $\delta^{13}C$ values have a negative correlation with TOC. They also suggest the decreasing availability of carbon within the depositional area. High C/N ratios and $\delta^{15}N$ isotopes suggest a nitrogen-limited system. Enriched Mo, U, and V show deposition occurred mostly within euxinic conditions. Ni and Cu values suggest the high production of marine algae. High production appears to be the most important cause of anoxia within this study area. Bioturbated textures are shown to retain high TOC wt %. Quartz, illite, and calcite are the major minerals in the Marcellus.

Reconstruction of the Paleo-Redox Conditions of Reservoir Facies using Chemostratigraphy and Core Descriptions of the Devonian Marcellus Formation, Pennsylvania

by

David W. Yeates, B.S.

A Thesis

Department of Geosciences

Stacy Atchley, Ph.D., Chairperson

Submitted to the Graduate Faculty of
Baylor University in Partial Fulfillment of the
Requirements for the Degree
of

Master of Science

Approved by Thesis Committee

Stephen I. Dworkin Ph.D., Chairperson

Stacy Atchley, Ph.D.

Charles M. Garner, Ph.D.

Accepted by the Graduate School

December 2017

J. Larry Lyon, Ph.D., Dean

Page bearing signatures is kept on file in the Graduate School.

TABLE OF CONTENTS

LIST OF FIGURES

LIST OF TABLES

ACKNOWLEDGMENTS

I would like to thank Anadarko Petroleum Company for providing the core and petrophysical data used in this project. I want to recognize Jared Hanson who was co-investigator on this project. I want to thank my advising committee, especially my advisor Dr. Steve Dworkin for the hours spent fixing geochemical equipment and setting up this project with Anadarko. I would also like to thank Baylor University's Department of Geoscience, Graduate School, and Applied Petroleum Systems Group for their financial support. I also thank my wife Kaelin for her support during this project.

CHAPTER ONE

Introduction

The Appalachian Basin is known for its thick accumulation of organic-rich mudrocks that punctuate the middle and late Devonian stratigraphic successions. Unlike Late Devonian black shale that has widespread geographic distributions (Algeo and Scheckler, 1998) the Middle Devonian black shale, known as the Marcellus Formation, represents a more isolated, although thick, occurrence of an organic rich-mudrock. This study investigates the geochemical character of Marcellus mudrocks and identifies a succession of chemofacies that documents the evolution of paleoceanographic conditions in the Appalachian basin that promoted the preservation of organic matter.

Persevered organic material is of great economic importance because it is the major source of hydrocarbons (Werne et al., 2002). The hydrocarbons sourced from Devonian black shales have been produced for the past 150 years (Van Tyne, 1983), but in the last decade improvements in production techniques, such as horizontal drilling combined with hydraulic fracturing, has made the Marcellus a much more successful venture for oil and gas companies. The Marcellus is one of the largest gas producing plays in the United States and has an estimated 500 trillion cubic feet of in-place gas reserves (Engelder and Lash, 2008).

Reconstructing paleoceanographic conditions during black shale deposition is difficult because of the lack of modern examples in which anoxic water columns are found (Algeo, 2004). The best example of a geographically widespread marine basin with an anoxic water column is the Black Sea. The Black Sea represents a highly restricted basin in which the decomposing organic matter removes oxygen from the water column resulting in anoxia. High organic matter deposition has also been identified in a few open marine locations where upwelling nutrient-rich water generate an oxygen minimum that encompasses much of the water column. These two endmember depositional settings for organic-rich mudrocks can be identified on the basis of relationships between organic matter abundance and trace metal concentrations.

Organic Carbon Preservation

The majority of the organic matter in black shales is derived from marine algae (Arthur and Sageman, 1994; Dean et al., 1986). In modern marine environments, the overwhelming majority of the marine organic matter sourced from algae will undergo oxidative decomposition resulting in the return of carbon to the atmosphere as carbon dioxide (CO_2) (Canfield, 1994; Thunell et al., 2000; Tribovillard et al., 2006; Meyers, 2014). If algae arrives to the sea floor, it may be buried and persevered within the sediment. The main controls on the abundance of organic matter preserved in the rock record (TOC) include marine productivity, oxidative destruction, and sediment dilution (Demaison and Moore, 1980; Pedersen and Calvert, 1990; Sageman et al., 2003).

The main control on marine primary productivity is the availability of nutrients, and the two most common growth limiting nutrients are nitrogen and phosphorous (Suess, 1980). Nutrients can be sourced from the atmosphere, such as carbon and nitrogen, but many others, such as phosphorus and iron, usually come from detrital sources (Emerson and Hedges, 1988). Nutrient recycling can also play a major role in maintaining high levels of photosynthesis (Murphy et al., 2000; Chen and Sharma, 2016) and high productivity most commonly when algal sourced dissolved nutrients are upwelled from deep water onto shallow shelves.

Nutrients can also be delivered to the oceans via riverine sources that in turn derive their dissolved constituents from the weathering of continental rocks (Algeo and Scheckler, 1998). This source is potentially important for Devonian marine ecosystems because of the prevailing climate combined with the evolution of land plants (Algeo and Scheckler, 1998). The greenhouse environment present in the Middle Devonian along with the development of vascular land plants may have increased mineral weathering rates resulting in elevated delivering of continentally sourced nutrients (Algeo and Scheckler, 1998; Gensel and Edwards, 2001; Helmond et al., 2014), which in turn may have resulted in high productivity without the necessity of upwelling.

The second important control on organic matter abundance in shales is the amount of free oxygen dissolved in the water column, which is a variable that controls the decomposition of the marine organic matter as it settles to the seafloor. The carbon in organic material is in a reduced form that can be readily oxidized by bacteria in the presence of free oxygen. Therefore, the more dissolved O_2 that is present in the water, the more organic matter is oxidized into CO_2 (Arthur and Sageman, 1994; Canfield, 1994; Hedges et al., 1999). Terms used to indicate the abundance of free oxygen gives a good indication of the likely preservation potential of organic matter. Oxic is used to signify normal marine conditions with an O_2 concentration > 2 (ml O_2/l H_2O). Dysoxic or suboxic is O_2 levels that are lower than normal marine but still can support some more resilient aquatic life. In suboxic/dysoxic conditions hydrogen sulfide (H_2S) occurrence is limited to below the sediment-water interface and O_2 concentration range between 2 (ml

O_2/l H_2O) and 0.2 (ml O_2/l H_2O). Anoxic conditions refer to O_2 levels that are low enough to drive the denitrification process and have O_2 concentration <0.2 (ml O_2/l H_2O). Euxinic conditions represent anoxia in which free H_2S exists in the water column. (Canfield, 1989; Tyson and Pearson, 1991; Tribovillard et al., 2006).

Stratification of dissolved oxygen concentrations is an important factor that controls organic matter preservation (Demaison and Moore, 1980). A stratified water body will prevent communication between surface waters and deeper parts of the water column, thus preventing the replenishment of O_2 to the sediment-water interface. Anoxic conditions can also be caused by high production of organic material. (Tribovillard et al., 2006; Saltzman and Thomas, 2012). Often a combination of high production and water stagnation creates widespread anoxia within the water column. (Tribovillard et al., 2006).

Lastly, sediment dilution is also an important factor in the amount of TOC that is found within mudrocks (Tyson, 2001). The lower rate of sediment delivery to the sea floor higher the proportion of organic matter within the sedimentary succession.

Study Area

The Marcellus Formation is found throughout the Appalachian Basin in the northeastern part of the United States. It underlies most of Pennsylvania and West Virginia and as well as large parts of New York, Ohio, and Virginia (Figure 1). The study area for this project is in the north-central part of Pennsylvania and partially covers Centre, Clinton, and Lycoming counties. It is an area approximately 35 miles east to west and 25 miles north to south. The geochemical data used in this study comes from three cored wells. These wells are COP Tract 259 A-1000 (COP 259), COP Tract 653 1000 (COP 653), COP Tract 289 1000PH (COP 289). The petrophysical data from the three cored wells and six nearby wells are also used in this study. These six wells are COP Tract 231 A-1000, WW Lite A-PH, Texas Gulf B A-4, COP Tract 678 B-1001, COP Tract 252B-1002, and COP Tract 356D-1019 (Figure 2).

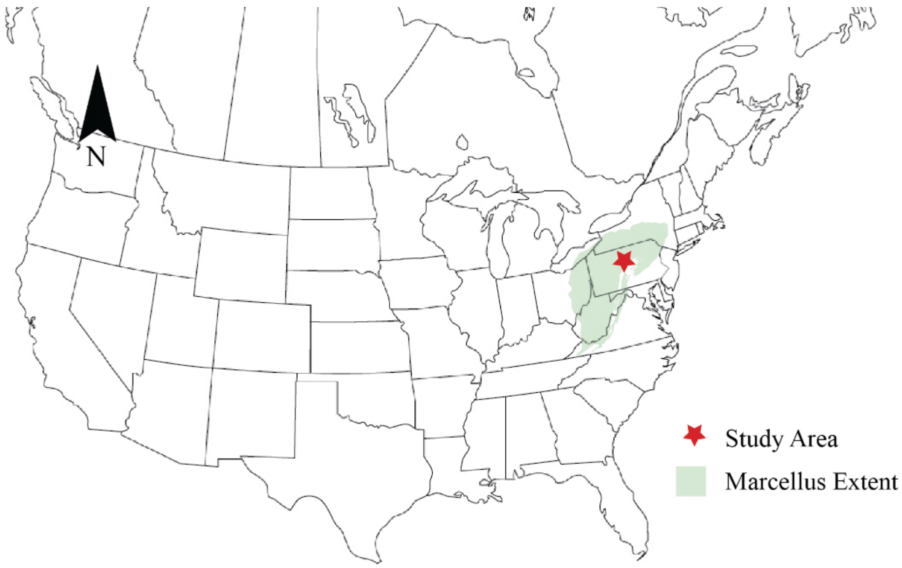

Figure 1. Marcellus shale extent and study area within the United States and the southern portion of Canada. The state and province outlines are courtesy of Bruce Jones Design Inc. Marcellus Extent modified from (Coleman et al., 2011).

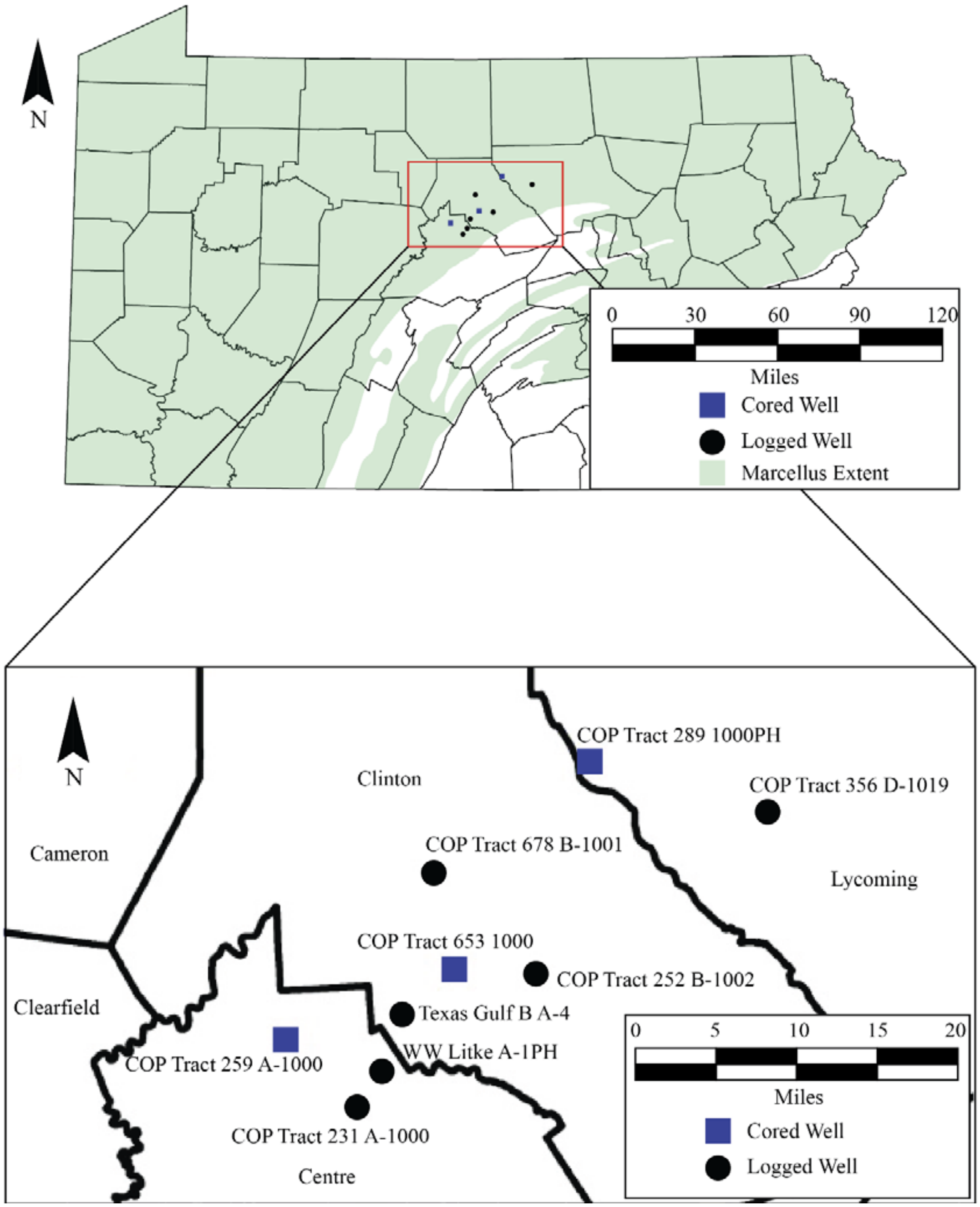

Figure 2. Cored and logged well locations from this study. The upper map is a county map of Pennsylvania, USA, while the lower map is zoomed into the area surrounding Clinton County. The well names are posted next to their locations. The county names are also present. Marcellus extent was modified from Pennsylvania Department of Environmental Protection eMapPA (http://www.depgis.state.pa.us/emappa/).

CHAPTER TWO

Geologic Setting

Regional Stratigraphy

The Marcellus Formation was deposited during the Middle Devonian and spans the Eifelain-Givetain boundary. The stratigraphic location of this boundary varies depending on author and study area. Zagorski et al. (2012) suggest that the bottom of the Marcellus as Eifelain-Givetain boundary while Milici and Swezey (2006) place the time boundary at top of the formation. Most studies suggest the boundary is somewhere within the Marcellus Formation, and it is often represented as the top of the Cherry Valley Member (Sageman et al., 2003; Ver Straeten and Brett, 2006; Brett et al., 2011; DeSantis and Brett, 2011; Ver Straeten et al., 2011; Wang and Carr, 2013; Kohl et al., 2014).

The Marcellus Formation has been the focus of many local and regional investigations. Therefore, the stratigraphic nomenclature and division of the members varies greatly. In this study, the Marcellus is designated as the lower part of the Hamilton group with the Mahantango Formation making up the upper part of this group. The Marcellus is separated into three separate units including the Union Springs Member, Cherry Valley Member, and Oatka Creek Member (Figure 3). The Union Springs Member and the Oatka Creek Member are clastic-dominated organic-rich mudstone with occasional fossils, whereas the Cherry Valley Member is a carbonate-rich mudstone with common allochems that separates the other two members (Ver Straeten and Brett, 2006; Lash and Engelder, 2011).

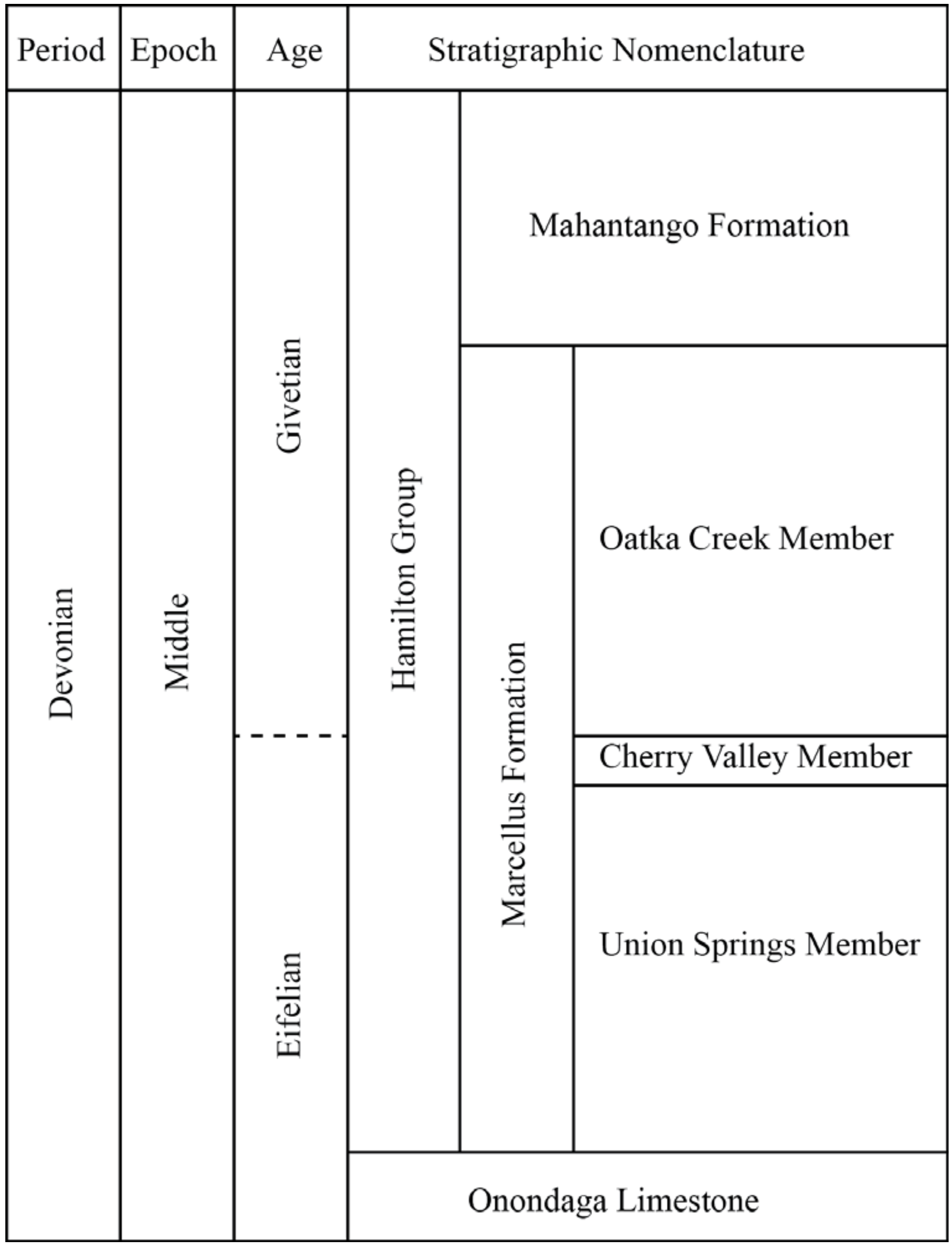

Figure 3. Stratigraphic nomenclature of the Marcellus used in this study. The dotted line signifies uncertainty in the timing of the boundary location. The relative thickness of these members is drawn to scale.

The Onondaga Limestone underlies the Marcellus Formation and the contact in this study area appears to be gradational and mostly conformable. This limestone is consists of poorly sorted fine-grained crinoids, bryozoans, and microspar skeletal replaced coral fragments. It contains terrigenous silt and clay contents ranging from 5-20 % (Lindholm, 1969). It also has bedded chert and has undergone partial dolomitization in some areas (Oliver, 1956). All three of the cores used in this study recover the top of the Onondaga. Overlying the Marcellus but still within the Hamilton group is the Mahantango Formation. The Mahantango Formation is mostly mudstone with interbedded quartz siltstone to sandstones with some diverse skeletal fragments (Duke et al., 1991; Prave et al., 1996). The abundance of sandstones decreases to the northwest away from the prograding Catskill Delta. Between 70 and 140 feet of the basal Mahantango Formation is present within the cores used in this study and is composed mainly of thinly laminated mudstone.

Paleogeography

The Appalachian Basin developed as the Iapetus Ocean was being consumed by the impingement of Laurentia and Gondwana moving during the Devonian (Scotese and McKerrow, 1990; Ettensohn, 2008). This collision caused the Acadian Orogeny that was located 25° to 35° south of the equator (Scotese and McKerrow, 1990) (Figure 4). Isostatic depression caused flexural subsidence resulting in the Arcadian Forearc Basin and a forebulge known as the Findlay and Algonquin Arch (Beaumont et al., 1988; Castle, 2001). Relatively high sea levels also promoted a period of deposition that created the Kaskaskia supersequence (Sloss, 1963; Brett et al., 2011).

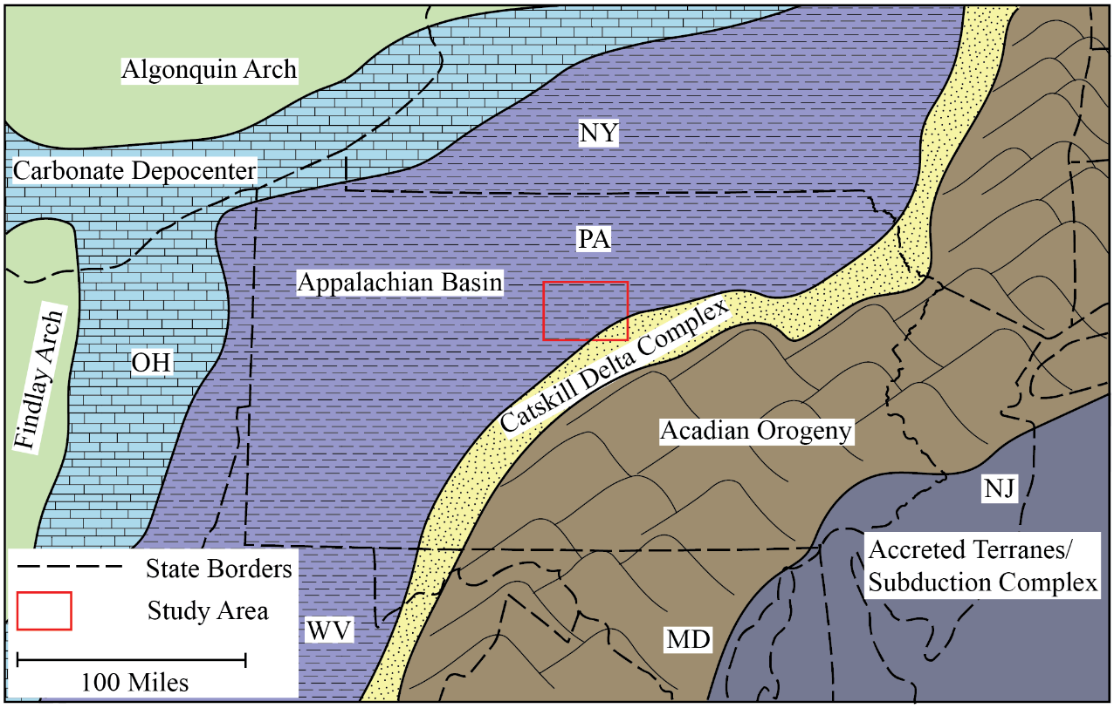

Figure 4. Regional paleogeography of the northeastern United States during the Middle Devonian.

The Appalachian Basin was a semi-restricted forearc basin bounded by the Acadian Orogeny highlands to the southeast and the Findlay/Algonquin Arch to the northeast. The basin trended from northeast to southwest and was connected to the Iapetus Ocean to the south and the Michigan basin to the northwest (Castle, 2001; Edinger et al., 2002; Brett et al., 2011; DeSantis and Brett, 2011). The Hamilton Group thickens to the east and southeast suggesting that the greatest accommodation was near the Acadian Mountains (Cooper, 1934; Lash and Engelder, 2011). $\delta\ ^{18}O$ values from brachiopods within the Hamilton Group suggest water temperatures that ranged from 25° to 35° C and likely characterized by normal marine salinity (Milici and Swezey, 2006). The eastern side of the basin was dominated by progradation of and filling by the Catskill Delta Complex (Ettensohn, 1985b; Faill, 1985). The Acadian mountains also affected the regional climate by putatively inducing a western rain shadow from easterly trade winds (Ettensohn, 1985a; Woodrow, 1985). The northwest side of the basin was a carbonate platform associated with the Findlay/Algonquin Arch (DeSantis and Brett, 2011; Kohl et al., 2014). The middle of the basin was dominated by fine-grained clastics with minor mixed carbonates (Ettensohn, 1985b).

CHAPTER THREE

Data and Methods

Data

This study is based on well logs and core provided by Anadarko Petroleum Company. The core consists of 1011 ft (308m) of whole core from three wells near Clinton County, Pennsylvania (Figure 2). Well logs from these three wells, along with well logs from six nearby wells, were used in the subsurface mapping chemofacies (Hanson, 2017). The core was described and sampled at Core Laboratories Inc. in Houston, Texas. After the description, the core was sampled at a 2 ft interval, for a total of 502 samples. This sampling density is approximately at the resolution of the petrophysical data. Thirty grams of each rock sample was powdered with a SPEX Shatterbox® and subsequently analyzed for TOC, elemental concentrations, and isotopic composition. All geochemical analyses were performed at Baylor University.

Core Descriptions

Rock type was identified and carbonates were classified using Dunham's classification scheme (Dunham, 1962), supplemented with a description of types of allochems as well as mechanical sedimentary structures. Effervescence was measured using 10% hydrochloric acid on a scale from 0-5 with 0 signifying no reaction and 5 as a very strong reaction. Bioturbation was recorded on a decimal scale from 0 (undisturbed) to 1 (completely bioturbated). The dry core color was recorded using a Munsell Color Chart and fracture density per foot was also recorded. Depth correction was made by comparing log gamma to measured TOC, which are well correlated within these wells (Hanson, 2017).

Organic Matter Analysis

Organic carbon and nitrogen abundance along with their corresponding isotopic compositions were measured by combustion analysis and mass spectrometry. For this analysis, five to thirty milligrams of a rock (depending on estimated TOC) was transferred into silver capsules and placed on a hot plate at 65° C. These samples were decarbonated with 10 % hydrochloric acid (HCl) added incrementally until reactions ceased. The capsules were then filled with HCl three times and allowed to dry for 24 hours. The decarbonated sample was wrapped in tin and placed into a desiccator to avoid rehydration. The samples then underwent combustion analysis in a Costech EA model 4010 and the carbon and nitrogen abundances were quantified. Standard USGS-40 yielded carbon and nitrogen values of 6.1 ± 0.13 wt. % and 0.46 ± 0.04 wt. % respectively. The gasses were conveyed to a Thermo Scientific™ Delta V™ Isotope Ratio Mass Spectrometer where the carbon and nitrogen isotope ratios were measured. The reproducibility of the isotope value was measured using Acetanilide (ACET) with the expected $\delta^{13}C$ value of -29.53 ± 0.01 ‰ and an expected $\delta^{15}N$ value of 1.18 ± 0.02 ‰. The average values from the $\delta^{13}C$ and $\delta^{15}N$ analyses are -29.41 ‰ ± 0.16 and 1.23 ‰ ± 0.16 respectively.

Weight % Carbonate

The abundance of calcite in Marcellus mudrocks was determined by subtracting the organic carbon abundance TOC from total carbon abundance (Equation 1) and multiplying the inorganic carbon value by the stoichiometric carbon weight ratio in calcite, i.e., 8.33 (Equation 2). The calcite within this study area has undergone a small amount of dolomitization which has the potential to cause some error in this calculation.

$$TC - OC = IC \qquad (1)$$

$$Wt.\%\,calcite = IC * 8.33 \qquad (2)$$

Major and Trace Elements

Major and trace element abundance was measured on a Rigaku wavelength dispersive X-ray fluorescence (XRF) instrument. For the XRF analysis, shatterbox pulverized samples were pressed into pellets. The elements analyzed include Si, Al, Fe, Ti, Mn, Ca, K, P, V, Cu, Zn, U, Ni, Mo, Th, and S. The standard deviations for analysis of each metal is reported in Table 1 based on duplicate analysis of standard TS-1. Drift corrections were calculated by repeatedly analyzing the standard TS-1.

Table 1. Precision of XRF analyses (+/- 1sd) using standard TS-1

Element Unit	SiO2 mass%	TiO2 mass%	Al2O3 mass%	Fe2O3 mass%	MnO mass%	CaO mass%	K2O mass%	P2O5 mass%
STDEV	0.0895	0.0019	0.0322	0.0095	0.0004	0.0006	0.0179	0.0024

Element Unit	V ppm	Cu ppm	Zn ppm	U ppm	Ni ppm	Th ppm	Mo ppm	S mass%
STDEV	5.17	1.56	1.10	0.78	1.38	1.41	0.60	0.0005

Redox-sensitive elements such as molybdenum (Mo), uranium (U), and vanadium (V) are reported in this study as enrichment factors (EF) in which they are normalized to Al concentration. Enrichment factors are calculated by normalizing the trace metal of interest to aluminum concentration and then dividing it by the trace metal to aluminum ratio of the average shale as shown in Equation 3 (Tribovillared et al., 2006) where x signifies the trace metal of interest.

$$EF_{element\ x} = \frac{\left(\frac{x}{Al}\right)_{Sample}}{\left(\frac{x}{Al}\right)_{average\ shale}} \tag{3}$$

Enrichment factors simplify the interpretation of the redox-sensitive metals because values above 1 indicate that the sample is more enriched than an average shale, while values below 1 suggest depletion. The values for the standard shale are taken from (Tribovillared et al., 2006) and are presented in Table 2.

Table 2. Trace element values for average shale

Element	Mn	Ba	Cd	Co	Cr	Cu	Mo	Ni	U	V	Zn	Al
Unit	ppm	ppm	ppm	ppm	ppm	ppm	ppm	ppm	ppm	ppm	ppm	wt%
Avg Shale	850	650	0.3	19	90	45	1.3	68	3	130	95	8.89

Chemofacies

Chemofacies were identified through stratigraphic analysis of the geochemical data and involved grouping stratigraphic intervals with similar geochemical trends and values. The most useful geochemical variables for identifying chemofacies in the Marcellus are $\delta\ ^{13}C$, TOC, EF-Mo, wt% calcite, and C/N ratios. Other data used to delineate chemofacies boundaries are $\delta\ ^{15}N$, EF-V, EF-U, S wt %, Fe wt %, Al wt %, Si wt %, Cu (ppm), and Ni (ppm).

Mineralogy

One representative sample from each chemofacies was analyzed for bulk mineralogy. These samples were finely powdered and analyzed on a Siemens D5000 X-ray diffractometer as random powder mount. Each sample was analyzed from 2° to 60°

two theta with a .05° step and a 5 seconds well time. The diffractograms were then interpreted with the software program JADE 7.

CHAPTER FOUR

Results and Discussion

Lithofacies Description

Eight lithofacies were recognized on the basis of sedimentary structures, bioturbation, Dunham classification for carbonate rock and texture for clastic rocks, faunal assemblage, and intensity of effervescence. A summary of each facies is given provided in Table 3. Core descriptions are found in the appendix (Figures A.1 - A.13) and a comparison of the facies occurrence in each well is provided in Figure 5. Color was not helpful in discriminating facies inasmuch as almost all mudstones had colors as dark as or darker than 2.5/N (Figure 6).

Description of Lithofacies

Black Laminated Mudstone (BLM). The BLM facies is clastic dominated fine-grained mudstone with mm lamination (Figures 6 and 7). It has a bioturbation index of 0-0.2 and effervescence ≤ 1. These mudstones have <10% fossil, but some rare small fossils are observed (Figure 8). Most of these fossils were brachiopods, however, nautiloids, crinoids, bryozoans, corals and encrusting red algae were occasionally found. This facies is believed to have been deposited offshore resulting from hemipelagic sedimentation.

Table 3. Facies Summary

Name	Black Laminated Mudstone	Mottled Black Mudstone	Calcareous Black Laminated Mudstone	Massive Mudstone	Skeletal Black Mudstone	Mud Supported Carbonate	Grain Supported Carbonate	Crypt Algal Boundstone
Environment	offshore	offshore	offshore	offshore	offshore to distal slope	offshore to distal slope	offshore to distal slope	shallow marine
Inferred process	pelagic to hemipelagic	pelagic to hemipelagic	pelagic to hemipelagic	burrowed pelagic to hemipelagic	turbidity flow	turbidity flow	turbidity flow	In-situ
Effervescence (0 to 5)	≤1	0 to 1	>1	4 to 5	≤2	>2	3 to 5	3 to 5
Physical sedimentary structures	mm lamina	discontinuous mm lamina	mm lamina	none	mm lamina	mm lamina, normal grading	normal grading	none
Bioturbation index (0-1.0)	0-.2	.3 -.9	0-.2	.9-1.0	0-.3	0-.6	0-1	<.1
Dunham classification	N/A	N/A	Mudstone	Mudstone	Wackestone	Wackestone	Packestone	Boundstone
Representative core photo	653_8289, 259_8093	289_8065	653_8333	289_8110	653_8447, 653_8325	259_8388	259_8227, 259_8289	653_8548.5
Facies	**BLM**	**MBM**	**CBLM**	**MM**	**SBM**	**MSC**	**GSC**	**CAB**

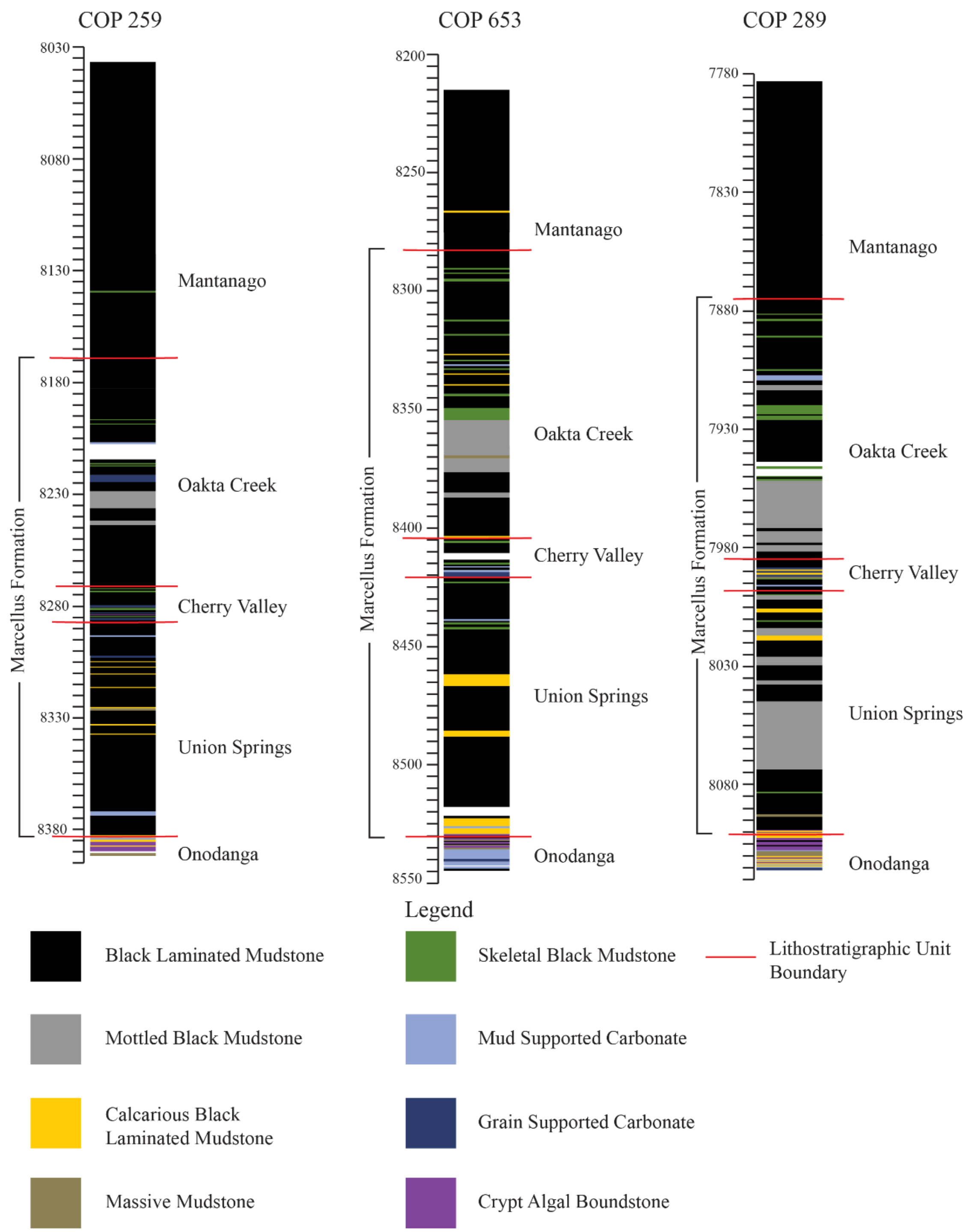

Figure 5. Distribution of lithofacies within each well. The red lines indicate lithostratigraphic boundaries.

Figure 6. Representative photo of BLM at well COP 259 at 8093 ft.

Figure 7. Representative photo of BLM from well COP 653 at 8289 ft.

Figure 8. BLM from well COP 653 at 8512 ft. This figure shows how BLM with occasional fossils. The fossils are the white dots and are diverse skeletal fragments.

Mottled Black Mudstone (MBM). MBMs is a clastic dominated fine-grained mudstone with discontinuous mm laminations (Figure 9). It is moderately bioturbated with a bioturbation index of 0.3-0.9. It has a low effervescence with values from 0-1. This facies is interpreted to have been deposited offshore from hemipelagic sedimentation.

Figure 9. Representative photo of MBM from well COP 289 at 8065 ft. This photo shows a bioturbation index of 0.5.

Calcareous Black Laminated Mudstone (CBLM). CBLM is a mixed carbonate and clastic rock and is a mudstone in the Dunham classification scheme (Figure 10). Most of the fossils found in CBLM are nautiloids. It has an effervescence >1 and mm laminations. The CBLM has very little to no bioturbation (index being from 0-0.2). The CBLM is interpreted to have been deposited offshore as pelagic to hemipelagic sediment.

Figure 10. Representative photo of CBLM from well COP 653 at 8333 ft.

Massive Mudstone (MM). MM is a carbonate-rich rock and is a mudstone in the Dunham classification (Figure 11). MM has no physical sedimentary structures and has a bioturbation index from 0.9-1. It exhibits strong effervescence with values from 4-5. MM is interpreted to have been deposited as offshore pelagic sediment.

Figure 11. Representative photo of MM from well COP 289 at 8110 ft. Saw blade marks in the lower 2/3 of the photo obscure the appearance.

Skeletal Black Mudstone (SBM). SBM is a clastic dominated mudstone with fossil content greater than >10% (Figures 12 and 13). Fossils observed in this facies are brachiopods, nautiloids, crinoids, gastropods, and serpulid worm tubes. The facies has an effervescence of ≤ 2 and mm laminations, and contains little to no bioturbation (index being from 0-0.3). This facies was likely deposited offshore. The fossils in the wackestone could be platform-swept skeletal grains deposited within pelagic to hemiplegic sediments. Most of the fossils are whole specimens suggesting in situ deposition or minimal transport.

Figure 12. Representative photo of SBM from well COP 653 at 8447 ft. The gold-brown color are allochems replaced by pyrite.

Figure 13. Representative photo of SBM from well COP 653 at 8325 ft.

Mud Supported Carbonate (MSC). MSC is a carbonate-dominated wackestone (Figure 14) with moderate effervescence (>2), mm laminations, and normal grading. This faices has a bioturbation index ranging from 0-.6. Fossils observed include brachiopods, nautiloids, and other skeletal fragments. This facies is interpreted as an offshore deposit, and owing to a common erosive base, at the distal end of turbidity flows.

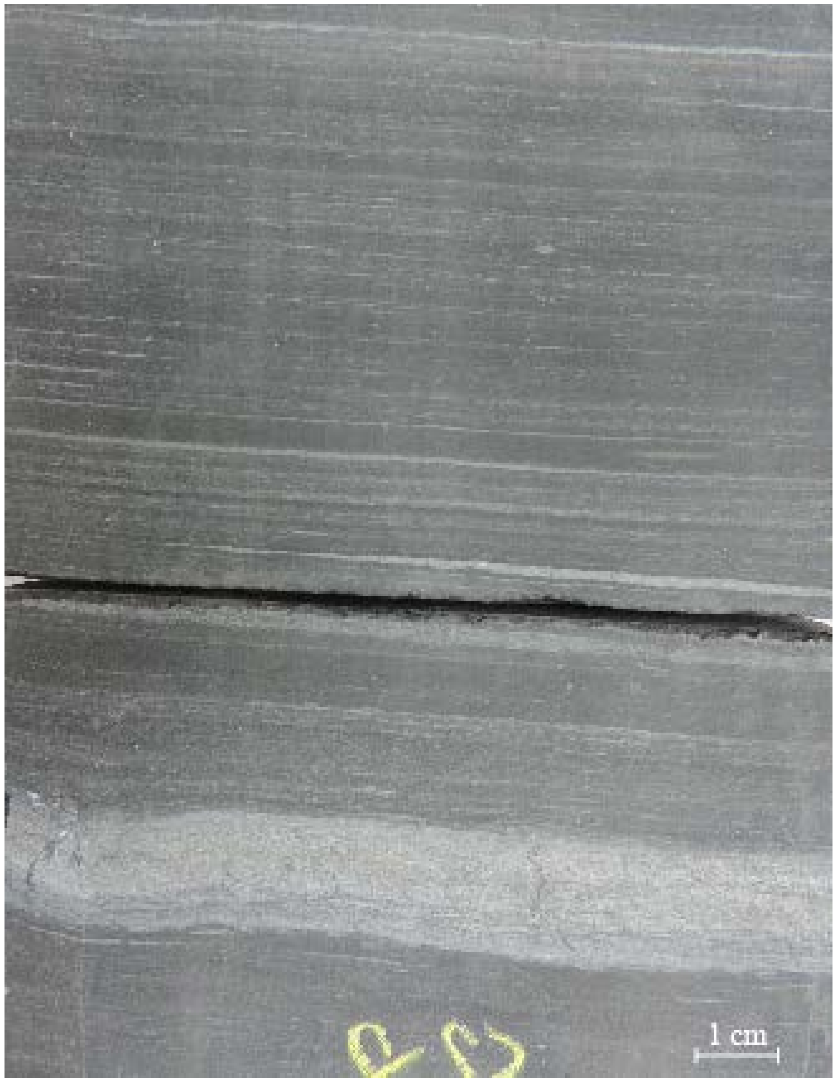

Figure 14. Representative photo of MSC from well COP 259 at 8388 ft.

Grain Supported Carbonate (GSC). GSC is a carbonate-dominated packstone (Figures 15 and 16). Fossil constituents include brachiopods, nautiloids, bivalves, bryozoans, gastropods, red crustal algae, and unidentified skeletal fragments. Sedimentary features consist of normally graded beds ranging in thickness from 2 to 20 cm. The GSC has effervescence from 3-5 and bioturbation index from 0-1. The GSC most likely accumulated as offshore turbidity flows.

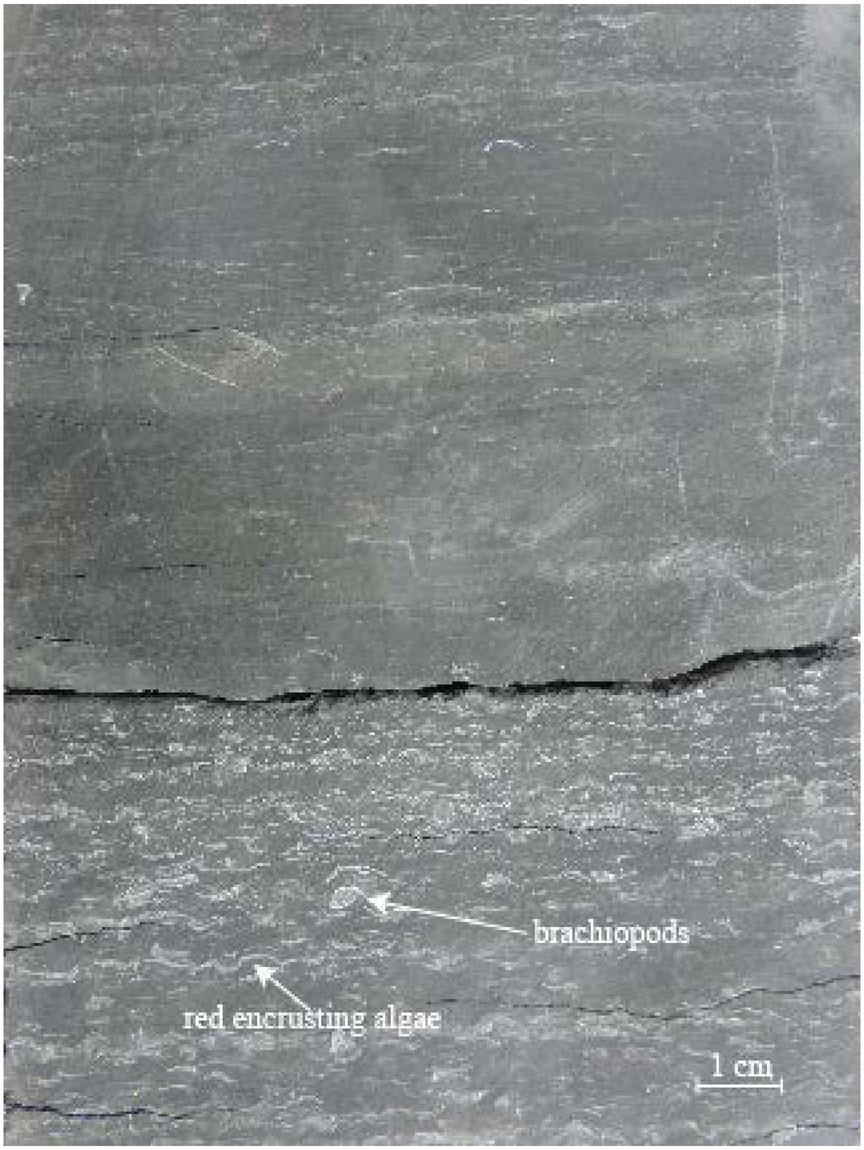

Figure 15. Representative photo of GSC from well COP 259 at 8227 ft. Allochems in this figure are mostly brachiopods. Some red encrusting algae is also present and can be seen as the white undulating lines.

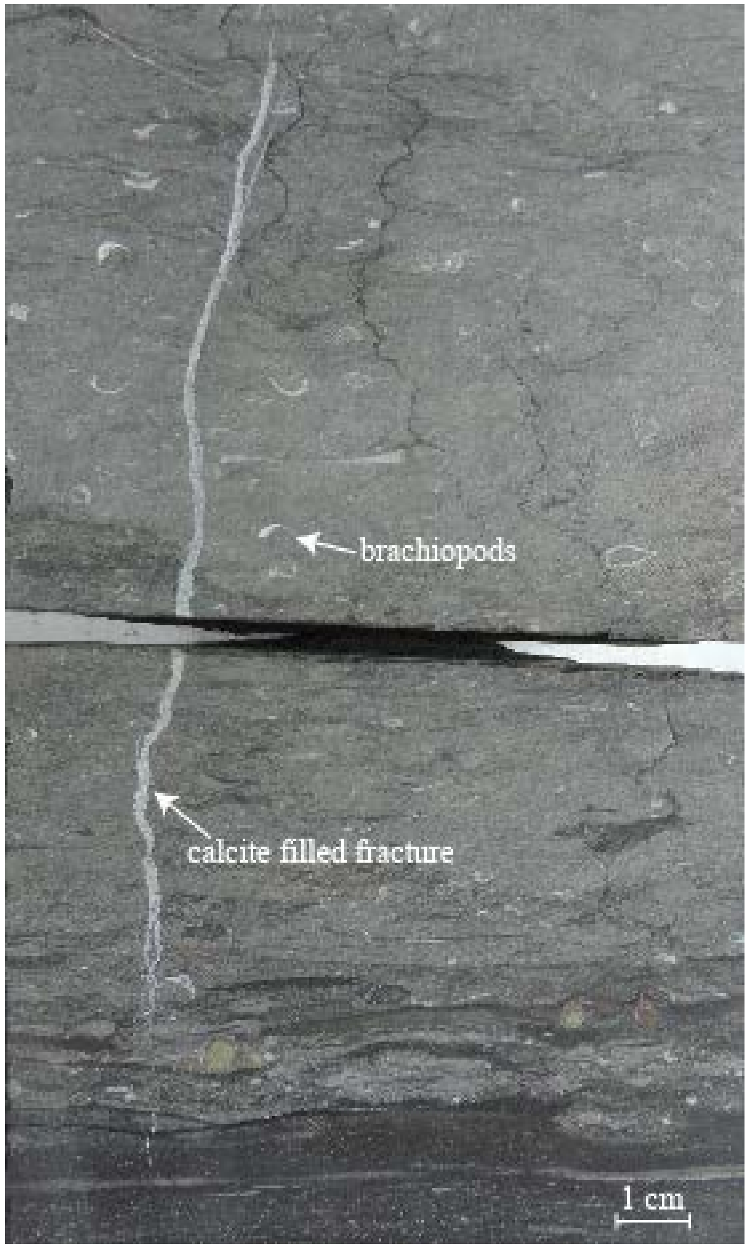

Figure 16. Representative photo of GSC from well COP 259 at 8289 ft. The white vertical feature is a calcite filled fracture.

Cryptalgal Boundstone (CB). CB is an encrusting red algal-carbonated boundstone (Figure 17). The CB has little to no bioturbation and effervescence intensity that ranges from 3-5. BS is interpreted to have been deposited in situ as an organically bound mound complex. Most of the CAB is concentrated within the transition between the Onondaga and Marcellus.

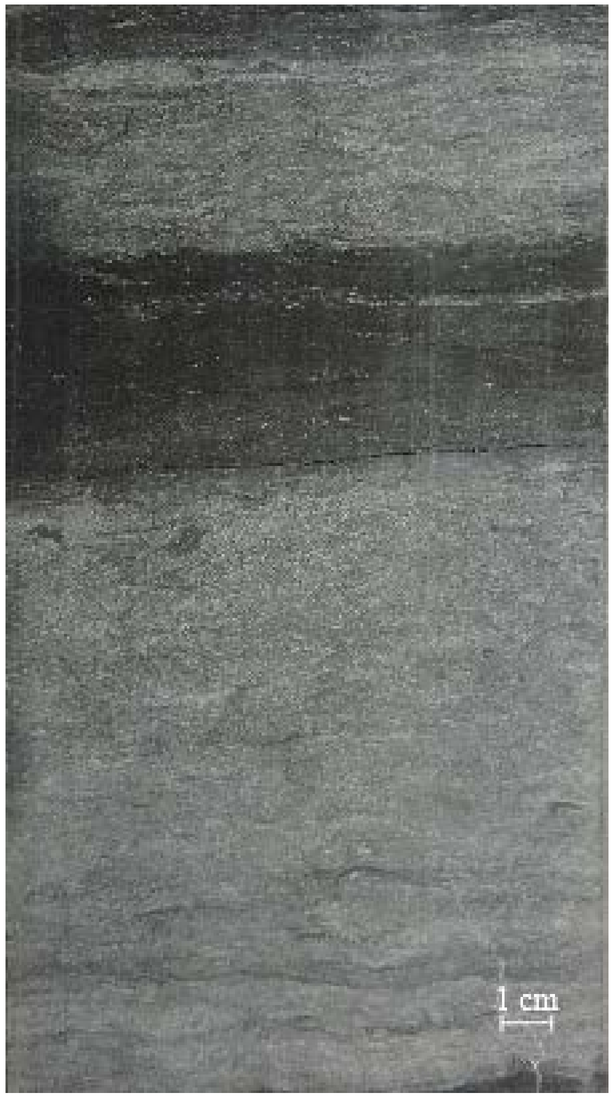

Figure 17. Representative photo of CAB from well COP 653 at 8548. The light gray portion of the rock is composed of encrusting red algae and is interbedded with organic rich black shale.

Chemofacies Description

Chemofacies are differentiated from each other by plotting geochemical data stratigraphically and then identifying stratigraphic intervals that have similar geochemical characteristic. Table 4 summarizes the attributes that distinguish chemofacies, and the chemofacies distribution in the three core are presented in Figures 18, 19, and 20. Geochemical data are summarized in appendix Thables A.1 through A.9. Several geochemical variables covary throughout the study interval. For example, stratigraphic packages with high TOC tend to have the most negative $\delta^{13}C$ values and high molybdenum, uranium, vanadium, nickel and copper concentrations (see correlation of geochemical variable with respect to organic matter abundance). The lowermost portion of the Marcellus has the highest concentration of organic matter, and concentrations decrease up section.

Table 4. Geochemical attributes of chemofacies

Chemofacies	Major attributes
A	High $CaCO_3$, positive $\delta^{13}C$
B	High TOC, negative $\delta^{13}C$, high SiO_2, high trace metal concentrations
C	Relatively higher Al_2O_3, decrease in SiO_2, high trace metal concentrations
D	High C/N ratios, high $CaCO_3$, variable enrichment factors, positive $\delta^{13}C$
E	Non-variable values in enrichment factors, high TOC, more negative $\delta^{13}C$
F	Positive $\delta^{13}C$ ratios, low enrichment factors, low productivity indicators
G	Variable but high Mo enrichment factors, negative $\delta^{13}C$
H	Low TOC, low enrichment factors, low productivity indictors, calcite abundance
I	Higher TOC, higher Mo enrichment factors
J	Low TOC, low trace metal enrichment factors

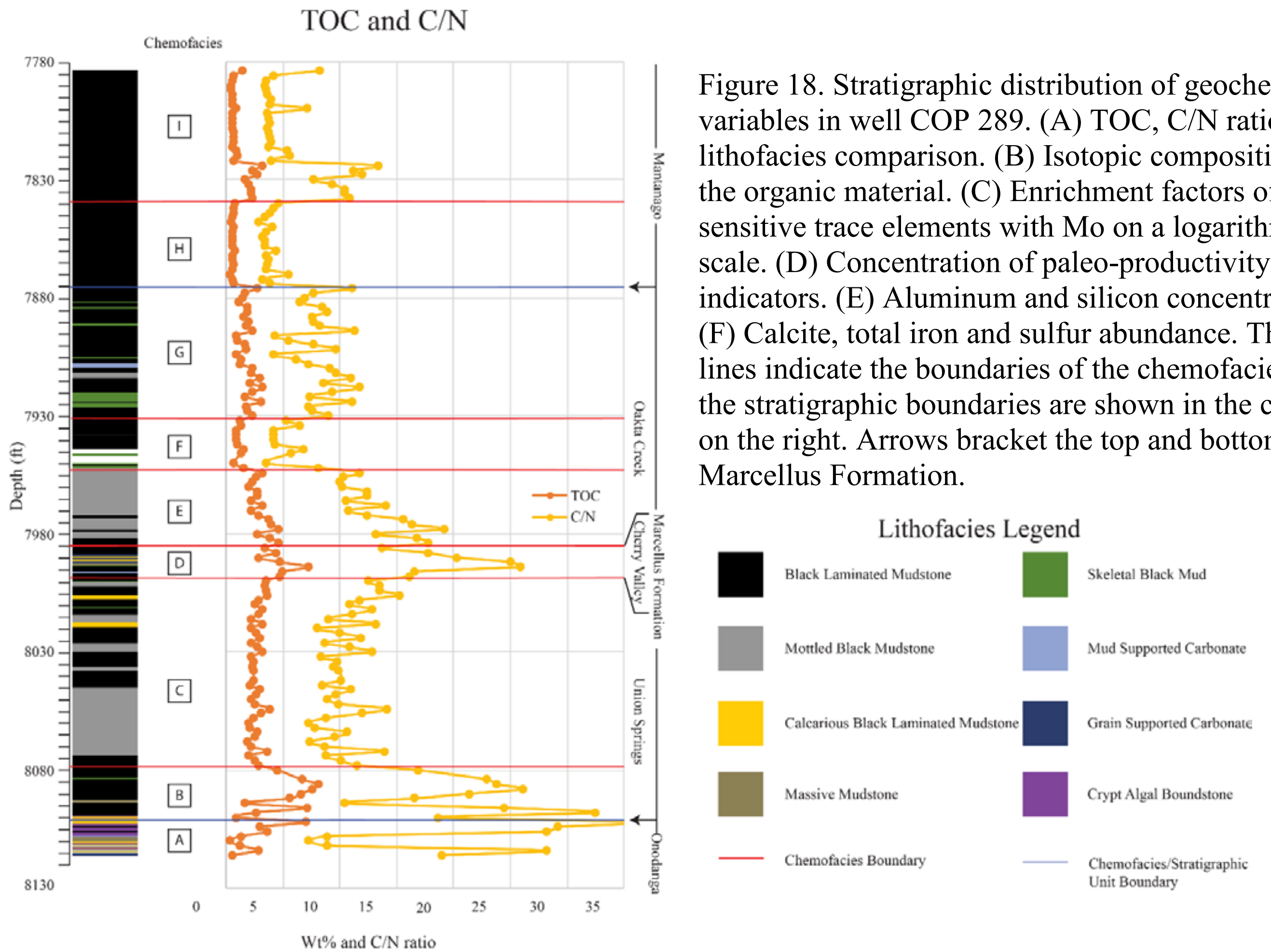

Figure 18 (A)

Figure 18. Stratigraphic distribution of geochemical variables in well COP 289. (A) TOC, C/N ratios, and lithofacies comparison. (B) Isotopic composition of the organic material. (C) Enrichment factors of redox-sensitive trace elements with Mo on a logarithmic scale. (D) Concentration of paleo-productivity indicators. (E) Aluminum and silicon concentrations. (F) Calcite, total iron and sulfur abundance. The red lines indicate the boundaries of the chemofacies and the stratigraphic boundaries are shown in the column on the right. Arrows bracket the top and bottom of the Marcellus Formation.

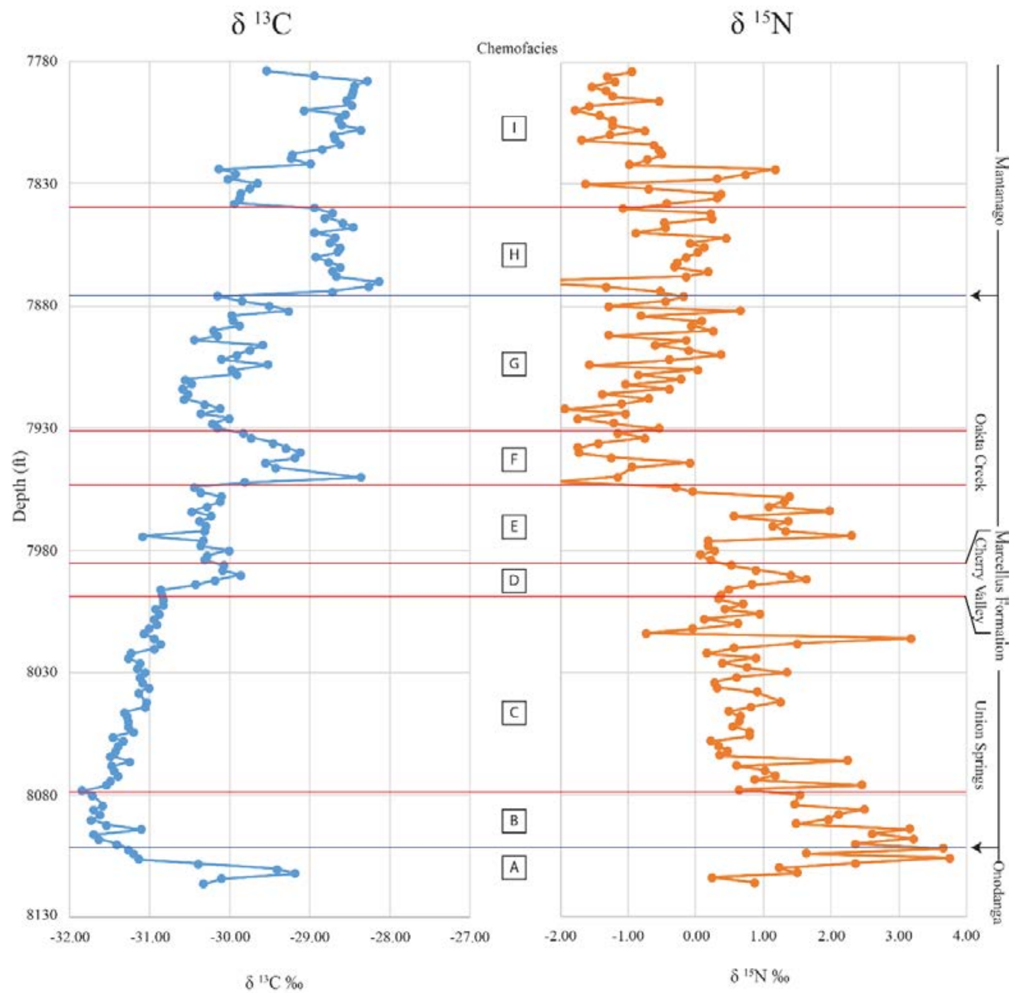

δ 13C
δ 15N
Chemofacies
Depth (ft)
I
H
G
F
E
D
C
B
A
Mantanago
Oakta Creek
Marcellus Formation
Cherry Valley
Union Springs
Onondaga
δ 13C ‰
δ 15N ‰

Figure 18 (B)

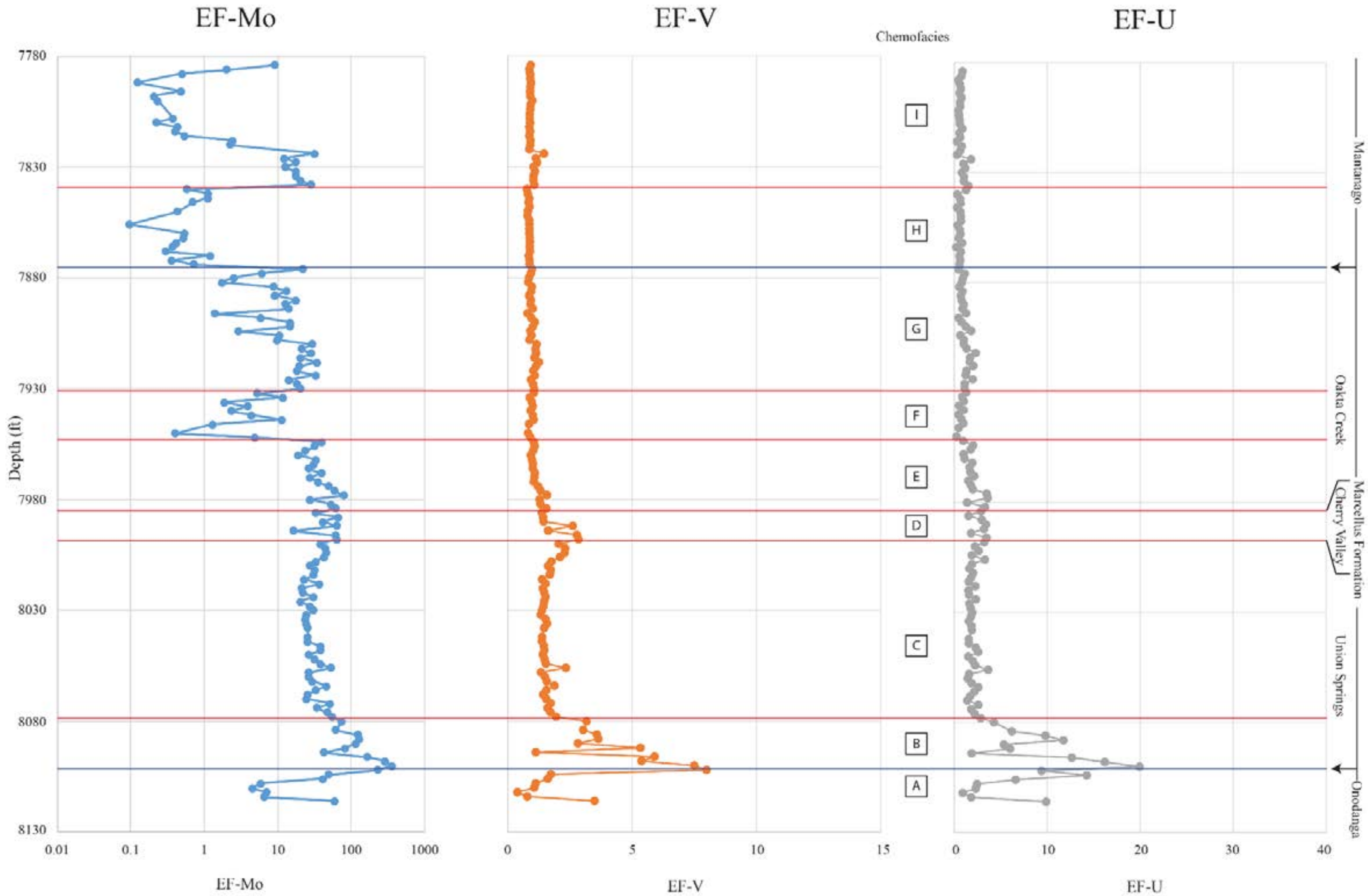

EF-Mo
EF-V
Chemofacies
EF-U
Depth (ft)
7780
7830
7880
7930
7980
8030
8080
8130
0.01
0.1
1
10
100
1000
EF-Mo
0
5
10
15
EF-V
0
10
20
30
40
EF-U
I
H
G
F
E
D
C
B
A
Mantanago
Oakta Creek
Marcellus Formation
Cherry Valley
Union Springs
Onodanga

Figure 18 (C)

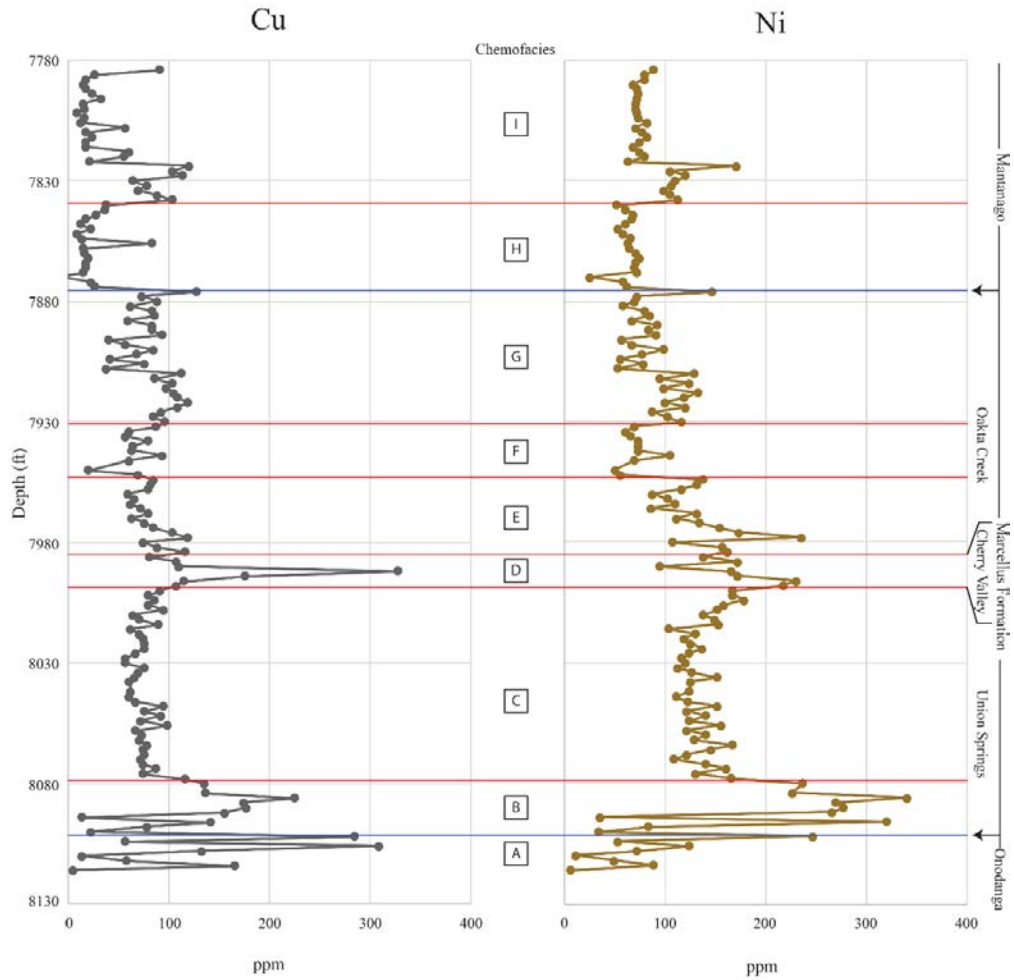
Cu
Ni
Chemofacies
Depth (ft)
7780
7830
7880
7930
7980
8030
8080
8130
0
100
200
300
400
ppm
I
H
G
F
E
D
C
B
A
Mantanago
Oakta Creek
Marcellus Formation
Cherry Valley
Union Springs
Onodanga

Figure 18 (D)

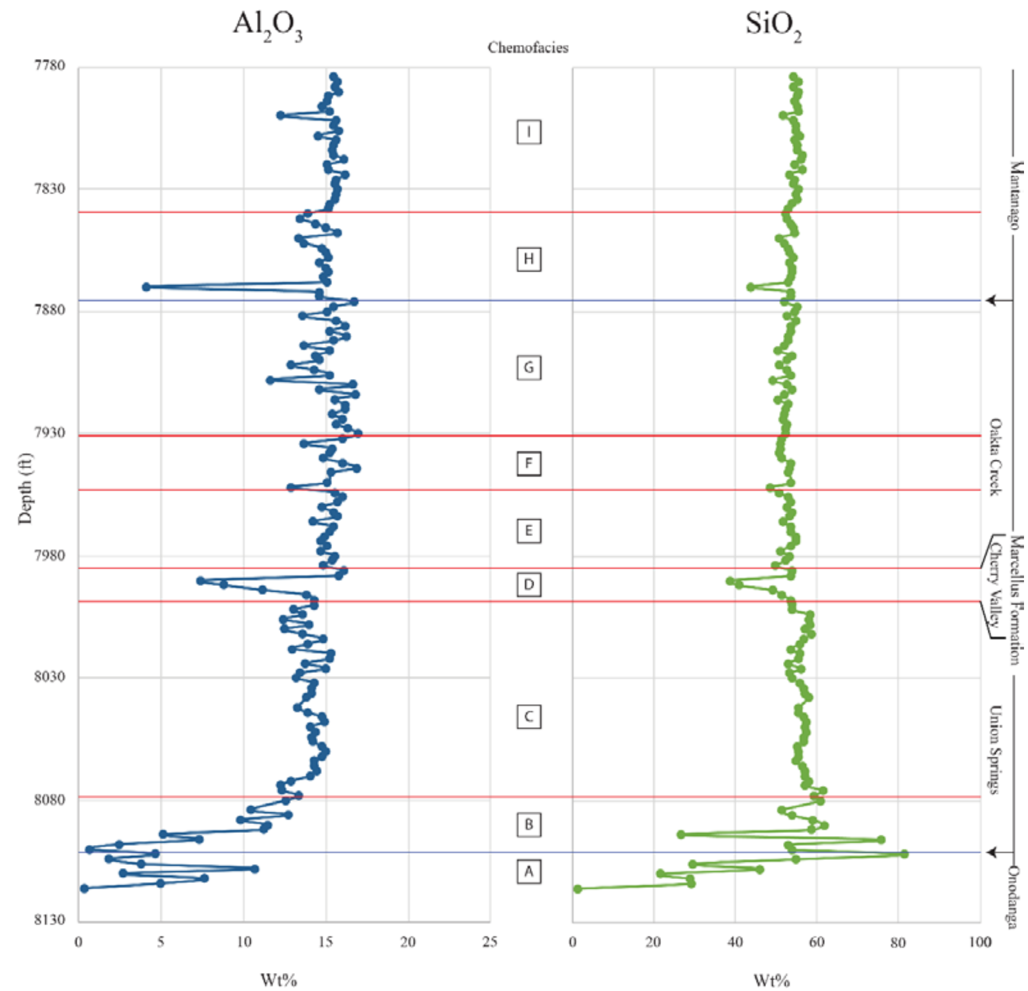

Al_2O_3
Chemofacies
SiO_2
7780
7830
7880
7930
7980
8030
8080
8130
Depth (ft)
I
H
G
F
E
D
C
B
A
0
5
10
15
20
25
Wt%
0
20
40
60
80
100
Wt%
Mantanago
Oakta Creek
Marcellus Formation
Cherry Valley
Union Springs
Onodanga

Figure 18 (E)

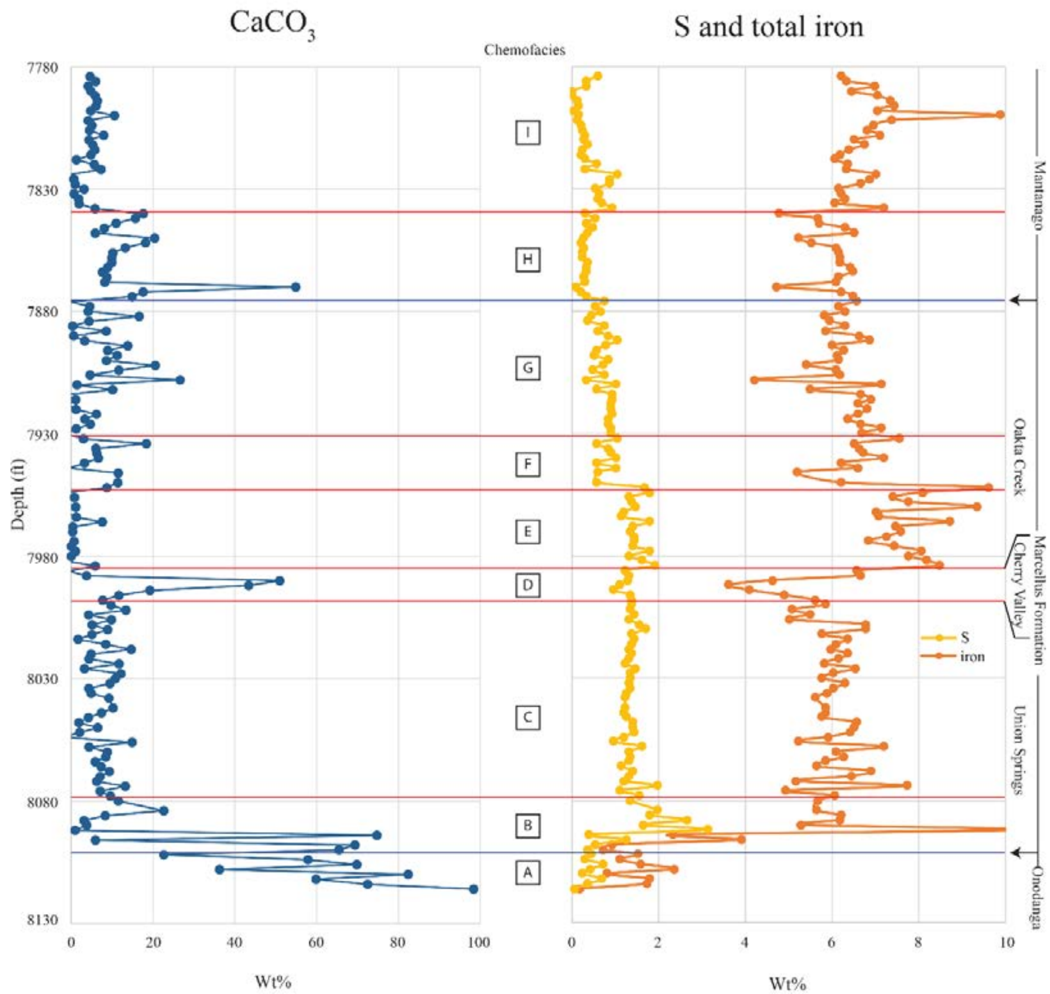

CaCO3
Chemofacies
S and total iron
Depth (ft)
7780
7830
7880
7930
7980
8030
8080
8130
0
20
40
60
80
100
Wt%
0
2
4
6
8
10
Wt%
I
H
G
F
E
D
C
B
A
S
iron
Mantanago
Oakta Creek
Marcellus Formation
Cherry Valley
Union Springs
Onodanga

Figure 18 (F)

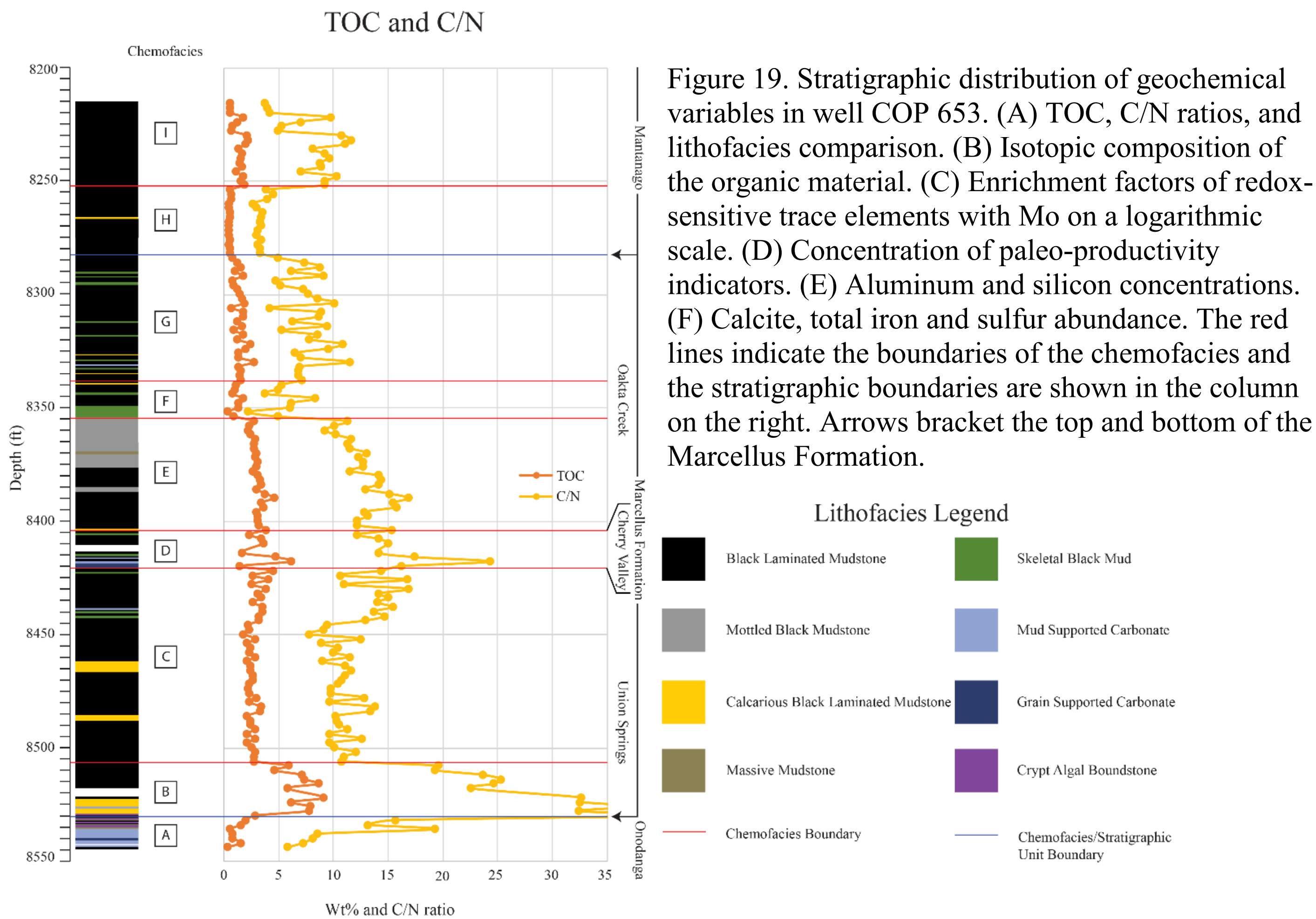

Figure 19. Stratigraphic distribution of geochemical variables in well COP 653. (A) TOC, C/N ratios, and lithofacies comparison. (B) Isotopic composition of the organic material. (C) Enrichment factors of redox-sensitive trace elements with Mo on a logarithmic scale. (D) Concentration of paleo-productivity indicators. (E) Aluminum and silicon concentrations. (F) Calcite, total iron and sulfur abundance. The red lines indicate the boundaries of the chemofacies and the stratigraphic boundaries are shown in the column on the right. Arrows bracket the top and bottom of the Marcellus Formation.

Figure 19 (A)

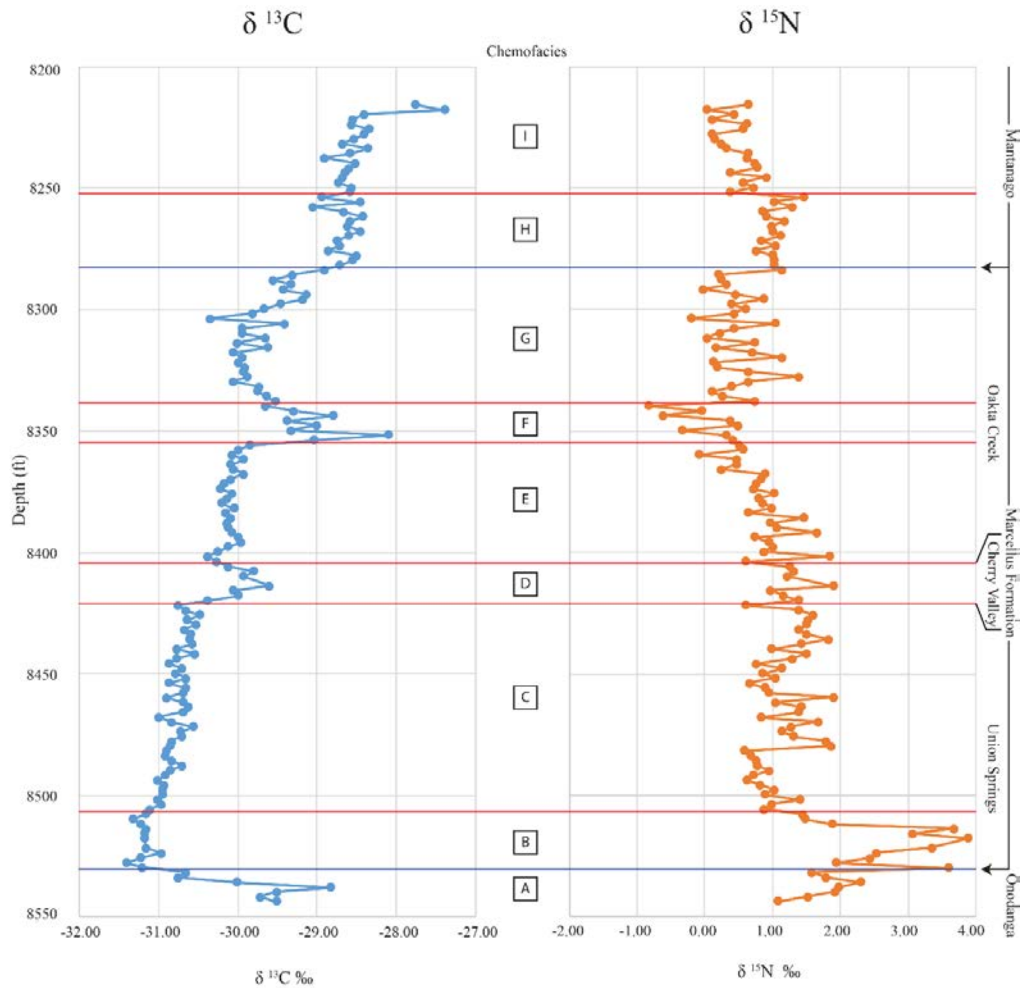

δ 13C
Chemofacies
δ 15N
Depth (ft)
8200
8250
8300
8350
8400
8450
8500
8550
-32.00
-31.00
-30.00
-29.00
-28.00
-27.00
δ 13C ‰
-2.00
-1.00
0.00
1.00
2.00
3.00
4.00
δ 15N ‰
I
H
G
F
E
D
C
B
A
Marcellus Formation
Mantango
Oakta Creek
Cherry Valley
Union Springs
Onodanga

Figure 19 (B)

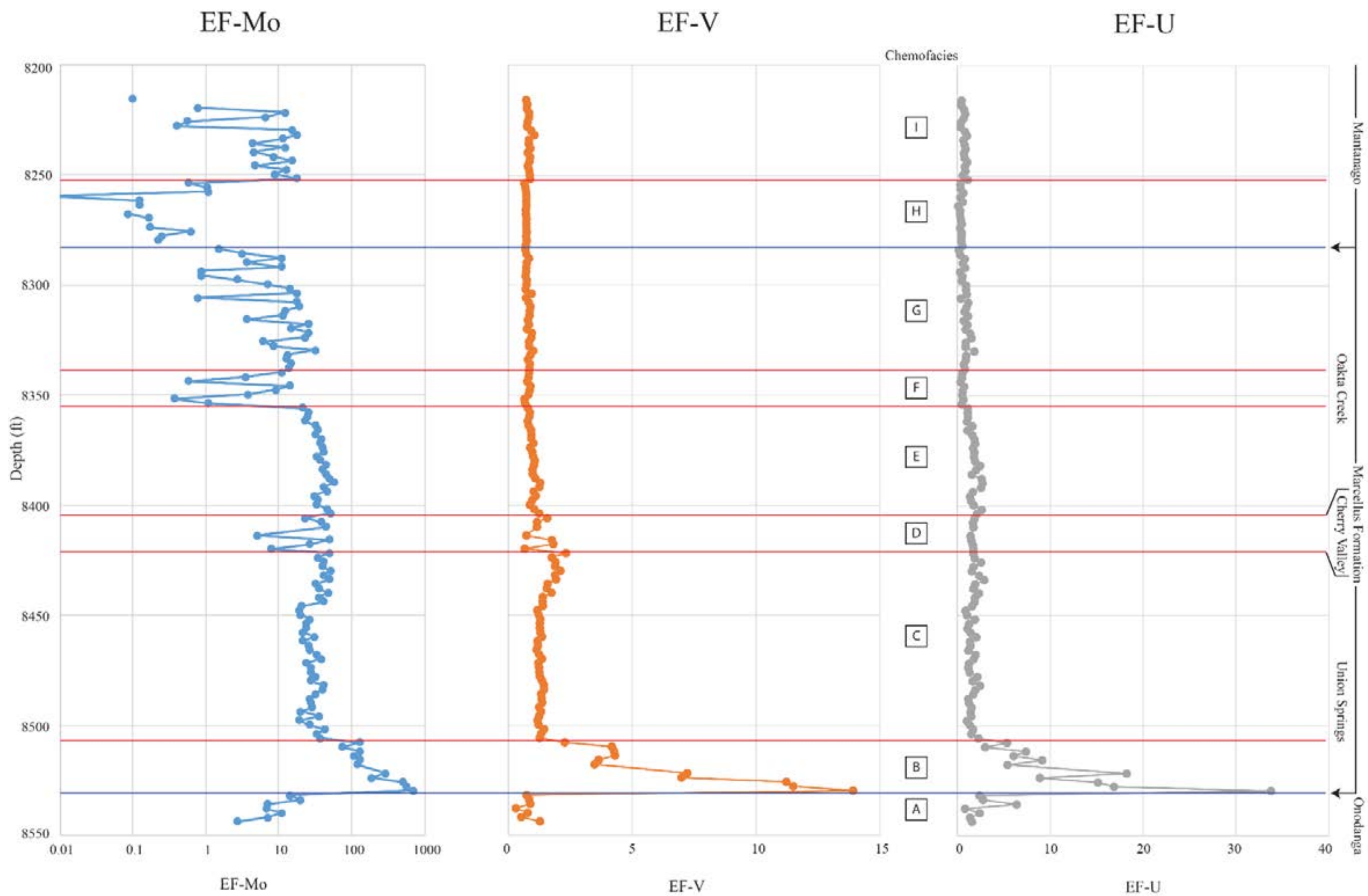
EF-Mo
EF-V
EF-U
Chemofacies
Depth (ft)
8200
8250
8300
8350
8400
8450
8500
8550
0.01
0.1
1
10
100
1000
EF-Mo
0
5
10
15
EF-V
0
10
20
30
40
EF-U
I
H
G
F
E
D
C
B
A
Mantango
Oakta Creek
Marcellus Formation
Cherry Valley
Union Springs
Onondaga

Figure 19 (C)

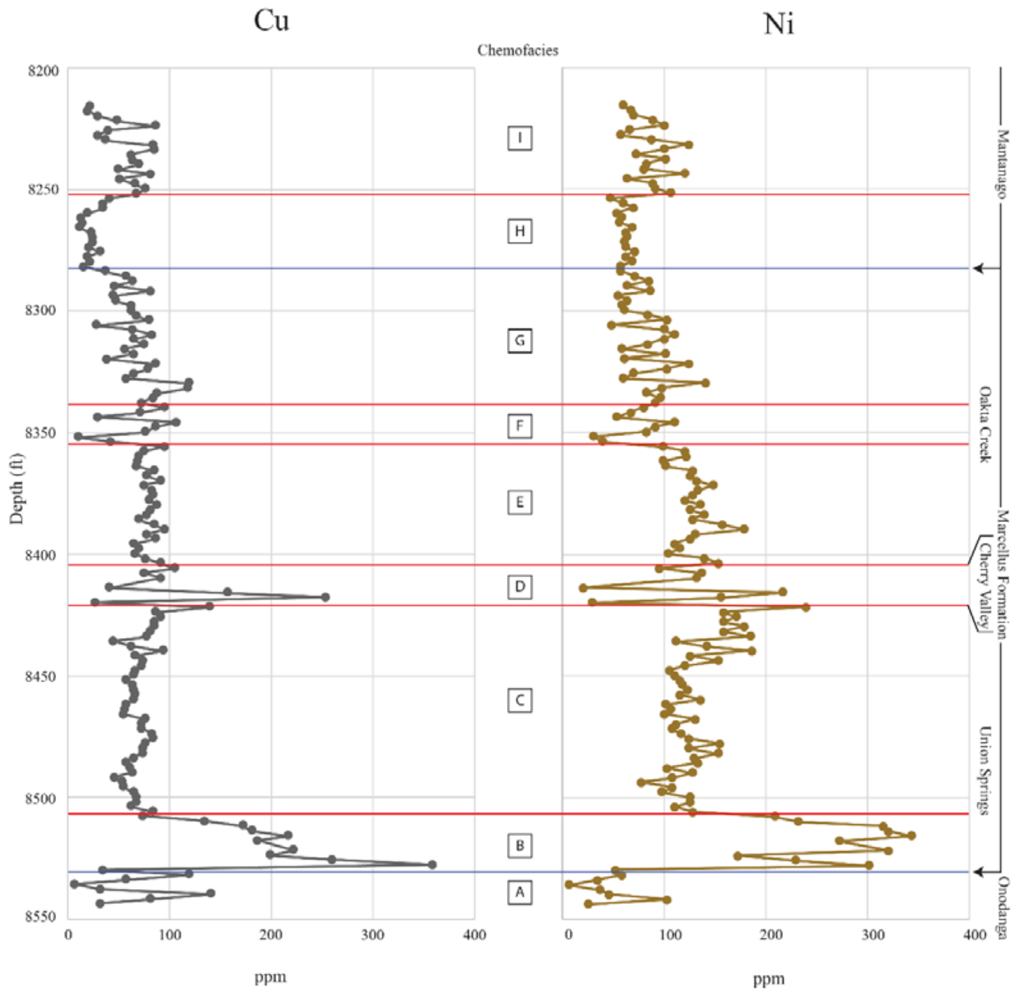

Cu
Ni
Chemofacies
8200
8250
8300
8350
8400
8450
8500
8550
Depth (ft)
I
H
G
F
E
D
C
B
A
0
100
200
300
400
ppm
Mantanago
Oakta Creek
Marcellus Formation
Cherry Valley
Union Springs
Onodanga

Figure 19 (D)

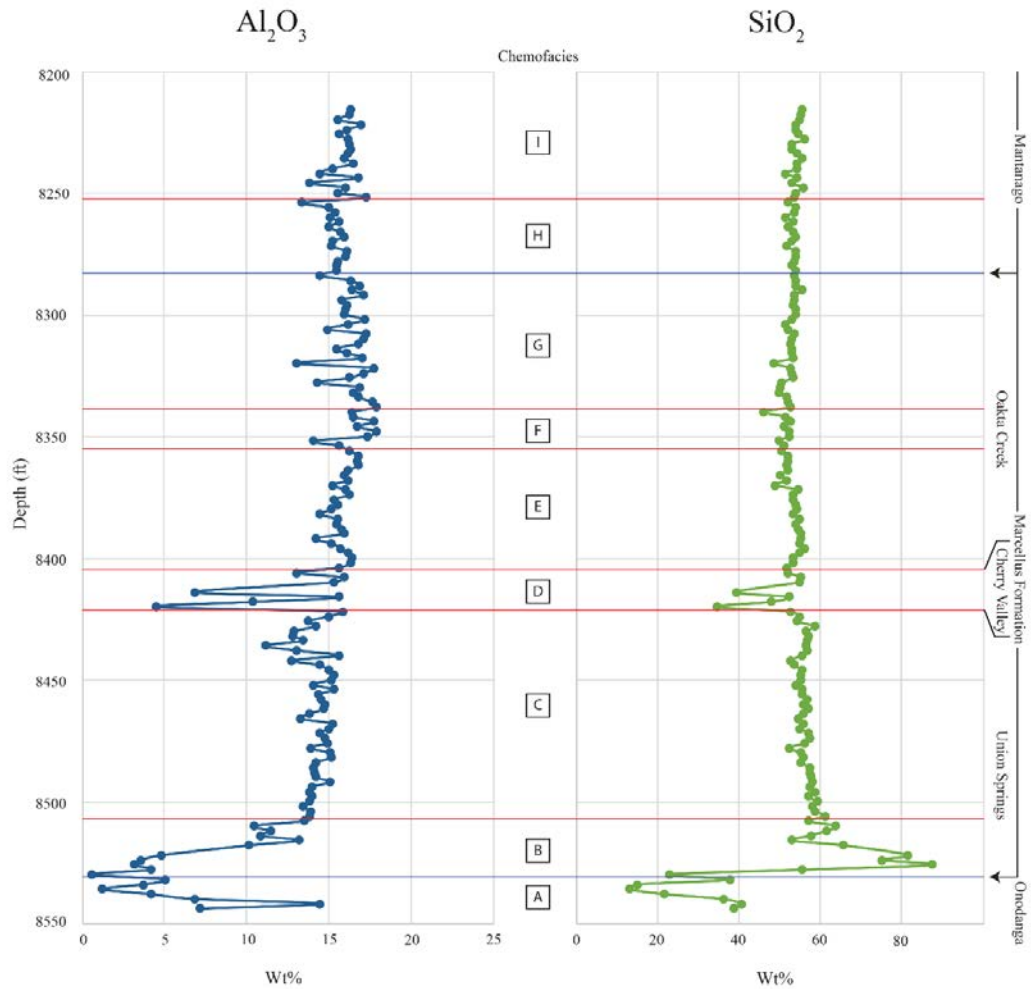
Al$_2$O$_3$
SiO$_2$
Chemofacies
Depth (ft)
8200
8250
8300
8350
8400
8450
8500
8550
I
H
G
F
E
D
C
B
A
0
5
10
15
20
25
Wt%
0
20
40
60
80
Wt%
Mantanago
Oakta Creek
Marcellus Formation
Cherry Valley
Union Springs
Oncdanga

Figure 19 (E)

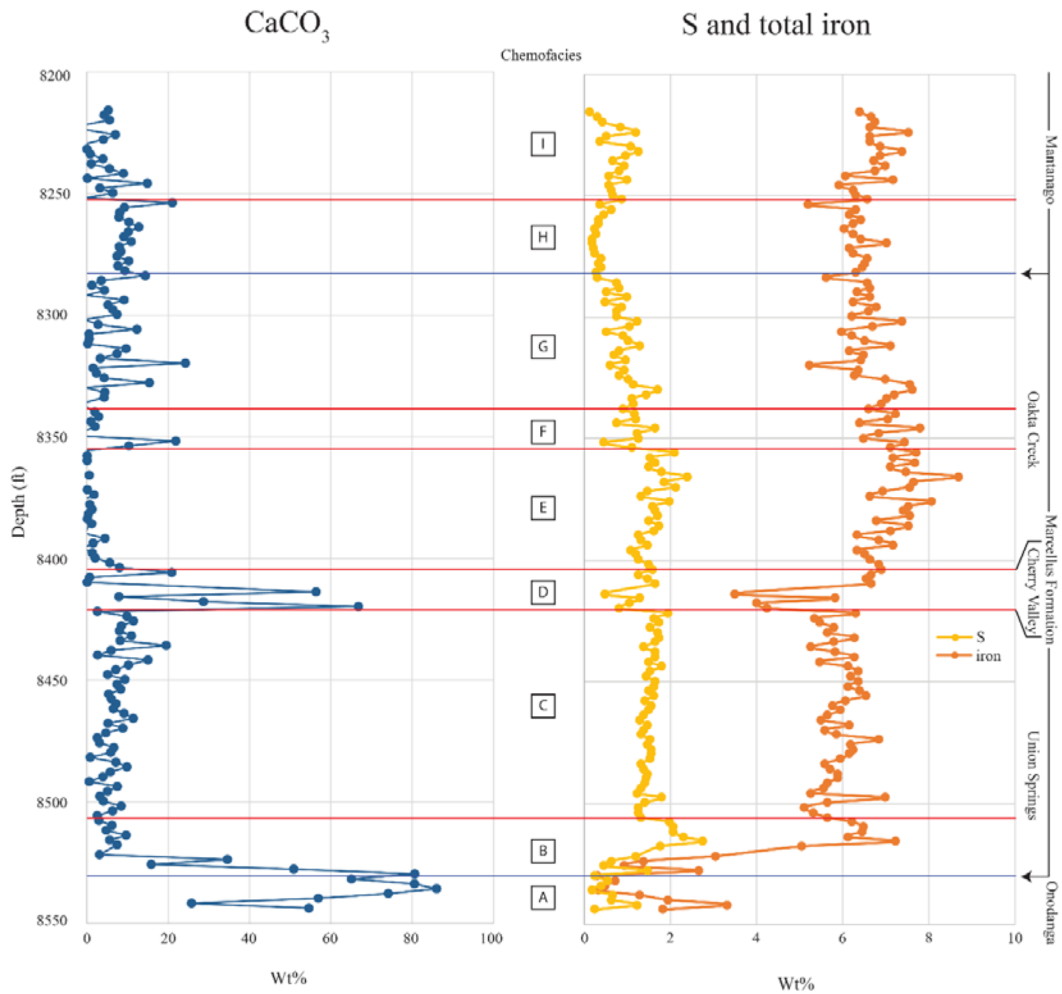
CaCO3
S and total iron
Chemofacies
Depth (ft)
8200
8250
8300
8350
8400
8450
8500
8550
0
20
40
60
80
100
Wt%
I
H
G
F
E
D
C
B
A
0
2
4
6
8
10
Wt%
S
iron
Mariatango
Oakta Creek
Marcellus Formation
Cherry Valley
Union Springs
Onondaga

Figure 19 (F)

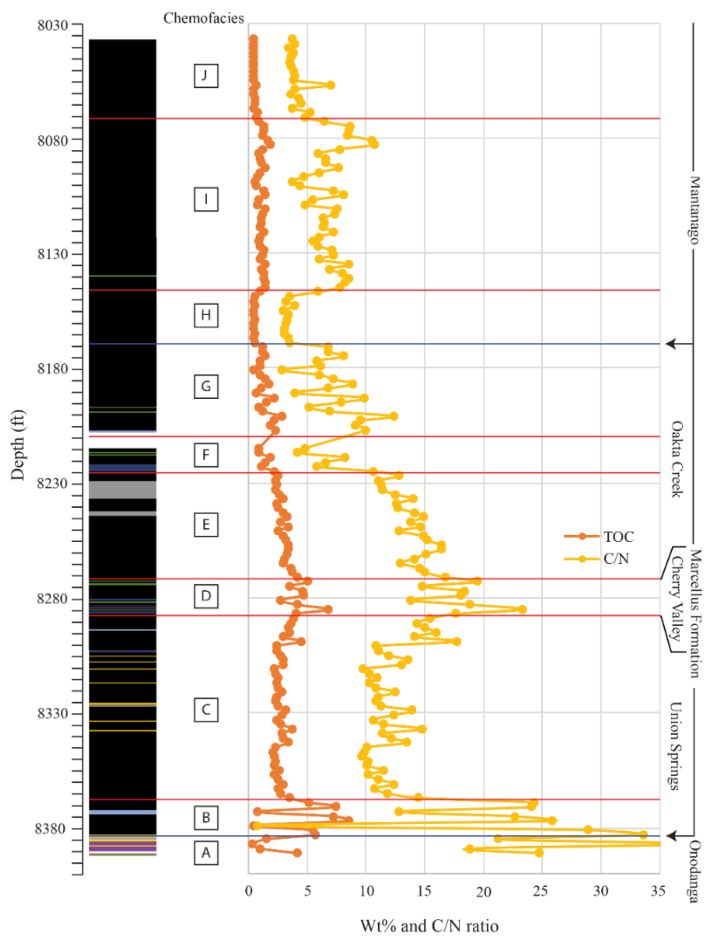

Figure 20. Stratigraphic distribution of geochemical variables in well COP 259. (A) TOC, C/N ratios, and lithofacies comparison. (B) Isotopic composition of the organic material. (C) Enrichment factors of redox-sensitive trace elements with Mo on a logarithmic scale. (D) Concentration of paleo-productivity indicators. (E) Aluminum and silicon concentrations. (F) Calcite, total iron and sulfur abundance. The red lines indicate the boundaries of the chemofacies and the stratigraphic boundaries are shown in the column on the right. Arrows bracket the top and bottom of the Marcellus Formation.

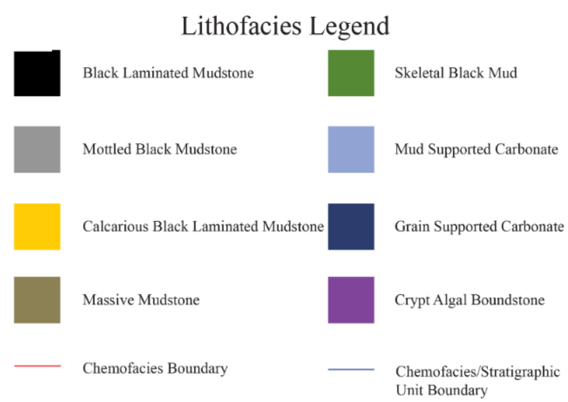

Figure 20 (A)

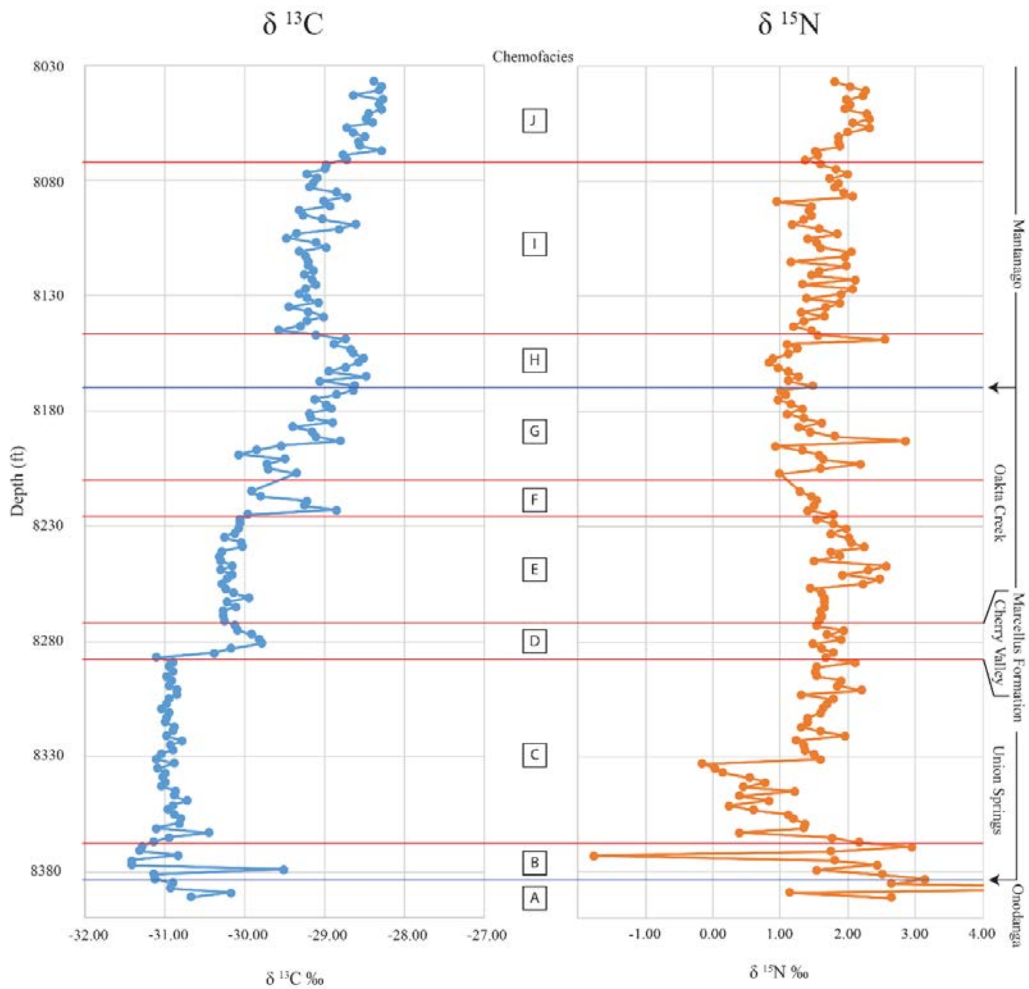
δ 13C
δ 15N
Chemofacies
Depth (ft)
8030
8080
8130
8180
8230
8280
8330
8380
J
I
H
G
F
E
D
C
B
A
-32.00
-31.00
-30.00
-29.00
-28.00
-27.00
δ 13C ‰
-1.00
0.00
1.00
2.00
3.00
4.00
δ 15N ‰
Mantango
Oakta Creek
Marcellus Formation
Cherry Valley
Union Springs
Onodanga

Figure 20 (B)

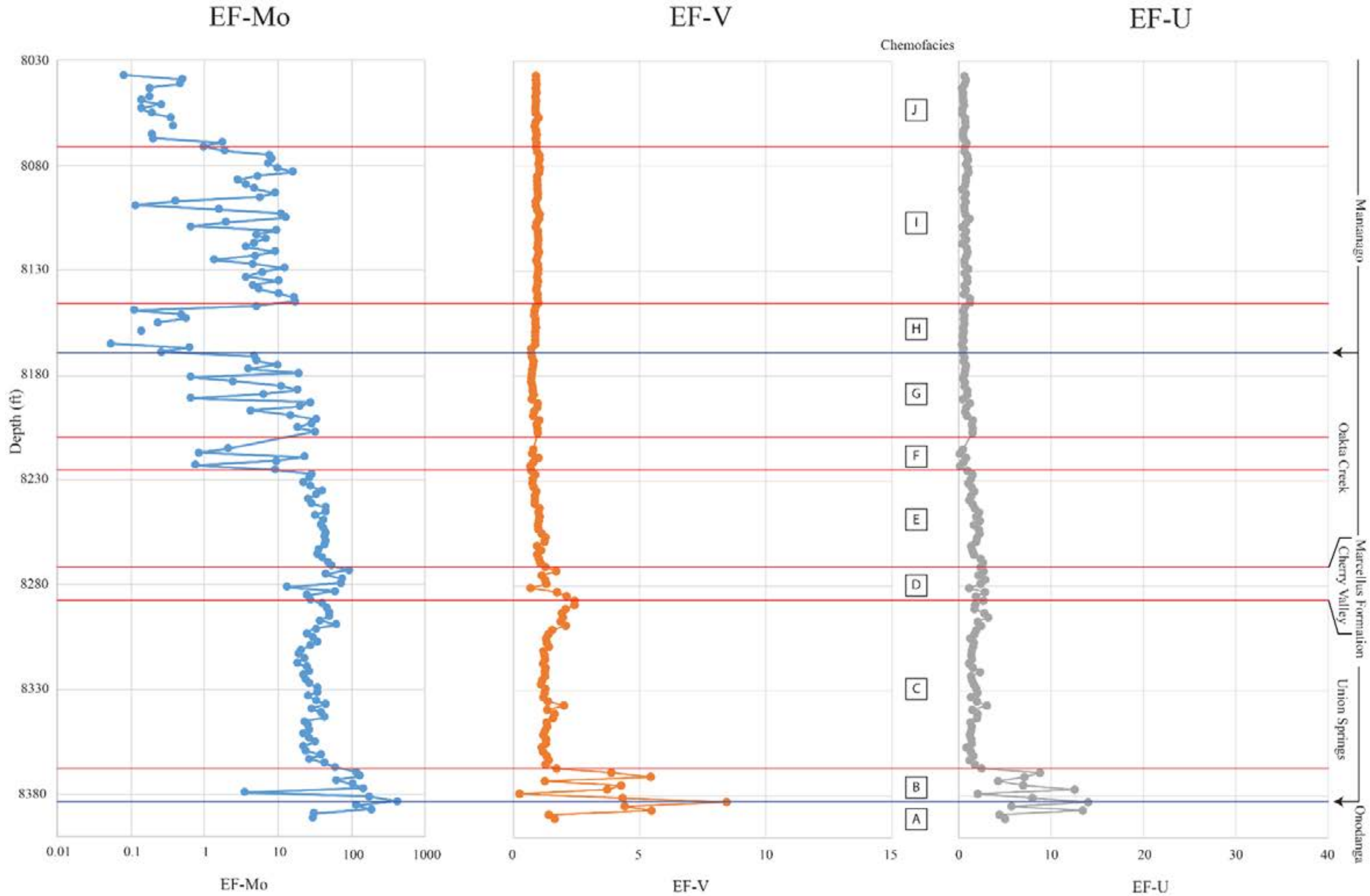

EF-Mo
EF-V
EF-U
Chemofacies
Depth (ft)
8030
8080
8130
8180
8230
8280
8330
8380
0.01
0.1
1
10
100
1000
EF-Mo
0
5
10
15
EF-V
0
10
20
30
40
EF-U
J
I
H
G
F
E
D
C
B
A
Mantanago
Oakta Creek
Marcellus Formation
Cherry Valley
Union Springs
Onodanga

Figure 20 (C)

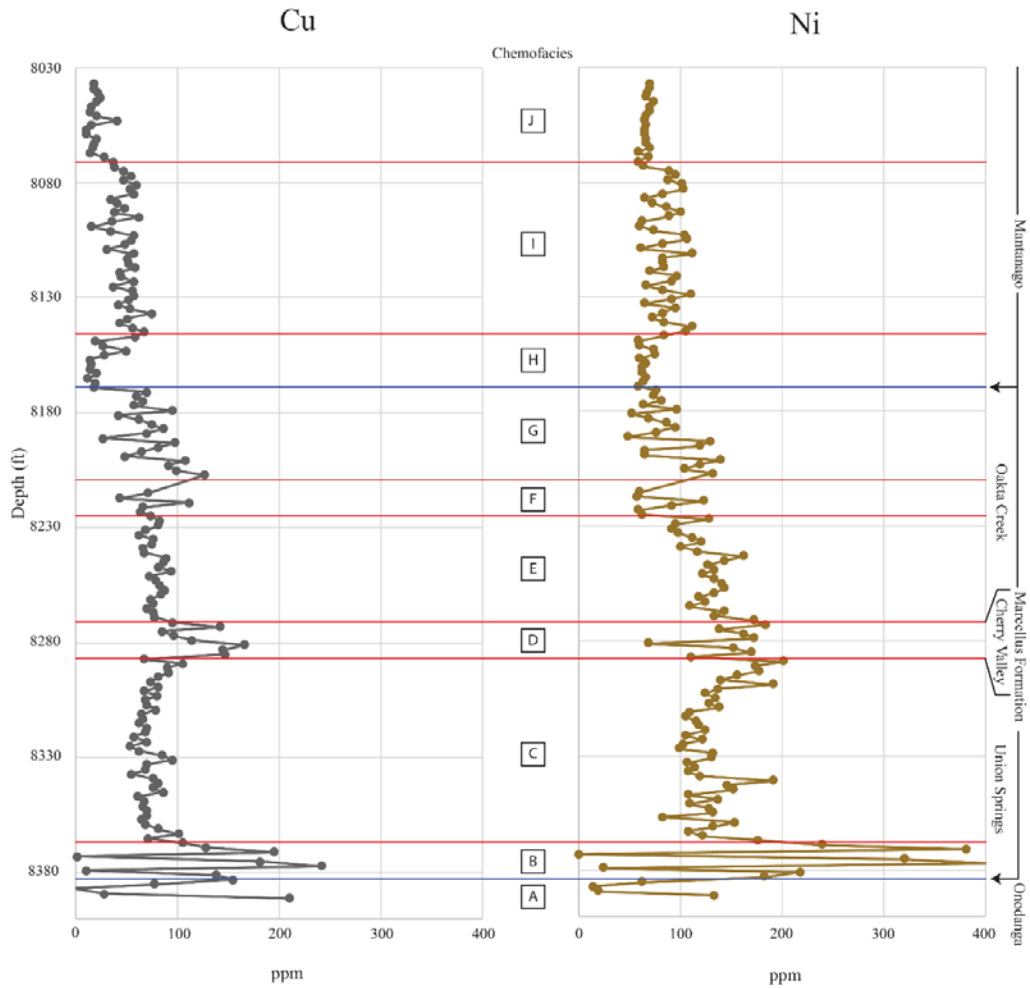
Cu
Ni
Chemofacies
Depth (ft)
8030
8080
8130
8180
8230
8280
8330
8380
0
100
200
300
400
ppm
J
I
H
G
F
E
D
C
B
A
Mantango
Oakta Creek
Marcellus Formation
Cherry Valley
Union Springs
Onondaga

Figure 20 (D)

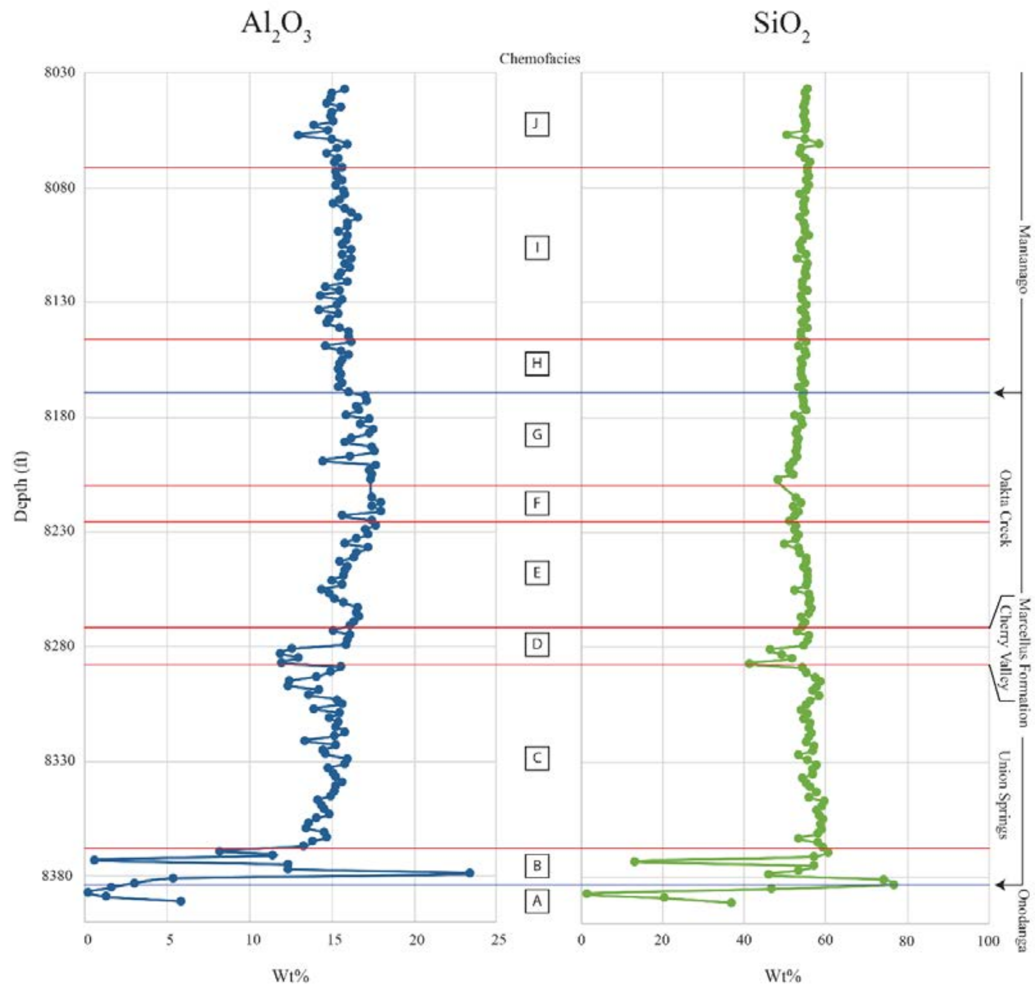

Al$_2$O$_3$
SiO$_2$
Chemofacies
Depth (ft)
8030
8080
8130
8180
8230
8280
8330
8380
J
I
H
G
F
E
D
C
B
A
0
5
10
15
20
25
0
20
40
60
80
100
Wt%
Wt%
Mantanago
Oakta Creek
Marcellus Formation
Cherry Valley
Union Springs
Onondaga

Figure 20 (E)

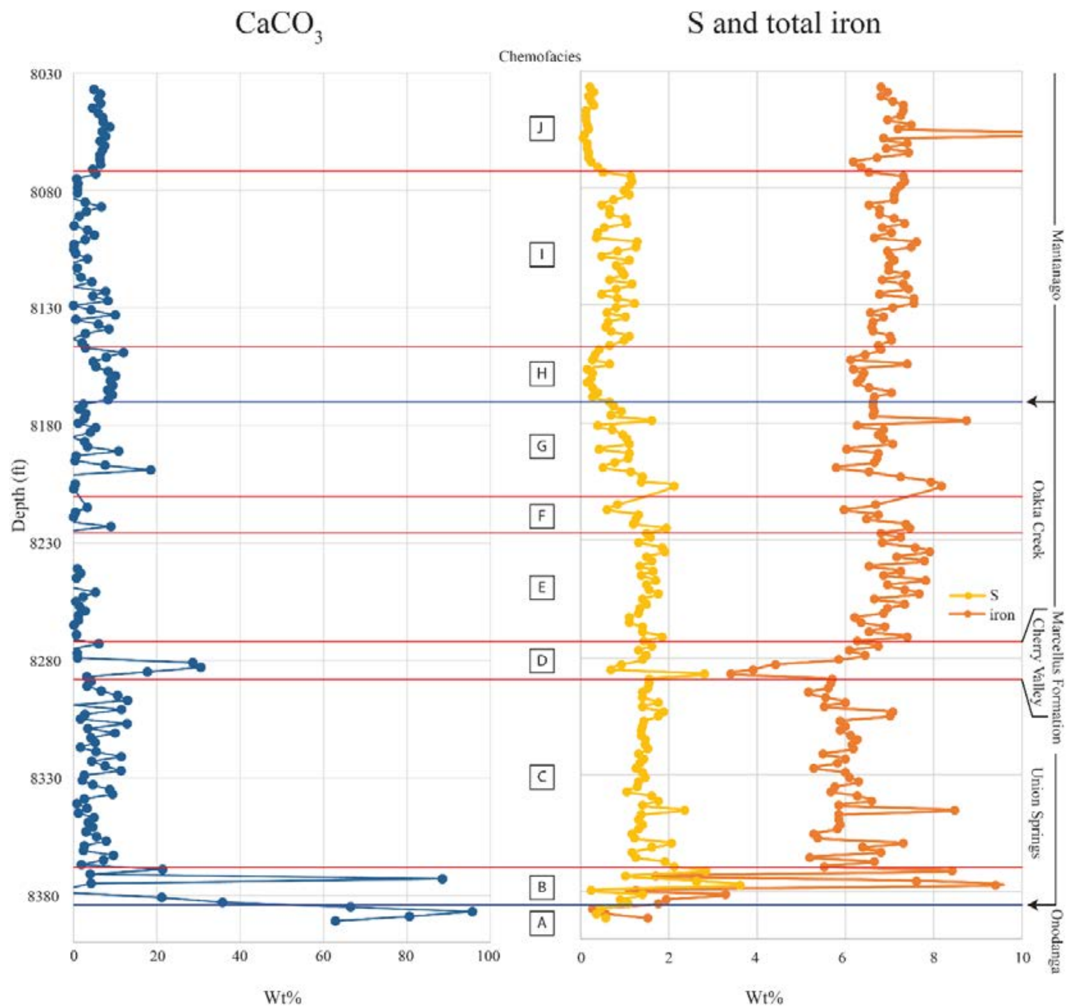

CaCO3
S and total iron
Chemofacies
Depth (ft)
8030
8080
8130
8180
8230
8280
8330
8380
J
I
H
G
F
E
D
C
B
A
0
20
40
60
80
100
Wt%
0
2
4
6
8
10
Wt%
S
iron
Mantanago
Oakta Creek
Marcellus Formation
Cherry Valley
Union Springs
Onondaga

Figure 20 (F)

Description of Chemofacies

Chemofacies A. Rocks in the base of all three wells correspond with the Onondoaga Limestone and have a distinctive chemistry characterized by low TOC associated with lower C/N ratios and more positive $\delta^{13}C$ values. Enrichment factors for trace metals in this facies are also relatively low (below 10 for Mo and U and below 1 for V). This stratigraphic interval tends to have a high concentration of inorganic carbon and relatively lower concentrations of Si and Al. The sulfur and iron concentration are also relatively low as are the Ni and Cu concentrations. The mineral assemblage of this chemofacies is dominated by calcite with lesser amounts of dolomite, quartz, pyrite, and illite (Figure 21). Wells COP 289 and COP 259 both appear to have transitional contacts between Chemofacies A and B. The transitional contact has rapidly changing TOC concentrations and spans 10-20 ft (Figures 18A and 20A).

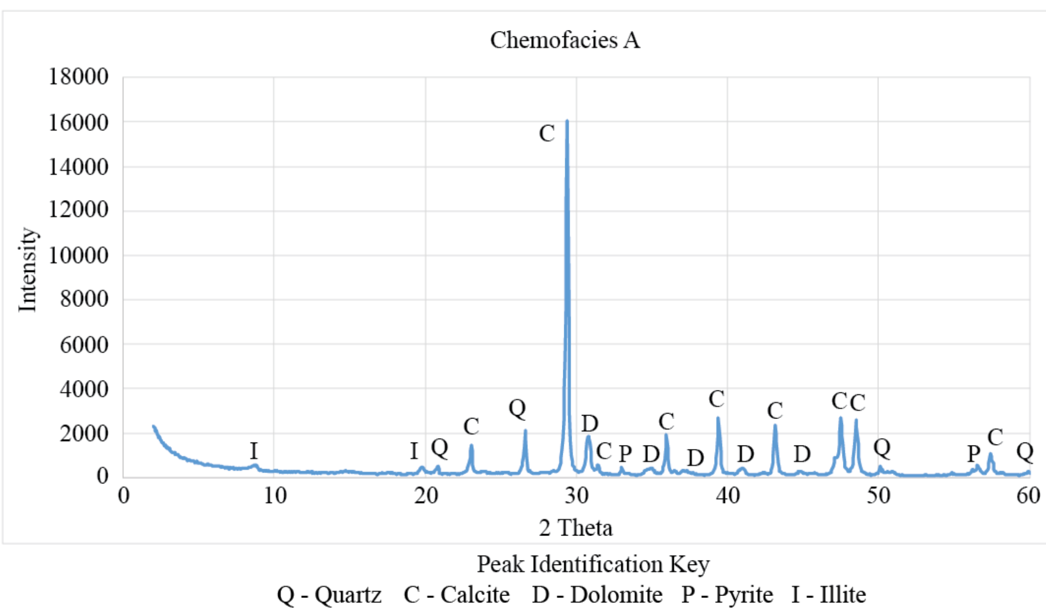

Figure 21. XRD random powder mount diffractogram of Chemofacies A from well COP 653 at 8544 ft. The most abundant mineral in this sample is calcite (C) with lesser amounts dolomite (D), quartz (Q), pyrite (P), and illite (I). The main calcite peak is very intense in this sample signifying a large proportion of calcite is present.

Chemofacies B. This stratigraphic interval generally has TOC values greater than 5 wt% and represents the most organic-rich chemofacies of the Marcellus. In wells 289 and 653 this TOC-rich interval is about 30 ft thick. The C/N ratios observed in this chemofacies tends to be greater than 20. There is an excursion of about -2‰ in $\delta^{13}C$ ratios at the bottom of this chemofacies that corresponds to an increase in TOC. The $\delta^{15}N$ values in this chemofacies are more positive particularly in wells COP 289 and COP 653. This chemofacies exhibits high enrichment factors for the redox sensitive trace metals (greater than 10 for U and V and greater than 100 for Mo). The Ni and Cu values are also very high in this interval. Chemofacies B also has elevated concentrations of S and total iron. This chemofacies has the greatest abundance of SiO_2, while Al_2O_3 and calcite abundance are low, compared to the other chemofacies. The dominant minerals found in this chemofacies are quartz with minor amounts of calcite, dolomite, pyrite, and illite (Figure 22).

Chemofacies C. This chemofacies ranges from 60 to 80 ft in thickness and is characterized by moderately high TOC (2-4 wt %), a trend of increasing aluminum and TOC content and enriched molybdenum. The C/N ratios are moderate from 8-15. The $\delta^{13}C$ values in well COP 289 is more negative near the base of this chemofacies and all three wells have delta values that are close to -31‰ at the top. $\delta^{15}N$ values exhibit large amplitude changes throughout but average at about 1‰. Redox-sensitive trace metals exhibit fairly consistent concentrations throughout Chemofacies C. This chemofacies has

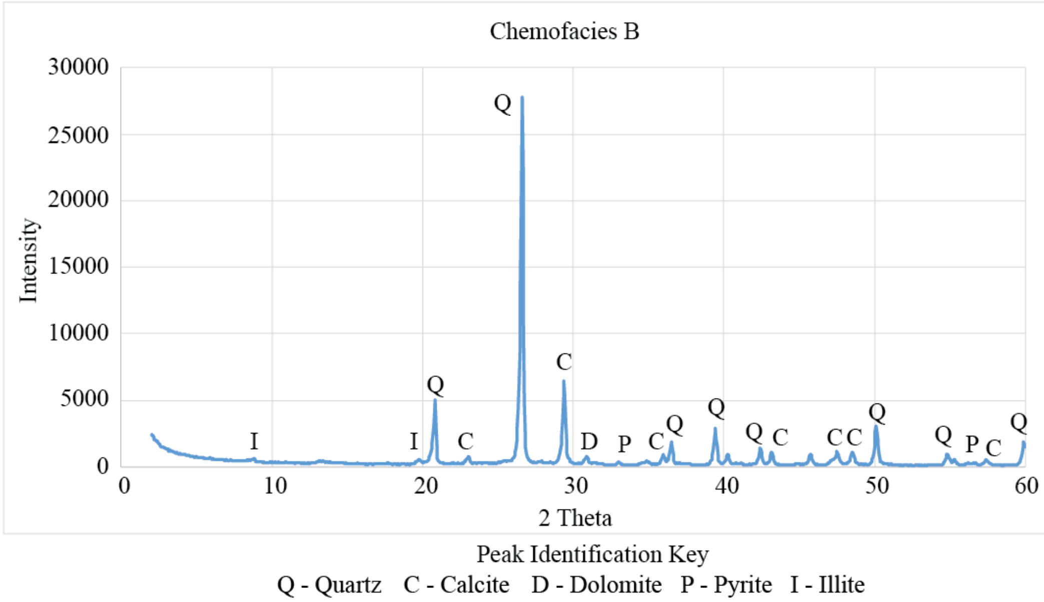

Figure 22. XRD random powder mount diffractogram of Chemofacies B from well COP 653 at 8532 ft. The major mineral in this sample is quartz (Q) with some calcite (C), dolomite (D), pyrite (P), and illite (I). The main quartz peak is very intense in this sample signifying a large proportion of quartz within this sample.

Mo enrichment factors that ranges between 20-50 while U and V are above 1 (enrichment factors range from 2-5). The sulfur concentration in this facies is relatively high from 1-2 wt. % whereas total iron content averages 6 wt. %. Al_2O_3 and SiO_2 concentrations are fairly uniform and average about 14 wt. % and 58 wt. %, respectively. The calcite abundance in this chemofacies is relatively low and ranges from about 0 to 15 wt. %. The Cu content is 80 ppm and the Ni increases near the top of the chemofacies from 120 to 180 ppm. The mineralogy of this chemofacies is dominated by quartz and illite with minor amounts of some smectite, kaolinite, calcite, dolomite, pyrite, and albite (Figure 23).

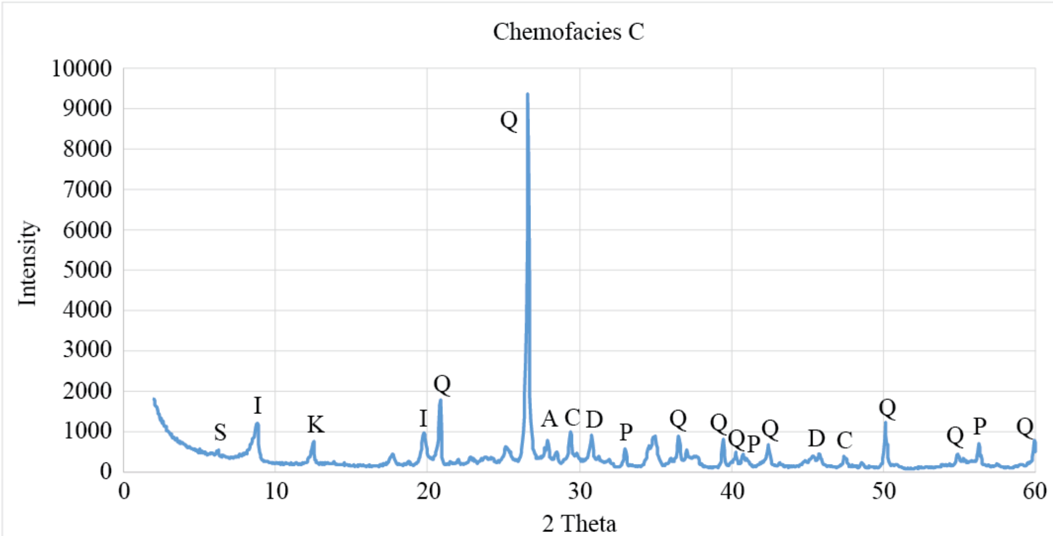

Figure 23. XRD random powder mount diffractogram of Chemofacies C from well COP 259 at 8340 ft. The major mineral in this chemofacies is quartz (Q) and illite (I). The lower intensity of the quartz shows that it is not as abundant as in Chemofacies B. The other minerals present are smectite (S), kaolinite (K), calcite (C), dolomite (D), Pyrite (P), and albite (A).

Chemofacies D. This chemofacies corresponds with the Cherry Valley Member of the Marcellus and is relatively thin with a thickness that ranges from 15 to 20 ft. This stratigraphic interval is characterized by high calcite abundance and low silica and aluminum concentrations. This chemofacies has a positive $\delta^{13}C$ excursion that can be correlated between all three wells. The TOC content is variable, and ranges from about 3 wt % to 7 wt %. The C/N ratios are mostly high with many of the samples being above 20. In wells COP 289 and COP 653 the $\delta^{15}N$ values have a positive excursion of 1‰ whereas well COP 259 remains near 1.8‰. The enrichment factors for the redox-sensitive trace elements are variable and many samples do not exhibit any enrichment. The total iron and S content of this facies tends to be lower than in Chemofacies C with the exception of well COP 259 where both elements slightly increase. The SiO_2 and

Al_2O_3 concentration are both much lower than in Chemofacies C. Calcite increases up to 70 wt %. Cu concentrations exhibit an increasing trend whereas Ni decreases. Minerals within this chemofacies include calcite, quartz, and illite with minor amounts of dolomite, smectite, kaolinite, pyrite, and albite (Figure 24).

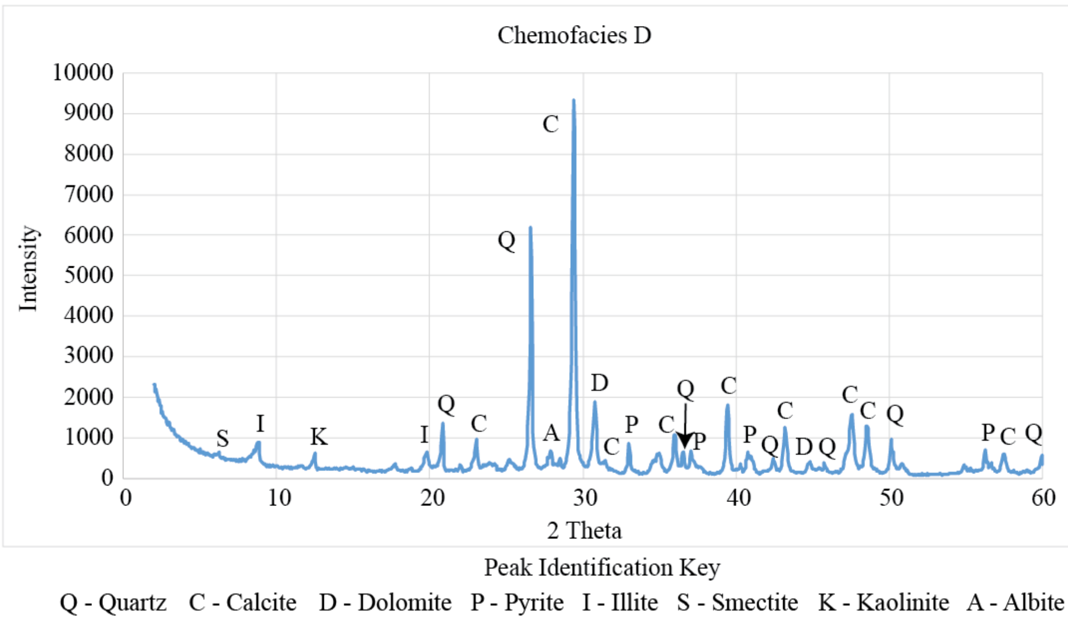

Figure 24. XRD random powder mount diffractogram of Chemofacies D from well COP 289 at 7992 ft. The major minerals in this sample are calcite (C), quartz (Q), and illite (I). The other minerals present are dolomite (D), smectite (S), kaolinite (K), pyrite (P), and albite (A).

Chemofacies E. Chemofacies E is from 30-50 ft thick and is characterized by decreasing C/N ratios (from 15 to 10), a low abundance of calcite, and enrichment in Mo. TOC decreases from 5 wt % at the base to 2.5 wt% at the top. The $\delta^{13}C$ values are more negative (about -30.0‰) than the values from Chemofacies D. Enrichment factors of the redox-sensitive trace metals slightly decreases within this facies. S and total iron are constant with S concentration at about 1.5 wt% and total iron from 6-8 wt %. The SiO_2 and Al_2O_3 values range from 53 to 55 wt% and 15 to 17 wt%, respectively. This chemofacies has very little calcite, and Cu and Ni concentrations are 80 ppm and 120 ppm, respectively. The mineral composition of this chemofacies is quartz and illite with minor amounts of smectite, kaolinite, pyrite, albite, and a small amount of calcite (Figure 25).

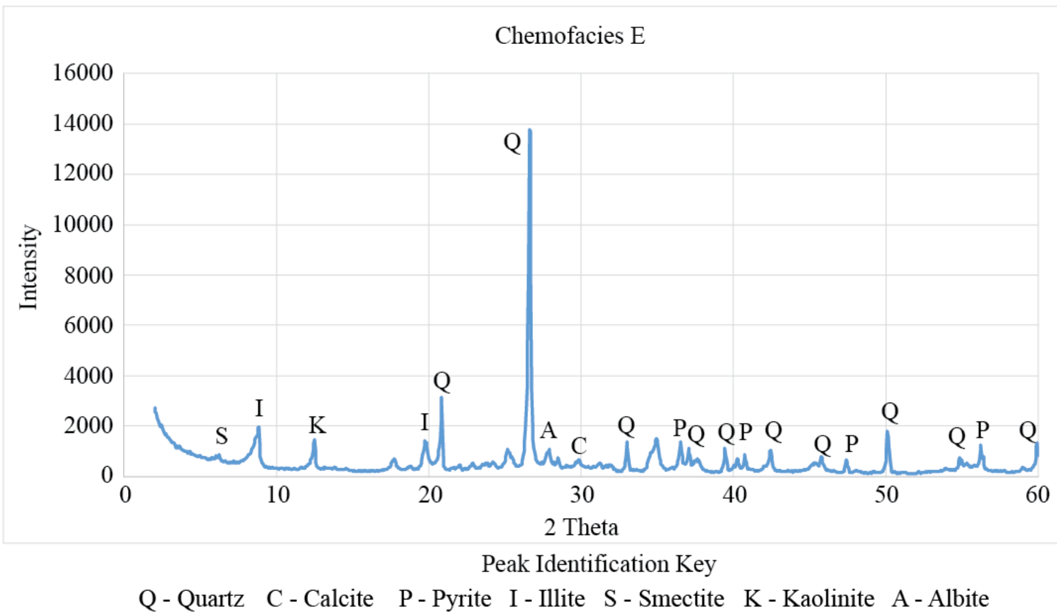

Figure 25. XRD random powder mount diffractogram of Chemofacies E from well COP 289 at 7972 ft. The major minerals of this chemofacies is quartz (Q) and illite (I). The other minerals present are smectite (S), kaolinite (K), pyrite (P), albite (A), and a small abundance of calcite (C).

Chemofacies F. Chemofacies F is from 10 to 20 ft thick and the top of the chemofacies correlates with the top of the Marcellus Formation. This chemofacies is characterized by a positive $\delta\ ^{13}C$ excursion, relatively low TOC (from 1-2 wt.%), and low enrichment factors from the redox-sensitive trace elements. The C/N ratios are also low are with values below 10. This chemofacies has a positive $\delta\ ^{13}C$ excursion of 1.5‰, and the $\delta\ ^{15}N$ ratios decrease. Mo has enrichment factors up to 10 whereas U and V are below 1. The S and total iron wt. % have concentrations of about 1 and 7 wt. %, respectively.

The Al_3O_2 and SiO_2 concentrations are around 17 and 53 wt. %, respectively. This chemofacies has a periodic increase in calcite wt% and relatively low Ni and Cu concentrations. The mineralogy is quartz, illite, and kaolinite with a minor amount of smectite, calcite, pyrite, and albite (Figure 26).

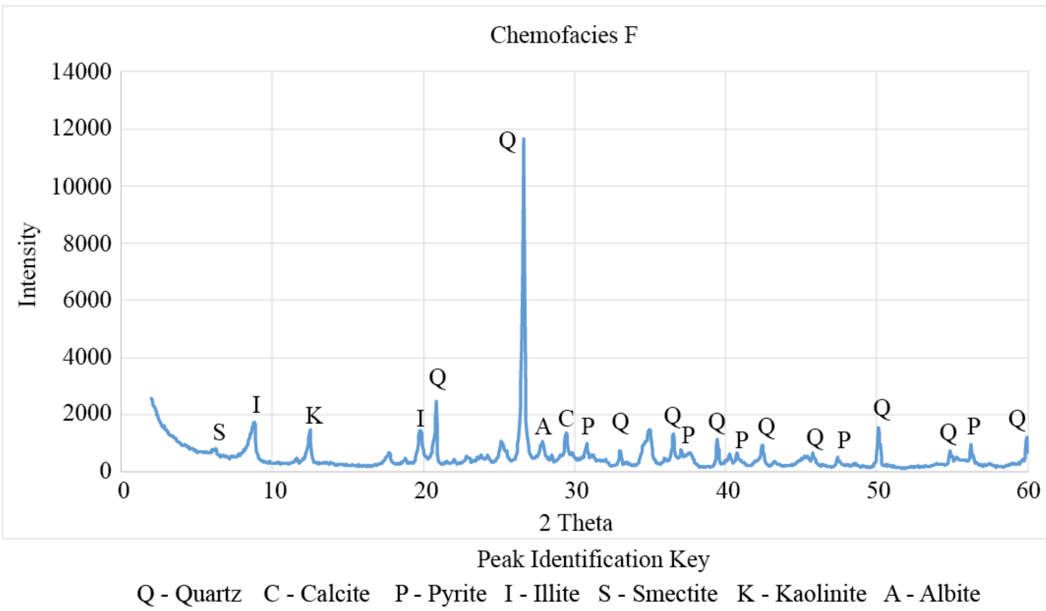

Figure 26. XRD random powder mount diffractogram of Chemofacies F from well COP 289 at 7940 ft. The major mineral present in this sample is quartz (Q), illite (I), and kaolinite (K). The other minerals present are smectite (S), calcite (C), pyrite (P), and albite (A).

Chemofacies G. This chemofacies is nearly 60 ft thick in wells COP 289 and COP 653 but only 30 ft thick in well COP 259. This chemofacies is characterized by an increase of TOC, enrichment of the redox-sensitive trace elements and more negative $\delta^{13}C$ values when compared to Chemofacies F. TOC ranges from 1 to 3 wt%. The C/N ratios range from 5 to 12. The $\delta^{15}N$ ratios are near 1.5‰ in well COP 259, 0.5‰ in well COP 653, and -0.3‰ in well COP 289. Mo enrichment factors are 10 while U and V are ≤1 within this chemofacies. The wt. % S generally decreases up stratigraphic section whereas the total iron increases from 6 to 7 wt %. The Al_2O_3 concentration is 15 wt % whereas SiO_2 ranges from 51 to 53 wt %. Calcite in this chemofacies averages about 10 wt % but is as high as 20 wt %. Cu and Ni concentrations are 70 ppm and 100 ppm respectively. The mineralogy of this sample is quartz, illite, and kaolinite with minor amounts of smectite, calcite, pyrite, and albite (Figure 27).

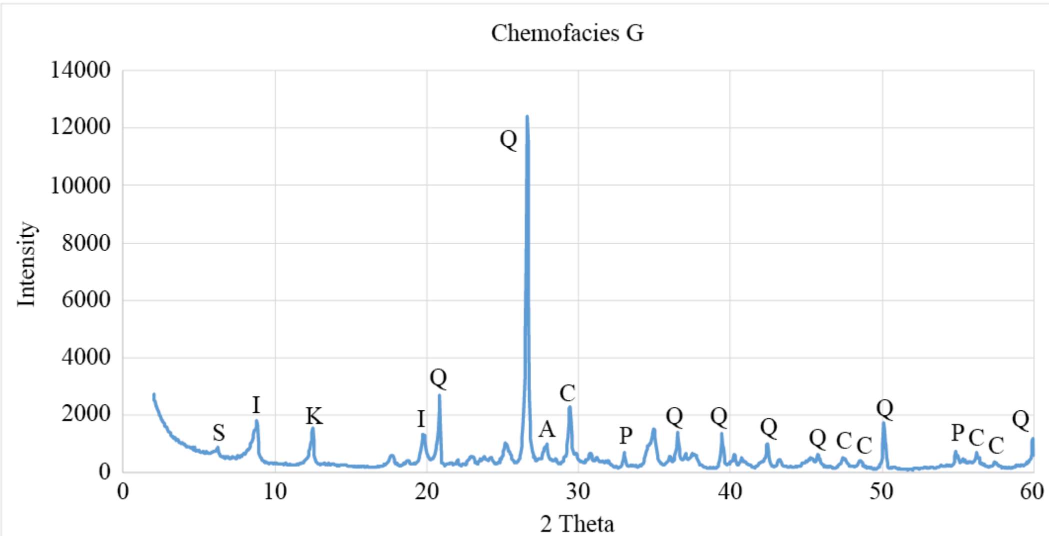

Peak Identification Key
Q - Quartz C - Calcite P - Pyrite I - Illite S - Smectite K - Kaolinite A - Albite

Figure 27. XRD random powder mount diffractogram of Chemofacies G from well COP 653 at 8320 ft. The major minerals of this sample are quartz (Q), illite (I), and kaolinite (K). The other minerals include smectite (S), calcite (C), pyrite (P), and albite (A).

Chemofacies H. This stratigraphic interval is 20 to 40 ft thick and is characterized by little to no organic matter. Chemofacies H has very low TOC (less than 1%) and low C/N ratios. The $\delta^{13}C$ ratios are -28.5‰. $\delta^{15}N$ ratios are inconsistent between each well with well COP 289 below 0‰, well COP 653 from 0-1‰, and well COP 259 just above 1‰. Redox-sensitive trace metals all have enrichment factors below 1. S concentration is near 0 whereas total iron ranges from 6-7 wt%. The SiO_2 and Al_2O_3 concentrations are 54 wt % and 15 wt % respectively. Calcite wt% averages 10 wt% and is consistently higher than in other chemofacies. Cu and Ni concentrations are significantly lower than Chemofacies G. Chemofacies H is dominated by quartz, illite, and smectite with minor amounts of kaolinite, calcite, dolomite, pyrite, and albite (Figure 28).

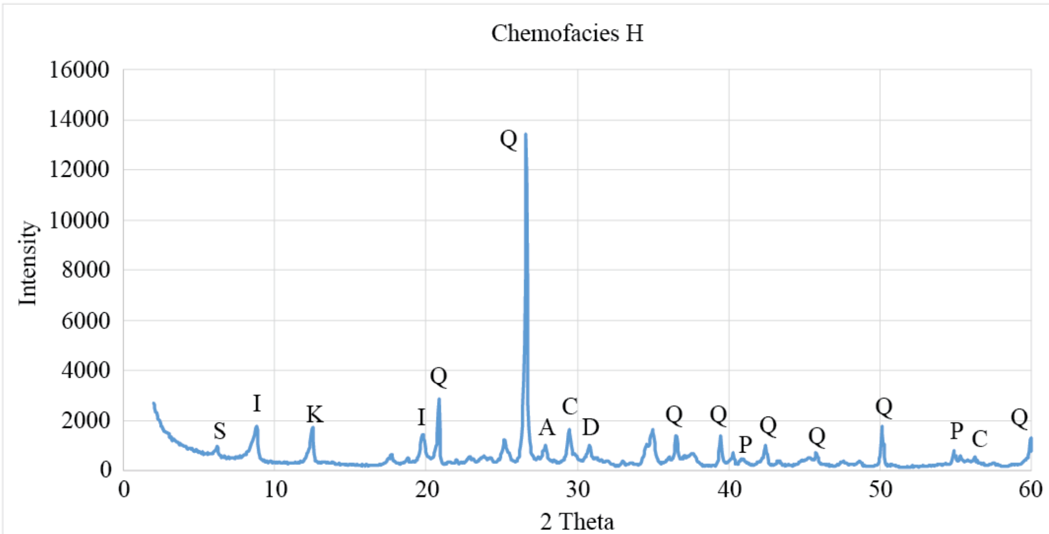

Figure 28. XRD random powder mount diffractogram of Chemofacies H from well COP 259 at 8162 ft. The major minerals of this sample are quartz (Q), illite (I), and smectite (S). This sample also contains kaolinite (K), calcite (C), dolomite (D), pyrite (P), and albite (A).

Chemofacies I. This stratigraphic interval is entirely recovered in well COP 259, (about 80 ft thick) and is petrophysically logged in all three wells (Hanson, 2017). The base of Chemofacies I has TOC values from 1-2.5 wt%. C/N ratios are near 10 in wells COP 289 and COP 653, but are in the range of 5-10 in well COP 259. This chemofacies has a prominent negative excursion $\delta^{13}C$ which reaches approximately -30‰. $\delta^{15}N$ values are more positive than the values from Chemofacies H. U and V enrichment factors exceed 1. Mo has enrichment factors of 10 or higher. S concentrations are approximately 1 wt%, and total iron concentration ranges from 6-7 wt %. Al_2O_3 content has a positive trend from 15 to 16 wt %. SiO_2 content increases from 53 to 55 wt %. Cu and Ni concentrations appear to increase relative to the underlying chemofacies The mineralogy is quartz, illite, and kaolinite with minor amounts of smectite, calcite, and albite (Figure 29).

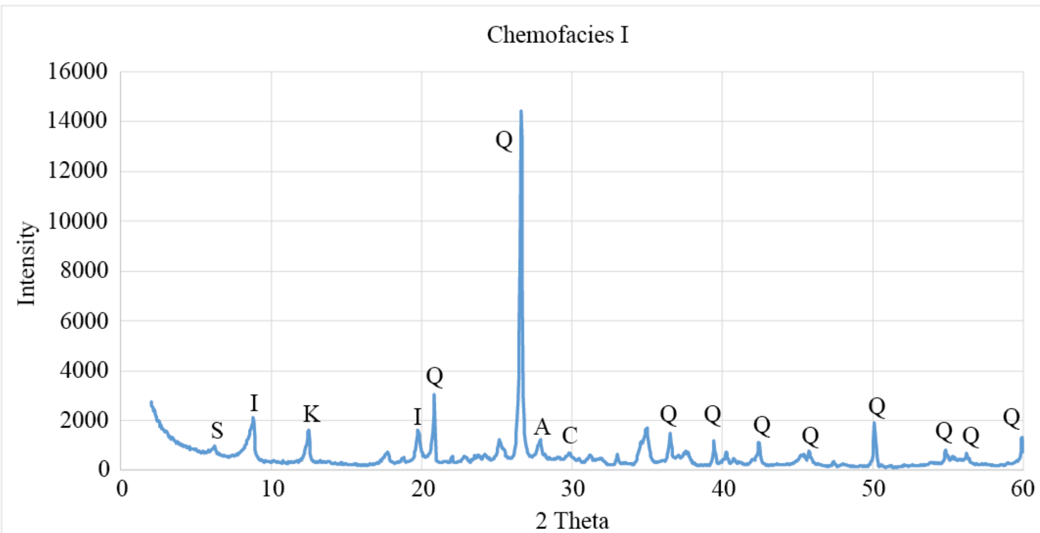

Peak Identification Key

Q - Quartz   C - Calcite   S - Smectite   K - Kaolinite   A - Albite

Figure 29. XRD random powder mount diffractogram of Chemofacies I from well COP 653 at 8258 ft. The major minerals of this sample are quartz (Q), illite (I), and kaolinite (K). Smectite (S), calcite (C), and albite (A) are also present.

Chemofacies J. Chemofacies J is only present in well COP 259 and is characterized by very low TOC values similar to Chemofacies H. Chemofacies J has low TOC (<1%) and C/N ratios less than 5. $\delta^{13}C$ values have a positive trend from -29‰ to -28.‰, and $\delta^{15}N$ values are at 2‰. This chemofacies is depleted in all three redox-sensitive trace elements: Mo reaching as low as 0.1, and V and U are slightly less than 1, and Cu and Ni concentrations average 20 and 70 ppm, respectively. S and total iron concentration are <1 wt% and 7 wt% respectively. The Al_2O_3 and SiO_2 values are similar to Chemofacies I with Al_2O_3 averaging 15 wt% and SiO_2 averaging 55 wt%. Calcite ranges from 5 to 10 wt%. The mineralogy of this stratigraphic interval is quartz and kaolinite with minor amounts of illlite, smectite, calcite, dolomite, and albite (Figure 30).

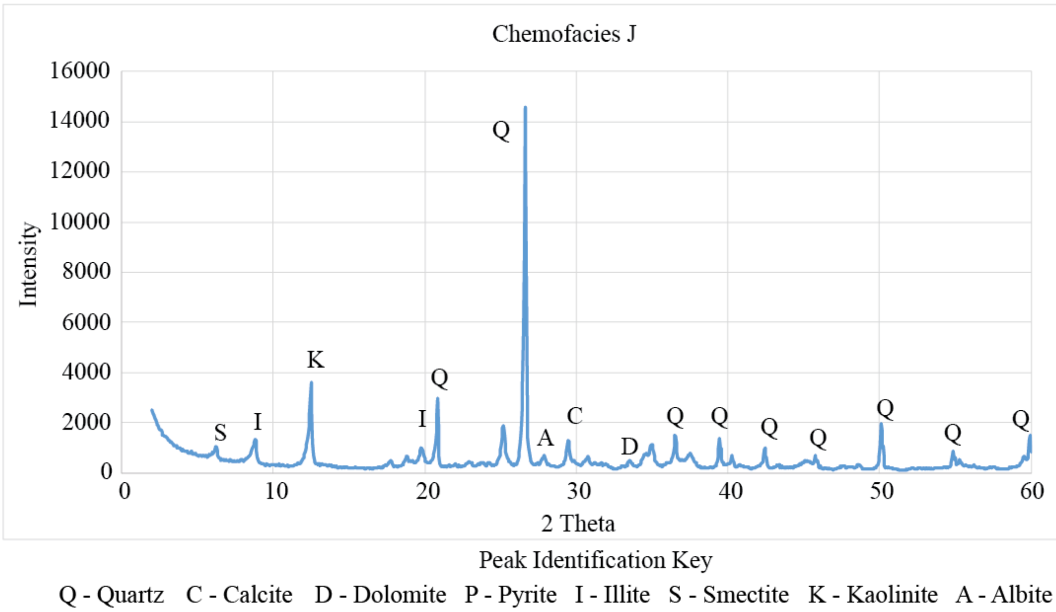

Figure 30. XRD random powder mount diffractogram of Chemofacies J from well 259 at 8060 ft. The major minerals in this sample are quartz (Q) and kaolinite (K). The other minerals present are illite (I), smectite (S), calcite (C), dolomite (D), and albite (A).

The Evolution of Redox and Productivity Conditions of the Appalachian Basin

There are several ways to reconstruct redox conditions in ancient marine depositional environments. One of the most commonly used methods to infer coeval redox dynamics is the abundance of organic matter preserved in the mudrock. High concentrations of preserved organic matter are usually interpreted as being indicative of reducing conditions in which free oxygen is absent from the water column. Under anoxic conditions it would be expected that the endolithic biota would be reduced or absent resulting in a laminated appearance to the mudrock. This texture is often used as a redox indicator. Elevated enrichment factors for redox-sensitive trace metals can also be used to elucidate redox conditions and can be effectively compared to the abundance of authigenic minerals (pyrite, for example) whose occurrence is controlled by the eH of the water column. Lastly, covariation or lack thereof among trace elements reveals information about the hydrodynamics of the basin (Algeo and Maynard, 2004).

Hydrographic Setting of the Appalachian Basin

Once sulfidic conditions have been achieved, the concentration of redox-sensitive trace metals within the water column, such as Mo, begins to deplete. Therefore, the concentration of the redox-sensitive trace metals becomes dependent on the ability of the water mass to replenish depleted trace metals. Mo/TOC ratios are used as an indicator of trace metal drawdown and a proxy for basin restriction (Algeo and Rowe, 2012). The trend-line slope of Mo vs TOC values can be compared to modern examples to describe the amount of basin restriction. The trend-line slopes found within these wells shows the Appalachian Basin had a similar water mass restriction (Figure 31) as the Cariaco Basin, which is 70-85% of open seawater conditions (Algeo and Rowe, 2012). Figure 32 shows that the study interval becomes slightly more restricted as deposition of the Marcellus progressed.

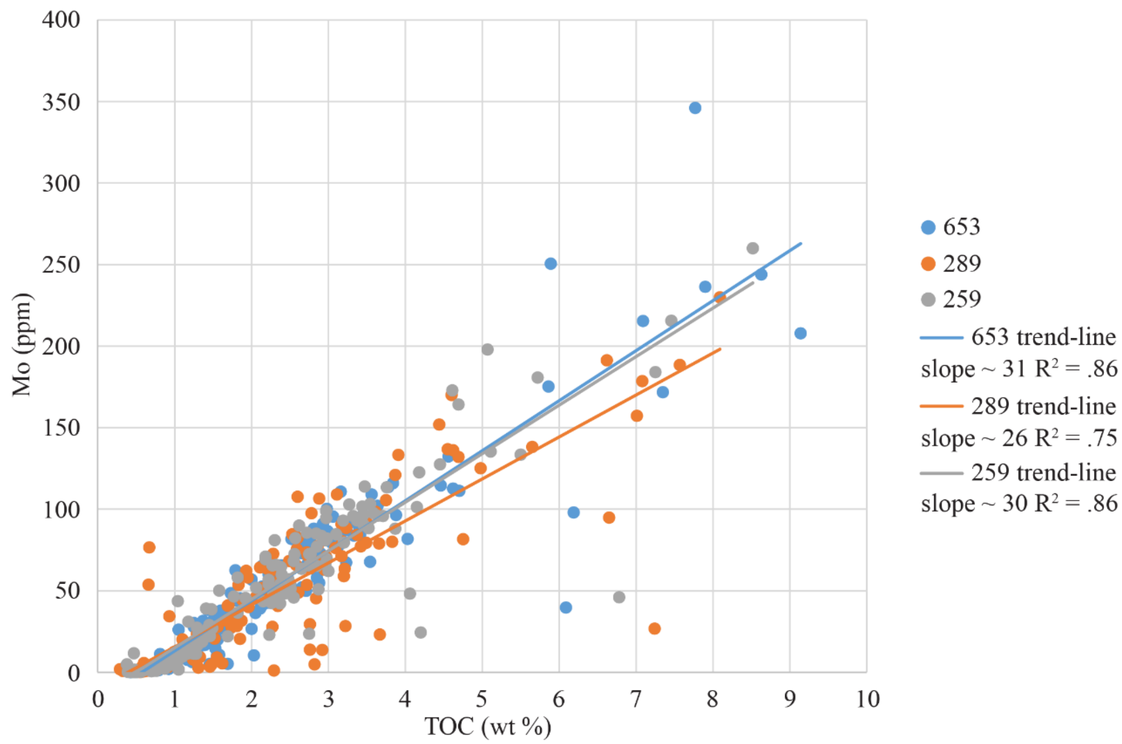

Figure 31. Mo vs. TOC. The trend-line slopes on these lines indicate that the Appalachian Basin during Marcellus deposition is about 80% open marine conditions by comparing the slopes of these lines to the slopes in modern examples as described in Algeo and Rowe (2012).

Organic Matter Abundance and Texture

The average TOC of the Marcellus Formation is much higher than the underlying Onondaga Formation and the overlying Mahantango Formation (Figures 18A, 19A, and 20A). The Marcellus also has a high proportion of laminated mudstone which suggests restriction of endolithic biota. These two trends suggest that the Marcellus was deposited under reducing conditions. The top portion of Chemofacies E in all three cores bioturbated suggesting that during the transition between Chemofacies E to F oxic to

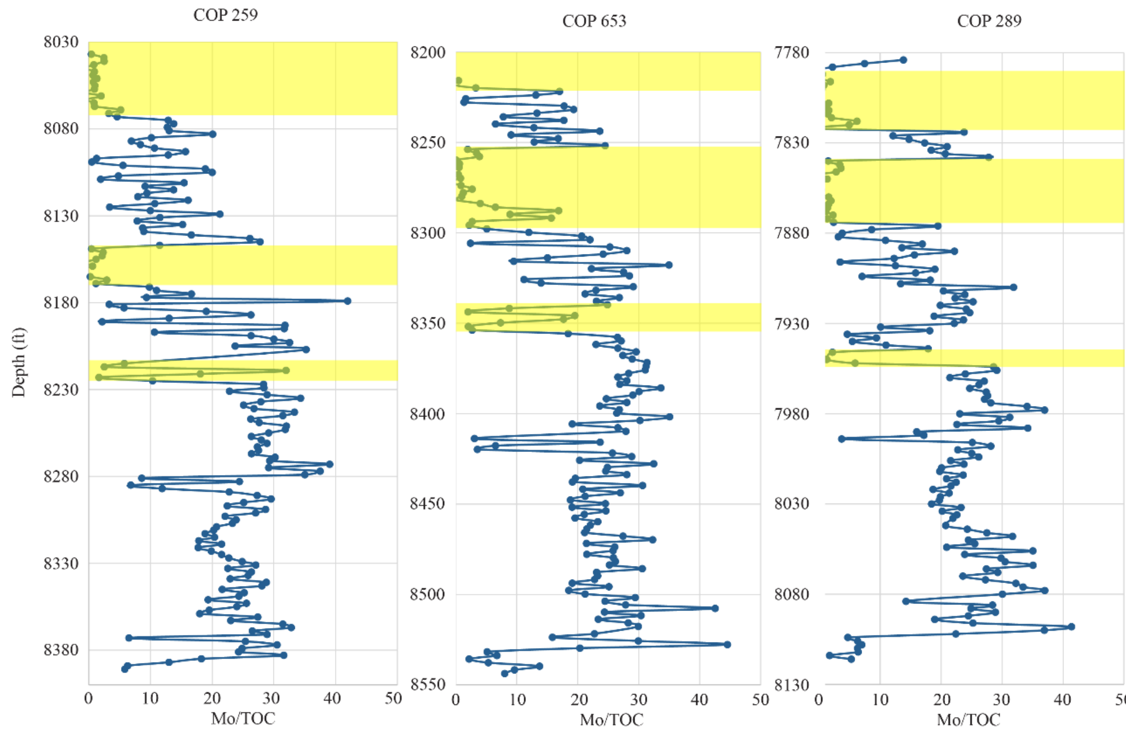

Figure 32.Mo/TOC within a stratigraphic succession. The Mo/TOC ratios indicate that the Appalachian Basin is increasing in restriction during deposition of the study interval. The yellow boxes indicate where Mo reducing conditions were not met so the basin restriction proxy becomes invalid.

suboxic conditions existed and conducive to endolithic fauna. A large portion of Chemofacies C in well COP 289 is bioturbated (Figure 9) even through the other geochemical proxies suggest euxinic conditions. The cause of this phenomena is unknown but the mottled texture may be misinterpreted as bioturbations.

Trace Metals

Molybdenum, uranium, and vanadium concentration in mudrocks can be used to reconstruct paleoceanographic redox conditions because these metals become enriched under variably reducing conditions. (Tribovillard et al., 2006). Under oxidizing conditions the trace metals will stay in solution but when condition becomes reducing they change valence. These reduced valence redox-sensitive trace metal are scavenged and adsorbed onto clay minerals, sulfides, and organic matter and are preserved in elevated concentrations.

When Mo becomes reduced it is often captured by Mn-oxyhydrates that are precipitating at the sediment-water interface (Bertine and Turekian, 1973; Erickson and Helz, 2000). Molybdenum only becomes reduced under anoxic conditions when free H_2S is present in the water column (Erickson and Helz, 2000; Tribovillard et al., 2006) under euxinic conditions. In contrast, uranium tends to become reduced at a higher eH that is coincident with the O_2 levels under which iron reduction occurs (Klinkhammer and Palmer, 1991; Crusius et al., 1996; Zheng et al., 2000). The reduced uranium adsorbs or precipitates onto clay particles as uraninite (Crusius et al., 1996; Morford et al., 2001; Chaillou et al., 2002). This process usually takes place within the sediment, which means that depositional and diffusion rates may play a role in the amount of uranium enrichment (Crusius and Thomson, 2000; Tribovillard et al., 2006). Reduced uranium also attaches itself to organic molecules as organometallic ligands by chelation (Swanson, 1960; Klinkhammer and Palmer, 1991; Zheng et al., 2000). Authigenic uranium can be remobilized if pore fluids become oxygenated post-deposition (Zheng et al., 2000; Morford et al., 2001). This can allow for vertical migration of the uranium especially in areas with bioturbation. The two reduction stages of vanadium can also be used to help determine the extent of anoxia (Calvert and Pedersen, 1993; Algeo and Maynard, 2004). V(IV) becomes reduced under mildly reducing conditions and precipitates as insoluble hydroxides (Emerson and Huested, 1991; Morford and Emerson, 1999). V(III) is present in euxinic conditions and precipitates as vanadium oxides or hydroxides (Breit and Wanty, 1991; Wanty and Goldhaber, 1992).

Using a combination of molybdenum, uranium, and vanadium it is possible to predict if the depositional redox conditions supported oxic, anoxic, or euxinic conditions (Tribovillard et al., 2006). If vanadium and uranium are enriched without molybdenum, anoxic denitrifying conditions exist. If molybdenum is enriched along with the other two elements, it indicates that aqueous sulfate was the terminal electron acceptor and results in free H_2S within the water column which is referred to as euxinic (Algeo and Maynard, 2004; Tribovillard et al., 2004, 2005, 2006).

Prior to Marcellus deposition (in Chemofacies A), low TOC values, low productivity, and low enrichment factors of redox-sensitive trace metals all indicate well-oxygenated open marine conditions. Within Chemofacies B all the redox-sensitive trace metals have enrichment factors for U (Figure 33) and V (Figure 34) greater than 10 whereas Mo (Figure 35) has an enrichment factors ≤ 1000. Mo enrichment indicates that euxinic conditions existed early in the deposition of the Marcellus, and illustrate strongly contrasting water chemistry between Onondaga through Marcellus deposition. After deposition of Chemofacies B there is a continual decline in Mo enrichment factors up section (Figures 18C, 19C and 20C). Within Chemofacies C, V and U are only slightly enriched whereas Mo has EF averages 50. Higher in the stratigraphic section V and U are near average shale values or even become depleted, whereas Mo remains enriched, as seen in Chemofacies G and I (Figures 18C, 19C, and 20C). The three redox-sensitive trace elements covary in the bottom of the study interval (Chemofacies A-F), but this covariation ceases in the upper portion of the section (Chemofacies G-J). The lack of covariation in the top of the section may be caused by a slight increase of basin restriction and resulting drawdown of U and V (Figure 32).

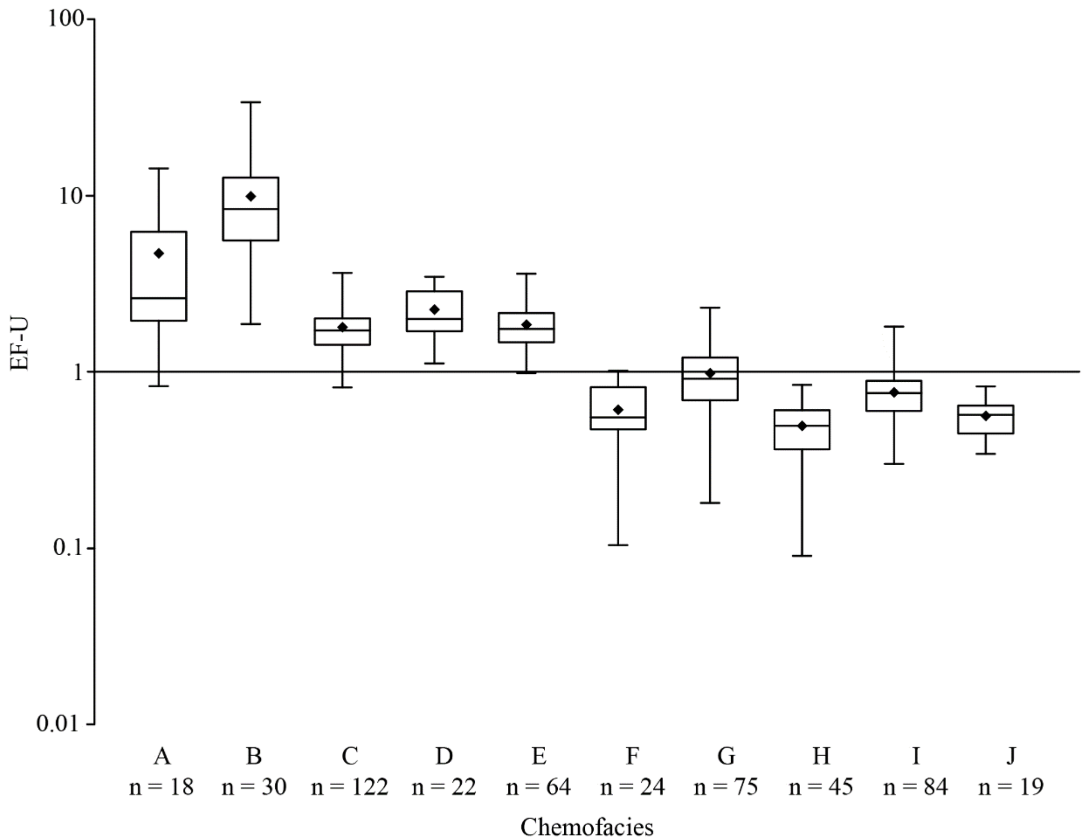

Figure 33. Boxplot of EF-U within each chemofacies. The black diamonds are the mean of each of chemofacies. Values greater than 1 are considered enriched and were deposited in anoxic conditions. Values below one are considered depleted. Uranium was likely undergoing the draw-down effect in the upper part of this section and conditions may have been more anoxic then these metals suggest.

Molybdenum enrichment follows a different stratigraphic pattern than the other two redox-sensitive trace metals and stays enriched throughout most of the section. Conversely, U and V are depleted in the upper half of study interval. The molybdenum response may be owing to the standard shale value being only 1.3 ppm whereas uranium and vanadium are 3 ppm and 130 ppm respectively. This indicates that bottom

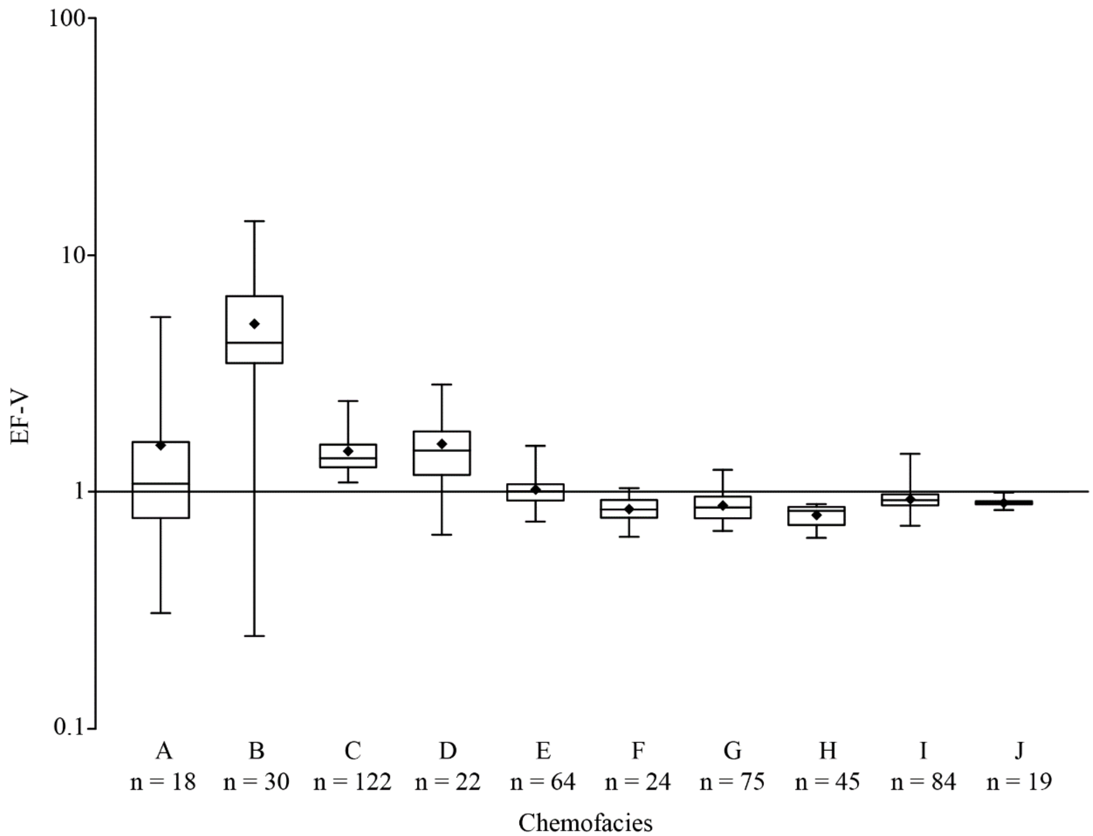

Figure 34. Boxplot of EF-V within each chemofacies. The black diamonds are the mean of each of chemofacies. Values greater than 1 are considered enriched and were deposited in anoxic conditions. Values below one are considered depleted.

normalization of Equation 3 will be less and allow for smaller changes in Mo concentrations to have a greater effect on EF values. For comparison, the trace metal concentration in well COP 653 is shown in Figure 36. This figure shows that Mo is generally more enriched than U or V. It is likely that drawdown of U and V cause less enrichment within the upper part of the study area interval even though the Mo/TOC ratio indicates fairly unrestricted conditions.

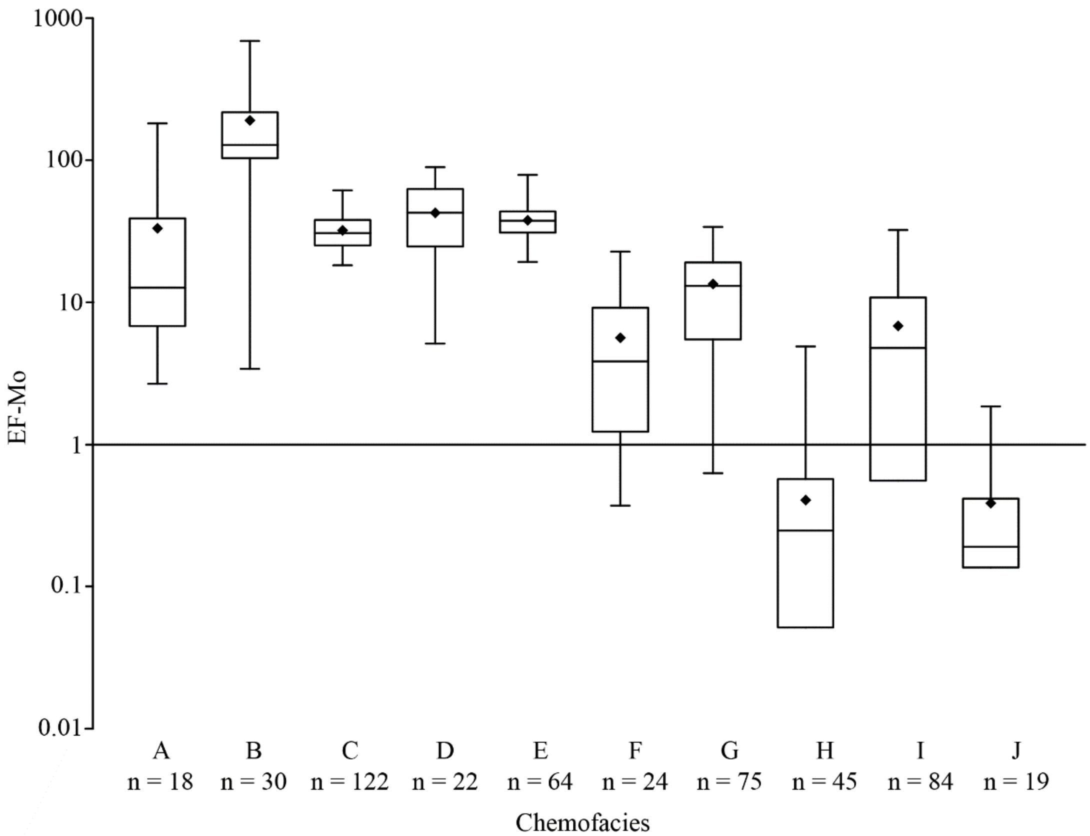

Figure 35. Boxplot of EF-Mo within each chemofacies. The black diamonds are the mean of each of chemofacies. Values greater than 1 are considered enriched and were deposited in euxinic conditions.

The enrichment of Mo and high TOC values of Chemofacies E, G, and parts of I indicate they were deposited in euxinic or anoxic conditions. The depleted to slightly elevated enrichment factors for uranium and vanadium in the upper portions of the Marcellus could have been caused by the drawdown effect. The drawdown effect describes trace metal behavior controlled by restricted seawater circulation resulting in trace metal removal at a rate exceeding seawater replenishment (Algeo, 2004; Algeo and Lyons, 2006; Tribovillard et al., 2006). In the lower portion of the study interval, high enrichment factors indicates that normal marine concentrations of dissolved trace metals could be reduced and deposited in the sediment.

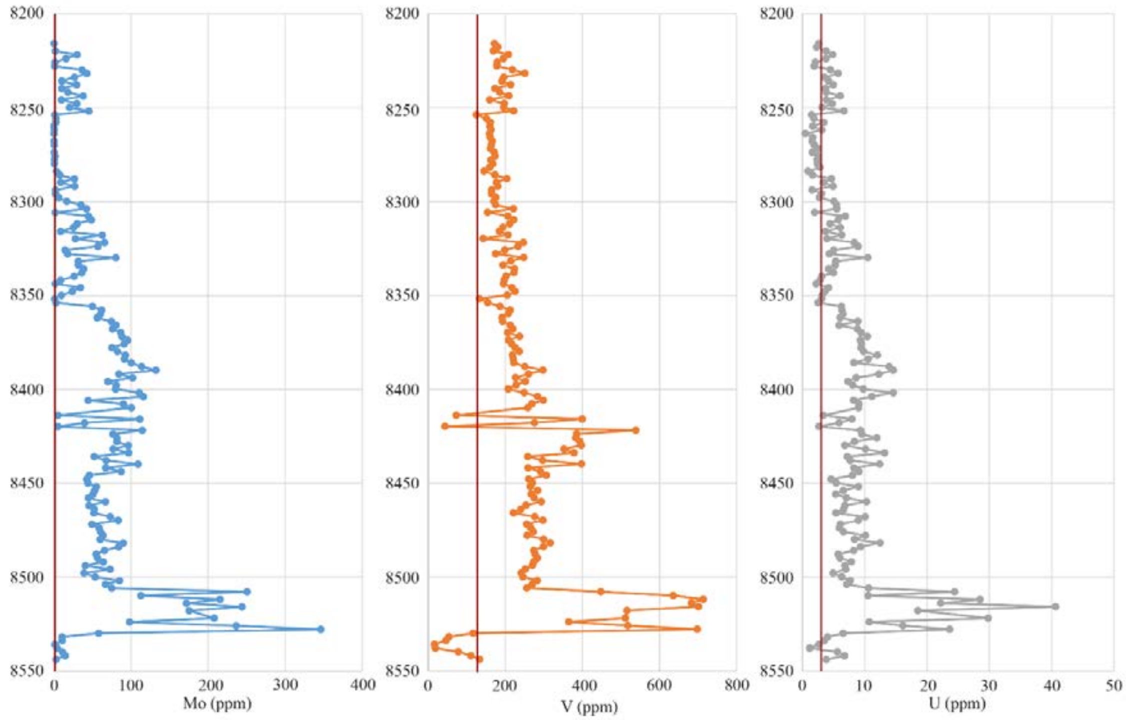

Figure 36. Redox-sensitive trace metal concentrations (in ppm) in well COP 653. The red line indicates the values for average shale. Mo has much higher ppm values than found in average shale meaning that the strong response of Mo is likely not only caused by how enrichment factors are calculated.

Paleoproductivity Indicators

Nickel and copper are useful paleoproductivity proxies because they behave as micronutrients, are incorporated into organic matter with organometallic ligands, and can remain in the sediment even if the organic material undergoes decomposition (Calvert and Pedersen, 1993; Whitfield, 2001; Achterberg et al., 2003; Algeo and Maynard, 2004). Both of these metals are scavenged from the water column by algae within the photic zone (Nameroff et al., 2004; Naimo et al., 2005).

Enrichment of Ni and Cu indicates high primary paleo-production (Huerta-Diaz and Morse, 1990, 1992, p.; Fernex et al., 1992; Morse and Luther, 1999). Copper and Nickel are both enriched through the majority of the Marcellus Formation in all three wells and indicate that high organic matter flux was partially responsible for creating anoxic to euxinic conditions (Figure 37 and 38). The greatest enrichment of these trace metals is found early in Marcellus deposition (Chemofacies B) which has concentrations of Cu and Ni several times greater than average shale values. Above Chemofacies B, the concentration of Co and Ni decrease up section. These productivity indicators covary with the redox-sensitive trace metals, $\delta^{13}C$ values, and organic carbon abundance. This suggests that high productivity induced into anoxic and euxinic conditions within the basin.

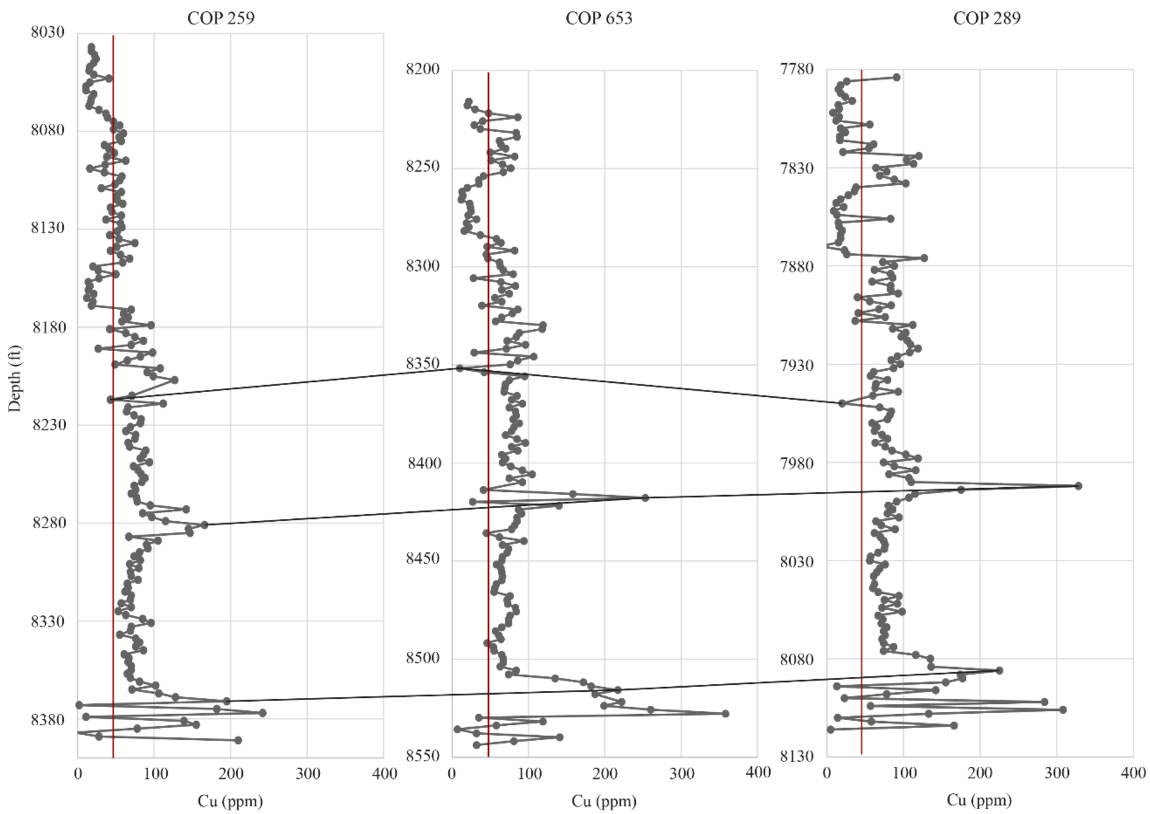

Figure 37. Cu concentration (ppm) in all three wells. The red line indicates the average shale values. The black lines show correlatable geochemical trends within the same stratigraphic horizon. The majority of this section has relatively high Cu concentrations.

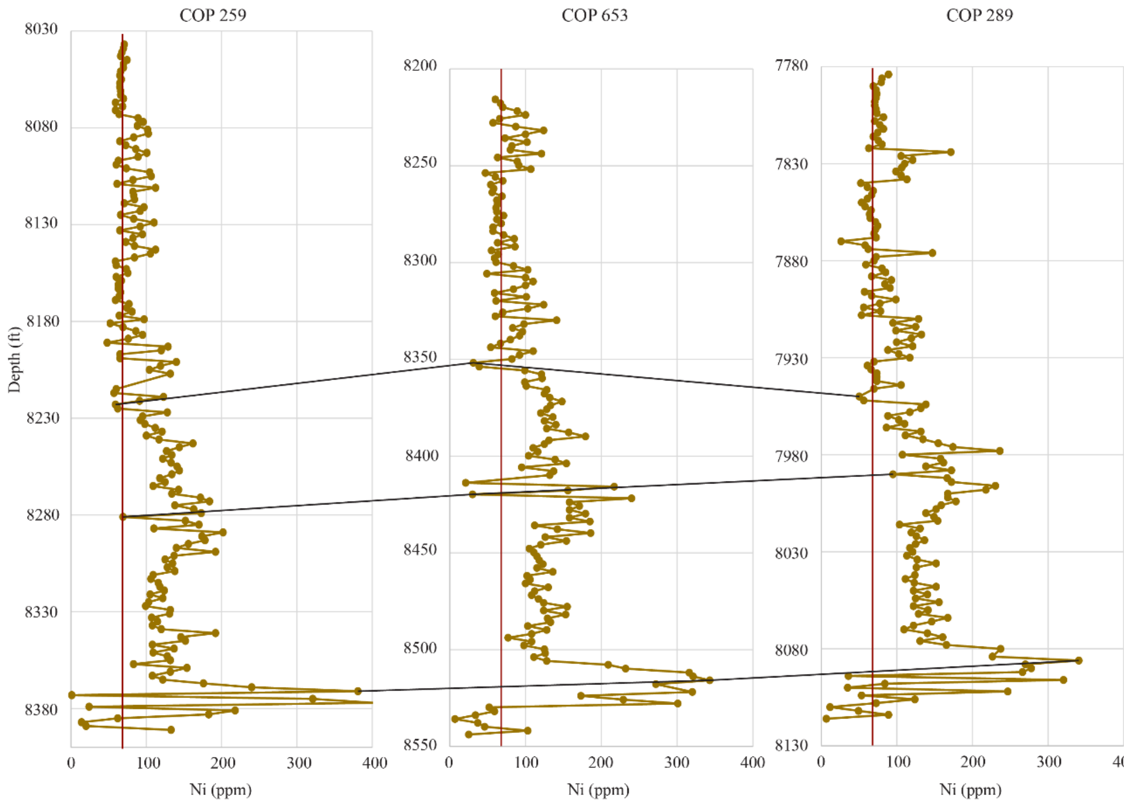

Figure 38. Ni concentration (ppm) in all three wells. The red line indicates the average shale values. The black lines show correlatable geochemical trends within the same stratigraphic horizon. The majority of this section has relatively high Ni concentrations.

Stratigraphic Patterns of Organic Matter Abundance in the Marcellus

The Marcellus Formation within study area has an average TOC of 2.8 wt% and the organic matter abundance exhibits considerable stratigraphic variation. The averages abundance of organic matter within individual chemofacies is presented in Figure 39. The overall high TOC values within the 250 ft of the Marcellus Formation indicate prolonged high productivity accompanied by anoxia. The stratigraphic intervals with the highest TOC values (> 5wt. %) occur at the bottom of the Union Springs Member (Chemofacies B) and a small portion with the Cherry Valley Member (Chemofacies D). The high concentrations of organic matter within Chemofacies B was likely influenced by low clastic dilution as indicated by the large quartz abundance. The organic-rich portion of Chemofacies D is unexpected because it is within the Cherry Valley Member which appears to have been deposited under relatively open marine conditions as indicated by the abundance of whole fossils and encrusting red algae.

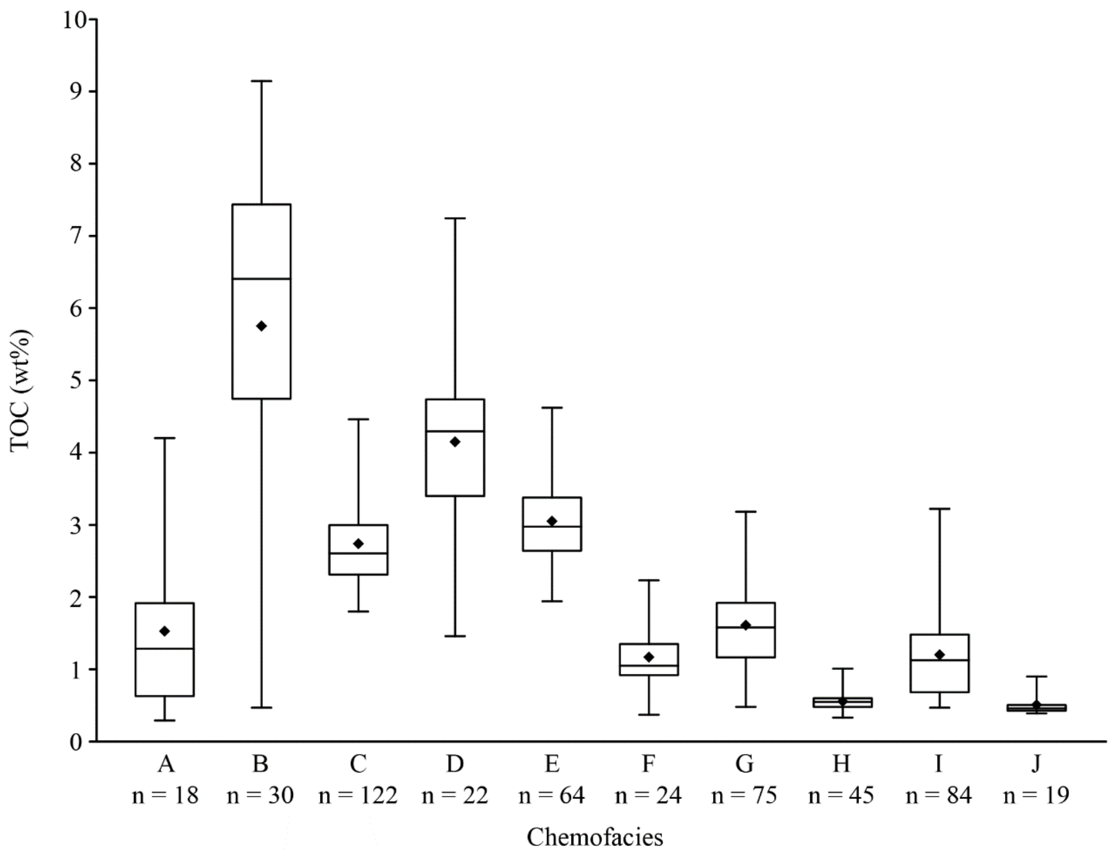

Figure 39. Box and whisker plot of chemofacies vs TOC. For this figure and all of the following boxplots, the black diamond represents the mean value, the horizontal line in the middle of the box is the median, horizontal line at top and bottom of the box represent the 75th and 25th percentiles of concentration, respectively. The whiskers show the minimum and maximum concentrations within each chemofacies. Chemofacies B and D have the highest TOC values found in the study area. The top of Chemofacies G is considered the top of the Marcellus Formation.

The C/N ratio of aquatic organic matter usually tpically from 5-10, but can also be as high as 15 (Emerson and Hedges, 1988; Khan et al., 2015). Aquatic organic matter usually has lower values than vascular plants because they are high in nitrogen-rich proteins that result in lower C/N ratios (Ohkouchi et al., 2003). Many C/N ratios in the Marcellus exceed 15 (Figure 40) and high C/N is often observed in organic-rich mudrocks (Sageman et al., 2003; Boling, 2013; Mills, 2015). High C/N ratios in marine rocks can be the result of terrestrial organic matter input (Meyers, 1994), but the organic matter within the Marcellus has a marine origin (Sageman et al., 2003). This phenomenon of very high C/N ratios in marine organic matter is also observed in Cretaceous black shales deposited during oceanic anoxic events (Ohkouchi et al., 2003; Meyers et al., 2009). This is likely caused by the elevated production of organic matter that results in the depletion of available nitrogen. This causes algae to produce nitrogen-poor carbohydrates or lipids instead of nitrogen-rich proteins (Ohkouchi et al., 2003) thus yielding organic matter with high C/N ratio. Organic matter abundance (Figure 39) and N wt% (Figure 41) do not covary and are likely due to the lack of available nitrogen.

The water chemistry within the Appalachian Basin had a distinct change between the deposition of the Onondaga and Marcellus formations as indicated by the sharp increase in the enrichment of redox-sensitive trace elements. Enrichments was likely driven by the high productivity of the basin at the beginning of Marcellus deposition. This allowed for the accumulation of a large amount of organic matter found in Chemofacies B. Organic matter richness decreased throughout deposition due to a decrease in organic matter production and concomitant increase in free oxygen partial pressure with the water column. Table 5 summarizes the redox conditions of each chemofacies.

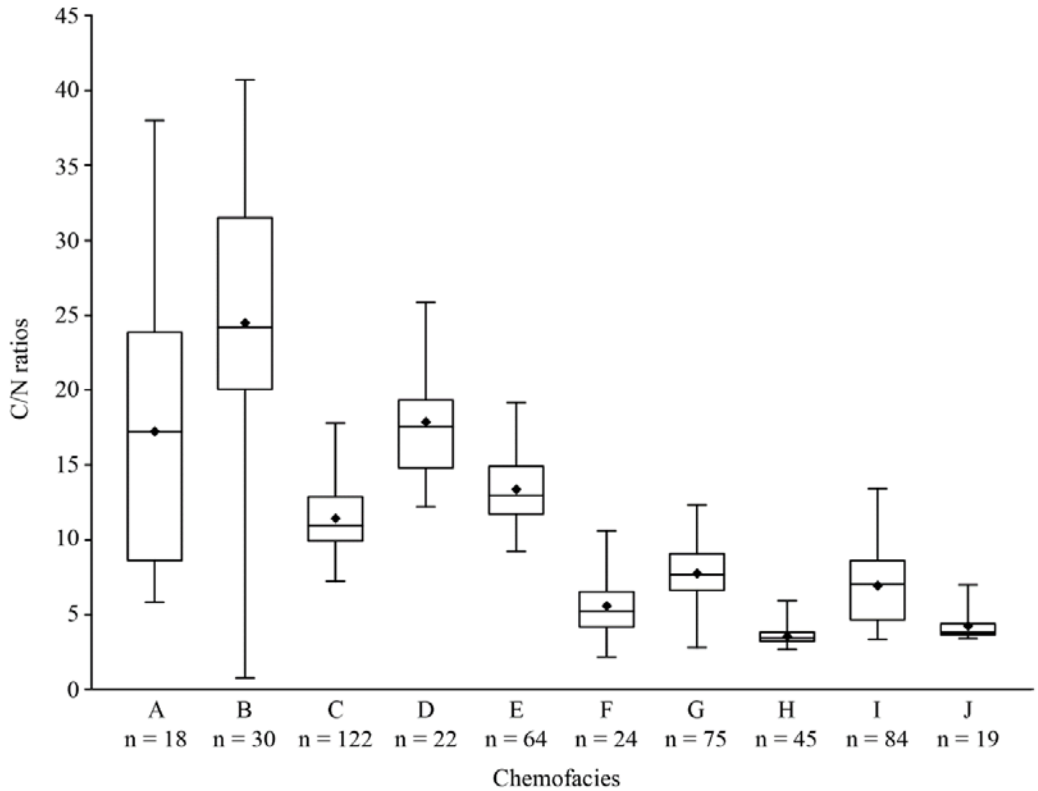

Figure 40. Boxplot of C/N ratios in each chemofacies. The black diamond is the mean values found within each chemofacies. Chemofacies B and D both have values that are unusually high for marine organic matter. These high C/N ratios were likely caused by a nitrogen limited system during the time of their depositions. The system was, to a lesser degree, likely also nitrogen-limited during Chemofacies C and E deposition as shown by their high C/N ratios.

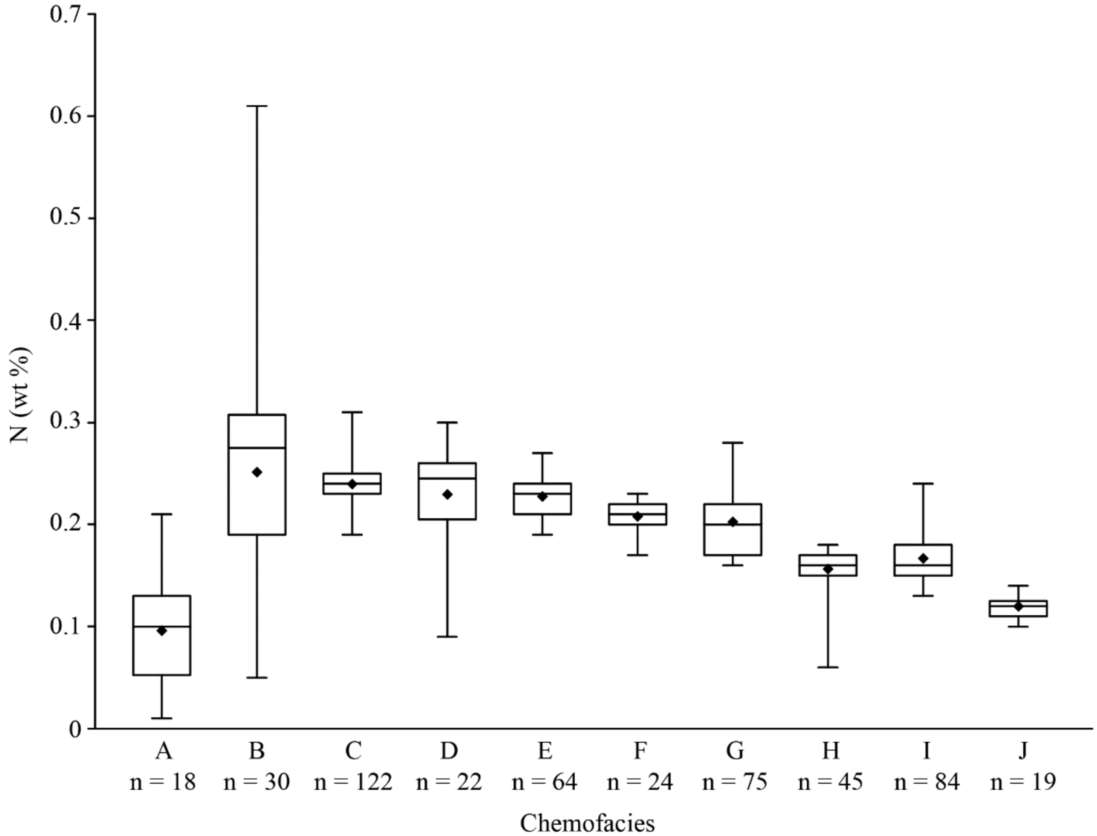

Figure 41. Boxplot of N abundance in each chemofacies. The black diamond is the mean values found within each chemofacies. The mean and median are relatively similar in Chemofacies B-G with as slight decrease moving up section. This trend does not have the same drastic changes as seen in the TOC chemofacies boxplot.

Table 5. Redox conditions of each chemofacies.

Chemofacies	redox conditions
J	Oxic
I	Anoixc
H	Oxic
G	Euxinic
F	Oxic to suboxic
E	Euxinic
D	Euxinic to suboxic
C	Euxinic
B	Euxinic
A	Oxic

The Isotopic Evolution of the Appalachian Basin

The carbon isotopic composition of the organic matter within the Marcellus ranges from -32‰ to -27‰ and has an average value of -29.93‰. The average carbon isotopic composition within each chemofacies is presented in Figure 42 and illustrates the overall carbon isotope trend toward more ^{13}C enriched organic matter. Most carbon isotope ratios worldwide during the Devonian organic matter exhibit enrichment in ^{12}C compared to modern marine algae (-20‰), and slightly more ^{12}C enrichment than other Phanerozoic black shales (-27‰) (Emerson and Hedges, 1988; Meyers, 1994, 2014; Galimov, 2006). Several processes could account for the negative $\delta^{13}C$ values. The pCO_2 of the atmosphere during the middle Devonian was much higher than it is today (Berner, 1990), an when carbon availability is limited, the discrimination against ^{12}C decreases. Therefore, when there is a greater availability of carbon, the isotopic discrimination increases which causes more negative values. The higher concentrations of CO_2 during the Middle Devonian perpetuates greater discrimination against C^{13} (Schubert and Jahren, 2012; Meyers, 2014) resulting in ^{12}C enriched organic matter. This process is more prominent in marine algae than in land plants (Popp et al., 1989; Sinninghe Damsté and Köster, 1998), because algae incorporate CO_2 through diffusion which is a concentration-dependent process. (Meyers, 2014).

Along with the availability of CO_2, negative $\delta^{13}C$ values in organic matter from the Marcellus could be caused by water stratification and carbon recycling. As organic material sinks towards the sea floor, some of it may be oxidized into CO_2. The liberated CO_2 from the degraded organic matter will have a more negative $\delta^{13}C$ value than the atmosphere (Küspert, 1982; Meyers, 2014). This CO_2 may be reincorporated by marine

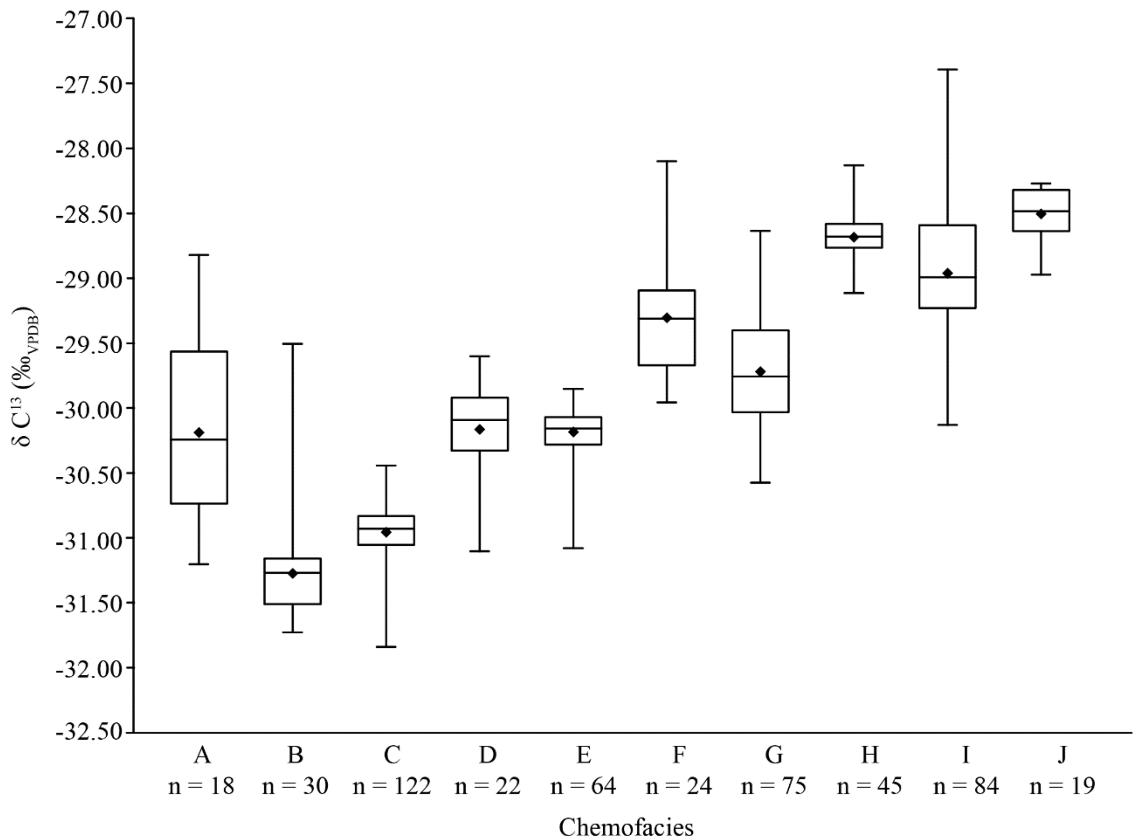

Figure 42. Boxplot of $\delta\ ^{13}C$ in each chemofacies. The black diamond is the mean values found within each chemofacies.

algae, leading to an even more pronounced negative carbon isotopic signature in the algae.

The ^{12}C enriched organic matter may also have been caused by selective diagenesis during decomposition. The bulk organic matter analyzed in this study is composed of many types of biomolecules. The most abundant of these include proteins, carbohydrates, and lipids. Proteins and carbohydrates tend to have more positive delta isotopic values and are more easily degraded then lipids (Galimov, 2006). If the lipids are preferentially persevered during diagenesis then the isotopically heavier proteins and carbohydrates will have degraded more than the lipids. This diagenetic alteration can cause the bulk organics to change their isotopic composition by -3‰ (Dean et al., 1986; Prahl et al., 1997; Meyers, 2014). Therefore, selective decomposition could explain some of the enrichment in ^{12}C, however, the amount of diagenetic alteration of the organic matter is unknown.

Nitrogen dynamics in the oceans are one of the major controls on marine productivity and can be reconstructed by measuring the nitrogen isotopic composition of preserved organic matter. The nitrogen isotopic composition of organic matter is a function of the nitrogen source (atmospheric versus dissolved) and the isotopic discrimination that takes place in the water column. The $\delta\ ^{15}N$ values in Marcellus ranges from +4‰ to -2‰ with an average of 1‰. The base of the study interval tends to have higher $\delta\ ^{15}N$ values of 3‰ to 4‰. These values are suggestive of terrestrial runoff which has an average value of 4‰ (Sigman, DiFiore, et al., 2009). The nitrogen isotope ratios could also be the result of early alteration or denitrification that took place within the sediment pore waters. Higher in the stratigraphic interval, the nitrogen isotopic ratios decrease toward 1‰. Nitrogen isotope ratios near zero are indicative of nitrogen that has been sourced from the atmosphere and fixed by cyanobacteria (Karl et al., 1997; Meyers et al., 2009; Saltzman and Thomas, 2012). When nitrogen dissolves into the water there is a slight discrimination of the nitrogen from 0.0‰ to 0.6‰ (Sigman, Karsh, et al., 2009) giving the observed data values slightly above zero. The nitrogen isotopic composition of Marcellus organic matter indicates that nitrogen was mainly sourced from the atmosphere. This along with high production are indicators that this was a nitrogen-limited system.

If nitrogen in the lower Marcellus (Chemofacies B) did not come from terrestrial runoff and was sourced from the air, the more positive values in the lower Marcellus may be explained by isotopic alteration during early burial. Early alteration can cause a 3 to 6‰ positive change in the nitrogen delta values (Altabet and Francois, 1994). However, this explanation is less likely because this phenomenon usually takes place in low organic nitrogen flux areas (Altabet and Francois, 1994; Robinson et al., 2012) and the base of the Marcellus has higher organic nitrogen values (Figure 43).

Denitrification is the major mechanism by which fixed nitrogen is lost from the ocean, and it is caused by bacteria using nitrates (NO_3^-) for respiration under anoxic conditions (Galbraith et al., 2004; Sigman, Karsh, et al., 2009; Robinson et al., 2012). This process discriminates against N^{14} and causes enrichment of N^{15} up to 25‰ in the remaining nitrogen if enrichment takes place above the sediment-water interface (Sigman, DiFiore, et al., 2009; Sigman, Karsh, et al., 2009). Conversely, enrichment in sediment pore waters minimizes discrimination because most of the nitrate is consumed and therefore restricts discrimination of ^{14}N and ^{15}N. Denitrification in the sediment pore water creates nitrogen values from 0‰ to 3‰ (Sigman, Karsh, et al., 2009; Robinson et al., 2012). This is also an alternative explanation for the positive nitrogen values observed near the base of the Union Springs Member. This would suggest that nitrogen that underwent denitrification escaped the pore fluids and was again fixed by cyanobacteria.

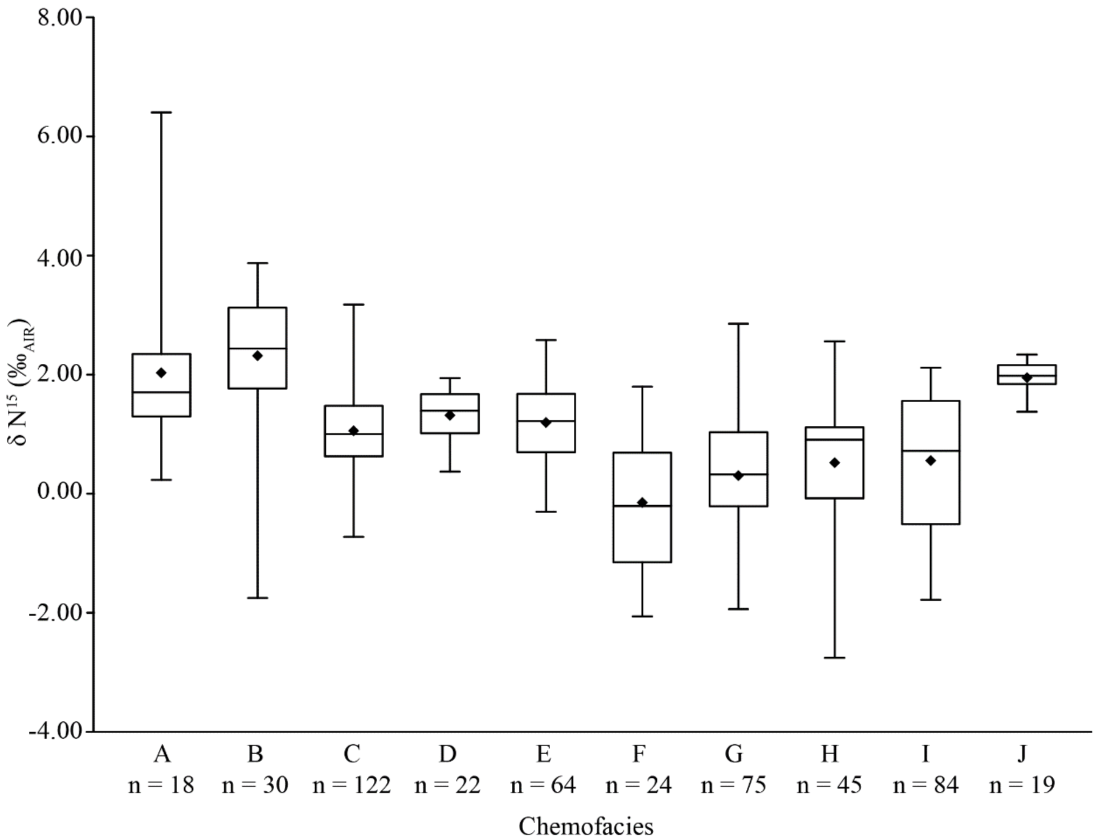

Figure 43. Boxplot of $\delta^{15}N$ within each chemofacies. The black diamonds are the mean. The higher nitrogen $\delta^{15}N$ values found in Chemofacies B are likely caused by denitrification within the sediment pore waters and the recycling of that nitrogen.

Correlation of Geochemical Variables with Respect to Organic Matter Abundance

Correlations between trace metal enrichments and TOC indicates that a lack of oxygen in the water column contributed in the preservation of organic matter, and subsequently the high TOC, observed within the Marcellus Formation (Figure 44).

There is also a strong negative correlation between $\delta^{13}C$ values and TOC (Figure 45). This correlation is consistent with carbon recycling caused by a stratified water body allowing for greater recycling of carbon and preventing O_2 from reaching the bottom waters resulting in the destruction of the organic carbon.

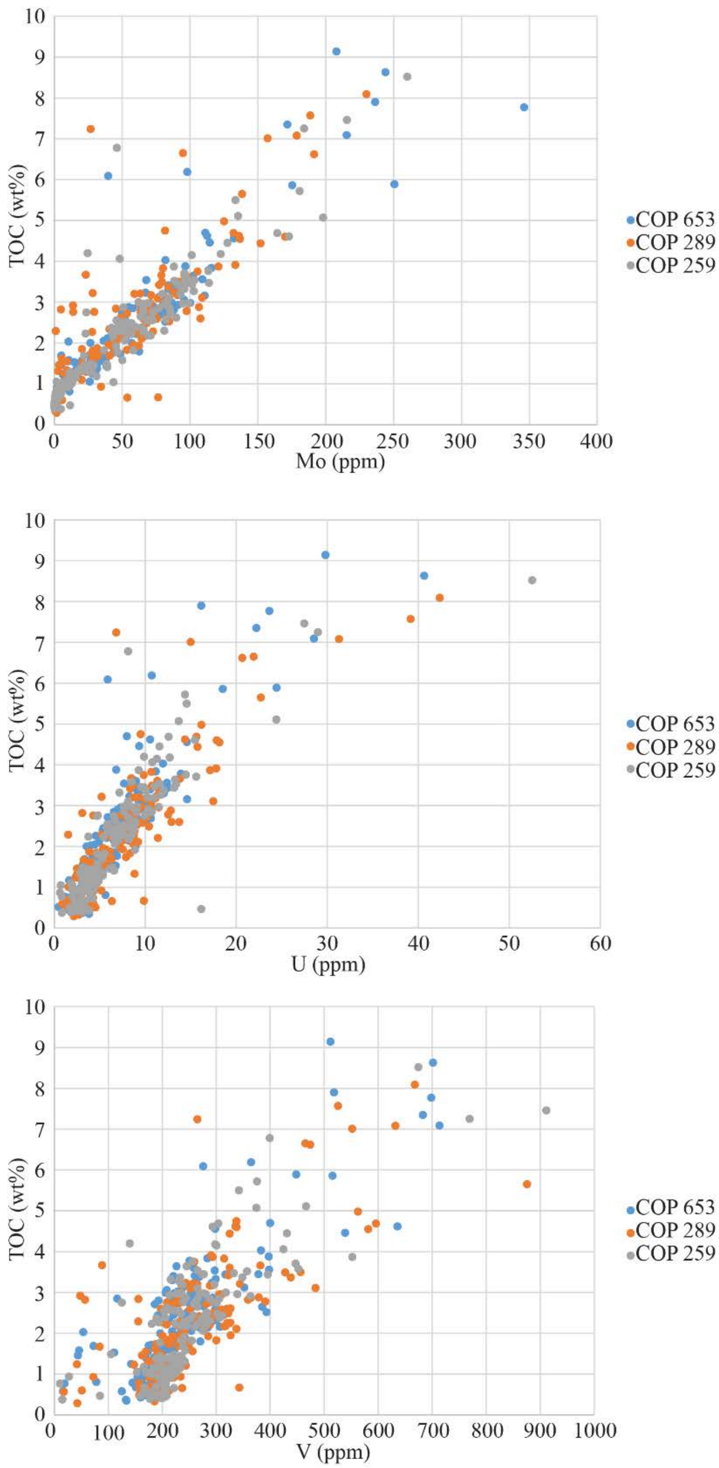

Figure 44. Correlation between redox-sensitive trace element (in ppm) and TOC. All three trace metals have a correlation. The correlation coefficient for Mo 0.82. The correlation coefficient for U is 0.76. The correlation coefficient for V is 0.62. These correlations suggest that anoxia is an important factor for preserving the organic matter within the study area.

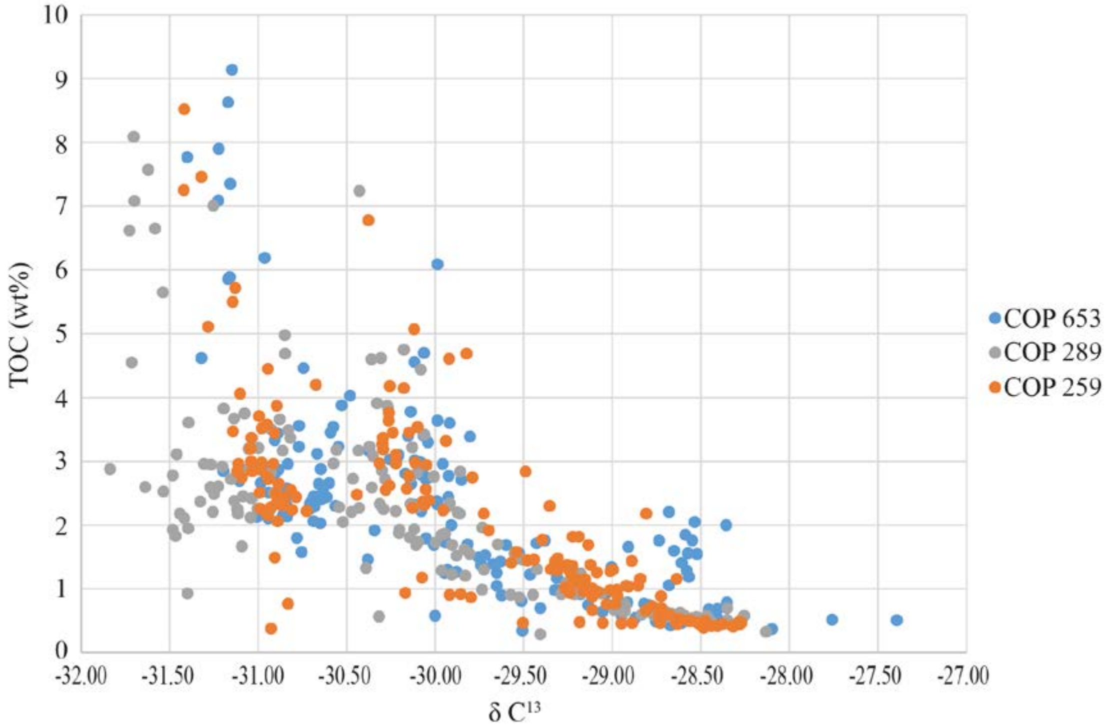

Figure 45. TOC vs. δ ^{13}C. A correlation between TOC and δ ^{13}C. Higher TOC correlated with increasingly negative δ ^{13}C.

The relationship between isotopic composition and organic matter abundance may be related to trapped methane within the mudrocks. When organic matter evolves into natural gas there is a strong discrimination against ^{13}C (Meyers, 2014). The carbon in methane often has isotopic ratios less than -40‰ (Rooney et al., 1995). In unconventional reservoirs such as the Marcellus, much of the porosity is microscopic (Kuila et al., 2014). A large proportion of porosity is located within the organic matter itself. As more of the organic matter matures to hydrocarbons the porosity within the organic material increase (Kuila et al., 2014). Therefore, the rocks with high organic matter are likely high in microporosity. Even with samples crushed into very fine powder, it is possible that some methane is trapped within the micro-pores and the isotopically light carbon within the methane subsequently decreases the overall $\delta\,^{13}C$ of the sample.

Geochemical Correlations between Wells

The compelling correlation of organic matter carbon isotope ratios between the three wells suggests a basin-wide cause. Global pCO_2 decrease throughout the middle and late Devonian (Berner, 1990, 1997; Mora et al., 1996; Driese et al., 2000). A decrease in pCO_2 concentration would cause less discrimination of ^{13}C and may account for the generally increasing $\delta\,^{13}C$ values observed throughout the study interval (Figure 46).

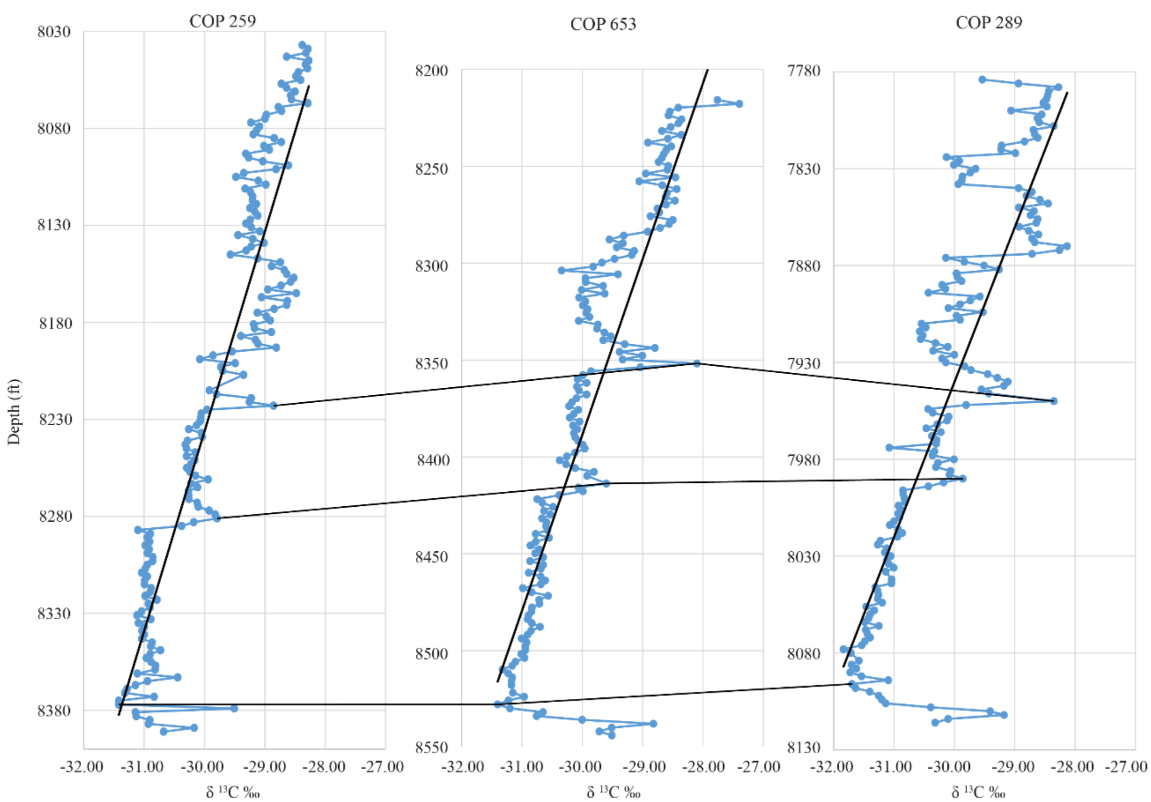

Figure 46. Comparison of stratigraphic variation in organic matter $\delta\,^{13}C$ values in all three well. Trend-lines are shown and have similar slopes suggesting the controlling processes is basin-wide. The black lines highlight correlatable geochemical trends within the same stratigraphic horizon. The most likely cause of the positive trend is declining carbon availability.

The only geochemical attribute that does not correlate between the three wells is the nitrogen isotopic ratio of the organic material. In well COP 259, the $\delta\ ^{15}N$ values are 3 ‰ at the base of the Marcellus and decrease to 0 ‰. A positive excursion occurs within Chemofacies C and remains between 1 and 2 ‰ throughout this stratigraphic interval. The $\delta\ ^{15}N$ values in well COP 653 have a positive excursion in Chemofacies B and then slightly decreases from 1.5 to 0 ‰ throughout this stratigraphic interval. The $\delta\ ^{15}N$ values in well COP 653 are between 3 and 4 ‰ in Chemofacies A and B. The $\delta\ ^{15}N$ values then decreases to approximately 1.5 ‰ and are succeeded by a sudden negative incursion to -1 ‰ near the boundary between Chemofacies E and F (Figure 47).

In contrast to C isotopes, the varying nitrogen isotopic patterns from these well indicate that the factors influencing nitrogen isotopes vary across the basin. The source of nitrogen in wells COP 259 and COP 653 is most likely a mixture of terrestrial runoff (4‰) and nitrogen-fixing from cyanobacteria (-2‰ to 0.5‰ (Sigman, Karsh, et al., 2009)). The water column near well COP 289 during the latter part of the Marcellus deposition may have been dominated by nitrogen fixation by cyanobacteria, or increased rainwater, which has $\delta\ ^{15}N$ ratios of -2 ‰ (Sigman, Karsh, et al., 2009), than the water columns near the other two wells.

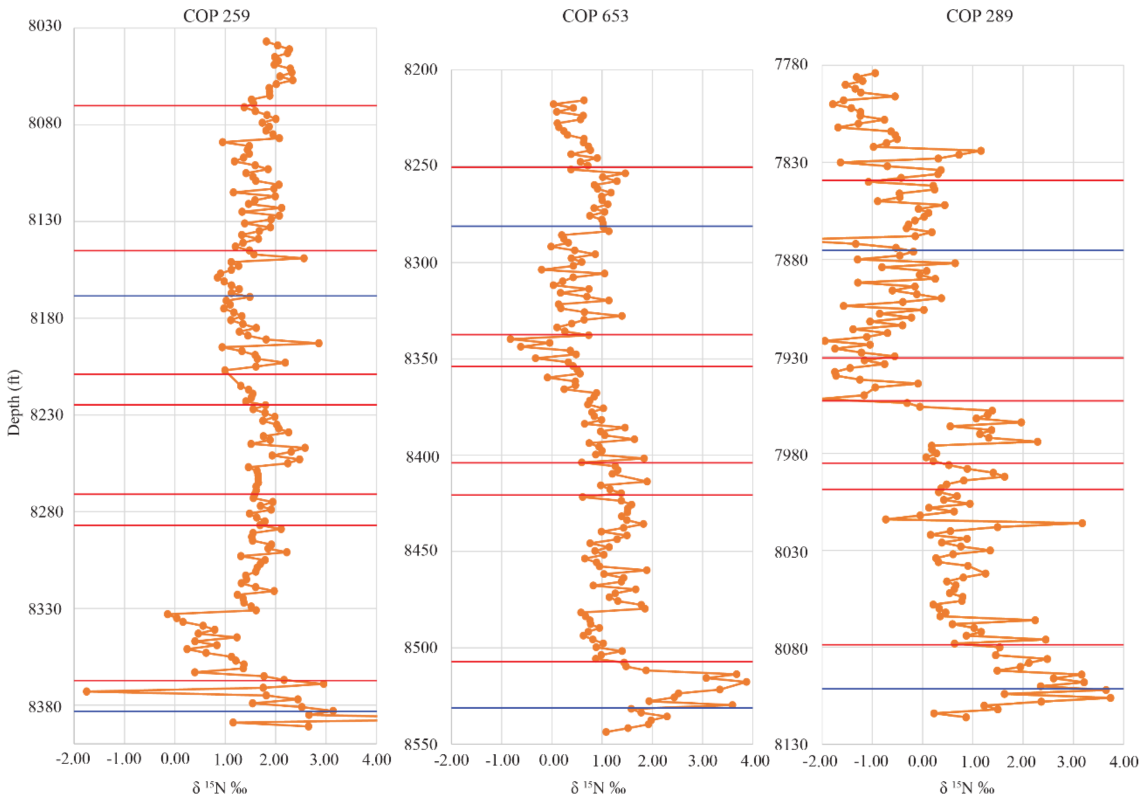

Figure 47. Comparison of stratigraphic variation in organic matter δ ^{15}N in all three well. Well COP 259 remains positive throughout the majority of the stratigraphic interval, well COP 653 has a negative trend, while well COP 289 has a strong negative excursion latter part of Marcellus deposition (transition from Chemofacies E to F). This suggests the dominant nitrogen source or process that affect the isotopic compositions were fairly localized when compared to the process affecting δ ^{13}C values.

Correlation of Physical Characteristics and Geochemical Attributes

TOC and lithofacies do not correlate. Bioturbated (mottled) mudstone is anticipated to have among the lowest TOC values; Figure 48 illustrates that bioturbated mudstone facies (Figure 9) has a higher average abundance of organic matter then the BLM facies. Bioturbation is usually considered evidence for O_2 at the sediment-water interface: however, these bioturbated intervals have high TOC (varying from 2-3 wt. %). A possible explanation is that mottled textures interpreted as bioturbation were caused by another process.

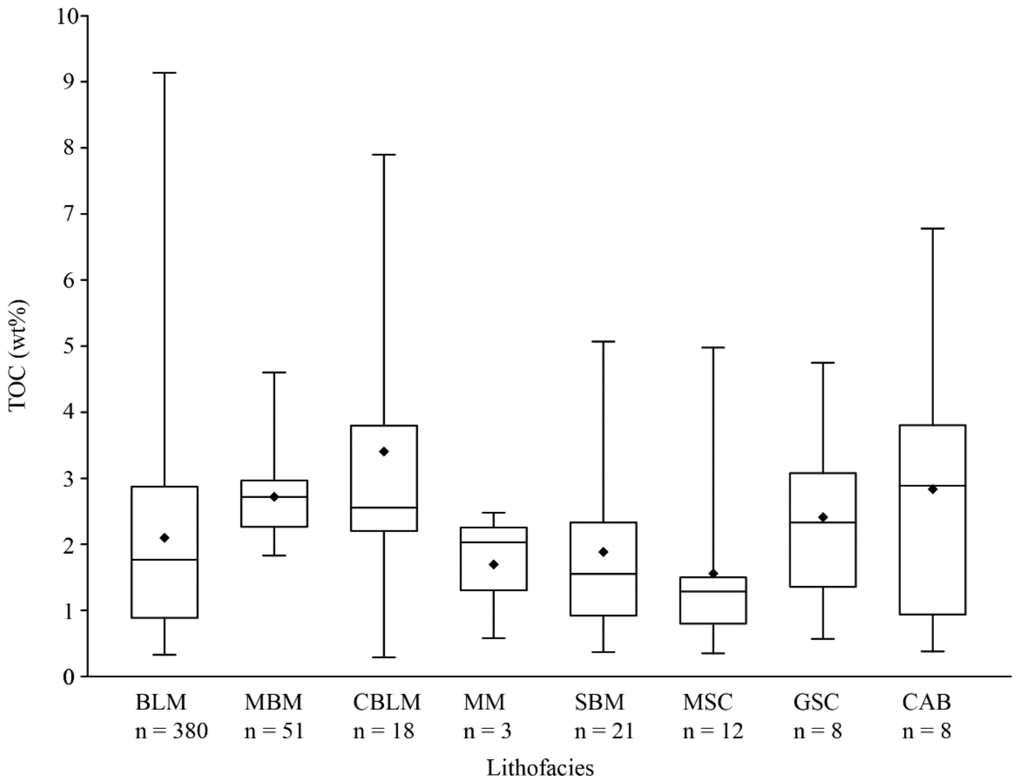

Figure 48. Boxplot of Lithofacies vs. TOC. The black diamond is the average value found within each lithofacies. CBLM has the highest average whereas while CAB has the highest median.

All three wells have a bioturbated interval just below Chemofacies F (Figure 18A, 19A, and 20A). Chemofacies F has redox-sensitive trace element concentrations that are indicative of oxic to dysoxic conditions, and C/N ratios and $\delta\ ^{13}C$ values that are closer to normal marine conditions. During this time, bioturbating organism could have entered the sediment and burrowed down into the top of sediments associated with Chemofacies E. If the bottom waters were dysoxic for an extended period of time, there may have been less destruction of organic matter and greater preservation of organic material. This hypothesis may explain the MBM in Chemofacies F observed in all three wells, but it cannot explain the bioturbation documented in Chemofacies C in well COP 289.

CHAPTER FIVE

Conclusion

Enriched Mo concentrations within the Marcellus and depleted concentrations found in the Onondaga Limestone and Mahantango Formation suggest the depositional water column in Appalachian Basin transitioned from oxic to euxinic and back to oxic conditions. The Mo/TOC proxy suggests that the basin was unrestricted to approximately 80% of open seawater conditions. High productivity indicators along with a lack of basin restriction suggests that organic matter production was a major factor in creating the euxinic conditions that existed during Marcellus deposition. The processes that provided nutrients to the water column decreased over time and concomitantly induced a trend of decreasing TOC within the study interval.

$\delta\,^{13}C$ values observed within in all three wells have a similar positive trend. This is likely caused by the decrease of ^{13}C discrimination because of the reduced availability of carbon within the system. The negative correlation of ^{13}C isotopes to TOC was possibly induced by a pycnocline and associated carbon recycling. The C/N ratios and the $\delta\,^{15}N$ values of the organic matter suggest that nitrogen was one of the limiting nutrients in the production of marine algae.

High TOC values observed within bioturbated intervals of the Marcellus are enigmatic. Intervals of bioturbation observed near the top of Chemofacies E may have been burrowed succeeding Chemofacies F deposition. Chemofacies F does appear to reach oxic to suboxic conditions, which could allow for a bioturbating organismst. This explanation cannot, however, explain the bioturbation and high TOC values observed within Chemofacies C of well COP 289. The mottled texture and its biological origin, however, may be a misinterpretation

APPENDIX

APPENDIX

Figures and Tables

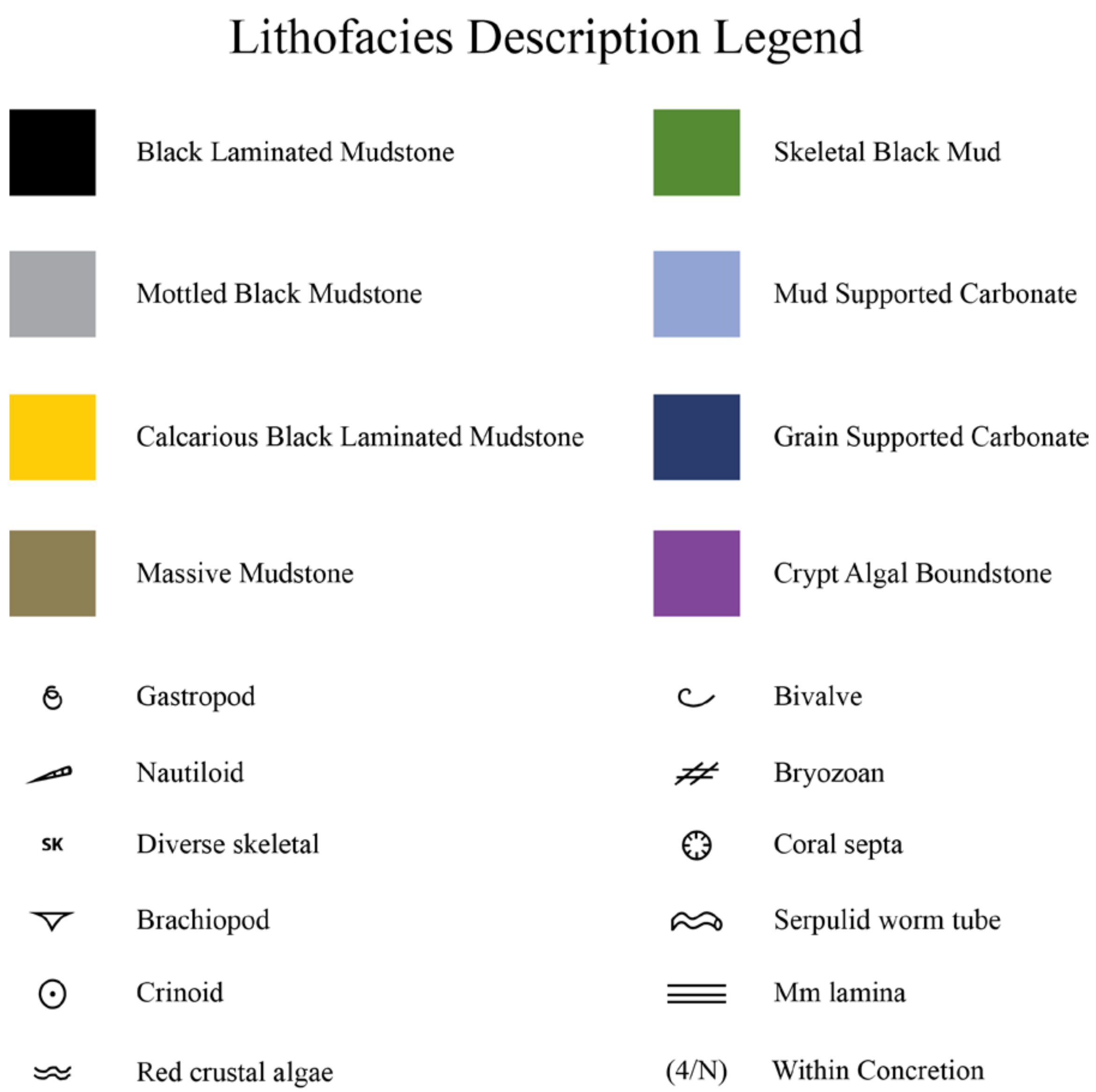

Figure A.1. Legend for the lithofacies descriptions

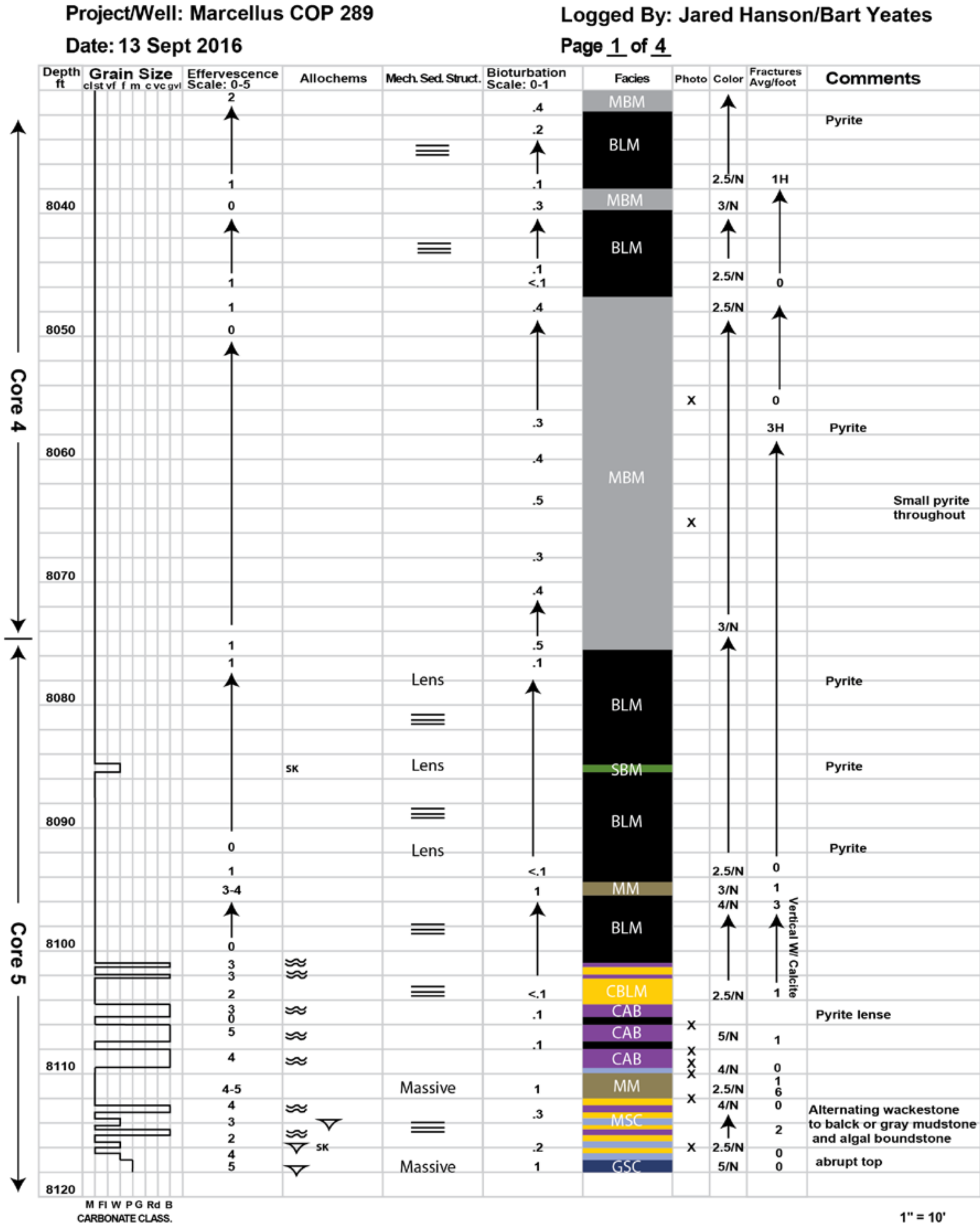

Figure A.2. Well COP 289 lithofacies description page 1 of 4.

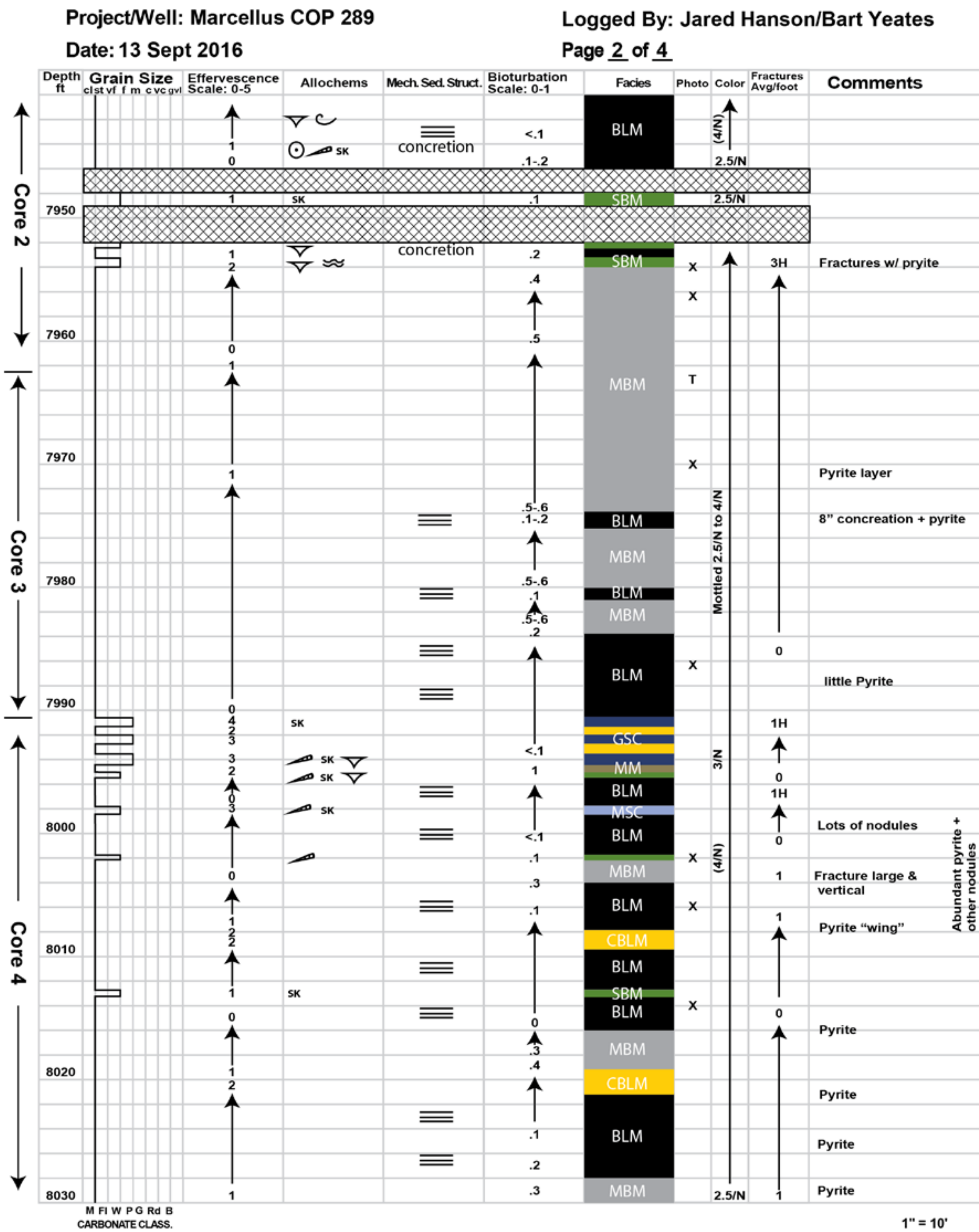

Figure A.3. Well COP 289 lithofacies description page 2 of 4

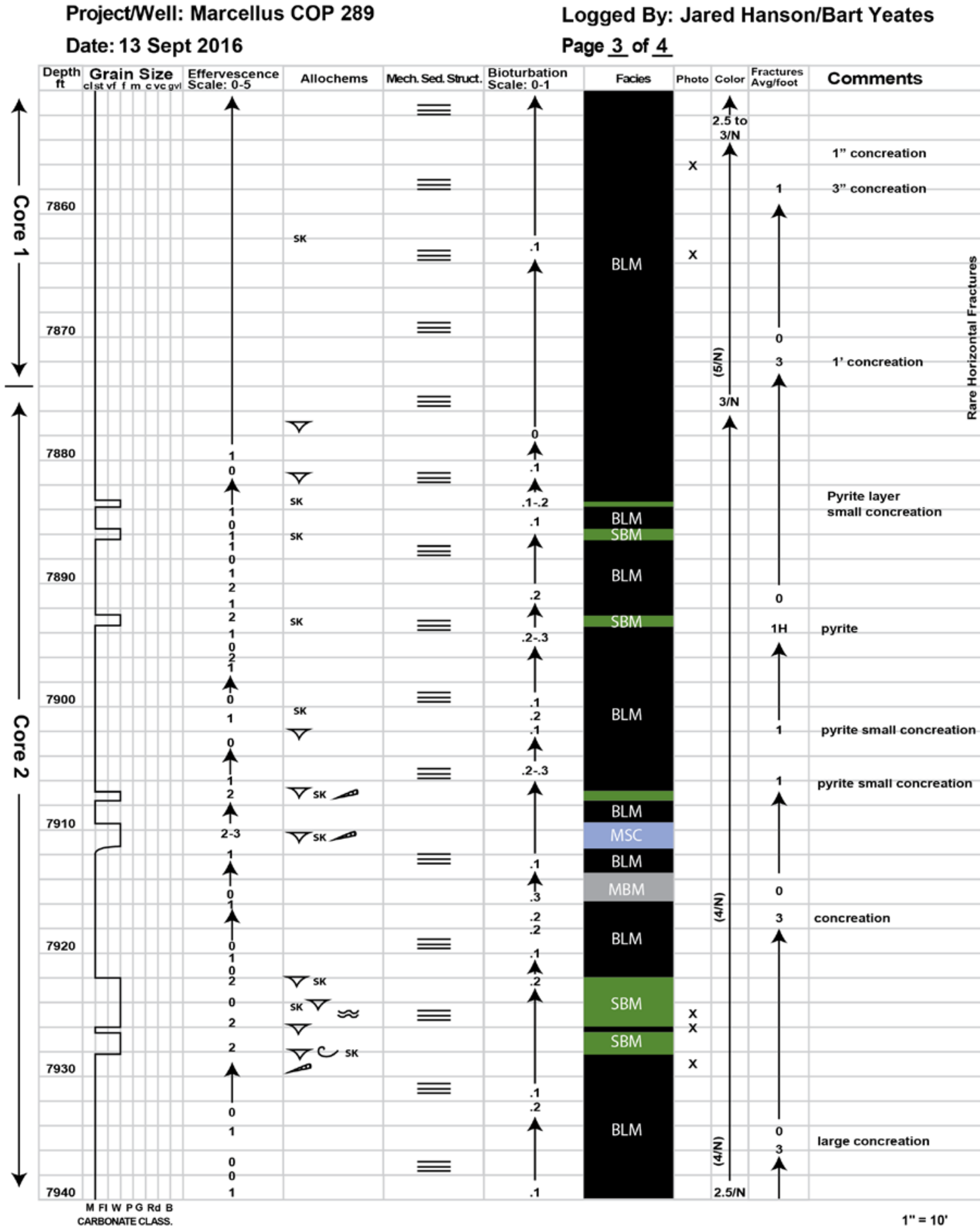

Figure A.4. Well COP 289 lithofacies description page 3 of 4

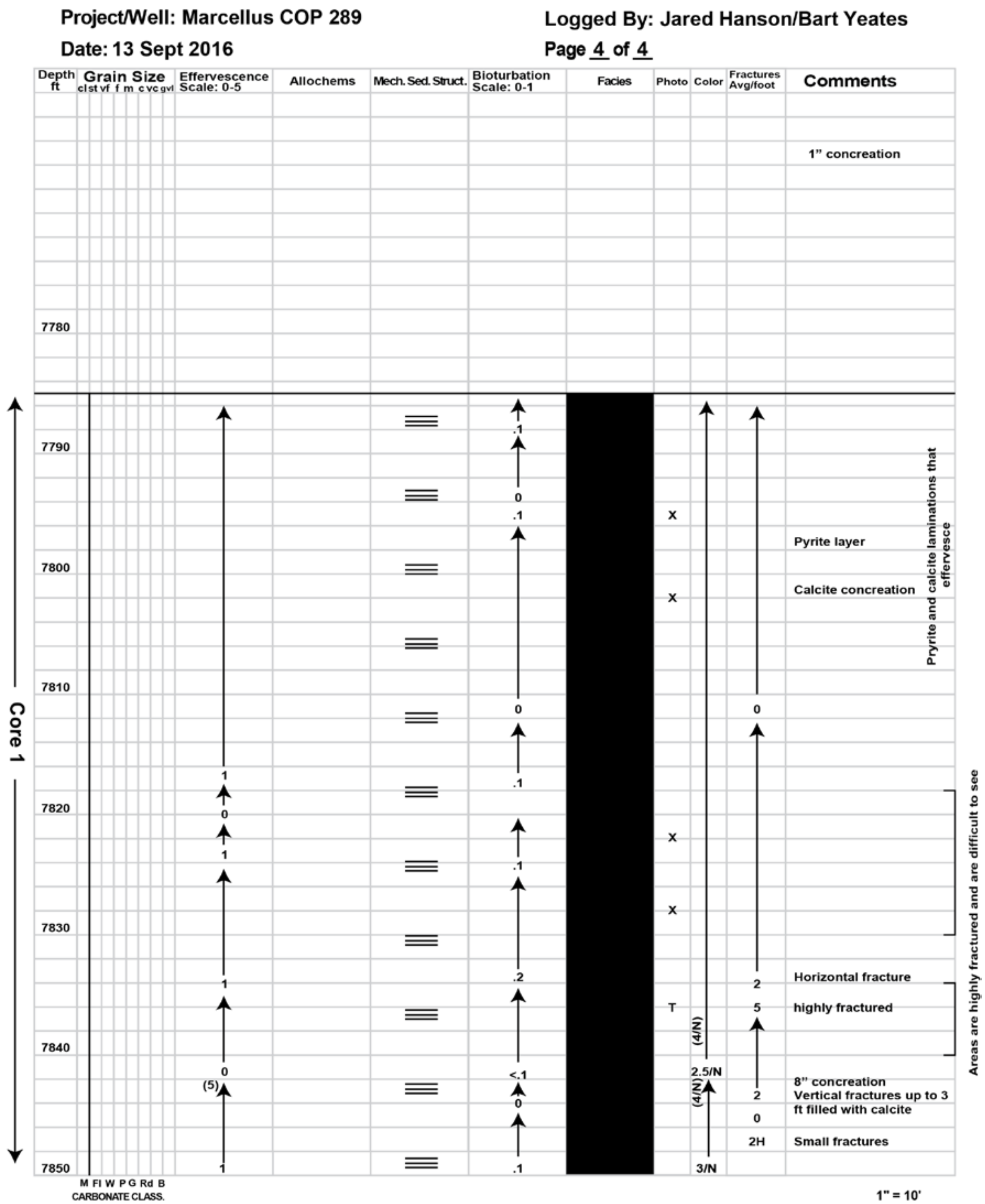

Figure A.5. Well COP 289 lithofacies description page 4 of 4

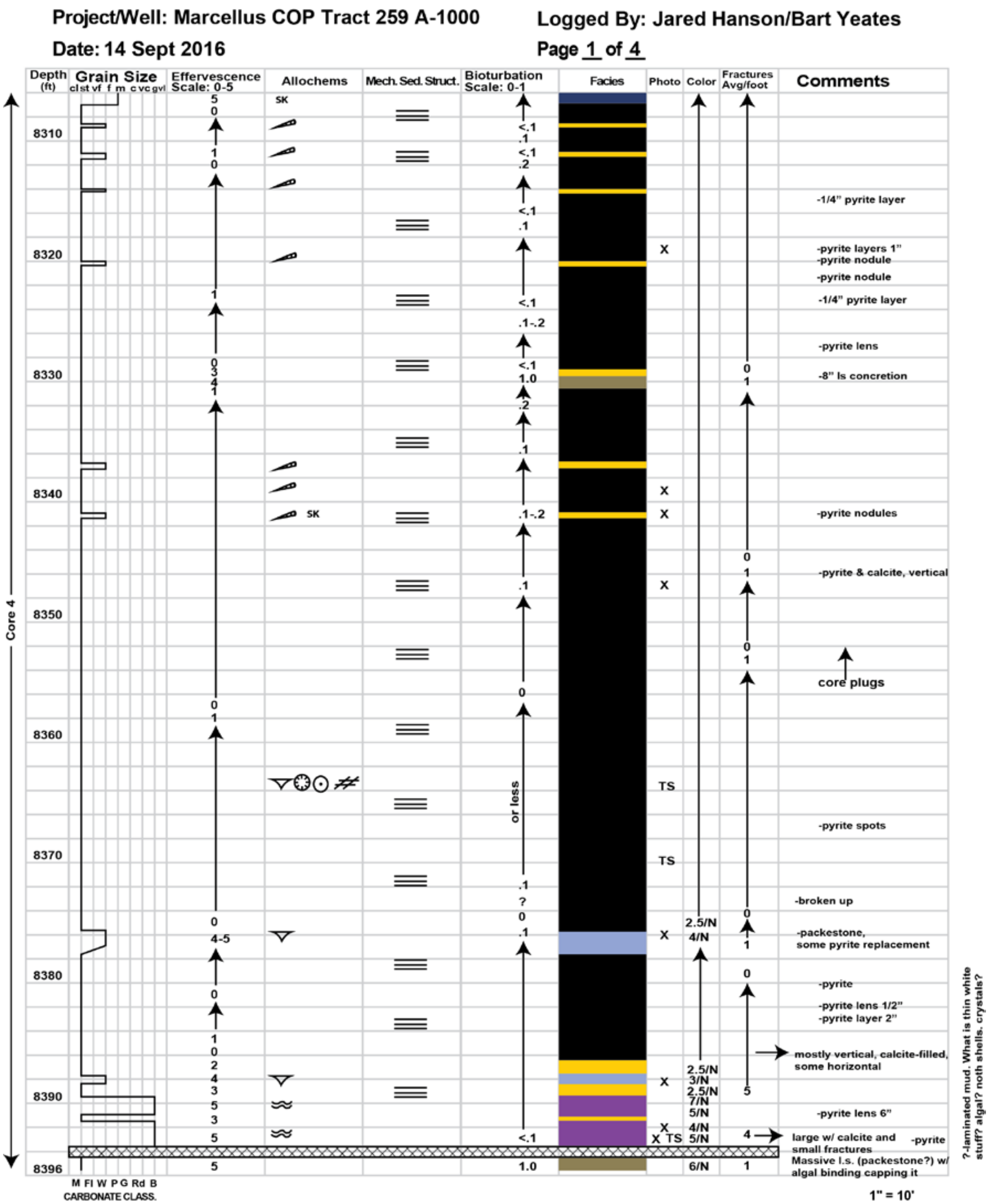

Figure 49. Well COP 259 lithofacies description page 1 of 4

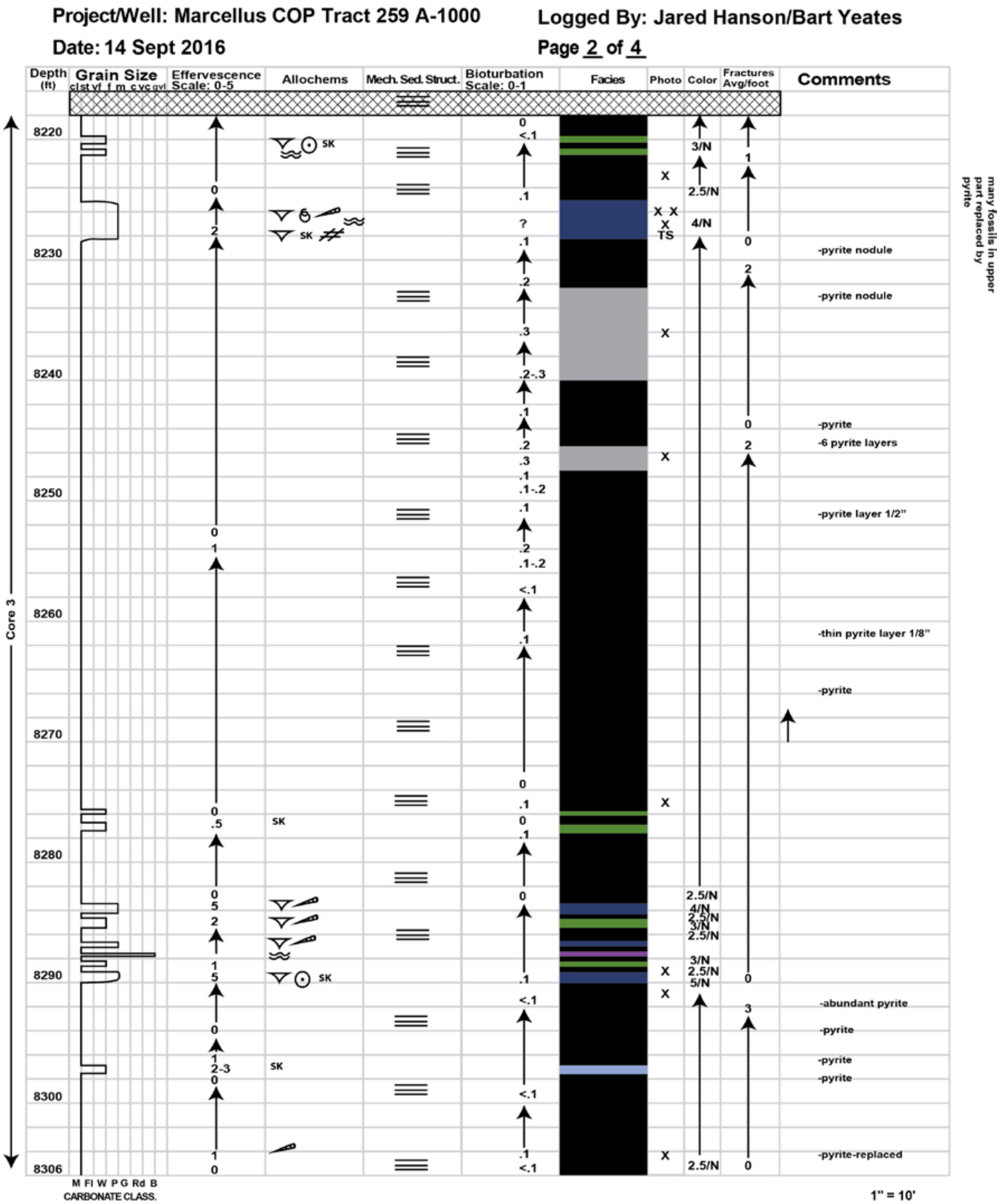

Figure A.7. Well COP 259 lithofacies description page 2 of 4

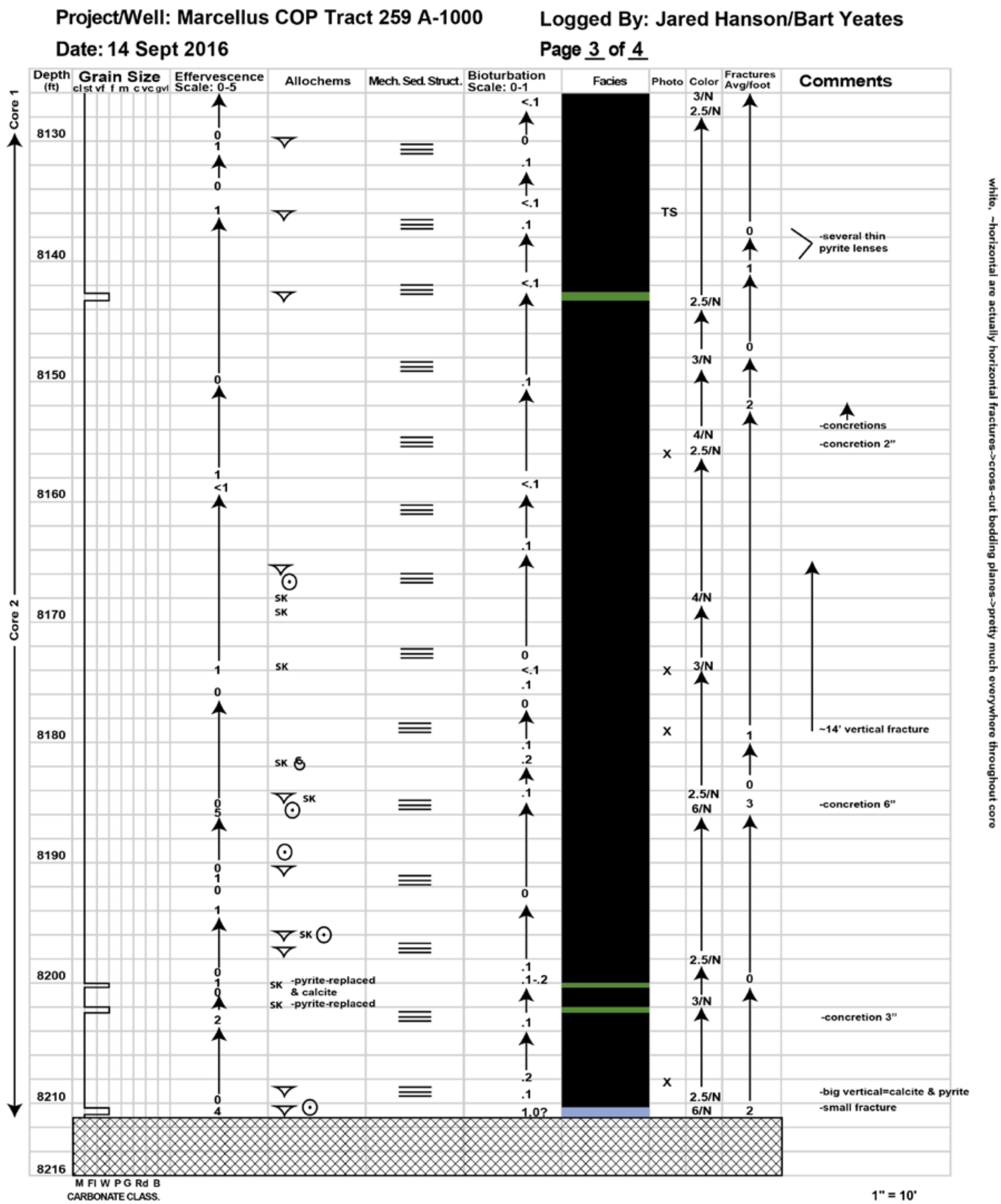

Figure A.8. Well COP 259 lithofacies description page 3 of 4

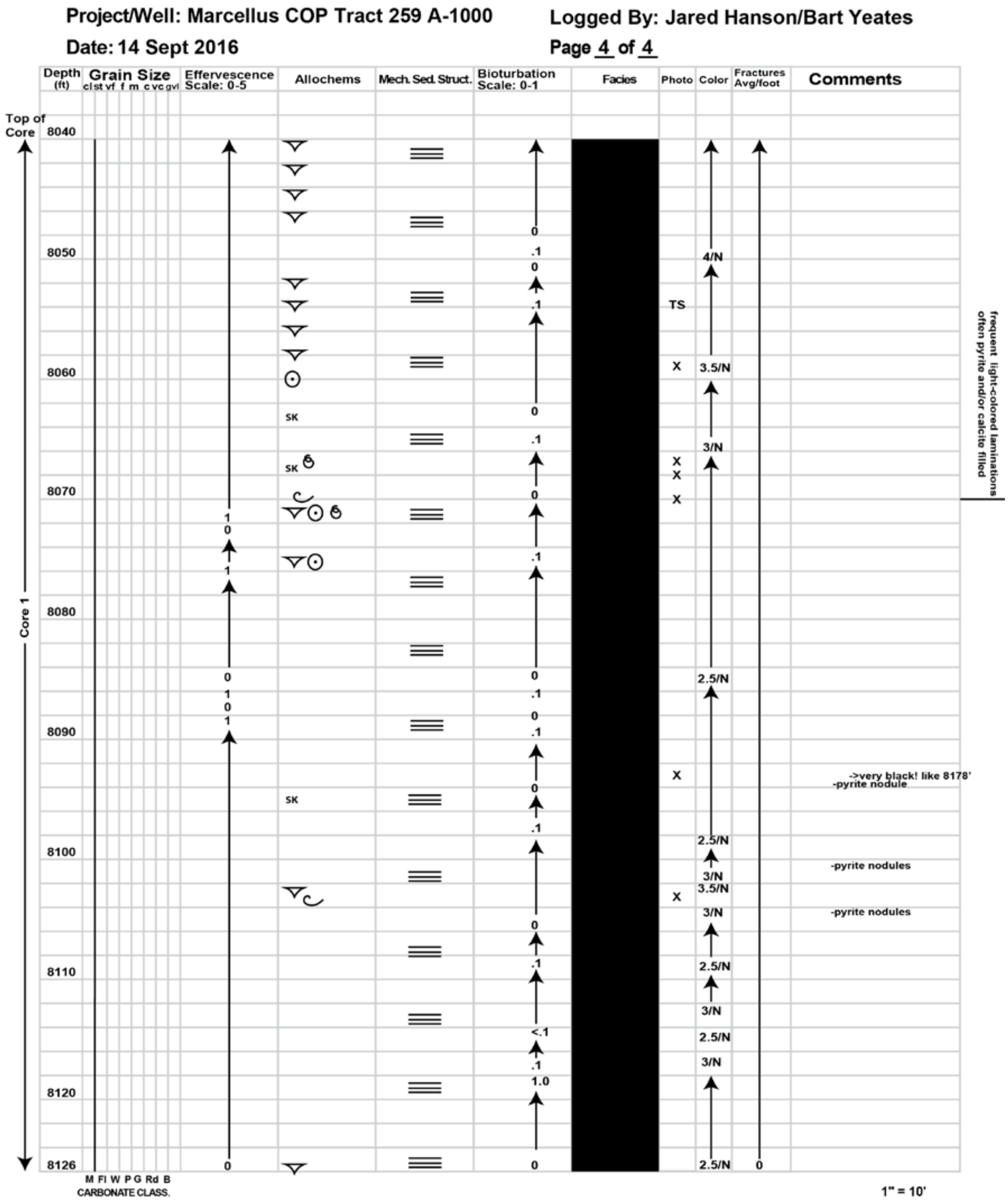

Figure A.9. Well COP 259 lithofacies description page 4 of 4

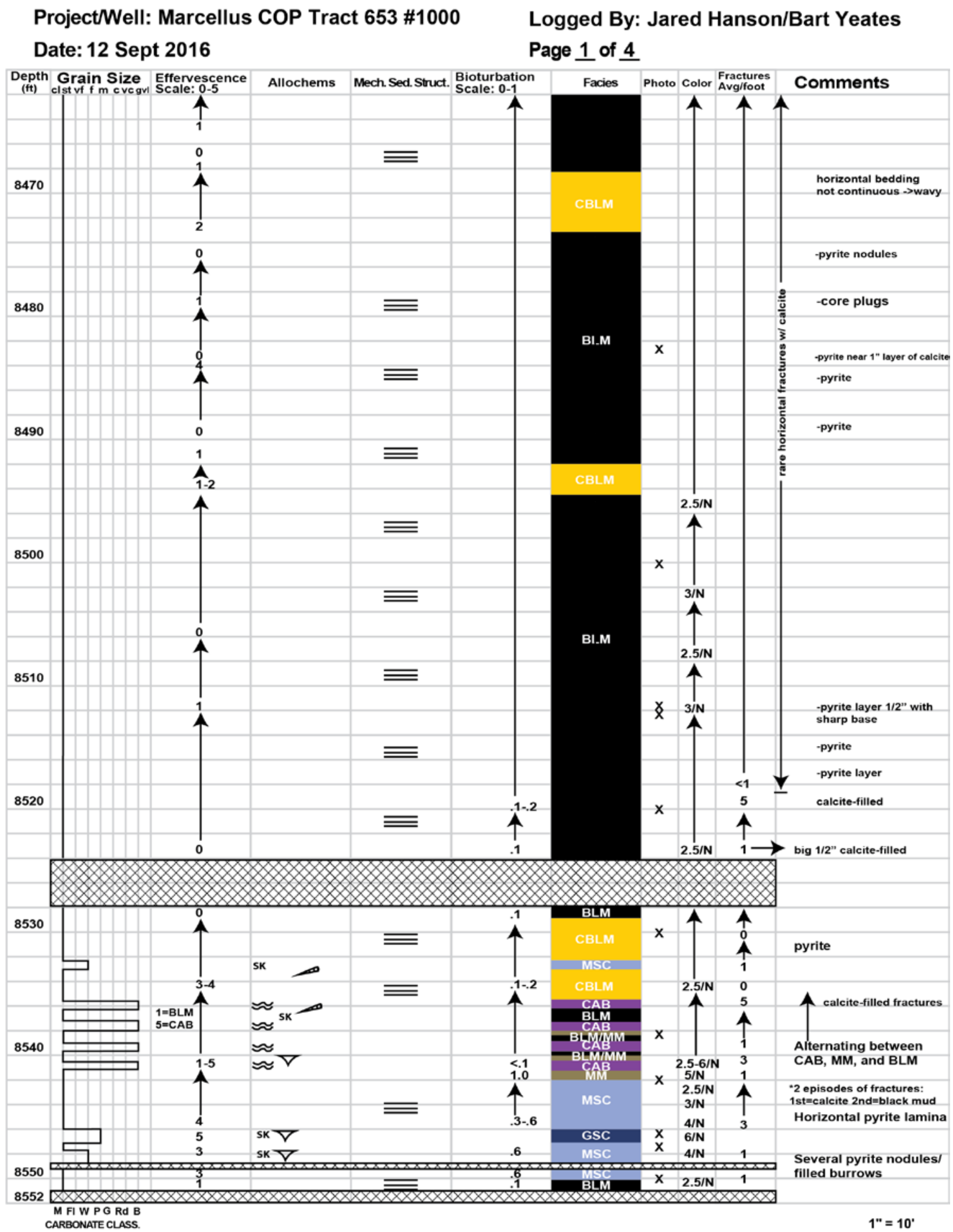

Figure A.10. Well COP 653 lithofacies description page 1 of 4

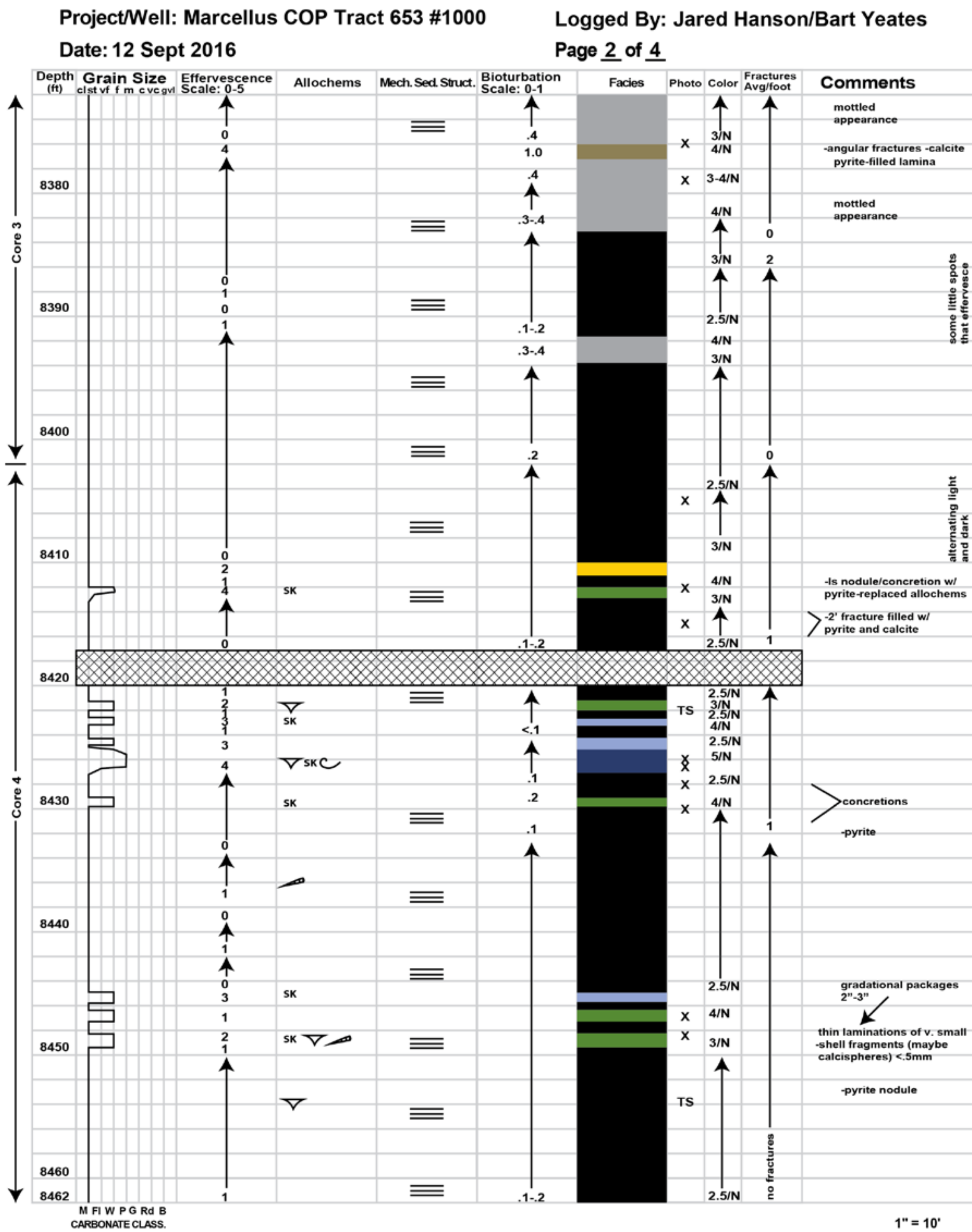

Figure A.11. Well COP 653 lithofacies description page 2 of 4

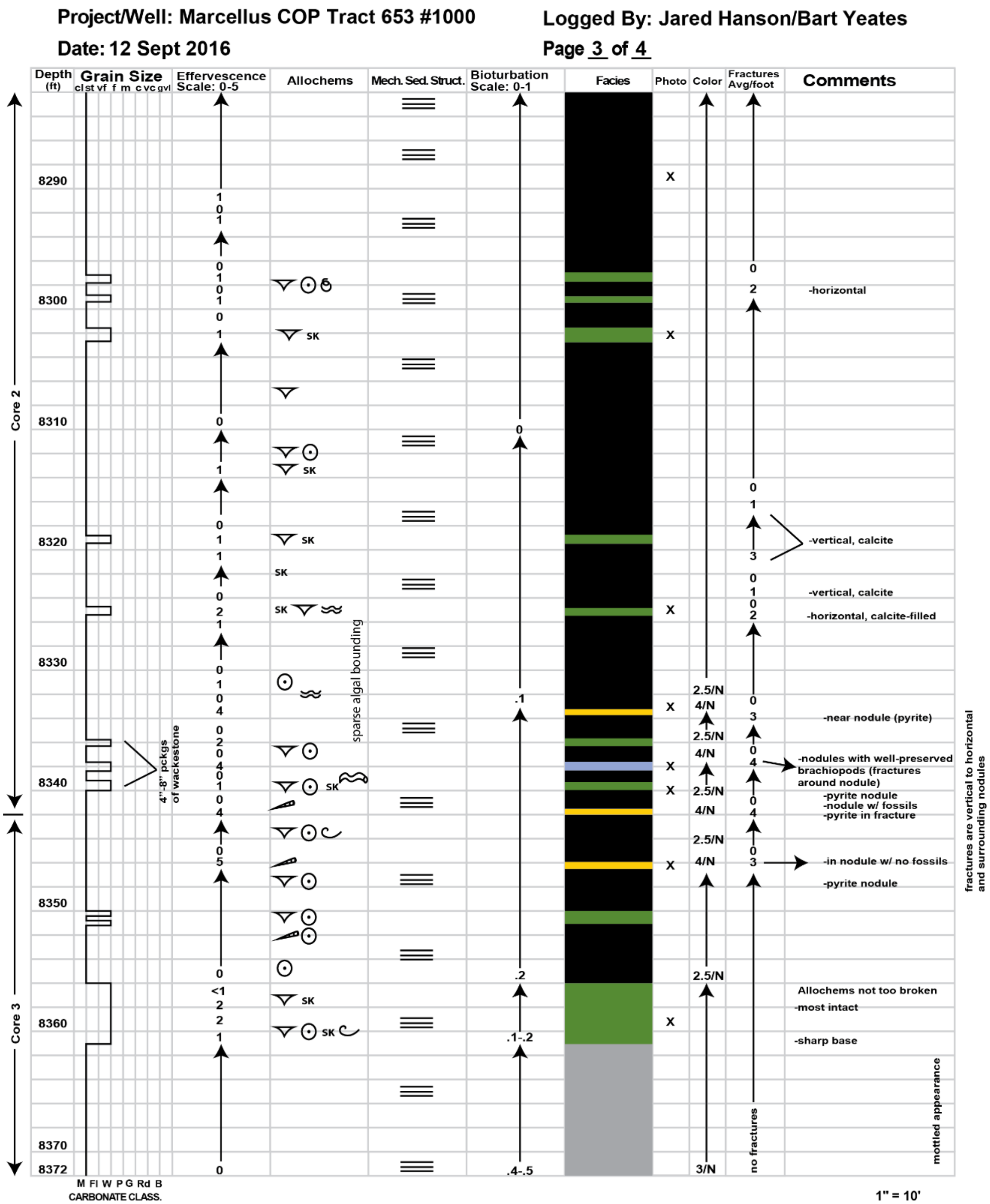

Figure A.12. Well COP 653 lithofacies description page 3 of 4

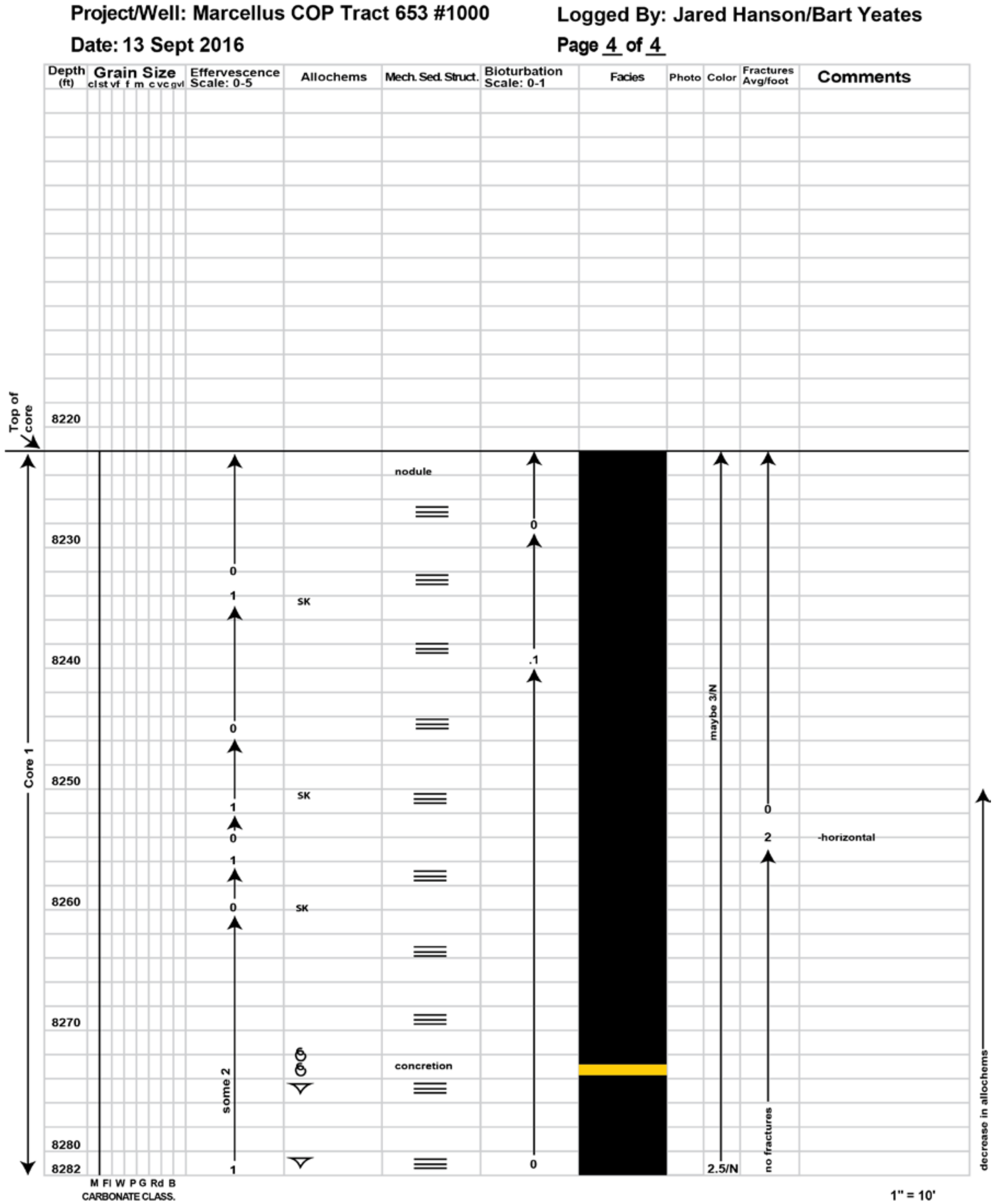

Figure A.13. Well COP 653 lithofacies description page 4 of 4.

Table A.1. Well COP 653 Carbon and Nitrogen Data

Depth ft	LC Depth ft	OC wt %	N wt %	δ ^{13}C ‰VPDB	δ ^{15}N ‰AIR	C/N N/A	IC wt %
8222	8215.75	0.52	0.14	-27.76	0.64	3.71	0.63
8224	8217.75	0.51	0.13	-27.39	0.03	3.92	0.51
8226	8219.75	0.54	0.13	-28.41	0.42	4.15	0.67
8228	8221.75	1.76	0.18	-28.55	0.10	9.78	-0.06
8230	8223.75	1.19	0.17	-28.57	0.62	7.00	-0.01
8232	8225.75	0.79	0.15	-28.35	0.57	5.27	0.84
8234	8227.75	0.69	0.14	-28.41	0.11	4.93	0.49
8236	8229.75	2.05	0.19	-28.54	0.14	10.79	-0.07
8238	8231.75	2.21	0.19	-28.68	0.24	11.63	0.01
8240	8233.75	2.00	0.18	-28.36	0.31	11.11	0.10
8242	8235.75	1.29	0.16	-28.58	0.64	8.06	0.48
8244	8237.75	1.66	0.18	-28.91	0.63	9.22	0.13
8246	8239.75	1.55	0.16	-28.52	0.73	9.69	0.67
8248	8241.75	1.41	0.16	-28.61	0.77	8.81	1.08
8250	8243.75	1.60	0.18	-28.65	0.38	8.89	0.02
8252	8245.75	1.06	0.15	-28.68	0.90	7.07	1.79
8254	8247.75	1.76	0.17	-28.74	0.56	10.35	0.38
8256	8249.75	1.56	0.17	-28.57	0.71	9.18	0.76
8258	8251.75	1.85	0.20	-28.59	0.38	9.25	-0.01
8260	8253.75	0.58	0.15	-28.95	1.46	3.87	2.52
8262	8255.75	0.68	0.15	-28.45	1.01	4.53	1.11
8264	8257.75	0.64	0.16	-29.06	1.29	4.00	0.97
8266	8259.75	0.43	0.16	-28.67	0.84	2.69	0.95
8268	8261.75	0.48	0.16	-28.43	0.91	3.00	1.24
8270	8263.75	0.52	0.15	-28.59	1.18	3.47	1.53
8272	8265.75	0.51	0.15	-28.62	0.99	3.40	1.22
8274	8267.75	0.49	0.15	-28.46	1.00	3.27	1.09
8276	8269.75	0.47	0.14	-28.61	1.11	3.36	1.31
8278	8271.75	0.49	0.16	-28.75	0.84	3.06	0.96
8280	8273.75	0.48	0.16	-28.72	1.05	3.00	1.01
8282	8275.75	0.55	0.16	-28.87	0.75	3.44	0.89
8284	8277.75	0.46	0.15	-28.50	0.99	3.07	1.24
8286	8279.75	0.52	0.16	-28.56	1.02	3.25	0.92
8288	8281.75	0.52	0.16	-28.71	1.03	3.25	1.12
8290	8283.75	0.79	0.16	-28.92	1.13	4.94	1.72
8292	8285.75	1.17	0.16	-29.31	0.20	7.31	0.43
8294	8287.75	1.58	0.18	-29.55	0.24	8.78	0.15
8296	8289.75	0.98	0.16	-29.33	0.32	6.13	0.52

Table A.1. Well COP 653 Carbon and Nitrogen Data Continued

Depth ft	LC Depth ft	OC wt %	N wt %	$\delta\,^{13}C$ ‰VPDB	$\delta\,^{15}N$ ‰AIR	C/N N/A	IC wt %
8298	8291.75	1.72	0.19	-29.43	-0.02	9.05	-0.02
8300	8293.75	0.75	0.16	-29.14	0.45	4.69	1.10
8302	8295.75	0.92	0.18	-29.18	0.86	5.11	0.63
8304	8297.75	1.23	0.17	-29.47	0.39	7.24	0.76
8306	8299.75	1.39	0.18	-29.67	0.59	7.72	0.89
8308	8301.75	1.70	0.20	-29.82	0.42	8.50	-0.07
8310	8303.75	1.92	0.19	-30.34	-0.21	10.11	0.33
8312	8305.75	0.70	0.17	-29.41	1.05	4.12	1.48
8314	8307.75	1.77	0.20	-29.95	0.42	8.85	0.06
8316	8309.75	1.73	0.20	-29.94	0.21	8.65	0.07
8318	8311.75	1.25	0.20	-29.65	0.03	6.25	0.03
8320	8313.75	1.69	0.18	-30.01	0.73	9.39	1.16
8322	8315.75	0.90	0.17	-29.63	0.17	5.29	0.89
8324	8317.75	1.79	0.21	-30.05	0.69	8.52	0.40
8326	8319.75	1.25	0.16	-29.95	1.13	7.81	2.91
8328	8321.75	2.38	0.22	-29.99	0.13	10.82	0.19
8330	8323.75	2.00	0.21	-29.91	0.18	9.52	0.28
8332	8325.75	1.30	0.20	-29.93	0.65	6.50	0.51
8334	8327.75	1.27	0.18	-29.88	1.39	7.06	1.85
8336	8329.75	2.76	0.24	-30.06	0.64	11.50	-0.07
8338	8331.75	1.37	0.20	-29.74	0.39	6.85	0.53
8340	8333.75	1.50	0.22	-29.76	0.10	6.82	0.51
8342	8335.75	1.43	0.21	-29.63	0.26	6.81	-0.02
8344	8337.75	1.56	0.22	-29.53	0.73	7.09	-0.02
8346	8339.75	1.05	0.20	-29.65	-0.83	5.25	0.23
8348	8341.75	0.98	0.20	-29.29	-0.04	4.90	0.35
8350	8343.75	0.75	0.20	-28.80	-0.62	3.75	0.12
8352	8345.75	1.76	0.21	-29.38	0.36	8.38	0.24
8354	8347.75	1.34	0.22	-29.01	0.48	6.09	-0.09
8356	8349.75	1.32	0.22	-29.33	-0.33	6.00	-0.05
8358	8351.75	0.37	0.17	-28.10	0.32	2.18	2.63
8360	8353.75	0.93	0.19	-29.04	0.42	4.89	1.25
8362	8355.75	2.71	0.24	-29.85	0.50	11.29	-0.10
8364	8357.75	2.33	0.23	-29.99	0.56	10.13	0.01
8366	8359.75	2.22	0.24	-30.08	-0.09	9.25	0.01
8368	8361.75	2.44	0.24	-29.93	0.46	10.17	-0.06
8370	8363.75	2.80	0.24	-30.09	0.47	11.67	-0.13
8372	8365.75	2.72	0.24	-30.05	0.24	11.33	0.07
8374	8367.75	2.77	0.24	-29.93	0.89	11.54	-0.13
8376	8369.75	2.99	0.23	-30.09	0.84	13.00	-0.05

Table A.1. Well COP 653 Carbon and Nitrogen Data Continued

Depth ft	LC Depth ft	OC wt %	N wt %	δ ^{13}C ‰VPDB	δ ^{15}N ‰AIR	C/N N/A	IC wt %
8378	8371.75	2.81	0.23	-30.17	0.75	12.22	0.02
8380	8373.75	3.06	0.24	-30.22	0.71	12.75	0.21
8386	8379.75	3.10	0.22	-30.21	0.84	14.09	0.16
8388	8381.75	3.30	0.23	-30.04	0.99	14.35	0.05
8390	8383.75	3.40	0.24	-30.15	0.65	14.17	0.02
8392	8385.75	2.98	0.23	-30.08	1.45	12.96	0.14
8394	8387.75	3.78	0.25	-30.14	0.97	15.12	0.00
8396	8389.75	4.56	0.27	-30.12	1.05	16.89	-0.03
8398	8391.75	3.41	0.22	-30.07	1.64	15.50	0.53
8400	8393.75	3.64	0.23	-29.99	0.74	15.83	0.19
8402	8395.75	2.96	0.23	-29.96	0.94	12.87	-0.10
8404	8397.75	3.02	0.23	-30.12	1.00	13.13	0.16
8406	8399.75	3.03	0.25	-30.26	0.87	12.12	0.24
8408	8401.75	3.16	0.26	-30.37	1.83	12.15	0.68
8410	8403.75	3.84	0.25	-30.27	0.59	15.36	0.96
8412	8405.75	2.32	0.19	-30.12	1.26	12.21	2.51
8414	8407.75	3.39	0.24	-29.80	1.31	14.13	0.08
8416	8409.75	3.60	0.24	-29.92	1.20	15.00	0.01
8420	8413.75	1.69	0.12	-29.60	1.89	14.08	6.77
8422	8415.75	4.70	0.27	-30.06	0.97	17.41	0.95
8424	8417.75	6.09	0.25	-29.99	1.15	24.36	3.44
8426	8419.75	1.46	0.09	-30.38	1.38	16.22	8.02
8428	8421.75	4.46	0.31	-30.75	0.61	14.39	0.31
8430	8423.75	2.65	0.25	-30.66	1.38	10.60	1.18
8432	8425.75	4.03	0.24	-30.48	1.59	16.79	1.37
8434	8427.75	2.52	0.23	-30.63	1.51	10.96	1.02
8436	8429.75	3.88	0.23	-30.53	1.50	16.87	0.97
8438	8431.75	3.12	0.22	-30.67	1.39	14.18	1.32
8440	8433.75	3.45	0.23	-30.59	1.49	15.00	0.98
8442	8435.75	2.66	0.19	-30.60	1.82	14.00	2.34
8444	8437.75	3.54	0.23	-30.58	1.43	15.39	0.71
8446	8439.75	3.56	0.26	-30.77	0.98	13.69	0.32
8448	8441.75	3.23	0.22	-30.55	1.49	14.68	1.81
8450	8443.75	3.23	0.25	-30.77	1.30	12.92	1.23
8452	8445.75	2.16	0.23	-30.86	0.76	9.39	0.85
8454	8447.75	2.26	0.25	-30.71	1.14	9.04	0.61
8456	8449.75	1.80	0.23	-30.78	0.86	7.83	1.12
8458	8451.75	2.88	0.23	-30.65	1.03	12.52	0.90
8460	8453.75	2.14	0.24	-30.86	0.65	8.92	1.00
8462	8455.75	2.40	0.23	-30.65	0.89	10.43	0.65

Table A.1. Well COP 653 Carbon and Nitrogen Data Continued

Depth	LC Depth	OC	N	δ ^{13}C	δ ^{15}N	C/N	IC
ft	ft	wt %	wt %	‰VPDB	‰AIR	N/A	wt %
8464	8457.75	2.29	0.23	-30.69	0.95	9.96	0.72
8466	8459.75	2.87	0.25	-30.89	1.89	11.48	0.86
8472	8465.75	2.45	0.21	-30.69	1.38	11.67	1.37
8474	8467.75	2.66	0.24	-30.99	0.82	11.08	0.63
8476	8469.75	2.58	0.24	-30.84	1.67	10.75	1.06
8478	8471.75	2.30	0.22	-30.56	1.26	10.45	0.56
8480	8473.75	2.25	0.23	-30.71	1.14	9.78	0.31
8482	8475.75	2.34	0.24	-30.71	1.31	9.75	0.37
8484	8477.75	2.96	0.23	-30.83	1.78	12.87	0.79
8486	8479.75	2.32	0.24	-30.84	1.85	9.67	0.71
8488	8481.75	3.44	0.25	-30.89	0.58	13.76	0.10
8490	8483.75	3.33	0.25	-30.91	0.67	13.32	0.85
8492	8485.75	2.14	0.21	-30.84	0.76	10.19	1.18
8494	8487.75	2.37	0.23	-30.70	0.77	10.30	0.69
8496	8489.75	2.43	0.23	-30.85	0.94	10.57	0.48
8498	8491.75	2.81	0.25	-30.91	0.72	11.24	0.07
8500	8493.75	2.13	0.22	-31.01	0.63	9.68	0.90
8502	8495.75	2.90	0.23	-30.92	0.81	12.61	0.61
8504	8497.75	2.11	0.22	-30.94	1.02	9.59	0.38
8506	8499.75	2.51	0.25	-30.94	0.88	10.04	0.49
8508	8501.75	2.89	0.24	-31.01	1.40	12.04	1.01
8510	8503.75	2.73	0.25	-30.96	0.98	10.92	0.76
8512	8505.75	2.69	0.25	-31.11	0.87	10.76	0.31
8514	8507.75	5.89	0.30	-31.16	1.43	19.63	0.36
8516	8509.75	4.62	0.24	-31.32	1.47	19.25	0.74
8518	8511.75	7.09	0.30	-31.23	1.87	23.63	0.58
8520	8513.75	7.35	0.29	-31.16	3.68	25.34	1.16
8522	8515.75	8.63	0.35	-31.17	3.07	24.66	0.67
8524	8517.75	5.86	0.26	-31.17	3.87	22.54	0.89
8528	8521.75	9.14	0.28	-31.15	3.34	32.64	0.37
8530	8523.75	6.19	0.19	-30.96	2.52	32.58	4.15
8532	8525.75	7.90	0.21	-31.22	2.43	37.62	1.90
8534	8527.75	7.77	0.24	-31.40	1.93	32.38	6.11
8536	8529.75	2.85	0.07	-31.20	3.60	40.71	9.68
8538	8531.75	2.03	0.13	-30.65	1.58	15.62	7.81
8540	8533.75	1.58	0.12	-30.76	1.78	13.17	9.67
8542	8535.75	0.58	0.03	-30.00	2.29	19.33	10.32
8544	8537.75	0.77	0.09	-28.82	1.97	8.56	8.90
8546	8539.75	0.81	0.10	-29.51	1.92	8.10	6.83
8548	8541.75	1.53	0.21	-29.72	1.51	7.29	3.09
8550	8543.75	0.35	0.06	-29.51	1.08	5.83	6.55

Table A.2. Well COP 259 Carbon and Nitrogen Data

Depth ft	LC Depth ft	OC wt %	N wt %	$\delta\ ^{13}C$ ‰VPDB	$\delta\ ^{15}N$ ‰AIR	C/N N/A	IC wt %
8040	8037	0.45	0.12	-28.38	1.81	3.75	0.59
8042	8039	0.44	0.11	-28.28	2.04	4.00	0.78
8044	8041	0.41	0.12	-28.32	2.27	3.42	0.72
8046	8043	0.46	0.12	-28.64	2.23	3.83	0.78
8048	8045	0.47	0.13	-28.27	1.98	3.62	0.55
8050	8047	0.42	0.12	-28.32	2.05	3.50	0.71
8052	8049	0.44	0.12	-28.29	1.97	3.67	0.84
8054	8051	0.42	0.11	-28.44	2.29	3.82	0.86
8056	8053	0.39	0.10	-28.49	2.32	3.90	1.05
8058	8055	0.42	0.11	-28.41	2.08	3.82	0.83
8060	8057	0.70	0.10	-28.72	2.34	7.00	0.92
8062	8059	0.47	0.12	-28.64	2.01	3.92	0.77
8064	8061	0.43	0.12	-28.50	1.87	3.58	0.89
8066	8063	0.51	0.12	-28.57	1.88	4.25	0.83
8068	8065	0.50	0.11	-28.56	1.88	4.55	0.76
8070	8067	0.48	0.13	-28.29	1.52	3.69	0.76
8072	8069	0.73	0.14	-28.77	1.56	5.21	0.78
8074	8071	0.67	0.14	-28.72	1.37	4.79	0.56
8076	8073	0.90	0.14	-28.97	1.60	6.43	0.64
8078	8075	1.30	0.15	-29.00	1.83	8.67	0.09
8080	8077	1.36	0.16	-29.23	2.00	8.50	0.13
8082	8079	1.26	0.15	-29.09	1.73	8.40	0.12
8084	8081	1.69	0.16	-29.14	1.87	10.56	0.11
8086	8083	1.82	0.17	-29.19	1.81	10.71	-0.07
8088	8085	1.16	0.15	-28.84	1.94	7.73	0.33
8090	8087	0.89	0.15	-28.72	2.07	5.93	0.80
8092	8089	0.98	0.15	-29.01	0.95	6.53	0.37
8094	8091	1.05	0.16	-28.92	1.47	6.56	0.16
8096	8093	1.38	0.18	-29.31	1.44	7.67	-0.06
8098	8095	1.02	0.17	-29.27	1.47	6.00	0.02
8100	8097	0.76	0.16	-29.03	1.36	4.75	0.40
8102	8099	0.52	0.14	-28.61	1.18	3.71	0.60
8104	8101	0.66	0.15	-28.81	1.59	4.40	0.33
8106	8103	1.31	0.18	-29.35	1.85	7.28	0.02
8108	8105	1.45	0.18	-29.48	1.41	8.06	0.00
8110	8107	0.93	0.17	-29.11	1.55	5.47	0.07
8112	8109	0.77	0.16	-28.98	1.60	4.81	0.40
8114	8111	1.43	0.19	-29.32	2.06	7.53	-0.08
8116	8113	1.25	0.17	-29.23	1.97	7.35	0.11
8118	8115	1.15	0.18	-29.20	1.16	6.39	-0.02

Table A.2. Well COP 259 Carbon and Nitrogen Data Continued

Depth ft	LC Depth ft	OC wt %	N wt %	$\delta^{13}C$ ‰VPDB	$\delta^{15}N$ ‰AIR	C/N N/A	IC wt %
8120	8117	1.10	0.17	-29.21	1.99	6.47	0.21
8122	8119	1.02	0.16	-29.14	1.59	6.38	0.53
8124	8121	1.31	0.18	-29.25	1.46	7.28	-0.02
8126	8123	0.96	0.16	-29.16	2.12	6.00	0.92
8128	8125	0.88	0.16	-29.11	1.33	5.50	0.56
8130	8127	0.94	0.16	-29.24	2.07	5.88	0.99
8132	8129	1.29	0.18	-29.31	1.91	7.17	0.00
8134	8131	1.16	0.16	-29.22	1.38	7.25	0.50
8136	8133	0.96	0.16	-29.08	1.89	6.00	1.20
8138	8135	1.46	0.17	-29.44	1.67	8.59	0.07
8140	8137	1.10	0.16	-29.20	1.32	6.88	0.72
8142	8139	1.28	0.16	-29.01	1.66	8.00	1.02
8144	8141	1.36	0.16	-29.23	1.35	8.50	0.34
8146	8143	1.48	0.18	-29.31	1.20	8.22	-0.04
8148	8145	1.41	0.18	-29.57	1.48	7.83	0.25
8150	8147	1.01	0.17	-29.11	1.57	5.94	0.34
8152	8149	0.56	0.16	-28.74	2.56	3.50	1.44
8154	8151	0.47	0.15	-28.89	1.11	3.13	0.94
8156	8153	0.60	0.15	-28.68	1.26	4.00	0.57
8158	8155	0.45	0.15	-28.63	1.12	3.00	0.64
8160	8157	0.47	0.14	-28.52	0.90	3.36	1.00
8162	8159	0.50	0.15	-28.57	0.84	3.33	1.21
8164	8161	0.47	0.15	-28.73	0.98	3.13	1.06
8166	8163	0.46	0.15	-28.95	1.12	3.07	1.13
8168	8165	0.50	0.16	-28.48	1.27	3.13	0.99
8170	8167	0.47	0.14	-29.05	1.12	3.36	1.12
8172	8169	0.53	0.15	-28.63	1.49	3.53	0.99
8174	8171	1.16	0.17	-28.64	1.02	6.82	0.28
8176	8173	1.16	0.17	-28.84	1.09	6.82	0.15
8178	8175	1.38	0.17	-29.12	0.97	8.12	0.35
8180	8177	0.99	0.17	-28.97	1.17	5.82	0.31
8182	8179	1.04	0.17	-28.91	1.33	6.12	0.14
8184	8181	0.48	0.17	-29.19	1.11	2.82	0.64
8186	8183	1.03	0.17	-29.17	1.35	6.06	0.49
8188	8185	1.44	0.20	-28.89	1.61	7.20	-0.05
8190	8187	1.77	0.20	-29.40	1.28	8.85	0.32
8192	8189	1.15	0.17	-29.16	1.45	6.76	0.40
8194	8191	0.67	0.17	-29.11	1.81	3.94	1.30
8196	8193	2.18	0.22	-28.81	2.86	9.91	0.07
8198	8195	1.58	0.20	-29.54	0.94	7.90	0.04

Table A.2. Well COP 259 Carbon and Nitrogen Data Continued

Depth ft	LC Depth ft	OC wt %	N wt %	$\delta^{13}C$ ‰VPDB	$\delta^{15}N$ ‰AIR	C/N N/A	IC wt %
8200	8197	0.92	0.18	-29.86	1.33	5.11	0.91
8202	8199	1.18	0.17	-30.08	1.59	6.94	2.22
8204	8201	2.84	0.23	-29.49	1.63	12.35	-0.03
8206	8203	2.18	0.23	-29.73	2.19	9.48	-0.06
8208	8205	1.92	0.21	-29.70	1.61	9.14	0.05
8210	8207	2.30	0.23	-29.35	0.99	10.00	0.01
8218	8215	0.91	0.19	-29.92	1.30	4.79	0.40
8220	8217	0.87	0.21	-29.80	1.46	4.14	0.05
8222	8219	1.82	0.22	-29.23	1.54	8.27	0.00
8224	8221	1.38	0.21	-29.26	1.51	6.57	-0.11
8226	8223	1.05	0.18	-28.86	1.41	5.83	1.07
8228	8225	2.23	0.21	-29.96	1.80	10.62	-0.15
8230	8227	2.56	0.20	-30.05	1.55	12.80	-0.09
8232	8229	2.32	0.21	-30.06	1.79	11.05	-0.10
8234	8231	2.37	0.21	-30.07	1.98	11.29	-0.03
8236	8233	2.27	0.20	-30.13	1.75	11.35	-0.14
8238	8235	2.62	0.21	-30.26	2.02	12.48	-0.18
8240	8237	2.94	0.21	-30.05	2.06	14.00	-0.06
8242	8239	2.39	0.19	-30.03	2.25	12.58	-0.04
8244	8241	2.55	0.20	-30.28	1.75	12.75	0.12
8246	8243	2.97	0.21	-30.32	1.89	14.14	0.21
8248	8245	3.27	0.22	-30.30	1.51	14.86	0.08
8250	8247	2.77	0.20	-30.15	2.58	13.85	-0.18
8252	8249	3.37	0.23	-30.30	2.30	14.65	-0.04
8254	8251	2.57	0.20	-30.16	1.93	12.85	0.63
8256	8253	2.97	0.20	-30.22	2.47	14.85	0.28
8258	8255	3.19	0.21	-30.29	2.24	15.19	0.07
8260	8257	3.45	0.21	-30.24	1.46	16.43	0.17
8262	8259	3.45	0.21	-30.15	1.63	16.43	0.33
8264	8261	3.32	0.22	-29.94	1.65	15.09	0.14
8266	8263	3.10	0.22	-30.22	1.65	14.09	0.14
8268	8265	2.98	0.23	-30.11	1.65	12.96	0.01
8270	8267	3.64	0.25	-30.26	1.61	14.56	-0.07
8272	8269	3.76	0.25	-30.26	1.61	15.04	0.08
8274	8271	4.18	0.25	-30.26	1.58	16.72	-0.10
8276	8273	5.07	0.26	-30.12	1.55	19.50	0.73
8278	8275	3.54	0.24	-30.10	1.94	14.75	-0.02
8280	8277	4.61	0.25	-29.92	1.70	18.44	0.11
8282	8279	4.69	0.26	-29.82	1.91	18.04	0.11
8284	8281	2.75	0.20	-29.79	1.48	13.75	3.43

Table A.2. Well COP 259 Carbon and Nitrogen Data Continued

Depth ft	LC Depth ft	OC wt %	N wt %	δ ^{13}C ‰VPDB	δ ^{15}N ‰AIR	C/N N/A	IC wt %
8286	8283	4.15	0.22	-30.18	1.62	18.86	3.66
8288	8285	6.78	0.29	-30.38	1.78	23.38	2.12
8294	8291	3.58	0.25	-30.95	1.55	14.32	0.39
8296	8293	3.44	0.23	-30.91	1.52	14.96	0.79
8298	8295	3.52	0.22	-30.98	1.54	16.00	1.27
8300	8297	2.96	0.21	-30.92	1.92	14.10	1.56
8302	8299	4.45	0.25	-30.95	1.85	17.80	-0.02
8304	8301	2.38	0.22	-30.86	2.22	10.82	1.38
8306	8303	2.43	0.22	-30.86	1.31	11.05	0.33
8308	8305	2.75	0.23	-30.95	1.79	11.96	0.20
8310	8307	2.98	0.22	-30.98	1.69	13.55	1.54
8312	8309	3.00	0.23	-31.04	1.63	13.04	0.41
8314	8311	2.15	0.22	-30.95	1.60	9.77	1.20
8316	8313	2.26	0.22	-30.99	1.40	10.27	0.50
8318	8315	2.51	0.23	-30.99	1.42	10.91	0.62
8320	8317	2.37	0.23	-30.88	1.32	10.30	0.20
8322	8319	2.50	0.23	-30.90	1.60	10.87	0.65
8324	8321	2.87	0.23	-30.98	1.97	12.48	1.37
8326	8323	2.44	0.22	-30.79	1.24	11.09	0.52
8328	8325	2.28	0.21	-30.93	1.35	10.86	0.91
8330	8327	2.48	0.22	-30.90	1.37	11.27	1.37
8332	8329	3.20	0.23	-31.04	1.51	13.91	0.31
8334	8331	2.85	0.23	-31.12	1.61	12.39	0.25
8336	8333	2.44	0.23	-30.89	-0.15	10.61	0.56
8338	8335	2.75	0.24	-31.09	0.03	11.46	1.04
8340	8337	3.71	0.25	-31.00	0.16	14.84	1.12
8342	8339	2.85	0.25	-31.03	0.56	11.40	0.31
8344	8341	2.91	0.24	-30.99	0.79	12.13	0.09
8346	8343	3.37	0.25	-31.04	0.46	13.48	0.39
8348	8345	2.31	0.23	-30.87	1.23	10.04	0.14
8350	8347	2.06	0.21	-30.89	0.40	9.81	0.59
8352	8349	2.22	0.23	-30.73	0.83	9.65	0.42
8354	8351	2.35	0.23	-30.90	0.24	10.22	0.55
8356	8353	2.22	0.22	-30.96	0.62	10.09	0.36
8358	8355	2.65	0.23	-30.89	1.12	11.52	0.66
8360	8357	2.24	0.22	-30.81	1.21	10.18	0.94
8362	8359	2.55	0.23	-30.82	1.37	11.09	0.31
8364	8361	2.96	0.24	-31.11	1.36	12.33	0.28
8366	8363	2.48	0.23	-30.44	0.40	10.78	1.15
8368	8365	2.72	0.23	-30.95	1.77	11.83	0.86

Table A.2. Well COP 259 Carbon and Nitrogen Data Continued

Depth ft	LC Depth ft	OC wt %	N wt %	$\delta^{13}C$ ‰VPDB	$\delta^{15}N$ ‰AIR	C/N N/A	IC wt %
8370	8367	3.47	0.24	-31.14	2.17	14.46	0.23
8372	8369	5.11	0.21	-31.28	2.95	24.33	2.56
8378	8375	7.25	0.32	-31.42	1.81	22.66	0.50
8380	8377	8.52	0.33	-31.42	2.44	25.82	-0.13
8382	8379	0.47	0.61	-29.51	1.54	0.77	-0.12
8384	8381	5.50	0.19	-31.14	2.52	28.95	2.54
8386	8383	5.72	0.17	-31.13	3.14	33.65	4.29
8388	8385	1.49	0.07	-30.91	2.66	21.29	7.98
8390	8387	0.38	0.01	-30.93	6.40	38.00	11.48
8392	8389	0.94	0.05	-30.17	1.15	18.80	9.67
8394	8391	4.20	0.17	-30.68	2.65	24.71	7.54

Table A.3. Well COP 289 Carbon and Nitrogen Data

Depth ft	LC Depth ft	OC wt %	N wt %	$\delta^{13}C$ ‰VPDB	$\delta^{15}N$ ‰AIR	C/N N/A	IC wt %
7786	7784	1.48	0.18	-29.54	-0.94	8.22	0.55
7788	7786	0.63	0.15	-28.94	-1.31	4.20	0.72
7790	7788	0.52	0.15	-28.27	-1.19	3.47	0.50
7792	7790	0.47	0.14	-28.44	-1.53	3.36	0.58
7794	7792	0.49	0.14	-28.45	-1.33	3.50	0.71
7796	7794	0.51	0.14	-28.47	-1.23	3.64	0.77
7798	7796	0.56	0.14	-28.53	-0.55	4.00	0.73
7800	7798	0.58	0.15	-28.47	-1.57	3.87	0.58
7802	7800	0.93	0.13	-29.06	-1.78	7.15	1.27
7804	7802	0.54	0.15	-28.55	-1.42	3.60	0.50
7806	7804	0.56	0.15	-28.63	-1.23	3.73	0.61
7808	7806	0.58	0.15	-28.59	-1.23	3.87	0.54
7810	7808	0.51	0.14	-28.35	-0.76	3.64	0.96
7812	7810	0.63	0.17	-28.69	-1.27	3.71	0.52
7814	7812	0.62	0.16	-28.67	-1.68	3.88	0.63
7816	7814	0.63	0.16	-28.62	-0.63	3.94	0.69
7818	7816	0.6	0.16	-28.84	-0.54	3.75	0.58
7820	7818	0.92	0.17	-29.22	-0.50	5.41	0.15
7822	7820	1.01	0.18	-29.23	-0.71	5.61	0.68
7824	7822	0.67	0.17	-28.99	-0.97	3.94	0.88
7826	7824	3.22	0.24	-30.13	1.16	13.42	-0.04
7828	7826	2.34	0.21	-29.92	0.73	11.14	0.08
7830	7828	2.76	0.23	-30.01	0.32	12.00	0.12

Table A.3. Well COP 289 Carbon and Nitrogen Data Continued

Depth ft	LC Depth ft	OC wt %	N wt %	δ ^{13}C ‰VPDB	δ ^{15}N ‰AIR	C/N N/A	IC wt %
7832	7830	1.7	0.22	-29.65	-1.63	7.73	0.38
7834	7832	1.96	0.21	-29.74	-0.70	9.33	0.09
7836	7834	2.18	0.21	-29.86	0.37	10.38	0.22
7838	7836	2.2	0.21	-29.88	0.31	10.48	0.23
7840	7838	2.29	0.21	-29.93	-0.42	10.90	0.70
7842	7840	0.78	0.17	-28.93	-1.07	4.59	2.11
7844	7842	0.67	0.16	-28.71	0.22	4.19	1.88
7846	7844	0.65	0.17	-28.81	0.24	3.82	1.32
7848	7846	0.55	0.16	-28.58	-0.46	3.44	0.97
7850	7848	0.49	0.17	-28.45	-0.45	2.88	0.71
7852	7850	0.65	0.16	-28.93	-0.89	4.06	2.45
7854	7852	0.57	0.16	-28.68	0.44	3.56	2.18
7856	7854	0.55	0.17	-28.74	-0.08	3.24	1.59
7858	7856	0.55	0.16	-28.62	0.12	3.44	1.22
7860	7858	0.57	0.17	-28.64	0.03	3.35	1.19
7862	7860	0.74	0.17	-28.93	-0.15	4.35	1.19
7864	7862	0.59	0.17	-28.77	-0.28	3.47	1.07
7866	7864	0.59	0.16	-28.61	-0.32	3.69	0.91
7868	7866	0.61	0.17	-28.71	0.19	3.59	1.05
7870	7868	0.6	0.17	-28.67	-0.14	3.53	0.99
7872	7870	0.33	0.06	-28.13	-2.75	5.50	6.59
7874	7872	0.58	0.18	-28.26	-1.33	3.22	2.11
7876	7874	0.66	0.17	-28.71	-0.53	3.88	1.79
7878	7876	2.76	0.25	-30.14	-0.18	11.04	-0.03
7880	7878	1.62	0.21	-29.84	-0.45	7.71	0.54
7882	7880	1.46	0.21	-29.51	-1.29	6.95	0.50
7884	7882	1.1	0.17	-29.26	0.65	6.47	2.00
7886	7884	1.85	0.22	-29.97	-0.80	8.41	0.53
7888	7886	1.87	0.21	-29.95	0.08	8.90	0.04
7890	7888	1.52	0.2	-29.88	-0.06	7.60	1.03
7892	7890	1.93	0.25	-30.20	0.25	7.72	0.07
7894	7892	1.81	0.22	-30.14	-1.28	8.23	0.39
7896	7894	2.27	0.2	-30.43	-0.15	11.35	1.66
7898	7896	0.91	0.21	-29.57	-0.60	4.33	1.07
7900	7898	0.99	0.18	-29.74	-0.11	5.50	1.35
7902	7900	1.69	0.22	-29.91	0.38	7.68	1.03
7904	7902	1.74	0.18	-30.10	-0.39	9.67	2.47
7906	7904	0.87	0.21	-29.53	-1.57	4.14	1.40
7908	7906	1.29	0.21	-29.97	0.03	6.14	0.55
7910	7908	1.23	0.17	-29.91	-0.85	7.24	3.20

Table A.3. Well COP 289 Carbon and Nitrogen Data Continued

Depth ft	LC Depth ft	OC wt %	N wt %	$\delta^{13}C$ ‰VPDB	$\delta^{15}N$ ‰AIR	C/N N/A	IC wt %
7912	7910	2.28	0.25	-30.54	-0.22	9.12	0.17
7914	7912	2.21	0.23	-30.47	-1.04	9.61	1.21
7916	7914	2.97	0.27	-30.58	-0.40	11.00	-0.16
7924	7922	1.69	0.23	-30.11	-1.94	7.35	0.74
7926	7924	3.09	0.28	-30.35	-1.04	11.04	0.40
7928	7926	1.73	0.24	-30.00	-1.74	7.21	0.56
7930	7928	1.88	0.25	-30.21	-1.21	7.52	0.15
7932	7930	2.33	0.26	-30.14	-0.55	8.96	-0.16
7934	7932	1.21	0.23	-29.83	-1.15	5.26	0.36
7936	7934	1.3	0.2	-29.73	-0.75	6.50	2.21
7938	7936	0.91	0.22	-29.45	-1.44	4.14	0.72
7940	7938	0.92	0.22	-29.29	-1.74	4.18	0.75
7942	7940	0.92	0.22	-29.11	-1.72	4.18	0.80
7944	7942	0.94	0.22	-29.18	-1.24	4.27	0.39
7946	7944	1.56	0.23	-29.55	-0.09	6.78	-0.06
7948	7946	1.31	0.23	-29.43	-0.94	5.70	1.38
7952	7950	0.7	0.2	-28.35	-1.16	3.50	1.37
7954	7952	1.55	0.19	-29.81	-2.06	8.16	1.04
7956	7954	3.17	0.27	-30.44	-0.30	11.74	-0.17
7958	7956	2.59	0.25	-30.36	-0.05	10.36	0.10
7960	7958	2.29	0.23	-30.10	1.39	9.96	-0.15
7962	7960	1.94	0.19	-30.12	1.30	10.21	0.13
7964	7962	2.72	0.22	-30.28	1.07	12.36	-0.18
7966	7964	2.73	0.22	-30.47	1.97	12.41	0.15
7968	7966	2.22	0.21	-30.22	0.55	10.57	0.91
7970	7968	3.23	0.23	-30.37	1.37	14.04	0.05
7972	7970	2.25	0.21	-30.29	1.14	10.71	0.04
7974	7972	2.86	0.23	-30.30	1.32	12.43	-0.17
7976	7974	3.75	0.24	-31.08	2.29	15.63	0.09
7978	7976	3.91	0.24	-30.33	0.19	16.29	0.01
7980	7978	4.6	0.24	-30.36	0.19	19.17	0.13
7982	7980	2.76	0.21	-30.01	0.28	13.14	0.00
7984	7982	3.87	0.23	-30.27	0.07	16.83	-0.14
7986	7984	4.62	0.26	-30.31	0.21	17.77	0.71
7988	7986	3.42	0.25	-30.06	0.53	13.68	-0.07
7990	7988	4.44	0.25	-30.08	0.89	17.76	0.45
7992	7990	2.84	0.14	-29.86	1.41	20.29	6.12
7994	7992	4.75	0.19	-30.18	1.63	25.00	5.21
7996	7994	7.24	0.28	-30.43	0.82	25.86	2.31
7998	7996	4.98	0.3	-30.85	0.48	16.60	1.40

Table A.3. Well COP 289 Carbon and Nitrogen Data Continued

Depth ft	LC Depth ft	OC wt %	N wt %	$\delta^{13}C$ ‰VPDB	$\delta^{15}N$ ‰AIR	C/N N/A	IC wt %
8000	7998	4.69	0.29	-30.85	0.37	16.17	0.92
8002	8000	3.49	0.28	-30.83	0.33	12.46	1.17
8008	8006	3.66	0.24	-30.88	0.95	15.25	1.18
8010	8008	2.82	0.24	-30.93	0.13	11.75	0.62
8012	8010	2.51	0.23	-30.91	0.63	10.91	1.07
8014	8012	3.21	0.25	-31.00	-0.05	12.84	0.61
8016	8014	2.87	0.26	-31.07	-0.73	11.04	0.20
8018	8016	2.24	0.25	-30.93	3.18	8.96	1.01
8020	8018	3.17	0.24	-30.86	1.49	13.21	1.76
8022	8020	2.17	0.27	-30.94	0.56	8.04	0.58
8024	8022	2.61	0.26	-31.23	0.16	10.04	0.52
8026	8024	2.95	0.25	-31.27	0.89	11.80	1.40
8028	8026	2.25	0.26	-31.12	0.39	8.65	0.39
8030	8028	2.72	0.25	-31.15	0.76	10.88	1.46
8032	8030	3.2	0.25	-31.06	1.35	12.80	1.29
8034	8032	2.18	0.26	-31.12	0.61	8.38	1.14
8036	8034	2.45	0.25	-31.09	0.27	9.80	0.52
8038	8036	2.26	0.24	-31.00	0.32	9.42	0.59
8040	8038	2.38	0.24	-31.14	0.90	9.92	1.11
8044	8042	2.42	0.24	-31.04	1.25	10.08	1.23
8046	8044	2.12	0.25	-31.04	0.81	8.48	0.89
8048	8046	2.96	0.27	-31.31	0.49	10.96	0.50
8050	8048	2.6	0.27	-31.27	0.66	9.63	0.23
8052	8050	2.21	0.25	-31.26	0.63	8.84	0.78
8054	8052	2.58	0.26	-31.27	0.54	9.92	0.25
8056	8054	3.83	0.27	-31.20	0.80	14.19	-0.20
8058	8056	3.11	0.26	-31.46	0.78	11.96	1.79
8060	8058	2.37	0.27	-31.33	0.22	8.78	0.52
8062	8060	1.95	0.27	-31.40	0.33	7.22	1.06
8064	8062	2.11	0.27	-31.42	0.46	7.81	1.02
8066	8064	2.78	0.26	-31.48	0.35	10.69	0.71
8068	8066	2.49	0.26	-31.25	2.24	9.58	0.88
8070	8068	1.83	0.25	-31.47	0.60	7.32	1.12
8072	8070	2.18	0.25	-31.44	1.03	8.72	0.85
8074	8072	3.61	0.26	-31.40	1.17	13.88	0.75
8076	8074	1.93	0.22	-31.48	0.87	8.77	1.59
8078	8076	2.53	0.25	-31.54	2.45	10.12	0.85
8080	8078	2.88	0.25	-31.84	0.64	11.52	1.15
8082	8080	4.55	0.27	-31.71	1.53	16.85	1.38
8086	8084	6.65	0.29	-31.58	1.46	22.93	2.72

Table A.3. Well COP 289 Carbon and Nitrogen Data Continued

Depth ft	LC Depth ft	OC wt %	N wt %	δ ^{13}C ‰VPDB	δ ^{15}N ‰AIR	C/N N/A	IC wt %
8088	8086	8.09	0.34	-31.70	2.48	23.79	0.99
8090	8088	7.57	0.29	-31.62	2.12	26.10	0.38
8096	8094	1.67	0.16	-31.09	3.17	10.44	8.97
8098	8096	7.08	0.29	-31.70	2.61	24.41	0.71
8100	8098	2.6	0.08	-31.64	3.21	32.50	8.32
8102	8100	0.93	0.05	-31.40	2.35	18.60	7.86
8104	8102	7.01	0.19	-31.25	3.65	36.89	2.72
8106	8104	2.92	0.1	-31.20	1.63	29.20	6.95
8108	8106	3.67	0.13	-31.14	3.74	28.23	8.38
8110	8108	1.33	0.15	-30.39	2.36	8.87	4.35
8112	8110	0.29	0.04	-29.41	1.23	7.25	9.88
8114	8112	1.24	0.14	-29.18	1.50	8.86	7.18
8116	8114	2.82	0.1	-30.10	0.23	28.20	8.69
8118	8116	0.57	0.03	-30.32	0.87	19.00	11.81

Table A.4. Well COP 653 XRF Trace Element Data

Depth ft	LC Depth ft	V ppm	Cu ppm	Zn ppm	U ppm	Ni ppm	Th ppm	Mo ppm
8222	8215.75	171.74	22	31	2.61	60	13	0.24
8224	8217.75	180.80	20	71	2.28	67	12	-0.40
8226	8219.75	169.44	30	73	3.79	70	12	1.77
8228	8221.75	207.90	48	34	4.86	89	15	29.94
8230	8223.75	195.12	86	45	3.79	100	12	15.64
8232	8225.75	178.97	40	40	2.06	66	11	1.29
8234	8227.75	178.34	29	112	1.91	57	11	0.93
8236	8229.75	218.35	37	62	4.46	87	14	36.42
8238	8231.75	250.47	84	24	5.73	124	13	42.73
8240	8233.75	196.24	85	50	3.55	100	13	26.61
8242	8235.75	191.43	62	53	4.19	73	13	10.04
8244	8237.75	214.14	64	58	4.97	102	14	29.39
8246	8239.75	173.20	70	84	3.69	82	11	10.09
8248	8241.75	185.28	50	53	3.82	80	10	18.04
8250	8243.75	209.28	82	1736	6.06	121	13	37.79
8252	8245.75	159.49	51	62	3.83	63	11	9.61
8254	8247.75	196.98	66	208	4.79	89	12	29.56
8256	8249.75	195.79	77	79	3.15	91	11	20.05
8258	8251.75	221.67	67	27	6.65	107	14	45.30
8260	8253.75	125.10	41	160	1.48	47	11	1.14

Table A.4. Well COP 653 XRF Trace Element Data Continued

Depth ft	LC Depth ft	V ppm	Cu ppm	Zn ppm	U ppm	Ni ppm	Th ppm	Mo ppm
8262	8255.75	151.15	35	32	1.83	60	9	2.29
8266	8259.75	159.94	20	21	1.66	54	13	0.02
8268	8261.75	163.38	13	25	3.12	58	11	0.28
8270	8263.75	159.08	14	23	0.46	56	11	0.27
8272	8265.75	160.88	12	57	1.64	69	10	-0.38
8274	8267.75	165.95	23	50	1.56	62	14	0.20
8276	8269.75	163.58	24	55	1.89	63	12	0.37
8278	8271.75	161.72	25	56	2.53	61	14	-0.62
8280	8273.75	171.43	21	57	1.60	62	11	0.41
8282	8275.75	173.53	32	65	2.52	71	14	1.47
8284	8277.75	162.62	19	79	2.36	62	12	0.56
8286	8279.75	167.85	22	30	2.39	68	11	0.50
8288	8281.75	159.57	16	45	2.81	57	12	0.00
8290	8283.75	144.63	37	162	0.88	57	9	3.16
8292	8285.75	173.19	58	63	1.63	71	12	7.60
8294	8287.75	203.86	64	103	4.67	85	15	26.63
8296	8289.75	177.18	46	33	3.35	63	12	8.71
8298	8291.75	180.48	82	50	4.91	86	16	26.96
8300	8293.75	164.91	45	27	1.56	55	14	2.00
8302	8295.75	163.94	47	90	3.07	64	12	2.02
8304	8297.75	175.20	62	39	2.71	59	12	6.25
8306	8299.75	169.92	63	47	5.07	61	14	16.64
8308	8301.75	174.84	67	86	5.45	84	14	35.10
8310	8303.75	221.07	80	67	5.52	103	14	42.26
8312	8305.75	154.13	28	14	1.93	49	10	1.67
8314	8307.75	206.78	64	127	6.89	100	14	44.71
8316	8309.75	222.07	83	100	5.74	110	14	48.52
8318	8311.75	211.61	65	95	4.44	100	17	30.20
8320	8313.75	193.37	75	72	6.08	84	12	25.39
8322	8315.75	184.68	56	38	3.73	59	12	8.55
8324	8317.75	207.09	65	63	6.32	101	14	62.60
8326	8319.75	142.45	39	91	3.95	61	9	27.82
8328	8321.75	247.16	86	131	8.34	124	16	65.52
8330	8323.75	232.85	79	70	8.92	103	13	56.96
8332	8325.75	198.50	65	119	5.01	70	13	14.53
8334	8327.75	175.02	57	47	4.32	60	10	17.77
8336	8329.75	247.77	119	234	10.50	141	13	80.32
8338	8331.75	213.79	118	33	5.34	98	13	31.49
8340	8333.75	193.69	88	24	5.25	83	12	31.79
8342	8335.75	223.81	84	107	4.19	96	15	38.36
8344	8337.75	222.25	72	140	4.98	92	16	35.97

Table A.4. Well COP 653 XRF Trace Element Data Continued

Depth ft	LC Depth ft	V ppm	Cu ppm	Zn ppm	U ppm	Ni ppm	Th ppm	Mo ppm
8346	8339.75	202.05	96	25	3.10	80	13	26.11
8350	8343.75	195.43	29	63	2.18	54	17	1.50
8352	8345.75	217.19	107	119	4.20	110	12	34.36
8354	8347.75	225.44	86	152	3.60	92	14	23.68
8356	8349.75	205.01	76	105	3.17	82	14	9.69
8358	8351.75	132.66	10	7	3.06	31	10	0.76
8360	8353.75	154.25	42	11	2.50	39	12	2.50
8362	8355.75	186.27	95	50	6.25	99	12	49.91
8364	8357.75	212.88	75	198	6.34	121	12	61.77
8366	8359.75	207.63	70	126	6.52	122	15	60.22
8368	8361.75	191.93	69	56	6.05	99	14	56.10
8370	8363.75	193.04	68	56	8.91	101	15	74.40
8372	8365.75	212.76	85	47	5.87	128	14	80.46
8374	8367.75	219.45	78	52	8.83	125	14	75.86
8376	8369.75	206.42	92	115	9.41	132	12	86.48
8378	8371.75	236.76	75	747	10.43	148	15	88.11
8380	8373.75	208.24	83	259	9.30	133	13	95.46
8382	8375.75	216.54	84	114	9.51	128	13	91.08
8384	8377.75	225.35	80	122	9.39	120	12	75.11
8386	8379.75	236.60	88	515	9.82	136	14	82.34
8388	8381.75	218.65	81	29	12.03	125	13	92.55
8390	8383.75	220.66	78	107	10.55	140	12	91.43
8392	8385.75	222.17	70	553	8.26	128	12	100.20
8394	8387.75	250.62	85	129	13.91	157	12	113.61
8396	8389.75	297.71	96	618	14.58	179	11	132.32
8398	8391.75	260.12	78	196	12.27	131	11	84.22
8400	8393.75	226.39	86	322	8.62	125	12	102.11
8402	8395.75	252.18	65	130	7.30	110	15	69.88
8404	8397.75	227.96	70	94	8.09	116	16	81.00
8406	8399.75	207.61	66	77	9.77	104	13	79.97
8408	8401.75	249.14	77	50	14.59	139	13	110.78
8410	8403.75	283.46	92	58	11.15	154	10	115.96
8412	8405.75	298.66	105	298	8.20	95	9	44.33
8414	8407.75	268.84	75	10	9.04	137	15	90.04
8416	8409.75	258.31	92	9	9.00	132	14	100.41
8420	8413.75	72.65	41	9	3.35	21	3	5.15
8422	8415.75	399.81	158	176	7.96	217	13	111.25
8424	8417.75	275.65	253	3409	5.88	156	8	39.72
8426	8419.75	43.75	27	46	2.65	30	4	5.16
8428	8421.75	538.51	140	16	9.32	240	12	114.57
8430	8423.75	385.01	87	7	9.55	158	9	76.43

Table A.4. Well COP 653 XRF Trace Element Data Continued

Depth ft	LC Depth ft	V ppm	Cu ppm	Zn ppm	U ppm	Ni ppm	Th ppm	Mo ppm
8432	8425.75	382.75	91	3	11.94	171	9	81.81
8436	8429.75	397.19	85	432	6.80	179	10	96.49
8438	8431.75	351.92	82	298	10.13	158	10	76.74
8440	8433.75	378.22	78	450	13.19	185	10	96.79
8442	8435.75	258.24	45	303	7.21	112	10	52.13
8444	8437.75	297.01	62	370	7.67	142	10	67.71
8446	8439.75	397.70	94	204	12.39	186	14	109.05
8448	8441.75	259.04	66	208	8.25	126	10	67.26
8450	8443.75	291.44	74	397	9.07	154	11	87.12
8452	8445.75	306.56	72	257	8.04	120	9	45.79
8454	8447.75	260.89	66	113	4.59	105	14	42.49
8456	8449.75	270.41	65	144	5.40	111	12	44.16
8458	8451.75	264.71	58	195	9.00	115	14	54.90
8460	8453.75	284.04	64	170	6.56	118	11	52.64
8462	8455.75	266.97	65	179	5.33	123	11	50.60
8464	8457.75	274.97	66	183	7.06	115	12	44.77
8466	8459.75	293.41	65	345	10.30	136	12	66.81
8468	8461.75	253.62	58	76	6.82	102	12	45.44
8470	8463.75	240.22	56	183	6.58	106	12	52.39
8472	8465.75	221.30	55	100	5.39	100	12	51.77
8474	8467.75	276.56	76	220	10.08	130	13	72.94
8476	8469.75	297.74	72	252	8.97	112	13	83.31
8478	8471.75	255.31	73	7	6.09	108	13	49.29
8480	8473.75	265.94	83	6	5.93	117	15	58.66
8482	8475.75	272.98	84	13	6.58	124	13	60.35
8484	8477.75	256.61	76	2	10.13	155	12	63.58
8486	8479.75	299.39	74	8	8.35	124	13	59.98
8488	8481.75	316.71	74	576	12.47	153	13	90.03
8490	8483.75	299.05	65	662	9.31	129	13	83.86
8492	8485.75	274.02	57	339	8.22	133	13	65.45
8494	8487.75	277.17	61	11	5.73	103	12	54.68
8496	8489.75	283.60	64	371	6.04	128	12	56.52
8498	8491.75	274.13	46	124	7.85	108	14	63.96
8500	8493.75	270.42	54	3	6.81	77	12	40.68
8502	8495.75	251.76	55	105	6.95	108	12	72.82
8504	8497.75	240.86	65	1	4.91	98	11	39.09
8506	8499.75	245.96	67	10	6.31	125	12	53.24
8508	8501.75	282.91	67	244	7.68	126	11	85.01
8510	8503.75	270.11	63	71	7.10	111	14	66.80
8512	8505.75	255.59	84	-4	10.63	128	11	74.92
8514	8507.75	448.05	74	186	24.42	209	11	250.53

Table A.4. Well COP 653 XRF Trace Element Data Continued

Depth ft	LC Depth ft	V ppm	Cu ppm	Zn ppm	U ppm	Ni ppm	Th ppm	Mo ppm
8516	8509.75	635.50	135	14	10.53	232	7	112.69
8518	8511.75	713.29	172	514	28.53	316	7	215.42
8520	8513.75	682.77	182	1189	22.20	321	9	171.72
8522	8515.75	701.42	217	61	40.64	343	10	243.94
8524	8517.75	515.44	187	994	18.52	272	10	175.30
8528	8521.75	511.58	222	121	29.81	320	3	207.83
8530	8523.75	364.54	199	38	10.72	173	3	97.99
8532	8525.75	517.97	260	316	16.14	229	2	236.39
8534	8527.75	698.07	358	855	23.64	301	3	346.12
8536	8529.75	116.60	35	373	6.53	52	-2	57.96
8538	8531.75	53.61	119	-21	4.03	59	2	10.44
8540	8533.75	45.94	58	-16	3.52	34	4	10.64
8542	8535.75	16.07	7	87	2.68	7	0	1.27
8544	8537.75	18.75	32	-30	1.16	37	5	4.11
8546	8539.75	77.89	141	-20	5.62	46	4	11.13
8548	8541.75	110.89	81	-2	6.76	103	10	14.73
8550	8543.75	133.62	32	22	3.82	25	7	2.80

Table A.5. Well COP 259 XRF Trace Element Data

Depth ft	LC Depth ft	V ppm	Cu ppm	Zn ppm	U ppm	Ni ppm	Th ppm	Mo ppm
8040	8037	206.10	18	46	3.18	70.67	13.00	0.18
8042	8039	195.26	18	49	3.80	69.70	15.89	1.07
8044	8041	200.18	22	163	3.11	67.76	15.89	1.02
8046	8043	191.29	24	81	1.70	65.83	15.89	0.37
8048	8045	208.20	21	53	2.39	74.54	15.89	-0.26
8050	8047	192.30	16	107	2.20	69.70	14.44	0.38
8052	8049	197.15	15	92	2.61	69.70	14.44	0.30
8054	8051	195.82	21	71	2.90	65.83	17.33	0.55
8056	8053	177.58	41	123	1.83	64.86	14.44	0.28
8058	8055	193.07	16	112	1.82	66.80	15.89	0.41
8060	8057	188.84	11	115	2.85	64.86	11.56	0.64
8062	8059	195.61	11	197	3.56	64.86	13.00	-0.31
8064	8061	196.32	21	89	3.86	65.83	13.00	0.85
8066	8063	200.36	18	104	2.65	65.83	15.89	-0.15
8068	8065	197.89	17	79	2.17	69.70	14.44	0.41
8070	8067	200.12	15	68	2.80	59.05	14.44	0.45
8072	8069	202.99	28	29	4.23	68.73	14.44	3.77
8074	8071	205.79	37	26	3.34	59.05	15.89	2.16

Table A.5. Well COP 259 XRF Trace Element Data Continued

Depth ft	LC Depth ft	V ppm	Cu ppm	Zn ppm	U ppm	Ni ppm	Th ppm	Mo ppm
8076	8073	209.26	39	24	3.19	63.89	11.56	4.13
8080	8077	237.05	55	25	5.32	95.84	14.44	18.71
8082	8079	221.87	47	24	4.03	88.09	17.33	16.03
8084	8081	238.07	60	50	5.25	101.65	14.44	21.99
8086	8083	237.08	54	41	5.54	102.62	15.89	36.55
8088	8085	212.60	57	73	4.02	83.25	13.00	11.76
8090	8087	209.20	35	103	3.89	64.86	10.11	6.14
8092	8089	220.61	41	159	3.63	72.60	10.11	8.18
8094	8091	224.75	48	47	1.98	86.16	18.78	11.16
8096	8093	237.13	38	31	4.21	100.68	18.78	21.62
8098	8095	224.79	63	23	3.28	89.06	15.89	13.11
8100	8097	206.67	36	43	3.96	62.92	14.44	0.94
8102	8099	200.50	16	22	3.02	60.02	17.33	0.25
8104	8101	221.65	35	58	3.40	73.57	15.89	3.65
8106	8103	241.81	58	22	3.88	104.55	15.89	24.75
8108	8105	235.40	55	30	6.15	106.49	15.89	29.01
8110	8107	217.48	49	47	4.28	82.29	17.33	4.46
8112	8109	203.15	31	208	1.98	60.99	15.89	1.47
8114	8111	229.95	57	1268	4.23	112.30	20.22	22.10
8116	8113	225.32	51	56	3.13	82.29	17.33	11.41
8118	8115	233.29	52	122	4.30	83.25	17.33	15.78
8120	8117	221.48	59	122	1.84	84.22	15.89	10.37
8122	8119	214.21	43	82	4.41	70.67	15.89	8.10
8124	8121	236.45	45	29	5.06	96.81	18.78	21.06
8126	8123	205.98	57	60	3.92	91.97	13.00	10.26
8128	8125	206.58	37	61	3.12	65.83	13.00	2.98
8130	8127	203.21	56	522	3.08	83.25	14.44	9.36
8132	8129	226.51	58	67	5.33	110.36	14.44	27.39
8134	8131	219.39	52	37	3.28	91.97	11.56	13.37
8136	8133	195.53	42	46	4.21	64.86	14.44	7.51
8138	8135	218.48	54	464	4.75	94.87	15.89	22.20
8140	8137	205.67	75	75	3.02	82.29	15.89	9.61
8142	8139	196.34	51	476	3.74	72.60	13.00	11.41
8144	8141	216.36	43	88	2.85	84.22	14.44	22.58
8146	8143	223.09	56	31	6.43	112.30	15.89	38.63
8148	8145	231.15	68	27	6.58	105.52	18.78	39.15
8150	8147	208.87	59	83	3.58	84.22	13.00	11.61
8152	8149	180.17	20	14	2.40	59.05	13.00	0.24
8154	8151	188.28	27	89	3.06	60.02	13.00	1.09
8156	8153	205.71	50	270	3.05	73.57	10.11	1.30
8158	8155	199.82	28	31	3.16	75.51	11.56	0.52

Table A.5. Well COP 259 XRF Trace Element Data Continued

Depth ft	LC Depth ft	V ppm	Cu ppm	Zn ppm	U ppm	Ni ppm	Th ppm	Mo ppm
8160	8157	201.54	14	30	2.55	60.02	11.56	-0.36
8164	8161	196.92	14	29	2.16	62.92	13.00	-0.99
8166	8163	196.45	21	30	2.76	62.92	13.00	-0.71
8168	8165	197.90	12	49	1.69	65.83	13.00	0.12
8170	8167	159.54	20	52	2.70	64.00	13.00	1.37
8172	8169	165.84	18	71	2.51	59.00	9.00	0.60
8174	8171	183.90	70	47	3.51	77.00	12.00	11.40
8176	8173	199.80	60	48	3.07	74.00	15.00	12.73
8178	8175	188.41	66	28	4.31	81.00	13.00	22.97
8180	8177	181.19	58	32	3.89	64.00	12.00	9.25
8182	8179	170.09	96	369	3.35	97.00	12.00	43.64
8184	8181	178.39	42	73	2.57	52.00	16.00	1.58
8186	8183	173.29	63	32	3.56	69.00	13.00	5.88
8188	8185	195.97	75	30	3.65	86.00	14.00	27.43
8190	8187	195.42	86	33	5.34	95.00	15.00	46.51
8192	8189	189.82	70	21	4.87	76.00	13.00	14.98
8194	8191	166.89	27	173	2.29	48.00	10.00	1.45
8196	8193	244.91	98	83	7.04	129.00	15.00	69.31
8198	8195	242.70	82	117	4.75	120.00	13.00	50.06
8200	8197	193.59	65	20	3.71	65.00	14.00	9.80
8202	8199	165.60	49	15	4.32	65.00	11.00	31.02
8204	8201	265.21	108	113	9.00	140.00	17.00	85.16
8206	8203	233.03	91	64	8.21	119.00	16.00	70.93
8208	8205	241.62	99	98	8.85	104.00	14.00	45.54
8210	8207	244.98	127	48	8.58	132.00	15.00	80.98
8218	8215	200.68	71	23	2.58	60.00	13.00	5.23
8220	8217	197.47	43	62	0.63	57.00	15.00	2.19
8222	8219	254.69	112	211	4.73	123.00	12.00	58.18
8224	8221	208.74	66	68	3.21	91.00	15.00	24.92
8226	8223	153.17	64	10	0.71	59.00	12.00	1.72
8228	8225	180.50	74	16	5.43	62.00	15.00	23.04
8230	8227	222.59	83	309	8.89	128.00	15.00	72.52
8232	8229	192.34	82	51	7.52	95.00	14.00	65.84
8234	8231	188.98	69	44	6.02	92.00	15.00	54.06
8236	8233	193.59	63	46	7.74	98.00	13.00	65.60
8238	8235	208.81	76	177	8.91	112.00	13.00	89.94
8240	8237	213.59	75	120	7.71	121.00	16.00	82.00
8242	8239	205.38	66	128	6.35	100.00	11.00	59.93
8244	8241	203.19	68	507	8.18	117.00	14.00	68.23
8246	8243	234.93	89	324	9.05	162.00	12.00	98.97
8248	8245	231.23	86	183	11.74	144.00	12.00	102.83

Table A.5. Well COP 259 XRF Trace Element Data Continued

Depth ft	LC Depth ft	V ppm	Cu ppm	Zn ppm	U ppm	Ni ppm	Th ppm	Mo ppm
8250	8247	239.45	82	136	10.03	127.00	12.00	72.73
8254	8251	214.09	73	91	8.28	122.00	11.00	82.32
8256	8253	226.88	79	61	11.47	133.00	12.00	94.59
8258	8255	237.21	83	155	10.96	141.00	11.00	93.00
8260	8257	276.88	88	801	9.86	144.00	11.00	90.87
8262	8259	273.66	84	220	9.56	134.00	12.00	96.50
8264	8261	215.75	74	248	7.16	118.00	11.00	95.83
8266	8263	265.19	76	177	8.11	125.00	15.00	84.68
8268	8265	228.04	70	85	9.10	109.00	14.00	82.02
8270	8267	244.96	77	84	13.27	143.00	12.00	95.96
8272	8269	256.02	78	169	14.45	134.00	12.00	113.52
8274	8271	298.18	95	88	12.69	172.00	13.00	122.56
8276	8273	374.23	142	159	13.67	184.00	13.00	197.96
8278	8275	265.27	85	12	11.56	138.00	10.00	103.18
8280	8277	293.25	97	77	15.46	163.00	11.00	172.85
8282	8279	303.61	115	38	12.56	173.00	11.00	164.26
8284	8281	125.05	166	-4	4.73	69.00	8.00	23.62
8286	8283	300.50	145	280	11.28	152.00	8.00	101.32
8288	8285	398.89	147	1548	8.11	170.00	12.00	46.06
8290	8287	424.26	67	1	10.76	110.00	5.00	48.20
8292	8289	552.08	105	124	9.27	202.00	13.00	88.08
8294	8291	452.09	90	19	8.53	174.00	11.00	97.68
8296	8293	395.48	92	3	13.14	178.00	9.00	101.59
8298	8295	357.04	81	177	13.37	156.00	10.00	88.35
8300	8297	338.75	74	251	8.58	140.00	9.00	66.39
8302	8299	430.76	82	358	11.56	192.00	10.00	127.54
8304	8301	306.36	68	303	8.62	137.00	13.00	64.38
8306	8303	311.50	80	13	8.75	125.00	11.00	53.66
8308	8305	296.04	69	173	6.55	135.00	12.00	65.61
8310	8307	269.92	70	213	7.63	128.00	10.00	69.35
8312	8309	317.68	79	155	8.01	138.00	12.00	62.07
8314	8311	259.90	65	137	7.01	109.00	13.00	43.49
8316	8313	276.50	66	145	7.08	106.00	12.00	42.60
8318	8315	281.65	62	144	7.23	116.00	11.00	51.16
8320	8317	273.09	70	154	5.97	118.00	12.00	42.22
8322	8319	283.43	69	158	7.76	124.00	13.00	53.77
8324	8321	243.77	57	162	10.30	105.00	11.00	50.84
8326	8323	279.13	70	200	6.90	122.00	14.00	48.44
8328	8325	240.32	53	110	7.02	103.00	11.00	49.06
8330	8327	234.59	63	43	8.07	99.00	11.00	56.32
8332	8329	296.59	85	166	10.24	132.00	13.00	79.53

Table A.5. Well COP 259 XRF Trace Element Data Continued

Depth ft	LC Depth ft	V ppm	Cu ppm	Zn ppm	U ppm	Ni ppm	Th ppm	Mo ppm
8334	8331	287.54	96	468	10.71	131.00	14.00	77.12
8338	8335	300.64	69	227	9.91	115.00	16.00	72.47
8340	8337	446.80	55	2741	15.61	108.00	13.00	95.84
8342	8339	305.60	76	9	7.61	120.00	14.00	65.26
8344	8341	363.30	81	265	10.32	192.00	11.00	83.72
8346	8343	348.23	76	517	10.05	146.00	13.00	94.56
8348	8345	288.41	86	2	6.43	152.00	8.00	49.91
8350	8347	275.80	61	11	6.67	108.00	13.00	51.88
8352	8349	264.58	67	159	6.51	137.00	12.00	53.99
8354	8351	251.90	66	12	5.90	109.00	12.00	45.44
8356	8353	282.25	70	68	6.78	128.00	13.00	56.76
8358	8355	265.32	70	314	6.64	132.00	12.00	63.57
8360	8357	223.58	65	8	3.75	83.00	10.00	43.70
8362	8359	230.42	69	6	5.83	154.00	9.00	45.81
8364	8361	280.56	81	255	7.69	132.00	12.00	81.03
8366	8363	301.56	102	254	5.76	108.00	11.00	57.04
8368	8365	258.46	71	146	8.11	122.00	11.00	85.55
8370	8367	332.60	106	1	11.04	176.00	9.00	113.89
8372	8369	466.15	128	200	24.40	240.00	5.00	135.40
8374	8371	911.10	195	738	27.47	381.00	9.00	215.53
8376	8373	10.44	2	-30	0.82	1.00	-1.00	5.00
8378	8375	769.13	182	563	28.97	321.00	9.00	184.07
8380	8377	674.25	242	7	52.52	401.00	9.00	260.04
8382	8379	84.60	11	-31	16.14	24.00	38.00	11.67
8384	8381	341.87	139	-11	14.54	218.00	4.00	133.49
8386	8383	375.44	155	955	14.37	183.00	-1.00	180.75
8388	8385	105.24	78	-33	3.13	62.00	0.00	27.17
8390	8387	14.89	-2	-36	0.84	14.00	0.00	4.93
8392	8389	27.22	28	-31	1.97	20.00	4.00	5.91
8394	8391	139.77	210	-28	9.87	133.00	5.00	24.50

Table A.6. Well COP 289 XRF Trace Element Data

Depth ft	LC Depth ft	V ppm	Cu ppm	Zn ppm	U ppm	Ni ppm	Th ppm	Mo ppm
7786	7784	206.75	91	76	4.63	89.06	11.56	20.46
7788	7786	199.14	26	26	4.17	80.35	11.56	4.69
7790	7788	202.51	18	77	2.29	79.38	14.44	1.14
7792	7790	207.27	15	27	3.17	68.73	13.00	-0.55
7794	7792	205.92	18	27	3.53	72.60	13.00	0.27
7796	7794	197.84	24	27	2.83	73.57	15.89	-0.17
7798	7796	192.52	33	49	3.88	72.60	14.44	1.03
7800	7798	201.22	15	42	3.19	70.67	13.00	0.45
7802	7800	175.90	16	157	2.68	70.67	10.11	0.42
7804	7802	207.41	8	119	2.37	72.60	14.44	-0.07
7806	7804	203.98	16	55	2.72	73.57	17.33	-0.14
7808	7806	202.51	12	55	2.94	82.29	14.44	-0.21
7810	7808	186.51	56	64	2.88	70.67	14.44	0.79
7812	7810	204.03	18	41	4.52	77.45	15.89	0.50
7814	7812	194.86	24	110	2.94	82.29	14.44	0.99
7816	7814	199.92	17	44	3.30	74.54	11.56	0.91
7818	7816	194.86	17	55	1.58	68.73	13.00	1.21
7820	7818	213.07	61	3425	4.29	75.51	14.44	5.69
7822	7820	197.92	55	33	3.24	80.35	11.56	4.96
7824	7822	191.40	21	29	1.56	62.92	11.56	-0.51
7826	7824	342.80	120	41	9.84	171.35	17.33	76.50
7828	7826	257.30	104	18	5.19	105.52	13.00	28.36
7830	7828	265.50	113	31	6.15	121.01	13.00	40.66
7832	7830	237.31	64	84	4.28	110.36	11.56	29.42
7834	7832	248.88	78	338	5.46	106.49	8.67	41.15
7836	7834	234.10	69	91	5.36	98.74	15.89	40.06
7838	7836	229.30	88	400	7.72	105.52	13.00	45.53
7840	7838	233.95	103	61	6.41	113.26	8.67	63.65
7842	7840	155.40	38	31	1.52	52.28	11.56	1.16
7844	7842	156.92	36	121	2.94	60.99	8.67	2.25
7846	7844	179.81	28	58	3.29	68.73	13.00	2.33
7848	7846	183.17	18	17	1.50	66.80	13.00	1.53
7850	7848	198.86	12	20	3.49	60.99	13.00	-0.55
7852	7850	157.28	22	12	3.11	53.24	11.56	0.86
7854	7852	157.99	9	12	3.29	58.08	11.56	-0.35
7856	7854	184.55	13	21	1.67	65.83	15.89	-0.58
7858	7856	188.98	83	391	3.07	63.89	13.00	0.21
7860	7858	191.71	15	57	3.39	64.86	14.44	-0.04
7862	7860	184.58	16	46	2.32	71.64	10.11	1.15

Table A.6. Well COP 289 XRF Trace Element Data Continued

Depth ft	LC Depth ft	V ppm	Cu ppm	Zn ppm	U ppm	Ni ppm	Th ppm	Mo ppm
7864	7862	192.57	20	117	4.26	74.54	14.44	1.15
7866	7864	195.63	18	53	1.14	71.64	14.44	0.91
7868	7866	190.00	18	36	3.55	69.70	17.33	0.82
7870	7868	195.50	15	29	2.82	72.60	11.56	0.66
7872	7870	50.95	-8	47	0.89	26.14	1.44	0.75
7874	7872	185.54	23	30	2.71	58.08	14.44	0.77
7876	7874	185.86	26	76	2.41	61.96	10.11	1.55
7878	7876	236.69	127	380	6.33	147.15	15.89	53.77
7880	7878	208.63	73	24	4.78	72.60	10.11	13.93
7882	7880	186.90	88	21	4.01	69.70	10.11	5.54
7884	7882	162.31	62	33	2.49	59.05	7.22	3.44
7886	7884	220.38	83	56	4.67	80.35	14.44	20.11
7888	7886	220.80	86	26	3.83	85.19	13.00	31.67
7890	7888	191.05	59	63	3.97	66.80	14.44	20.61
7892	7890	219.17	83	36	5.63	92.93	15.89	42.85
7894	7892	204.48	83	19	4.57	84.22	13.00	28.29
7896	7894	198.59	93	40	5.79	91.00	8.67	27.90
7898	7896	175.44	40	54	2.31	57.12	15.89	3.13
7900	7898	198.32	56	60	3.82	66.80	11.56	12.40
7902	7900	230.85	84	72	6.10	98.74	13.00	32.07
7904	7902	188.38	68	156	7.88	77.45	10.11	27.53
7906	7904	188.12	41	55	3.04	56.15	10.11	6.14
7908	7906	210.25	76	36	5.28	78.41	11.56	23.52
7910	7908	147.61	37	9	3.99	53.24	7.22	16.45
7912	7910	279.74	112	228	7.48	128.75	13.00	72.69
7914	7912	236.74	86	56	11.38	94.87	10.11	45.04
7916	7914	278.22	103	135	9.60	124.88	14.44	70.93
7918	7916	242.30	97	21	8.71	98.74	11.56	45.68
7920	7918	293.72	105	633	11.09	132.63	13.00	80.32
7922	7920	266.02	109	133	7.17	119.07	13.00	46.29
7924	7922	229.19	119	34	6.30	99.71	13.00	40.75
7926	7924	252.21	108	94	10.66	121.01	13.00	76.34
7928	7926	213.15	92	51	5.95	88.09	13.00	32.62
7930	7928	242.85	84	169	6.12	102.62	13.00	44.50
7932	7930	261.15	96	3476	7.31	117.14	14.44	51.64
7934	7932	243.72	87	71	4.65	69.70	17.33	12.21
7936	7934	174.31	61	6	4.66	60.99	10.11	23.57
7938	7936	215.35	57	29	2.72	65.83	14.44	4.19
7940	7938	221.64	79	106	5.17	73.57	10.11	8.64
7942	7940	199.74	64	20	2.32	73.57	15.89	5.00
7944	7942	234.08	63	95	4.05	73.57	13.00	10.31

Table A.6. Well COP 289 XRF Trace Element Data Continued

Depth ft	LC Depth ft	V ppm	Cu ppm	Zn ppm	U ppm	Ni ppm	Th ppm	Mo ppm
7946	7944	256.09	93	108	5.50	105.52	17.33	27.88
7952	7950	179.08	20	11	1.25	50.34	17.33	0.87
7954	7952	169.32	69	9	4.17	56.15	5.78	9.13
7956	7954	235.94	84	22	10.64	138.43	18.78	90.70
7958	7956	250.89	82	18	9.40	131.66	15.89	75.49
7960	7958	232.53	79	267	5.21	117.14	17.33	54.87
7962	7960	200.13	59	98	5.44	88.09	8.67	41.58
7964	7962	218.25	65	64	10.19	102.62	17.33	73.66
7966	7964	230.36	62	69	8.66	110.36	15.89	71.51
7968	7966	208.76	72	12	8.27	86.16	11.56	54.82
7970	7968	244.02	79	17	11.23	131.66	11.56	88.48
7972	7970	237.12	63	30	7.75	111.33	17.33	62.15
7974	7972	228.18	76	15	8.89	134.56	15.89	77.56
7976	7974	259.50	85	690	9.83	154.89	11.56	105.54
7978	7976	290.28	103	210	17.79	174.25	17.33	133.35
7980	7978	337.52	119	542	17.85	236.21	11.56	170.06
7982	7980	289.69	74	31	7.30	107.46	14.44	63.64
7984	7982	293.25	88	14	17.12	157.79	13.00	120.97
7986	7984	335.43	116	22	14.36	161.67	14.44	136.11
7988	7986	322.49	81	14	8.34	138.43	14.44	77.27
7990	7988	324.84	107	16	15.74	172.32	14.44	151.97
7992	7990	155.80	110	-2	8.57	94.87	1.44	45.40
7994	7992	337.20	328	6054	9.48	166.51	7.22	81.64
7996	7994	265.12	175	379	6.81	172.32	11.56	26.74
7998	7996	562.31	115	8	16.17	230.40	13.00	125.11
8000	7998	595.65	107	39	15.62	217.81	13.00	132.10
8002	8000	427.50	91	10	10.73	167.48	13.00	79.36
8004	8002	437.96	80	219	11.52	167.48	10.11	84.30
8006	8004	456.12	86	290	8.62	178.12	15.89	91.60
8008	8006	381.81	79	227	13.79	158.76	11.56	78.92
8010	8008	358.71	94	241	9.01	151.99	11.56	66.95
8012	8010	295.88	64	205	6.89	138.43	13.00	50.44
8014	8012	344.03	71	232	9.26	149.08	14.44	63.51
8016	8014	364.10	89	248	9.11	153.92	13.00	67.75
8018	8016	279.46	62	48	7.32	103.58	14.44	46.80
8020	8018	288.18	70	264	9.94	130.69	11.56	71.25
8022	8020	314.68	74	138	7.84	119.07	13.00	46.89
8024	8022	326.40	76	138	8.10	125.85	15.89	48.78
8026	8024	305.13	75	44	10.85	136.50	14.44	62.84
8028	8026	319.95	67	113	8.24	124.88	13.00	44.76
8030	8028	281.69	57	322	7.97	117.14	13.00	53.60

Table A.6. Well COP 289 XRF Trace Element Data Continued

Depth ft	LC Depth ft	V ppm	Cu ppm	Zn ppm	U ppm	Ni ppm	Th ppm	Mo ppm
8032	8030	265.10	56	174	8.66	121.01	11.56	58.95
8036	8034	314.53	69	197	7.48	126.82	10.11	49.46
8038	8036	326.11	65	313	8.74	151.99	14.44	51.04
8040	8038	294.25	61	247	8.82	125.85	15.89	52.24
8044	8042	267.92	62	199	6.98	123.91	10.11	50.23
8046	8044	277.65	60	116	7.33	111.33	11.56	51.50
8048	8046	310.76	67	129	11.48	122.94	14.44	81.41
8050	8048	319.77	94	6	12.87	151.99	13.00	82.44
8052	8050	288.33	75	28	7.16	121.98	14.44	54.10
8054	8052	309.53	92	4	9.67	140.37	11.56	65.82
8056	8054	314.35	72	3016	10.66	124.88	11.56	80.09
8058	8056	483.92	98	2152	17.47	155.86	15.89	108.99
8060	8058	286.67	67	2	8.01	121.98	14.44	56.58
8062	8060	326.70	73	6	7.32	141.34	17.33	58.18
8064	8062	337.34	71	4	9.21	128.75	14.44	64.35
8066	8064	390.97	78	551	12.51	167.48	10.11	97.49
8068	8066	322.52	74	8	10.40	146.18	11.56	68.28
8070	8068	300.11	76	-4	8.32	121.98	5.78	53.61
8072	8070	317.53	72	-4	6.60	109.39	8.67	51.35
8074	8072	324.92	74	228	11.32	140.37	8.67	98.48
8076	8074	285.04	87	122	7.51	160.70	7.22	62.25
8078	8076	309.13	74	-2	9.08	130.69	8.67	84.63
8080	8078	378.60	116	-1	12.79	165.54	13.00	106.59
8082	8080	581.56	135	36	18.14	237.18	11.56	136.75
8086	8084	465.00	136	80	21.91	226.53	10.11	94.78
8088	8086	667.62	225	451	42.36	340.76	13.00	229.91
8090	8088	525.51	174	38	39.16	270.09	2.89	188.47
8092	8090	473.99	177	235	20.65	277.84	8.67	191.36
8094	8092	875.60	155	0	22.70	266.22	7.22	138.26
8096	8094	83.94	13	-31	3.23	35.82	8.67	31.64
8098	8096	631.75	142	108	31.29	320.43	7.22	178.57
8100	8098	197.19	78	1687	13.72	84.22	-2.89	107.61
8102	8100	72.33	23	-7	4.44	34.85	-1.44	34.35
8104	8102	551.78	284	51	14.99	246.86	2.89	157.20
8106	8104	47.97	57	-6	9.14	53.24	-1.44	13.73
8108	8106	88.61	308	12	8.45	123.91	1.44	23.21
8110	8108	174.64	133	-14	8.82	72.60	8.67	9.31
8112	8110	42.53	14	-21	2.14	11.62	-2.89	1.83
8114	8112	42.07	58	-26	2.32	49.37	11.56	7.95
8116	8114	56.92	166	-24	3.07	89.06	0.00	4.83
8118	8116	17.61	5	54	1.15	6.78	-2.89	3.00

Table A.7. Well COP 653 XRD Major Element Data

Depth ft	LC Depth ft	SiO_2 wt %	TiO_2 wt %	Al_2O_3 wt %	Fe_2O_3 wt %	MnO wt %	CaO wt %	K_2O wt %	P_2O_5 wt %	S wt %
8222	8215.75	55.55	0.91	16.29	6.38	0.06	1.92	3.49	0.07	0.13
8224	8217.75	55.07	0.89	16.25	6.65	0.06	1.62	3.48	0.06	0.31
8226	8219.75	54.99	0.84	15.55	6.74	0.07	2.02	3.28	0.07	0.42
8228	8221.75	53.99	0.94	16.92	6.63	0.03	0.24	3.78	0.06	0.85
8230	8223.75	53.97	0.88	16.11	7.51	0.04	0.70	3.47	0.06	1.20
8232	8225.75	54.45	0.76	15.65	6.61	0.06	2.77	3.40	0.06	0.53
8234	8227.75	56.05	0.82	16.14	6.63	0.05	1.53	3.46	0.05	0.37
8236	8229.75	52.89	0.89	16.24	6.86	0.03	0.38	3.65	0.05	1.09
8238	8231.75	52.89	0.87	16.29	7.38	0.03	0.57	3.60	0.06	1.26
8240	8233.75	54.29	0.83	16.16	6.86	0.03	0.82	3.55	0.05	0.96
8242	8235.75	55.54	0.81	15.96	6.71	0.04	1.69	3.44	0.06	0.66
8244	8237.75	54.07	0.90	16.46	6.97	0.03	0.48	3.64	0.06	0.93
8246	8239.75	54.21	0.75	15.26	6.74	0.05	2.73	3.31	0.06	0.82
8248	8241.75	51.46	0.70	14.44	6.06	0.06	3.87	3.24	0.07	0.59
8250	8243.75	54.12	0.88	16.76	7.16	0.03	0.41	3.65	0.06	1.01
8252	8245.75	52.90	0.64	13.83	5.92	0.07	6.30	3.03	0.07	0.59
8254	8247.75	55.66	0.78	16.05	6.25	0.04	1.30	3.53	0.06	0.65
8256	8249.75	53.76	0.73	15.52	6.29	0.04	2.62	3.41	0.07	0.67
8258	8251.75	53.60	0.86	17.30	6.56	0.03	0.20	3.86	0.05	0.86
8260	8253.75	52.08	0.57	13.37	5.19	0.08	8.56	2.91	0.05	0.37
8262	8255.75	54.04	0.68	14.97	6.30	0.07	4.15	3.27	0.05	0.64
8264	8257.75	53.44	0.78	15.37	6.16	0.07	3.55	3.34	0.06	0.46
8266	8259.75	51.44	0.80	15.06	6.42	0.07	2.56	3.32	0.07	0.35
8268	8261.75	53.36	0.79	15.63	6.23	0.07	3.76	3.39	0.07	0.34
8270	8263.75	52.15	0.76	14.98	6.03	0.07	4.98	3.25	0.07	0.26
8272	8265.75	53.30	0.79	15.67	6.23	0.07	3.75	3.39	0.06	0.29
8274	8267.75	53.79	0.80	15.96	6.42	0.07	3.41	3.41	0.06	0.19
8276	8269.75	52.94	0.80	15.22	7.00	0.08	4.11	3.19	0.07	0.20
8278	8271.75	51.62	0.80	15.18	6.15	0.06	2.89	3.35	0.06	0.21
8280	8273.75	53.83	0.83	16.08	6.23	0.07	3.20	3.47	0.07	0.24
8282	8275.75	53.88	0.84	16.01	6.57	0.07	2.75	3.42	0.07	0.40
8284	8277.75	53.52	0.81	15.53	6.51	0.08	3.72	3.32	0.07	0.34
8286	8279.75	52.83	0.83	15.49	6.46	0.07	2.93	3.36	0.07	0.39
8288	8281.75	54.04	0.79	15.49	6.31	0.07	3.55	3.35	0.06	0.27
8290	8283.75	53.63	0.62	14.44	5.60	0.06	5.90	3.14	0.05	0.32
8292	8285.75	54.04	0.80	16.31	6.58	0.04	1.83	3.54	0.06	0.75
8294	8287.75	53.84	0.86	16.84	6.64	0.03	0.77	3.70	0.06	0.81
8296	8289.75	55.49	0.79	16.39	6.32	0.04	1.80	3.56	0.05	0.52

Table A.7. Well COP 653 XRD Major Element Data Continued

Depth ft	LC Depth ft	SiO_2 wt %	TiO_2 wt %	Al_2O_3 wt %	Fe_2O_3 wt %	MnO wt %	CaO wt %	K_2O wt %	P_2O_5 wt %	S wt %
8298	8291.75	53.46	0.84	17.07	6.62	0.03	0.57	3.76	0.05	1.00
8300	8293.75	53.47	0.74	15.77	6.24	0.06	3.40	3.44	0.06	0.50
8306	8299.75	53.90	0.79	15.91	6.21	0.04	3.38	3.44	0.06	0.75
8308	8301.75	53.11	0.91	17.16	7.37	0.03	0.44	3.68	0.06	1.25
8310	8303.75	51.27	0.85	16.19	6.69	0.03	0.95	3.59	0.06	1.04
8312	8305.75	51.92	0.71	14.90	5.97	0.07	4.99	3.25	0.06	0.53
8314	8307.75	53.73	0.88	17.28	6.21	0.03	0.70	3.80	0.06	0.91
8316	8309.75	53.10	0.84	17.11	6.52	0.03	0.80	3.78	0.05	1.04
8318	8311.75	52.71	0.88	16.79	7.09	0.03	0.84	3.67	0.06	1.29
8320	8313.75	52.91	0.73	15.46	6.15	0.06	4.02	3.40	0.05	0.82
8322	8315.75	53.05	0.78	16.09	6.48	0.06	2.99	3.50	0.06	0.71
8324	8317.75	53.29	0.75	17.02	6.42	0.03	1.66	3.72	0.06	0.95
8326	8319.75	48.56	0.50	13.07	5.24	0.08	9.85	2.78	0.06	0.59
8328	8321.75	52.70	0.84	17.71	6.37	0.02	0.25	3.90	0.05	0.95
8330	8323.75	53.11	0.78	17.11	6.28	0.03	0.99	3.77	0.05	0.83
8332	8325.75	53.14	0.80	16.28	6.99	0.04	1.84	3.53	0.06	1.02
8334	8327.75	50.53	0.65	14.29	7.55	0.07	5.18	2.93	0.06	1.13
8336	8329.75	50.16	0.85	16.91	7.62	0.02	0.28	3.69	0.07	1.72
8338	8331.75	49.66	0.80	16.48	7.19	0.03	2.55	3.59	0.06	1.45
8340	8333.75	51.72	0.79	16.79	7.01	0.03	1.75	3.66	0.05	1.11
8342	8335.75	52.06	0.86	17.67	6.91	0.02	0.26	3.91	0.05	1.15
8344	8337.75	52.57	0.92	17.92	6.60	0.02	0.23	3.93	0.06	0.91
8346	8339.75	45.93	0.88	16.42	7.21	0.03	1.04	3.70	0.06	1.18
8348	8341.75	51.30	0.83	16.46	7.05	0.04	1.62	3.59	0.05	1.19
8350	8343.75	52.63	0.84	17.76	6.39	0.03	0.96	3.89	0.05	0.75
8352	8345.75	50.95	0.75	16.72	7.79	0.03	1.51	3.56	0.05	1.64
8354	8347.75	52.30	0.87	17.89	6.83	0.02	0.22	3.89	0.05	1.24
8356	8349.75	52.35	0.88	17.35	6.48	0.03	0.66	3.82	0.04	1.25
8358	8351.75	49.65	0.70	14.01	7.44	0.10	7.38	2.83	0.07	0.47
8360	8353.75	50.93	0.76	15.61	7.10	0.06	4.11	3.29	0.05	1.12
8362	8355.75	50.42	0.81	16.26	7.71	0.02	0.41	3.59	0.06	2.10
8364	8357.75	52.04	0.86	16.80	7.17	0.02	0.20	3.71	0.06	1.54
8366	8359.75	52.13	0.86	16.72	7.68	0.02	0.32	3.65	0.06	1.65
8368	8361.75	51.72	0.88	16.80	7.11	0.02	0.21	3.73	0.05	1.51
8370	8363.75	51.95	0.87	16.20	7.46	0.02	0.19	3.59	0.05	1.80
8372	8365.75	50.25	0.82	15.91	8.69	0.02	0.40	3.41	0.05	2.40
8374	8367.75	51.76	0.84	16.18	7.65	0.02	0.24	3.59	0.06	1.87
8376	8369.75	48.94	0.81	15.22	7.54	0.02	1.09	3.48	0.06	2.12

Table A.7. Well COP 653 XRD Major Element Data Continued

Depth ft	LC Depth ft	SiO_2 wt %	TiO_2 wt %	Al_2O_3 wt %	Fe_2O_3 wt %	MnO wt %	CaO wt %	K_2O wt %	P_2O_5 wt %	S wt %
8378	8371.75	54.40	0.86	16.02	6.93	0.02	0.31	3.58	0.05	1.48
8380	8373.75	53.15	0.82	16.21	6.63	0.02	0.78	3.66	0.05	1.31
8382	8375.75	53.22	0.80	15.32	8.05	0.02	0.37	3.34	0.06	1.97
8384	8377.75	53.94	0.83	15.50	7.53	0.02	0.60	3.41	0.07	1.60
8394	8387.75	54.62	0.86	15.74	7.10	0.02	0.42	3.51	0.06	1.61
8396	8389.75	55.13	0.84	15.91	6.33	0.02	0.50	3.65	0.05	1.26
8398	8391.75	55.18	0.77	14.19	6.84	0.03	1.99	3.16	0.08	1.34
8400	8393.75	54.73	0.83	15.16	7.17	0.02	0.75	3.41	0.06	1.48
8402	8395.75	56.04	0.86	15.70	6.32	0.02	0.65	3.59	0.05	1.09
8404	8397.75	54.74	0.89	16.20	6.52	0.02	0.53	3.71	0.05	1.20
8406	8399.75	53.29	0.86	16.39	6.61	0.02	0.76	3.73	0.04	1.26
8408	8401.75	53.12	0.88	16.36	6.83	0.02	0.70	3.73	0.05	1.51
8410	8403.75	51.65	0.81	15.61	6.88	0.03	2.27	3.50	0.05	1.58
8412	8405.75	51.95	0.65	13.05	6.65	0.05	6.50	2.82	0.08	1.26
8414	8407.75	55.18	0.91	15.91	6.55	0.02	0.50	3.63	0.06	1.48
8416	8409.75	54.71	0.86	15.31	6.66	0.02	0.91	3.45	0.06	1.65
8420	8413.75	39.41	0.26	6.88	3.49	0.07	25.84	1.33	0.06	0.48
8422	8415.75	52.20	0.85	15.58	5.83	0.03	2.92	3.43	0.06	1.29
8424	8417.75	47.79	0.52	10.38	3.99	0.04	14.64	2.17	0.08	1.04
8426	8419.75	34.55	0.22	4.53	4.24	0.07	33.84	0.76	0.10	0.82
8428	8421.75	52.75	0.81	15.84	6.31	0.02	1.32	3.64	0.06	1.93
8430	8423.75	54.76	0.77	14.97	5.36	0.03	2.90	3.49	0.07	1.61
8432	8425.75	54.26	0.74	13.78	5.47	0.03	4.70	3.22	0.06	1.74
8434	8427.75	58.54	0.77	14.23	5.80	0.02	2.23	3.25	0.05	1.52
8436	8429.75	56.57	0.70	12.91	5.64	0.03	4.67	2.91	0.05	1.70
8438	8431.75	56.95	0.71	12.79	6.28	0.03	3.92	2.89	0.05	1.73
8440	8433.75	56.61	0.73	13.45	5.80	0.03	3.54	3.06	0.06	1.66
8442	8435.75	56.58	0.62	11.16	5.24	0.04	8.29	2.49	0.09	1.39
8444	8437.75	56.91	0.75	13.06	5.82	0.03	3.92	2.96	0.07	1.64
8446	8439.75	55.43	0.92	15.61	6.26	0.02	0.66	3.53	0.05	1.64
8448	8441.75	52.73	0.68	12.76	5.46	0.03	7.42	2.86	0.10	1.51
8450	8443.75	53.49	0.82	14.42	6.11	0.03	3.01	3.26	0.05	1.79
8452	8445.75	55.60	0.82	15.00	6.35	0.02	2.20	3.37	0.06	1.53
8454	8447.75	55.26	0.84	15.29	6.18	0.03	2.52	3.38	0.05	1.45
8456	8449.75	55.05	0.86	15.15	6.37	0.03	2.31	3.41	0.05	1.64
8458	8451.75	53.85	0.81	14.02	6.11	0.03	3.87	3.14	0.07	1.62
8460	8453.75	55.45	0.89	15.29	6.40	0.02	1.78	3.42	0.05	1.50
8462	8455.75	55.57	0.84	14.36	6.55	0.03	2.36	3.18	0.05	1.62
8464	8457.75	56.76	0.81	14.54	6.06	0.03	2.60	3.22	0.05	1.42
8466	8459.75	55.81	0.85	14.79	5.77	0.02	1.94	3.37	0.07	1.57

Table A.7. Well COP 653 XRD Major Element Data Continued

Depth ft	LC Depth ft	SiO_2 wt %	TiO_2 wt %	Al_2O_3 wt %	Fe_2O_3 wt %	MnO wt %	CaO wt %	K_2O wt %	P_2O_5 wt %	S wt %
8468	8461.75	56.94	0.84	14.70	5.93	0.02	2.05	3.32	0.05	1.50
8470	8463.75	55.79	0.77	13.79	5.65	0.03	4.32	3.14	0.06	1.38
8476	8469.75	54.94	0.82	15.03	5.59	0.02	2.58	3.47	0.08	1.38
8478	8471.75	57.09	0.80	14.42	5.85	0.02	2.38	3.25	0.06	1.31
8480	8473.75	57.42	0.81	14.72	6.84	0.02	1.49	3.26	0.06	1.52
8482	8475.75	56.16	0.85	14.90	6.17	0.02	1.42	3.38	0.06	1.49
8484	8477.75	52.28	0.82	13.86	6.24	0.03	3.42	3.15	0.11	1.55
8486	8479.75	55.25	0.89	15.05	6.15	0.02	1.84	3.41	0.05	1.57
8488	8481.75	55.81	0.89	15.16	5.95	0.02	0.87	3.47	0.06	1.53
8490	8483.75	55.29	0.80	14.19	5.59	0.03	3.08	3.32	0.07	1.32
8492	8485.75	57.27	0.81	14.08	5.72	0.03	2.65	3.22	0.06	1.40
8494	8487.75	57.46	0.82	14.13	5.87	0.03	2.12	3.22	0.06	1.47
8496	8489.75	57.76	0.83	14.20	5.88	0.02	1.95	3.24	0.06	1.44
8498	8491.75	57.87	0.88	15.04	5.64	0.02	0.99	3.43	0.06	1.43
8500	8493.75	57.49	0.78	13.98	5.56	0.03	3.18	3.15	0.05	1.32
8502	8495.75	58.62	0.79	13.81	5.26	0.02	2.30	3.20	0.05	1.22
8504	8497.75	57.09	0.77	13.99	6.98	0.02	1.82	3.08	0.05	1.79
8506	8499.75	59.13	0.79	13.81	5.64	0.02	2.11	3.09	0.06	1.41
8508	8501.75	58.09	0.73	13.46	5.11	0.02	3.97	3.06	0.07	1.26
8510	8503.75	58.67	0.79	13.89	5.30	0.02	3.06	3.11	0.06	1.26
8512	8505.75	61.03	0.73	13.83	5.65	0.02	1.14	3.00	0.05	1.34
8514	8507.75	57.09	0.74	13.49	6.22	0.02	1.86	3.11	0.08	1.99
8516	8509.75	63.78	0.54	10.41	6.49	0.02	2.98	2.33	0.05	2.05
8518	8511.75	61.49	0.58	11.45	6.44	0.01	2.18	2.60	0.06	2.07
8520	8513.75	57.56	0.52	10.85	6.12	0.02	5.86	2.47	0.05	2.29
8522	8515.75	52.89	0.64	13.16	7.22	0.02	2.99	2.98	0.06	2.74
8524	8517.75	65.59	0.52	10.14	5.05	0.01	4.57	2.30	0.06	1.78
8528	8521.75	81.57	0.21	4.84	3.05	0.01	5.92	1.14	0.06	1.20
8530	8523.75	75.03	0.12	3.57	1.40	0.01	20.73	0.74	0.07	0.63
8532	8525.75	87.52	0.12	3.16	0.93	0.01	15.25	0.71	0.09	0.46
8534	8527.75	55.49	0.17	4.15	2.65	0.01	24.40	0.90	0.09	1.48
8536	8529.75	22.81	-0.02	0.57	0.32	0.02	47.90	0.12	0.05	0.25
8538	8531.75	37.81	0.14	5.01	0.74	0.01	32.03	1.18	0.04	0.54
8540	8533.75	15.11	0.05	3.74	0.48	0.02	40.44	0.74	0.06	0.38
8542	8535.75	13.01	0.02	1.24	0.35	0.02	44.07	0.33	0.04	0.18
8544	8537.75	21.75	0.10	4.16	1.29	0.02	35.33	0.96	0.06	0.68
8546	8539.75	36.15	0.27	6.87	1.96	0.02	25.31	1.76	0.12	0.63
8548	8541.75	40.56	0.76	14.46	3.32	0.02	9.08	4.02	0.08	1.25
8550	8543.75	38.86	0.32	7.18	1.84	0.04	24.64	2.04	0.04	0.26

Table A.8. Well COP 259 XRF Major Element Data

Depth ft	LC Depth ft	SiO_2 wt %	TiO_2 wt %	Al_2O_3 wt %	Fe_2O_3 wt %	MnO wt %	CaO wt %	K_2O wt %	P_2O_5 wt %	S wt %
8040	8037	55.598	ND	15.811	6.803	0.078	1.544	3.3976	0.066	0.212
8042	8039	54.718	ND	15.016	6.953	0.088	2.049	3.1871	0.068	0.308
8044	8041	55.236	ND	14.928	6.818	0.087	2.043	3.1243	0.072	0.2
8046	8043	54.871	ND	14.732	7.073	0.09	2.191	3.034	0.074	0.238
8048	8045	54.413	ND	15.548	7.301	0.069	1.6	3.2679	0.073	0.323
8050	8047	54.797	ND	15.041	7.326	0.092	1.882	3.1169	0.078	0.127
8052	8049	54.386	ND	14.948	7.256	0.09	2.349	3.0744	0.076	0.143
8054	8051	54.84	ND	15.073	6.968	0.099	2.223	3.0861	0.074	0.142
8056	8053	55.075	ND	13.955	7.483	0.11	2.849	2.7289	0.084	0.162
8058	8055	54.93	ND	14.751	7.204	0.091	2.343	3.0074	0.078	0.182
8060	8057	50.244	ND	12.964	12.161	0.102	2.936	2.1485	0.097	0.115
8062	8059	54.881	ND	15.054	6.866	0.083	2.221	3.1445	0.073	0.08
8064	8061	58.169	ND	15.983	7.408	0.104	2.544	3.2338	0.073	0.156
8066	8063	54.02	ND	15.299	6.915	0.087	2.172	3.1988	0.069	0.157
8068	8065	53.585	ND	14.683	7.443	0.08	2.119	3.0191	0.094	0.197
8070	8067	54.928	ND	15.415	6.716	0.084	1.969	3.2827	0.068	0.189
8072	8069	55.931	ND	15.204	6.18	0.057	2.429	3.3168	0.051	0.253
8074	8071	55.372	ND	15.628	6.356	0.054	1.809	3.4188	0.051	0.4
8076	8073	55.593	ND	15.266	6.543	0.056	1.963	3.3093	0.055	0.525
8078	8075	55.89	ND	15.333	7.301	0.039	0.706	3.2296	0.052	1.129
8080	8077	55.083	ND	15.686	7.347	0.032	0.457	3.3263	0.051	1.166
8082	8079	55.706	ND	15.241	7.257	0.036	0.617	3.2126	0.054	1.124
8084	8081	55.111	ND	15.701	7.145	0.031	0.519	3.3582	0.053	0.981
8086	8083	53.65	ND	15.774	7.092	0.028	0.247	3.4677	0.052	1.101
8088	8085	54.901	ND	15.469	7.111	0.044	1.128	3.3487	0.053	0.743
8090	8087	54.401	ND	15.137	6.543	0.062	2.415	3.3401	0.058	0.495
8092	8089	54.415	ND	15.829	6.778	0.046	1.27	3.4783	0.058	0.681
8094	8091	54.786	ND	16.19	6.776	0.037	0.806	3.5474	0.052	0.657
8096	8093	53.461	ND	16.598	7.111	0.025	0.186	3.5974	0.057	1.033
8098	8095	54.627	ND	15.966	7.351	0.033	0.483	3.4092	0.055	1.043
8100	8097	54.904	ND	15.996	6.843	0.052	1.289	3.4624	0.051	0.545
8102	8099	54.849	ND	15.412	7.039	0.065	1.765	3.2976	0.06	0.405
8104	8101	55.641	ND	15.991	6.655	0.046	1.096	3.4645	0.059	0.365
8106	8103	54.296	ND	15.897	7.601	0.027	0.362	3.388	0.053	1.279
8108	8105	53.605	ND	15.654	7.491	0.026	0.215	3.3859	0.053	1.272
8110	8107	53.876	ND	16.178	6.946	0.034	0.581	3.5219	0.052	0.838
8112	8109	55.198	ND	15.641	7.013	0.051	1.329	3.354	0.049	0.488
8114	8111	53.074	ND	16.202	7.103	0.026	0.207	3.5326	0.055	1.125
8116	8113	55.344	ND	15.807	6.991	0.035	0.784	3.4061	0.056	0.81
8118	8115	55.185	ND	16.117	6.987	0.027	0.235	3.4581	0.052	0.922

Table A.8. Well COP 259 XRF Major Element Data Continued

Depth ft	LC Depth ft	SiO_2 wt %	TiO_2 wt %	Al_2O_3 wt %	Fe_2O_3 wt %	MnO wt %	CaO wt %	K_2O wt %	P_2O_5 wt %	S wt %
8120	8117	54.714	ND	15.55	7.371	0.036	0.819	3.3306	0.054	0.981
8122	8119	55.111	ND	15.424	6.841	0.044	1.503	3.3274	0.065	0.665
8124	8121	54.295	ND	15.986	7.3	0.027	0.276	3.4656	0.055	1.166
8126	8123	54.034	ND	14.634	7.429	0.063	2.757	3.1201	0.067	0.818
8128	8125	55.462	ND	15.525	6.765	0.053	1.539	3.3731	0.055	0.48
8130	8127	53.896	ND	14.303	7.541	0.065	2.946	3.0489	0.069	0.856
8132	8129	54.264	ND	15.646	7.539	0.029	0.297	3.3529	0.051	1.232
8134	8131	55.124	ND	15.36	7.073	0.044	1.316	3.3093	0.057	0.817
8136	8133	53.737	ND	14.256	6.563	0.061	3.63	3.1095	0.067	0.594
8138	8135	54.971	ND	15.378	6.866	0.033	0.666	3.3316	0.053	1.013
8140	8137	55.249	ND	14.85	6.633	0.048	2.328	3.2264	0.058	0.625
8142	8139	54.105	ND	14.747	6.604	0.057	3.002	3.2296	0.061	0.591
8144	8141	55.294	ND	15.468	6.625	0.042	1.407	3.3922	0.058	0.687
8146	8143	53.749	ND	16.057	7.025	0.027	0.225	3.489	0.054	1.109
8148	8145	53.926	ND	16.035	7.033	0.036	1.041	3.489	0.057	0.987
8150	8147	55.008	ND	16.188	6.761	0.038	1.262	3.4773	0.05	0.677
8152	8149	53.339	ND	14.659	6.809	0.076	4.273	3.1754	0.052	0.422
8154	8151	54.667	ND	15.568	6.443	0.064	2.557	3.4294	0.051	0.351
8156	8153	55.228	ND	16.009	6.116	0.048	1.632	3.5676	0.05	0.286
8158	8155	53.759	ND	15.661	7.399	0.06	1.837	3.4007	0.059	0.68
8160	8157	54.156	ND	15.476	6.169	0.059	2.754	3.4581	0.056	0.17
8162	8159	53.854	ND	15.447	6.408	0.066	3.198	3.4071	0.061	0.282
8164	8161	53.877	ND	15.586	6.368	0.062	2.86	3.4496	0.054	0.253
8166	8163	54.277	ND	15.5	6.279	0.064	3.006	3.4209	0.056	0.175
8168	8165	54.74	ND	15.665	6.536	0.062	2.641	3.4422	0.056	0.285
8170	8167	53.293	0.802	15.415	7.053	0.07	3.387	3.309	0.065	0.394
8172	8169	54.428	0.804	16.05	6.655	0.065	2.855	3.477	0.059	0.265
8174	8171	54.266	0.881	17.087	6.635	0.034	0.943	3.78	0.063	0.671
8176	8173	54.599	0.926	17.147	6.618	0.033	0.683	3.794	0.058	0.76
8178	8175	54.344	0.87	16.534	6.669	0.033	1.238	3.629	0.065	0.921
8180	8177	55.193	0.821	16.682	6.616	0.037	1.053	3.669	0.056	0.684
8182	8179	52.338	0.775	15.914	8.736	0.032	1.07	3.35	0.052	1.629
8184	8181	54.013	0.823	17.276	6.275	0.051	1.691	3.825	0.055	0.409
8186	8183	54.236	0.807	16.751	6.854	0.039	1.321	3.669	0.059	0.731
8188	8185	53.013	0.889	17.549	6.744	0.026	0.316	3.896	0.054	0.962
8190	8187	52.481	0.877	17.331	6.877	0.028	0.828	3.817	0.053	1.042
8192	8189	53.112	0.802	16.192	7.064	0.038	1.603	3.55	0.06	1.118
8194	8191	52.963	0.732	15.797	6.046	0.061	3.852	3.497	0.056	0.433
8196	8193	52.925	0.873	17.445	6.753	0.023	0.281	3.912	0.05	1.119
8198	8195	52.742	0.883	17.637	6.703	0.024	0.23	3.944	0.053	1.089

Table A.8. Well COP 259 XRF Major Element Data Continued

Depth ft	LC Depth ft	SiO_2 wt %	TiO_2 wt %	Al_2O_3 wt %	Fe_2O_3 wt %	MnO wt %	CaO wt %	K_2O wt %	P_2O_5 wt %	S wt %
8200	8197	53.017	0.767	16.107	6.643	0.05	2.673	3.57	0.058	0.782
8202	8199	51.948	0.573	14.457	5.786	0.068	6.856	3.156	0.059	0.51
8208	8205	52.093	0.844	17.42	7.951	0.027	0.315	3.821	0.058	1.391
8210	8207	48.066	0.886	17.36	8.19	0.021	0.164	3.855	0.072	2.119
8218	8215	52.736	0.812	17.427	6.676	0.035	1.166	3.9	0.053	0.841
8220	8217	53.792	0.856	18.033	5.965	0.029	0.453	4.063	0.049	0.595
8222	8219	52.105	0.843	17.473	6.733	0.025	0.505	3.921	0.05	1.309
8224	8221	53.168	0.918	17.972	6.469	0.022	0.197	3.989	0.049	1.269
8226	8223	52.169	0.716	15.658	7.359	0.056	3.6	3.312	0.059	1.216
8228	8225	50.95	0.877	17.459	7.459	0.025	0.396	3.822	0.049	1.942
8230	8227	52.698	0.857	17.664	6.801	0.02	0.142	3.942	0.052	1.492
8232	8229	52.408	0.863	17.08	7.24	0.02	0.232	3.807	0.049	1.579
8234	8231	53.246	0.879	17.21	6.822	0.022	0.264	3.86	0.046	1.337
8236	8233	52.641	0.864	16.487	7.579	0.021	0.263	3.675	0.049	1.854
8238	8235	49.741	0.806	15.798	7.914	0.021	0.382	3.497	0.052	1.918
8240	8237	53.122	0.832	17.197	7.172	0.02	0.315	3.857	0.051	1.491
8242	8239	53.605	0.85	16.52	7.778	0.022	0.451	3.605	0.054	1.634
8244	8241	55.181	0.857	16.348	6.533	0.024	0.562	3.719	0.053	1.354
8246	8243	55.082	0.764	15.515	7.257	0.026	1.001	3.477	0.05	1.657
8248	8245	54.557	0.833	15.93	6.865	0.024	0.978	3.576	0.063	1.371
8250	8247	55.486	0.826	15.771	7.812	0.022	0.441	3.417	0.063	1.718
8252	8249	55.577	0.834	15.733	6.956	0.02	0.343	3.552	0.062	1.502
8254	8251	55.485	0.765	15.001	7.349	0.035	1.672	3.327	0.053	1.57
8256	8253	55.121	0.801	15.656	7.659	0.024	0.822	3.474	0.056	1.757
8258	8255	52.345	0.792	14.434	6.65	0.019	0.413	3.316	0.052	1.409
8260	8257	55.852	0.786	14.873	7.335	0.028	1.337	3.299	0.066	1.516
8262	8259	56.109	0.802	15.183	6.965	0.027	1.27	3.377	0.054	1.351
8264	8261	55.746	0.857	15.718	6.854	0.024	0.804	3.558	0.069	1.32
8266	8263	56.471	0.868	16.556	6.215	0.02	0.474	3.81	0.047	1.111
8268	8265	55.633	0.87	16.475	6.357	0.024	0.721	3.784	0.05	1.105
8270	8267	53.883	0.848	16.635	6.906	0.02	0.677	3.792	0.043	1.405
8272	8269	54.691	0.863	16.354	6.539	0.023	0.944	3.762	0.053	1.424
8274	8271	54.203	0.872	16.09	7.388	0.019	0.808	3.622	0.051	1.872
8276	8273	52.974	0.748	15.129	6.258	0.025	3.201	3.49	0.065	1.429
8278	8275	55.622	0.902	16.151	6.753	0.02	0.717	3.631	0.057	1.616
8280	8277	55.294	0.877	15.973	6.102	0.019	0.688	3.633	0.054	1.311
8282	8279	54.626	0.859	15.869	6.436	0.022	1.005	3.497	0.062	1.498
8284	8281	46.219	0.581	12.594	5.858	0.05	10.606	2.479	0.045	1.422
8286	8283	49.193	0.591	11.893	4.424	0.039	12.184	2.597	0.058	0.938
8288	8285	51.521	0.684	12.968	3.928	0.031	8.55	2.928	0.081	0.704

Table A.8. Well COP 259 XRF Major Element Data Continued

Depth ft	LC Depth ft	SiO_2 wt %	TiO_2 wt %	Al_2O_3 wt %	Fe_2O_3 wt %	MnO wt %	CaO wt %	K_2O wt %	P_2O_5 wt %	S wt %
8290	8287	41.089	0.557	11.957	3.405	-0.004	1.809	2.891	0.392	2.811
8292	8289	54.126	0.821	15.601	5.691	0.02	1.143	3.637	0.056	1.549
8298	8295	58.757	0.66	12.446	5.153	0.026	4.832	2.903	0.063	1.424
8300	8297	57.799	0.662	12.385	5.565	0.028	5.006	2.838	0.05	1.408
8302	8299	56.726	0.862	14.206	6.015	0.021	0.942	3.324	0.057	1.757
8304	8301	58.394	0.769	13.59	5.53	0.026	3.346	3.12	0.058	1.4
8306	8303	56.138	0.829	15.358	7.082	0.02	1	3.43	0.046	1.893
8308	8305	55.062	0.901	15.631	7.011	0.02	0.83	3.485	0.051	1.779
8310	8307	53.937	0.756	13.958	5.874	0.03	4.647	3.164	0.059	1.453
8312	8309	55.582	0.884	15.456	5.987	0.021	1.344	3.549	0.046	1.424
8314	8311	54.587	0.796	14.87	5.87	0.027	3.585	3.353	0.063	1.374
8316	8313	56.207	0.884	15.394	6.135	0.025	1.943	3.481	0.05	1.383
8318	8315	55.658	0.901	15.264	6.278	0.026	1.985	3.425	0.048	1.483
8320	8317	56.546	0.917	15.827	6.165	0.022	1.22	3.59	0.044	1.482
8322	8319	55.881	0.856	15.205	6.184	0.024	2.181	3.438	0.049	1.54
8324	8321	55.001	0.732	13.4	5.497	0.029	5.134	3.071	0.076	1.314
8326	8323	56.934	0.846	15.241	5.99	0.021	1.543	3.532	0.055	1.432
8328	8325	56.635	0.807	14.454	5.813	0.026	3.356	3.302	0.062	1.353
8330	8327	53.269	0.8	14.628	5.296	0.029	4.803	3.45	0.077	1.255
8332	8329	55.519	0.89	15.952	6.009	0.021	0.991	3.686	0.056	1.408
8334	8331	57.519	0.858	15.833	6.099	0.019	0.798	3.671	0.052	1.472
8336	8333	56.853	0.827	14.779	6.296	0.025	2.398	3.35	0.068	1.321
8338	8335	56.669	0.826	15.113	5.767	0.024	2.053	3.515	0.07	1.289
8340	8337	54.204	0.828	15.251	5.673	0.03	2.998	3.52	0.093	1.061
8342	8339	55.237	0.921	15.616	6.284	0.024	1.315	3.605	0.054	1.607
8344	8341	56.057	0.857	15.261	6.601	0.019	0.658	3.523	0.05	1.767
8346	8343	57.601	0.834	15.167	5.848	0.022	1.478	3.541	0.051	1.405
8348	8345	55.808	0.819	14.975	8.472	0.019	1.061	3.33	0.049	2.351
8350	8347	59.711	0.841	14.145	5.862	0.023	2.003	3.248	0.057	1.383
8352	8349	58.868	0.838	14.4	5.851	0.023	1.643	3.306	0.058	1.316
8354	8351	57.735	0.81	14.546	5.871	0.023	2.34	3.352	0.058	1.415
8356	8353	58.147	0.871	14.846	5.833	0.022	1.062	3.389	0.055	1.328
8358	8355	59.349	0.781	14.048	5.29	0.023	2.655	3.278	0.06	1.18
8360	8357	58.704	0.748	13.634	5.376	0.026	3.823	3.165	0.064	1.229
8362	8359	59.019	0.77	13.449	7.311	0.018	1.485	2.958	0.059	2.058
8364	8361	58.092	0.817	14.535	6.383	0.018	1.126	3.315	0.063	1.622
8366	8363	53.097	0.744	14.704	6.812	0.042	3.666	3.108	0.08	1.188
8368	8365	57.898	0.754	13.857	5.205	0.024	3.415	3.192	0.062	1.25
8370	8367	59.346	0.741	13.307	6.647	0.017	1.412	3.012	0.056	1.914
8372	8369	60.453	0.358	8.223	5.518	0.021	11.046	1.85	0.169	2.137

Table A.8. Well COP 259 XRF Major Element Data Continued

Depth ft	LC Depth ft	SiO_2 wt %	TiO_2 wt %	Al_2O_3 wt %	Fe_2O_3 wt %	MnO wt %	CaO wt %	K_2O wt %	P_2O_5 wt %	S wt %
8374	8371	56.99	0.58	11.454	8.416	0.014	1.894	2.573	0.059	2.84
8376	8373	12.981	-0.013	0.572	1.705	0.061	44.128	0.114	0.413	1.018
8382	8379	45.85	0.648	23.445	1.251	0.002	0.189	3.714	0.076	0.239
8384	8381	74.031	0.238	5.406	3.295	0.011	13.273	1.147	0.047	1.408
8386	8383	76.636	0.091	3.04	1.949	0.014	22.318	0.611	0.068	0.901
8388	8385	46.661	0.024	1.631	1.757	0.037	39.918	0.257	0.088	1.088
8390	8387	1.427	-0.028	0.186	0.27	0.034	49.243	0.046	0.09	0.456
8392	8389	20.298	0.024	1.329	0.585	0.022	45.202	0.289	0.048	0.36
8394	8391	36.762	0.235	5.841	1.54	0.018	28.285	1.505	0.153	0.585

Table A.9. Well COP 289 XRF Major Element Data

Depth ft	LC Depth ft	SiO_2 wt %	TiO_2 wt %	Al_2O_3 wt %	Fe_2O_3 wt %	MnO wt %	CaO wt %	K_2O wt %	P_2O_5 wt %	S wt %
7786	7784	54.25	ND	15.50	6.22	0.04	2.04	3.42	0.05	0.62
7788	7786	55.42	ND	15.75	6.34	0.06	2.57	3.49	0.06	0.34
7790	7788	54.21	ND	15.59	7.00	0.07	1.64	3.42	0.06	0.34
7792	7790	55.42	ND	15.79	6.44	0.07	1.70	3.42	0.07	0.01
7794	7792	55.25	ND	15.17	7.06	0.08	2.31	3.22	0.09	0.02
7796	7794	54.40	ND	15.11	7.35	0.09	2.46	3.16	0.09	0.12
7798	7796	55.02	ND	14.76	7.46	0.09	2.46	3.04	0.09	0.17
7800	7798	55.46	ND	15.28	7.05	0.08	2.06	3.20	0.08	0.04
7802	7800	51.70	ND	12.30	9.89	0.15	4.91	2.15	0.11	0.17
7804	7802	54.37	ND	15.63	7.39	0.06	1.65	3.33	0.06	0.14
7806	7804	54.87	ND	15.48	6.95	0.07	2.01	3.31	0.06	0.21
7808	7806	54.82	ND	15.82	6.82	0.06	1.86	3.45	0.06	0.25
7810	7808	55.74	ND	14.53	7.11	0.12	2.65	3.01	0.06	0.32
7812	7810	54.60	ND	15.69	6.51	0.06	1.94	3.46	0.06	0.29
7814	7812	55.06	ND	15.47	6.75	0.07	2.09	3.34	0.06	0.36
7816	7814	55.17	ND	15.39	6.41	0.07	2.40	3.39	0.06	0.25
7818	7816	56.41	ND	15.53	6.19	0.07	2.17	3.40	0.06	0.22
7820	7818	56.26	ND	16.13	6.06	0.04	0.94	3.64	0.05	0.31
7822	7820	54.44	ND	15.11	6.36	0.06	2.73	3.39	0.04	0.57
7824	7822	56.30	ND	15.15	6.33	0.07	2.89	3.32	0.05	0.31
7826	7824	53.15	ND	16.17	7.03	0.03	0.32	3.69	0.04	1.06
7828	7826	54.54	ND	15.62	6.87	0.04	1.09	3.49	0.04	0.87
7830	7828	54.24	ND	15.56	6.67	0.03	0.79	3.54	0.05	0.88
7832	7830	55.62	ND	15.70	6.15	0.04	1.50	3.57	0.05	0.56

Table A.9. Well COP 289 XRF Major Element Data Continued

Depth ft	LC Depth ft	SiO_2 wt %	TiO_2 wt %	Al_2O_3 wt %	Fe_2O_3 wt %	MnO wt %	CaO wt %	K_2O wt %	P_2O_5 wt %	S wt %
7834	7832	54.91	ND	15.64	6.21	0.04	1.07	3.58	0.05	0.64
7836	7834	55.15	ND	15.61	6.32	0.06	1.23	3.56	0.05	0.62
7842	7840	52.38	ND	13.91	4.80	0.06	7.45	3.17	0.04	0.31
7844	7842	52.50	ND	13.49	5.67	0.07	6.90	3.01	0.05	0.56
7846	7844	53.70	ND	14.38	5.72	0.07	4.65	3.23	0.05	0.34
7848	7846	54.20	ND	15.03	6.32	0.07	3.34	3.33	0.06	0.48
7850	7848	54.66	ND	15.70	6.53	0.06	2.27	3.46	0.06	0.36
7852	7850	50.76	ND	13.39	5.24	0.08	8.44	2.96	0.06	0.27
7854	7852	52.10	ND	13.73	5.54	0.09	7.28	3.03	0.06	0.23
7856	7854	53.02	ND	14.78	6.10	0.08	4.56	3.26	0.06	0.27
7858	7856	53.33	ND	15.04	6.15	0.07	3.73	3.34	0.06	0.25
7860	7858	54.06	ND	15.17	6.20	0.07	3.67	3.32	0.06	0.24
7862	7860	53.15	ND	14.65	6.20	0.07	3.93	3.24	0.06	0.36
7864	7862	53.91	ND	14.99	6.42	0.07	3.28	3.28	0.06	0.33
7866	7864	53.89	ND	15.15	6.48	0.07	2.98	3.31	0.06	0.34
7868	7866	53.64	ND	14.89	6.16	0.07	3.54	3.29	0.06	0.28
7870	7868	52.96	ND	15.09	6.10	0.06	3.42	3.36	0.06	0.30
7872	7870	43.93	ND	4.17	4.73	0.28	27.10	0.73	0.12	0.11
7874	7872	53.66	ND	14.63	6.22	0.08	3.84	3.20	0.06	0.22
7876	7874	53.44	ND	14.65	6.50	0.08	4.40	3.15	0.06	0.33
7878	7876	51.88	ND	16.71	6.57	0.03	0.39	3.82	0.05	0.75
7880	7878	55.27	ND	15.48	6.17	0.04	2.10	3.44	0.04	0.54
7882	7880	54.60	ND	15.07	6.32	0.04	2.33	3.32	0.04	0.67
7884	7882	52.74	ND	13.58	5.82	0.07	6.37	3.00	0.05	0.47
7886	7884	54.90	ND	15.69	5.96	0.04	2.00	3.53	0.05	0.37
7888	7886	53.69	ND	16.19	6.32	0.03	0.82	3.62	0.05	0.75
7890	7888	53.46	ND	15.27	5.87	0.04	3.63	3.34	0.05	0.61
7892	7890	53.00	ND	16.31	6.63	0.03	0.88	3.56	0.05	0.84
7894	7892	53.07	ND	15.46	6.86	0.03	1.77	3.38	0.05	1.05
7896	7894	52.14	ND	13.67	6.00	0.05	5.47	2.99	0.06	0.80
7898	7896	50.42	ND	15.22	6.27	0.05	4.06	3.24	0.06	0.57
7900	7898	53.82	ND	14.43	6.14	0.06	4.44	3.15	0.06	0.51
7902	7900	52.70	ND	14.66	6.15	0.04	3.98	3.23	0.06	0.85
7904	7902	50.64	ND	12.90	5.42	0.06	9.19	2.77	0.05	0.74
7906	7904	52.52	ND	14.33	6.12	0.06	4.48	3.15	0.05	0.48
7908	7906	53.60	ND	15.27	6.19	0.04	3.12	3.36	0.05	0.74
7910	7908	49.13	ND	11.66	4.23	0.07	10.84	2.60	0.06	0.34
7912	7910	52.51	ND	16.70	7.15	0.02	0.16	3.69	0.05	1.02
7914	7912	53.90	ND	14.60	5.50	0.04	4.20	3.23	0.05	0.57
7916	7914	52.13	ND	16.80	6.67	0.02	0.27	3.74	0.05	0.93

Table A.9. Well COP 289 XRF Major Element Data Continued

Depth ft	LC Depth ft	SiO_2 wt %	TiO_2 wt %	Al_2O_3 wt %	Fe_2O_3 wt %	MnO wt %	CaO wt %	K_2O wt %	P_2O_5 wt %	S wt %
7918	7916	50.28	ND	15.54	6.89	0.02	0.56	3.43	0.04	0.95
7920	7918	53.02	ND	16.18	6.60	0.02	0.53	3.60	0.05	0.89
7926	7924	51.68	ND	16.03	6.36	0.03	1.89	3.58	0.05	0.86
7928	7926	52.64	ND	15.65	6.67	0.04	2.12	3.44	0.05	0.85
7930	7928	52.41	ND	16.39	7.14	0.03	0.85	3.58	0.05	0.92
7932	7930	52.45	ND	16.97	6.70	0.02	0.26	3.75	0.05	0.92
7934	7932	51.33	ND	16.03	7.56	0.04	1.16	3.51	0.05	1.07
7936	7934	51.08	ND	13.66	6.53	0.10	6.56	2.94	0.05	0.57
7938	7936	51.20	ND	15.41	6.65	0.05	2.45	3.46	0.05	0.84
7940	7938	50.77	ND	15.26	6.72	0.05	2.48	3.43	0.05	0.91
7942	7940	51.22	ND	14.90	7.19	0.05	2.63	3.31	0.05	1.04
7944	7942	53.72	ND	16.08	6.21	0.04	1.52	3.62	0.05	0.57
7946	7944	53.29	ND	16.93	6.60	0.02	0.17	3.75	0.04	1.02
7948	7946	52.95	ND	15.34	5.21	0.05	4.69	3.37	0.04	0.61
7952	7950	53.63	ND	15.09	6.21	0.08	4.05	3.33	0.07	0.59
7954	7952	48.46	ND	12.87	9.61	0.08	4.91	2.60	0.06	1.69
7956	7954	50.64	ND	15.60	8.10	0.02	0.10	3.44	0.05	1.80
7958	7956	52.81	ND	16.02	7.43	0.02	0.08	3.49	0.05	1.32
7960	7958	53.51	ND	15.74	7.76	0.02	0.17	3.36	0.05	1.38
7962	7960	52.53	ND	14.80	9.37	0.03	0.79	3.07	0.09	1.47
7964	7962	53.81	ND	15.50	7.04	0.02	0.18	3.35	0.04	1.22
7966	7964	53.14	ND	15.69	7.09	0.03	0.60	3.46	0.05	1.13
7968	7966	51.66	ND	14.27	8.72	0.04	2.54	3.01	0.05	1.81
7970	7968	53.56	ND	15.51	7.49	0.02	0.39	3.40	0.05	1.40
7972	7970	53.52	ND	15.29	7.59	0.02	0.32	3.29	0.05	1.37
7974	7972	54.98	ND	14.95	7.27	0.02	0.27	3.18	0.05	1.44
7976	7974	54.71	ND	14.67	6.86	0.02	0.23	3.19	0.05	1.43
7978	7976	53.56	ND	15.11	7.43	0.02	0.46	3.27	0.07	1.40
7980	7978	51.00	ND	14.72	8.08	0.02	0.42	3.17	0.06	1.79
7982	7980	53.40	ND	15.58	7.78	0.02	0.34	3.36	0.05	1.31
7984	7982	52.45	ND	15.39	8.20	0.02	0.36	3.33	0.05	1.63
7986	7984	49.90	ND	14.84	8.48	0.02	1.79	3.19	0.04	1.92
7988	7986	53.90	ND	16.16	6.59	0.02	0.49	3.54	0.04	1.23
7990	7988	53.58	ND	15.78	6.66	0.02	0.85	3.40	0.05	1.34
7992	7990	38.83	ND	7.45	4.63	0.06	21.69	1.47	0.05	1.30
7994	7992	40.95	ND	8.85	3.63	0.03	18.76	1.82	0.18	1.13
7996	7994	49.25	ND	11.22	4.10	0.03	11.20	2.37	0.08	0.97
7998	7996	51.47	ND	13.87	4.89	0.03	5.68	3.12	0.07	1.37
8000	7998	53.74	ND	14.34	5.62	0.03	3.58	3.19	0.06	1.38
8002	8000	53.94	ND	14.30	5.85	0.03	3.41	3.18	0.06	1.38

Table A.9. Well COP 289 XRF Major Element Data Continued

Depth ft	LC Depth ft	SiO_2 wt %	TiO_2 wt %	Al_2O_3 wt %	Fe_2O_3 wt %	MnO wt %	CaO wt %	K_2O wt %	P_2O_5 wt %	S wt %
8004	8002	53.91	ND	13.04	5.09	0.03	6.17	2.89	0.06	1.36
8006	8004	58.29	ND	13.65	5.50	0.02	2.31	3.01	0.04	1.44
8012	8010	57.05	ND	12.55	6.78	0.03	3.99	2.64	0.06	1.70
8014	8012	58.64	ND	13.62	5.77	0.02	1.94	2.94	0.05	1.38
8016	8014	56.62	ND	14.84	6.37	0.02	0.83	3.22	0.04	1.44
8018	8016	55.66	ND	13.92	6.10	0.03	4.01	2.97	0.05	1.39
8020	8018	53.48	ND	13.03	5.99	0.03	5.63	2.80	0.06	1.34
8022	8020	55.71	ND	15.35	6.38	0.02	1.33	3.29	0.04	1.38
8024	8022	55.48	ND	15.28	6.17	0.02	1.28	3.32	0.04	1.34
8026	8024	52.92	ND	13.80	5.82	0.03	3.36	3.04	0.05	1.23
8028	8026	56.11	ND	15.01	6.56	0.02	1.09	3.22	0.04	1.46
8030	8028	53.35	ND	13.47	6.03	0.03	4.32	2.90	0.06	1.35
8032	8030	53.83	ND	13.21	5.76	0.03	5.04	2.86	0.05	1.34
8034	8032	55.86	ND	14.32	6.31	0.03	2.39	3.08	0.05	1.34
8036	8034	56.71	ND	14.19	6.05	0.02	1.87	3.07	0.04	1.35
8038	8036	57.07	ND	14.14	5.89	0.02	1.85	3.06	0.04	1.26
8040	8038	57.94	ND	13.85	5.63	0.02	2.79	3.01	0.06	1.23
8044	8042	55.55	ND	13.33	5.86	0.03	4.33	2.88	0.06	1.24
8046	8044	55.44	ND	13.90	5.85	0.03	2.94	3.02	0.05	1.22
8048	8046	56.86	ND	14.79	5.77	0.02	1.04	3.28	0.05	1.27
8050	8048	57.53	ND	14.92	6.57	0.02	0.68	3.23	0.05	1.42
8052	8050	56.94	ND	14.08	6.53	0.02	1.88	3.04	0.05	1.40
8054	8052	57.42	ND	14.39	6.43	0.02	1.35	3.13	0.06	1.45
8056	8054	56.69	ND	14.15	5.94	0.03	1.82	3.12	0.07	1.21
8058	8056	56.62	ND	14.23	5.23	0.02	2.65	3.18	0.10	0.98
8060	8058	55.30	ND	14.80	7.21	0.02	1.15	3.18	0.04	1.62
8062	8060	55.50	ND	15.03	6.11	0.02	1.56	3.29	0.05	1.31
8064	8062	55.63	ND	14.80	6.28	0.02	1.70	3.20	0.05	1.36
8066	8064	54.93	ND	14.31	5.86	0.02	1.16	3.22	0.04	1.33
8068	8066	56.54	ND	14.30	5.64	0.02	2.53	3.13	0.06	1.14
8070	8068	57.03	ND	14.50	6.90	0.02	1.96	3.07	0.04	1.43
8072	8070	57.03	ND	14.05	6.45	0.02	2.48	2.99	0.04	1.31
8074	8072	58.04	ND	12.94	5.19	0.02	3.39	2.84	0.04	1.20
8076	8074	57.22	ND	12.27	7.74	0.02	3.68	2.49	0.05	1.97
8078	8076	61.59	ND	12.35	4.93	0.02	1.70	2.67	0.05	1.11
8080	8078	59.30	ND	13.36	6.07	0.02	1.24	2.86	0.04	1.58
8082	8080	60.82	ND	12.57	5.67	0.02	2.36	2.69	0.05	1.35
8086	8084	51.39	ND	10.50	5.64	0.02	9.96	2.24	0.07	2.00
8088	8086	53.80	ND	12.77	6.23	0.02	3.57	2.83	0.05	1.81
8090	8088	59.01	ND	9.89	6.20	0.00	1.69	2.12	0.06	2.68

Table A.9. Well COP 289 XRF Major Element Data Continued

Depth ft	LC Depth ft	SiO_2 wt %	TiO_2 wt %	Al_2O_3 wt %	Fe_2O_3 wt %	MnO wt %	CaO wt %	K_2O wt %	P_2O_5 wt %	S wt %
8092	8090	61.76	ND	11.50	5.30	0.01	3.11	2.47	0.05	1.64
8094	8092	58.67	ND	11.24	10.34	0.00	1.16	1.93	0.07	3.14
8096	8094	26.69	ND	5.13	2.35	0.19	21.93	0.73	0.04	0.39
8098	8096	75.60	ND	7.33	3.93	0.01	5.24	1.37	0.07	1.27
8100	8098	52.96	ND	2.51	0.93	0.02	35.26	0.46	0.09	0.54
8102	8100	54.05	ND	0.66	0.72	0.02	38.67	0.13	0.04	0.37
8104	8102	81.28	ND	4.72	1.54	0.01	12.33	0.94	0.04	0.46
8106	8104	54.97	ND	1.90	1.13	0.02	33.26	0.38	0.04	0.30
8108	8106	29.58	ND	3.80	1.59	0.01	32.80	0.91	0.06	0.72
8110	8108	46.10	ND	10.71	2.38	0.02	14.32	2.89	0.11	0.42
8112	8110	21.73	ND	2.76	0.82	0.02	37.87	0.73	0.04	0.25
8114	8112	28.93	ND	7.63	1.82	0.02	25.08	1.95	0.08	0.70
8116	8114	29.29	ND	4.98	1.74	0.02	27.94	1.40	0.06	0.37
8118	8116	1.47	ND	0.35	0.20	0.02	46.28	0.10	0.04	0.06

BIBLIOGRAPHY

Achterberg, E.P., van den Berg, C.M.G., and Colombo, C., 2003, High resolution monitoring of dissolved Cu and Co in coastal surface waters of the Western North Sea: Continental Shelf Research, v. 23, p. 611–623, doi: 10.1016/S0278-4343(03)00003-7.

Algeo, T.J., 2004, Can marine anoxic events draw down the trace element inventory of seawater? Geology, v. 32, p. 1057–1060, doi: 10.1130/G20896.1.

Algeo, T.J., and Lyons, T.W., 2006, Mo–total organic carbon covariation in modern anoxic marine environments: Implications for analysis of paleoredox and paleohydrographic conditions: Paleoceanography, v. 21, p. PA1016, doi: 10.1029/2004PA001112.

Algeo, T.J., and Maynard, J.B., 2004, Trace-element behavior and redox facies in core shales of Upper Pennsylvanian Kansas-type cyclothems: Chemical Geology, v. 206, p. 289–318, doi: 10.1016/j.chemgeo.2003.12.009.

Algeo, T.J., and Rowe, H., 2012, Paleoceanographic applications of trace-metal concentration data: Chemical Geology, v. 324, p. 6–18, doi: 10.1016/j.chemgeo.2011.09.002.

Algeo, T.J., and Scheckler, S.E., 1998, Terrestrial-marine teleconnections in the Devonian; links between the evolution of land plants, weathering processes, and marine anoxic events: Philosophical Transactions - Royal Society of London. Biological Sciences, v. 353, p. 113–130, doi: 10.1098/rstb.1998.0195.

Altabet, M.A., and Francois, R., 1994, Sedimentary nitrogen isotopic ratio as a recorder for surface ocean nitrate utilization: Global Biogeochemical Cycles, v. 8, p. 103–116, doi: 10.1029/93GB03396.

Arthur, M.A., and Sageman, B.B., 1994, Marine Black Shales: Depositional Mechanisms and Environments of Ancient Deposits: Annual Review of Earth and Planetary Sciences, v. 22, p. 499–551, doi: 10.1146/annurev.ea.22.050194.002435.

Beaumont, C., Quinlan, G., and Hamilton, J., 1988, Orogeny and stratigraphy: Numerical models of the Paleozoic in the eastern interior of North America: Tectonics, v. 7, p. 389–416, doi: 10.1029/TC007i003p00389.

Berner, R.A., 1990, Atmospheric Carbon Dioxide Levels Over Phanerozoic Time: Science, v. 249, p. 1382–1386, doi: 10.1126/science.249.4975.1382.

Berner, R.A., 1997, Geochemistry and Geophysics: The Rise of Plants and Their Effect on Weathering and Atmospheric CO2: Science, v. 276, p. 544–546, doi: 10.1126/science.276.5312.544.

Bertine, K.K., and Turekian, K.K., 1973, Molybdenum in marine deposits: Geochimica et Cosmochimica Acta, v. 37, p. 1415–1434, doi: 10.1016/0016-7037(73)90080-X.

Boling, K., 2013, Controls on the Accumulation of Organic Matter in the Eagle Ford Group, Central Texas, USA:

Breit, G.N., and Wanty, R.B., 1991, Vanadium accumulation in carbonaceous rocks: A review of geochemical controls during deposition and diagenesis: Chemical Geology, v. 91, p. 83–97, doi: 10.1016/0009-2541(91)90083-4.

Brett, C.E., Baird, G.C., Bartholomew, A.J., DeSantis, M.K., and Ver Straeten, C.A., 2011, Sequence stratigraphy and a revised sea-level curve for the Middle Devonian of eastern North America: Palaeogeography, Palaeoclimatology, Palaeoecology, v. 304, p. 21–53, doi: 10.1016/j.palaeo.2010.10.009.

Calvert, S.E., and Pedersen, T.F., 1993, Geochemistry of Recent oxic and anoxic marine sediments: Implications for the geological record: Marine Geology, v. 113, p. 67–88, doi: 10.1016/0025-3227(93)90150-T.

Canfield, D.E., 1994, Factors influencing organic carbon preservation in marine sediments: Chemical Geology, v. 114, p. 315–329, doi: 10.1016/0009-2541(94)90061-2.

Canfield, D.E., 1989, Sulfate reduction and oxic respiration in marine sediments: implications for organic carbon preservation in euxinic environments: Deep Sea Research Part A. Oceanographic Research Papers, v. 36, p. 121–138, doi: 10.1016/0198-0149(89)90022-8.

Castle, J.W., 2001, Appalachian Basin stratigraphic response to convergent-margin structural evolution: Basin Research, v. 13, p. 397–418.

Chaillou, G., Anschutz, P., Lavaux, G., Schäfer, J., and Blanc, G., 2002, The distribution of Mo, U, and Cd in relation to major redox species in muddy sediments of the Bay of Biscay: Marine Chemistry, v. 80, p. 41–59, doi: 10.1016/S0304-4203(02)00097-X.

Chen, R., and Sharma, S., 2016, Role of alternating redox conditions in the formation of organic-rich interval in the MiddleDevonian MarcellusShale, Appalachian Basin,USA: Palaeogeography, Palaeoclimatology, Palaeoecology, v. 446, p. 85–97.

Coleman, J.L., Cook, R.C., Charpentier, R.R., Kirschbaum, M., Klett, T.R., Pollastro, R.M., and Schenk, C.J., 2011, Assessment of undiscovered oil and gas resources of the Devonian Marcellus Shale of the Appalachian Basin Province: U.S. Geological Survey Fact Sheet, v. 2011–3092.

Cooper, G.A., 1934, Stratigraphy of the Hamilton Group, eastern New York: American Journal of Science, v. Series 5 Vol. 27, p. 1–12, doi: 10.2475/ajs.s5-27.157.1.

Crusius, J., Calvert, S., Pedersen, T., and Sage, D., 1996, Rhenium and molybdenum enrichments in sediments as indicators of oxic, suboxic and sulfidic conditions of deposition: Earth and Planetary Science Letters, v. 145, p. 65–78, doi: 10.1016/S0012-821X(96)00204-X.

Crusius, J., and Thomson, J., 2000, Comparative behavior of authigenic Re, U, and Mo during reoxidation and subsequent long-term burial in marine sediments: Geochimica et Cosmochimica Acta, v. 64, p. 2233–2242, doi: 10.1016/S0016-7037(99)00433-0.

Dean, W.E., Arthur, M.A., and Claypool, G.E., 1986, Depletion of 13C in Cretaceous marine organic matter: Source, diagenetic, or environmental sigal? Marine Geology, v. 70, p. 119–157, doi: 10.1016/0025-3227(86)90092-7.

Demaison, G.J., and Moore, G.T., 1980, Anoxic environments and oil source bed genesis: Organic Geochemistry, v. 2, p. 9–31, doi: 10.1016/0146-6380(80)90017-0.

DeSantis, M.K., and Brett, C.E., 2011, Late Eifelian (Middle Devonian) biocrises: Timing and signature of the pre-Kačák Bakoven and Stony Hollow Events in eastern North America: Palaeogeography, Palaeoclimatology, Palaeoecology, v. 304, p. 113–135, doi: 10.1016/j.palaeo.2010.10.013.

Driese, S.G., Mora, C.I., and Elick, J.M., 2000, The paleosol record of increasing plant diversity and depth of rooting and changes in atmospheric pCO2 in the Siluro-Devonian: The Paleontological society,.

Duke, W.L., Prave, A.R., and PennStrat, 1991, Storm- and Tide-Influenced Prograding Shoreline Sequences in the Middle Devonian Mahantango Formation, Pennsylvania: , p. 349–369.

Dunham, R.J., 1962, Classification of Carbonate Rocks According to Depositional Textures: v. 38, p. 108–121.

Edinger, E.N., Copper, S.P., Risk, M.J., and Atmojo, W., 2002, Oceanography and reefs of recent and Paleozoic tropical epeiric seas: Facies, v. 47, p. 127–149, doi: 10.1007/BF02667710.

Emerson, S., and Hedges, J.I., 1988, Processes controlling the organic carbon content of open ocean sediments: Paleoceanography, v. 3, p. 621–634, doi: 10.1029/PA003i005p00621.

Emerson, S.R., and Huested, S.S., 1991, Ocean anoxia and the concentrations of molybdenum and vanadium in seawater: Marine Chemistry, v. 34, p. 177–196, doi: 10.1016/0304-4203(91)90002-E.

Engelder, T., and Lash, G.G., 2008, Marcellus Shale Play's Vast Resource Potential Creating Stir In Appalachia: The American Oil and Gas Reporter, v. 51, p. 76–87.

Erickson, B.E., and Helz, G.R., 2000, Molybdenum(VI) speciation in sulfidic waters: Geochimica et Cosmochimica Acta, v. 64, p. 1149–1158, doi: 10.1016/S0016-7037(99)00423-8.

Ettensohn, F.R., 2008, Chapter 4 The Appalachian Foreland Basin in Eastern United States, *in* Sedimentary Basins of the World, Elsevier, v. 5, p. 105–179, doi: 10.1016/S1874-5997(08)00004-X.

Ettensohn, F.R., 1985a, Controls on development of Catskill Delta complex basin-facies: Geological Society of America Special Papers, v. 201, p. 65–78, doi: 10.1130/SPE201-p65.

Ettensohn, F.R., 1985b, The Catskill Delta complex and the Acadian Orogeny: A model: Geological Society of America Special Papers, v. 201, p. 39–50, doi: 10.1130/SPE201-p39.

Faill, R.T., 1985, The Acadian orogeny and the Catskill Delta, *in* Geological Society of America Special Papers, Geological Society of America, v. 201, p. 15–38, doi: 10.1130/SPE201-p15.

Fernex, F., Février, G., Bénaïm, J., and Arnoux, A., 1992, Copper, lead and zinc trapping in Mediterranean deep-sea sediments: probable coprecipitation with Mn and Fe: Chemical Geology, v. 98, p. 293–306, doi: 10.1016/0009-2541(92)90190-G.

Galbraith, E.D., Kienast, M., Pedersen, T.F., and Calvert, S.E., 2004, Glacial-interglacial modulation of the marine nitrogen cycle by high-latitude O_2 supply to the global thermocline: MODULATION OF THE N CYCLE BY O_2 SUPPLY: Paleoceanography, v. 19, p. n/a-n/a, doi: 10.1029/2003PA001000.

Galimov, E.M., 2006, Isotope organic geochemistry: Organic Geochemistry, v. 37, p. 1200–1262, doi: 10.1016/j.orggeochem.2006.04.009.

Gensel, P.G., and Edwards, D., 2001, Plants Invade the Land: Evolutionary and Environmental Perspectives: Columbia University Press, 321 p.

Hanson, J., 2017, Characterizing the Reservoir Quality of Marcellus Formation Mudrocks through a Comparison of Chemostratigraphic Character and Petrophysical Response in North-Central Pennsylvania: Baylor University,.

Hedges, J.I., Hu, F.S., Devol, A.H., Hartnett, H.E., Tsamakis, E., and Keil, R.G., 1999, Sedimentary organic matter preservation; a test for selective degradation under oxic conditions: American Journal of Science, v. 299, p. 529–555, doi: 10.2475/ajs.299.7-9.529.

Helmond, N.A.G.M. van, Sluijs, A., Reichart, G.-J., Damsté, J.S.S., Slomp, C.P., and Brinkhuis, H., 2014, A perturbed hydrological cycle during Oceanic Anoxic Event 2: Geology, v. 42, p. 123–126, doi: 10.1130/G34929.1.

Huerta-Diaz, M.A., and Morse, J.W., 1990, A quantitative method for determination of trace metal concentrations in sedimentary pyrite: Marine Chemistry, v. 29, p. 119–144, doi: 10.1016/0304-4203(90)90009-2.

Huerta-Diaz, M.A., and Morse, J.W., 1992, Pyritization of trace metals in anoxic marine sediments: Geochimica et Cosmochimica Acta, v. 56, p. 2681–2702, doi: 10.1016/0016-7037(92)90353-K.

Karl, D., Letelier, R., Tupas, L., Dore, J., Christian, J., and Hebel, D., 1997, The role of nitrogen fixation in biogeochemical cycling in the subtropical North Pacific Ocean: Nature, v. 388, p. 533–538, doi: 10.1038/41474.

Khan, N.S., Vane, C.H., Horton, B.P., Hillier, C., Riding, J.B., and Kendrick, C.P., 2015, The application of $\delta^{13}C$, TOC and C/N geochemistry to reconstruct Holocene relative sea levels and paleoenvironments in the Thames Estuary, UK: HOLOCENE RELATIVE SEA LEVELS AND PALEOENVIRONMENTS IN THE THAMES ESTUARY: Journal of Quaternary Science, v. 30, p. 417–433, doi: 10.1002/jqs.2784.

Klinkhammer, G.P., and Palmer, M.R., 1991, Uranium in the oceans: Where it goes and why: Geochimica et Cosmochimica Acta, v. 55, p. 1799–1806, doi: 10.1016/0016-7037(91)90024-Y.

Kohl, D., Slingerland, R., Arthur, M., Bracht, R., and Engelder, T., 2014, Sequence stratigraphy and depositional environments of the Shamokin (Union Springs) Member, Marcellus Formation, and associated strata in the middle Appalachian Basin: AAPG Bulletin, v. 98, p. 483–513, doi: 10.1306/08231312124.

Kuila, U., McCarty, D.K., Derkowski, A., Fischer, T.B., Topór, T., and Prasad, M., 2014, Nano-scale texture and porosity of organic matter and clay minerals in organic-rich mudrocks: Fuel, v. 135, p. 359–373, doi: 10.1016/j.fuel.2014.06.036.

Küspert, W., 1982, Environmental Changes During Oil Shale Deposition as Deduced from Stable Isotope Ratios, *in* Cyclic and Event Stratification, Springer, Berlin, Heidelberg, p. 482–501, doi: 10.1007/978-3-642-75829-4_36.

Lash, G.G., and Engelder, T., 2011, Thickness trends and sequence stratigraphy of the Middle Devonian Marcellus Formation, Appalachian Basin: Implications for Acadian foreland basin evolution: AAPG Bulletin, v. 95, p. 61–103, doi: 10.1306/06301009150.

Lindholm, R.C., 1969, Carbonate Petrology of the Onondaga Limestone (Middle Devonian), New York: a Case for Calcisiltite: Journal of Sedimentary Research, v. 39, http://archives.datapages.com/data/sepm/journals/v38-41/data/039/039001/0268.htm (accessed May 2017).

McManus, J., Berelson, W.M., Klinkhammer, G.P., Hammond, D.E., and Holm, C., 2005, Authigenic uranium: Relationship to oxygen penetration depth and organic carbon rain: Geochimica et Cosmochimica Acta, v. 69, p. 95–108, doi: 10.1016/j.gca.2004.06.023.

Meyers, P.A., 1994, Preservation of elemental and isotopic source identification of sedimentary organic matter: Chemical Geology, v. 114, p. 289–302, doi: 10.1016/0009-2541(94)90059-0.

Meyers, P.A., 2014, Why are the d13Corg values in Phanerozoic black shales more negative than in modern marine organic matter? Geochemistry, Geophysics, Geosystems, v. 15, p. 3085–3106, doi: 10.1002/2014GC005305.

Meyers, P.A., Bernasconi, S.M., and Yum, J.-G., 2009, 20My of nitrogen fixation during deposition of mid-Cretaceous black shales on the Demerara Rise, equatorial Atlantic Ocean: Organic Geochemistry, v. 40, p. 158–166, doi: 10.1016/j.orggeochem.2008.11.006.

Milici, R.C., and Swezey, C.S., 2006, Assessment of Appalachian Basin Oil and Gas Resources: Devonian Shale–Middle and Upper Paleozoic Total Petroleum System: U.S. Geological Survey Open File Report 2006–1237, https://pubs.usgs.gov/of/2006/1237/.

Mills, T., 2015, Paleoceanographic Conditions that Resulted in the Accumulation of Organic Matter in the Middle Pennsylvanian Hermosa Group, Southwestern Shelf, Paradox Basin, Utah:

Mora, C.I., Driese, S.G., and Colarusso, L.A., 1996, Middle to late Paleozoic atmospheric CO2 levels from soil carbonate and organic matter: Science; Washington, v. 271, p. 1105.

Morford, J.L., and Emerson, S., 1999, The geochemistry of redox sensitive trace metals in sediments: Geochimica et Cosmochimica Acta, v. 63, p. 1735–1750, doi: 10.1016/S0016-7037(99)00126-X.

Morford, J.L., Russell, A.D., and Emerson, S., 2001, Trace metal evidence for changes in the redox environment associated with the transition from terrigenous clay to diatomaceous sediment, Saanich Inlet, BC: Marine Geology, v. 174, p. 355–369, doi: 10.1016/S0025-3227(00)00160-2.

Morse, J.W., and Luther, G.W., 1999, Chemical influences on trace metal-sulfide interactions in anoxic sediments: Geochimica et Cosmochimica Acta, v. 63, p. 3373–3378, doi: 10.1016/S0016-7037(99)00258-6.

Murphy, A.E., Sageman, B.B., Hollander, D.J., Lyons, T.W., and Brett, C.E., 2000, Black shale deposition and faunal overturn in the Devonian Appalachian Basin: Clastic starvation, seasonal water-column mixing, and efficient biolimiting nutrient recycling: Paleoceanography, v. 15, p. 280–291, doi: 10.1029/1999PA000445.

Naimo, D., Adamo, P., Imperato, M., and Stanzione, D., 2005, Mineralogy and geochemistry of a marine sequence, Gulf of Salerno, Italy: Quaternary International, v. 140, p. 53–63, doi: 10.1016/j.quaint.2005.05.004.

Nameroff, T.J., Calvert, S.E., and Murray, J.W., 2004, Glacial-interglacial variability in the eastern tropical North Pacific oxygen minimum zone recorded by redox-sensitive trace metals: Paleoceanography, v. 19, p. PA1010, doi: 10.1029/2003PA000912.

Ohkouchi, N., Kuroda, J., Okada, M., and Tokuyama, H., 2003, Why Cretaceous black shales have high C/N ratios: Implications from SEM-EDX observations for Livello Bonarelli black shales at the Cenomanian-Turonian boundary: FRONTIER RESEARCH ON EARTH EVOLUTION, v. Vol 1, p. 239–241.

Oliver, W.A., 1956, STRATIGRAPHY OF THE ONONDAGA LIMESTONE IN EASTERN NEW YORK: Geological Society of America Bulletin, v. 67, p. 1441, doi: 10.1130/0016-7606(1956)67[1441:SOTOLI]2.0.CO;2.

Pedersen, T.F., and Calvert, S.E., 1990, Anoxia vs. Productivity: What Controls the Formation of Organic-Carbon-Rich Sediments and Sedimentary Rocks? AAPG Bulletin, v. 74, p. 454–466.

Popp, B.N., Takigiku, R., Hayes, J.M., Louda, J.W., and Baker, E.W., 1989, The post-Paleozoic chronology and mechanism of 13 C depletion in primary marine organic matter: American Journal of Science, v. 289, p. 436–454, doi: 10.2475/ajs.289.4.436.

Prahl, F.G., De Lange, G.J., Scholten, S., and Cowie, G.L., 1997, A case of post-depositional aerobic degradation of terrestrial organic matter in turbidite deposits from the Madeira Abyssal Plain: Organic Geochemistry, v. 27, p. 141–152, doi: 10.1016/S0146-6380(97)00078-8.

Prave, A.R., Duke+, W.L., and Slattery, W., 1996, A depositional model for storm- and tide-influenced prograding siliciclastic shorelines from the Middle Devonian of the central Appalachian foreland basin, USA: Sedimentology, v. 43, p. 611–629, doi: 10.1111/j.1365-3091.1996.tb02017.x.

Robinson, R.S., Kienast, M., Luiza Albuquerque, A., Altabet, M., Contreras, S., De Pol Holz, R., Dubois, N., Francois, R., Galbraith, E., Hsu, T.-C., Ivanochko, T., Jaccard, S., Kao, S.-J., Kiefer, T., et al., 2012, A review of nitrogen isotopic alteration in marine sediments: N ISOTOPIC ALTERATION IN MARINE SEDIMENT: Paleoceanography, v. 27, doi: 10.1029/2012PA002321.

Rooney, M.A., Claypool, G.E., and Moses Chung, H., 1995, Modeling thermogenic gas generation using carbon isotope ratios of natural gas hydrocarbons: Chemical Geology, v. 126, p. 219–232, doi: 10.1016/0009-2541(95)00119-0.

Sageman, B.B., Murphy, A.E., Werne, J.P., Ver Straeten, C.A., Hollander, D.J., and Lyons, T.W., 2003, A Tale of Shales: The Relative Roles of Production, Decomposition, and Dilution in the Accumulation of Organic-Rich Strata, Middle–Upper Devonian, Appalachian Basin: Chemical Geology, v. 195, p. 229–273, doi: 10.1016/S0009-2541(02)00397-2.

Saltzman, M.R., and Thomas, E., 2012, Carbon isotope stratigraphy, *in* United Kingdom, Elsevier : Oxford, United Kingdom, p. 207–232, doi: 10.1016/B978-0-444-59425-9.00011-1.

Schubert, B.A., and Jahren, A.H., 2012, The effect of atmospheric CO2 concentration on carbon isotope fractionation in C3 land plants: Geochimica et Cosmochimica Acta, v. 96, p. 29–43, doi: 10.1016/j.gca.2012.08.003.

Scotese, C.R., and McKerrow, W.S., 1990, Revised World maps and introduction: Geological Society, London, Memoirs, v. 12, p. 1–21, doi: 10.1144/GSL.MEM.1990.012.01.01.

Sigman, D.M., DiFiore, P.J., Hain, M.P., Deutsch, C., and Karl, D.M., 2009, Sinking organic matter spreads the nitrogen isotope signal of pelagic denitrification in the North Pacific: Geophysical Research Letters, v. 36, doi: 10.1029/2008GL035784.

Sigman, D.M., Karsh, K.L., and Casciotti, K.L., 2009, Nitrogen Isotopes in the Ocean, *in* Encyclopedia of Ocean Sciences, Elsevier, p. 40–54, doi: 10.1016/B978-012374473-9.00632-9.

Sinninghe Damsté, J.S., and Köster, J., 1998, A euxinic southern North Atlantic Ocean during the Cenomanian/Turonian oceanic anoxic event: Earth and Planetary Science Letters, v. 158, p. 165–173, doi: 10.1016/S0012-821X(98)00052-1.

Sloss, L.L., 1963, Sequences in the Cratonic Interior of North America: Geological Society of America Bulletin, v. 74, p. 93–114, doi: 10.1130/0016-7606(1963)74[93:SITCIO]2.0.CO;2.

Suess, E., 1980, Particulate organic carbon flux in the oceans: Surface and oxygen utilization: Nature,.

Swanson, V.E., 1960, Oil Yield and Uranium Content of Black Shales: Geological Survey, Washington, DC (USA) TID-27491, https://www.osti.gov/scitech/biblio/7314404 (accessed May 2017).

Thunell, R.C., Varela, R., Llano, M., Collister, J., -Karger, F.M., and Bohrer, R., 2000, Organic carbon fluxes, degradation, and accumulation in an anoxic basin: Sediment trap results from the Cariaco Basin: Limnology and Oceanography, v. 45, p. 300–308, doi: 10.4319/lo.2000.45.2.0300.

Tribovillard, N., Algeo, T.J., Lyons, T., and Riboulleau, A., 2006, Trace metals as paleoredox and paleoproductivity proxies; an update: Chemical Geology, v. 232, p. 12–32, doi: 10.1016/j.chemgeo.2006.02.012.

Tribovillard, N., Ramdani, A., and Trentesaux, A., 2005, Controls on Organic Accumulation in Upper Jurassic Shales of Northwestern Europe as Inferred from Trace-Metal Geochemistry:, http://archives.datapages.com/data/sepm_sp/SP82/Controls_on_Organic_Accumulation.htm (accessed June 2017).

Tribovillard, N., Riboulleau, A., Lyons, T., and Baudin, F., 2004, Enhanced trapping of molybdenum by sulfurized marine organic matter of marine origin in Mesozoic limestones and shales: Chemical Geology, v. 213, p. 385–401, doi: 10.1016/j.chemgeo.2004.08.011.

Tyson, R.V., 2001, Sedimentation rate, dilution, preservation and total organic carbon: some results of a modelling study: Organic Geochemistry, v. 32, p. 333–339, doi: 10.1016/S0146-6380(00)00161-3.

Tyson, R.V., and Pearson, T.H., 1991, Modern and ancient continental shelf anoxia: an overview: Geological Society, London, Special Publications, v. 58, p. 1–24, doi: 10.1144/GSL.SP.1991.058.01.01.

Van Tyne, A.M., 1983, Natural gas potential of the Devonian black shales of New York: Northeastern Geology, v. 5, p. 209–16.

Ver Straeten, C.A., and Brett, C.E., 2006, Pragian to Eifelian strata (middle Lower to lower Middle Devonian), northern Appalachian Basin: Stratigraphic nomenclatural changes: Northeastern Geology & Environmental Sciences, v. 28, p. 80–95.

Ver Straeten, C.A., Brett, C.E., and Sageman, B.B., 2011, Mudrock sequence stratigraphy: A multi-proxy (sedimentological, paleobiological and geochemical) approach, Devonian Appalachian Basin: Palaeogeography, Palaeoclimatology, Palaeoecology, v. 304, p. 54–73, doi: 10.1016/j.palaeo.2010.10.010.

Wang, G., and Carr, T.R., 2013, Organic-rich Marcellus Shale lithofacies modeling and distribution pattern analysis in the Appalachian Basin: AAPG Bulletin, v. 97, p. 2173–2205, doi: 10.1306/05141312135.

Wanty, R.B., and Goldhaber, M.B., 1992, Thermodynamics and kinetics of reactions involving vanadium in natural systems: Accumulation of vanadium in sedimentary rocks: Geochimica et Cosmochimica Acta, v. 56, p. 1471–1483, doi: 10.1016/0016-7037(92)90217-7.

Werne, J.P., Sageman, B.B., Lyons, T.W., and Hollander, D.J., 2002, An integrated assessment of a “type euxinic” deposit: Evidence for multiple controls on black shale deposition in the middle Devonian Oatka Creek formation: American Journal of Science, v. 302, p. 110–143, doi: 10.2475/ajs.302.2.110.

Whitfield, M., 2001, Interactions between phytoplankton and trace metals in the ocean: Advances in Marine Biology, v. 41, p. 1–128, doi: 10.1016/S0065-2881(01)41002-9.

Woodrow, D.L., 1985, Paleogeography, paleoclimate, and sedimentary processes of the Late Devonian Catskill Delta: Geological Society of America Special Papers, v. 201, p. 51–64, doi: 10.1130/SPE201-p51.

Zagorski, W.A., Wrightstone, G.R., and Bowman, D.C., 2012, The Appalachian Basin Marcellus Gas Play: Its History of Development, Geologic Controls on Production, and Future Potential as a World-class Reservoir: AAPG Memoir, v. 97, p. 172–200, doi: 10.1306/13321465M973491.

Zheng, Y., Anderson, R.F., van Geen, A., and Kuwabara, J., 2000, Authigenic molybdenum formation in marine sediments: a link to pore water sulfide in the Santa Barbara Basin: Geochimica et Cosmochimica Acta, v. 64, p. 4165–4178, doi: 10.1016/S0016-7037(00)00495-6.